**Horizon 2020**

**Societal Challenge: Improving the air quality and reducing the carbon footprint of European cities**

ICARUS

**Project: 690105 – ICARUS**

Full project title:

**Integrated Climate forcing and Air pollution Reduction in Urban Systems**

# D3.3: Report on AQ and GHGs concentration at the ground level in the ICARUS cities

**WP3 Integrated atmospheric modelling for connecting pressures to the environment to concentrations at the regional and urban scales**

Lead beneficiary: AUTH

Date: October 2018

Nature: Report

Dissemination level: Public

# Table of Contents

## Document Information

| | | | |
|---|---|---|---|
| **Grant Agreement Number** | 690105 | **Acronym** | ICARUS |
| **Full title** | Integrated Climate forcing and Air pollution Reduction in Urban Systems | | |
| **Project URL** | www.icarus2020.eu | | |
| **Project Officer** | Mirjam Witschke - Mirjam.WITSCHKE@ec.europa.eu | | |

| | | | | |
|---|---|---|---|---|
| **Delivery date** | **Contractual** | October 2017 | **Actual** | October 2018 |
| **Status** | Draft ☐ | | Final √ | |
| **Nature** | Demonstrator ☐ | Report √ | Prototype ☐ | Other ☐ |
| **Dissemination level** | Confidential ☐ | Public √ | | |

| | | | | |
|---|---|---|---|---|
| **Responsible Author (Partners)** | AUTH | | | |
| **Responsible Author** | Denis Sarigiannis | | **Email** | denis@eng.auth.gr |
| | **Partner** | AUTH | **Phone** | +30-2310-994562 |
| **Other partners (Institution)** | NCSRD, USTUTT, CMCC | | | |

## *Document History*

| Name (Institution) | Date | Version |
|---|---|---|
| AUTH | January 2018 | First draft |
| CMCC | March 2018 | Second draft |
| AUTH | June 2018 | Third draft |
| AUTH | October 2018 | Final |

# 1. Objective

The main objective of this report is to provide high space and time resolution ground concentrations reflecting climatic trends for the period 2001-2050.

- on major air pollutants ($PM_{10}$, $PM_{2.5}$, $NO_2$, $O_3$, BaP)
- on major Greenhouse Gases ($CO_2$, $CH_4$)

in Europe, focusing on nine (9) cities i.e. Thessaloniki, Athens, Madrid, Stuttgart, Ljubljana, Brno, Milan, Basel and Copenhagen/Roskilde using

- appropriate climatic and emission scenarios and
- appropriate air modelling and statistical tools.

The changes on climate and emissions over time, on the air concentration levels of the abovementioned pollutants need to be assessed.

## 2. Background

In a general description the statistical changes in the climate system over long periods of time defines the widely used term of "climate change". The last decades the extensively human activities considerably altered climate and earth's temperature by burning fossil fuels, cutting down rainforests and farming livestock. As a result, enormous amounts of greenhouse gases are produced and are added to those naturally occurring in the atmosphere, increasing the greenhouse effect (https://ec.europa.eu/clima/change/causes_en). Anthropogenic causes affected the climate both in terms of the global warming and the increase of greenhouse gas levels. The fact that emissions, transport, dilution, chemical transformation, and eventual deposition of air pollutants all can be significantly influenced by weather patterns as a result affecting the level of Air Quality (Kinney, 2008). Meteorological parameters like wind conditions and atmospheric boundary height could affect pollutants' transport and their accumulation. Also, temperature variation, solar radiation and air's humidity could impact on the chemical reaction rates and pollutants' emission. Global and large-scale climate changes through years affects urban and local conditions. The meteorological, topographic and land use variability could influence significantly the spatial and temporal patterns on the air quality and air pollutants concentrations.

Projections of changes in the climate system can be performed taking into consideration prescribed socio-economic and emission scenarios. One result of such a systematic effort prompted by the Intergovernmental Panel on Climate Change (IPCC) was the generation of the four (4) Representative Concentration Pathways (RCPs) scenarios. The main aim was that the RCPs need to refer to emissions and land use compatible with the full range of scenarios existing in the literature including extreme as well as intermediate scenarios. The four RCPs (i.e. RCP2.6, RCP4.5, RCP6, RCP8.5) together span the range of year 2100 radiative forcing values found in the open literature i.e. from 2.6W/m$^2$ to 8.5W/m$^2$. (van Vuuren et al., 2011). The RCP characteristics are given in Table 2.1.

*Table 2.1: The Representative Concentration Pathways (RCP) (van Vuuren et al., 2011)*

| | Description | Publication-Integrated Assessment Model |
|---|---|---|
| RCP8.5 | Rising radiative forcing pathway leading to 8.5 W/m$^2$ (~1370 ppm $CO_2$ eq) by 2100. | (Riahi et al., 2007)—MESSAGE |
| RCP2.6 | Stabilization without overshoot pathway to 6 W/m2 (~850 ppm $CO_2$ eq) at stabilization after 2100 | (Fujino et al., 2006; Hijioka et al., 2008)—AIM |
| RCP4.5 | Stabilization without overshoot pathway to 4.5 W/m$^2$ (~650 ppm $CO_2$ eq) at stabilization after 2100 | (Clarke et al., 2007; Smith and Wigley 2006; Wise et al., 2009)—GCAM |

| | | |
|---|---|---|
| RCP2.6 | Peak in radiative forcing at ~3 W/m$^2$ (~490 ppm $CO_2$ eq) before 2100 and then decline (the selected pathway declines to 2.6 W/m$^2$ by 2100). | (Van Vuuren et al., 2007a; van Vuuren et al., 2006)—IMAGE |

The high pathway (RCP8.5) for which radiative forcing reaches >8.5 W/m$^2$ by 2100 and continues to rise for some amount of time; two intermediate "stabilization pathways" (RCP 6-4.5) in which radiative forcing is stabilized at approximately 6 W/m$^2$ and 4.5 W/m$^2$ after 2100; and one pathway (RCP2.6) where radiative forcing peaks at approximately 3 W/m$^2$ before 2100 and then declines.

The RCP exercise has provided a comprehensive dataset with respect to emissions a land cover as shown in Table 2.2. This database allows the user to preview and download data both at the level of aggregated regions and in gridded format. The database can be accessed by the following link:

http://tntcat.iiasa.ac.at:8787/RcpDb/dsd?Action=htmlpage&page=welcome

*Table 2.2: The RCP available information (van Vuuren et al.,2011)*

| | Resolution (sectors) | Resolution (geographical) |
|---|---|---|
| **Emissions of greenhouse gases** | | |
| $CO_2$ | Energy/industry, land | Global and for 5 regions |
| $CH_4$ | 12 sectors | 0.5°×0.5° grid |
| $N_2O$, HFCs, PFCs, CFCs, SF6 | Sum | Global and for 5 regions |
| **Emissions aerosols and chemically active gases** | | |
| $SO_2$, Black Carbon (BC), Organic Carbon (OC), CO, NOx, VOCs, $NH_3$ | 12 sectors | 0.5°×0.5° grid |
| Speciation of VOC emissions | | 0.5°×0.5° grid |
| **Concentration of greenhouse gases** | | |
| ($CO_2$, $CH_4$, $N_2O$, HFCs, PFCs, CFCs, SF6) | - | Global |
| **Concentrations of aerosols and chemically active gases** | | |
| ($O_3$, Aerosols, N deposition, S deposition) | - | 0.5°×0.5° grid |
| **Land-use/land-cover data** | Cropland, pasture, primary vegetation, secondary vegetation, forests | 0.5°×0.5° grid with subgrid fractions, (annual maps and transition matrices including wood harvesting) |

RCP Database was used for the new climate model simulations carried out under the framework of the Coupled Model Intercomparison Project Phase 5 (CMIP5) of the World Climate Research Programme (Taylor et al., 2012). More specifically, the Community Earth System Model (CESM) a coupled global climate model comprised of four component models that simulate the atmosphere, ocean, land surface and sea-ice has been used for this purpose. More info can be found in http://www.cesm.ucar.edu/. Model outputs have been successfully produced based on RCP 4.5, 6.0 and 8.5 and are available for further use from NCAR's CISL Research Data Archive (http://rda.ucar.edu/datasets/ds316.0), and from the Earth System Grid Q Program for Climate Model Diagnosis and Intercomparison (ESGQ-PCMDI) gateway at Lawrence Livermore National Laboratory (http://pcmdi3.llnl.gov/esgcet/home.htm).

# 3. Methodology

## 3.1. Overall Strategy

Trying to follow climatic changes on local meteorology and air quality is a very demanding effort in terms of computational capability and computational time.

Thus, the present methodological strategy is based on the following principles:

1. Minimize the required CPU time;
2. Provide a methodological approach to avoid unnecessary additional computational runs.

Based on the above principles and taking into consideration the modeling state of the art, the project contractual requirements and the available resources the following decisions have been made:

1. Provide the necessary meteorological input for the future years following the IPCC scenarios based on the Fifth Assessment Report (AR5) and on the Representative Concentration Pathways (RCP);
2. Investigate the possibility to provide air quality future trends and representative detailed results following the concept of weather clustering/classification;
3. Produce the abovementioned detailed results by using WRF-Chem methodology to provide hourly concentrations of air pollutants in both regional and local scale on the selected representative days.

## 3.2. The study areas

The selected cities and their center locations are given in Table 3.1.

*Table 3.1: Location of the study areas*

| Point of domain's center | Longitude | Latitude |
|---|---|---|
| Stuttgart | 9.13 | 48.80 |
| Athens | 23.77 | 37.97 |
| Thessaloniki | 22.87 | 40.78 |
| Milan | 9.23 | 45.49 |
| Madrid | 356.30 | 40.46 |
| Basel | 7.55 | 47.55 |
| Brno | 16.66 | 49.14 |
| Copenhagen wider area | 12.56 | 55.64 |
| Roskilde wider area | 12.08 | 55.63 |
| Ljubljana | 14.53 | 46.01 |

In each city a local domain of an area 50km*50km is considered surrounding the city center. Given rather the small size of Roskilde city area it is considered to is adequate to be selected a 25km*25km area.

## 3.3. The climatic scenario

RCP4.5 seems to be a realistic scenario and therefore it is selected for the present analysis. It is a low-to-moderate emissions scenario with GHG radiative forcing reaching 4.5W/m$^2$ near 2100. It represents a trajectory that may be plausible if, for instance, GHG emissions pricing were introduced to limit radiative forcing (Thomson et al., 2011).

## 3.4. The Weather clustering approach

### 3.4.1 Weather classification

Meteorological temporal and spatial processes and conditions influence air pollutants' transport, accumulation and concentrations. Also, large time scale changes in the weather conditions may affect air pollutants' level (Austin et al., 2014). To investigate the climatic, meteorological and air quality conditions in a particular area for a wide time period, the identification of weather patterns has a significant role. Performing weather classification is a way to create distinguished groups of different weather patterns. These sets of weather regimes could help to identify weather conditions that produces pollution episodes and furthermore to forecast when these conditions occur in the future (Serra et al., 1999). Weather pattern classification shows relationship with atmospheric air quality levels (Demuzere and van Lipzig, 2010) such as in PM variations (Rimetz-Planchon et al., 2008; Chang and Zhan, 2017). Also, when it comes to estimate pollutants' concentrations, using advanced modeling tools, it is time-wise to apply these modeling approaches of large data sets in alternative smaller periods which are described by consistent weather characteristics (Sfetsos et al., 2005).

Cluster analysis is a statistical method able to identify, from a large dataset, subgroups with some degree of homogeneity. Based on nesting technique (partitioning or hierarchical), their approach (fuzzy or crisp clustering), or special purpose sequential data set, very large database. In hierarchical technique clusters are classified at various levels, whereas in partitioning technique clusters are optimized by specific clustering criterion (such as the number of clusters). In crisp clustering method the boundary between clusters is fully defined while when the boundaries between clusters cannot be clearly defined fuzzy clustering methods such as Fuzzy c-means, Mountain or subtractive clustering method or Partition Simplification Fuzzy C-means method work better (Moertini, 2002).

Within the nonhierarchical crisp techniques, k-means method (Huth et al. 2008) seems to perform well through various methods in the field of weather pattern identification (Beck and Philipp, 2010, Cahynova and Huth, 2010). It is noticed that k–means has been widely used for weather clustering (Serra et al., 1999; Bejaran et al., 2003; Hoffmann and Schlunzen, 2013; Austin et al., 2014). Thus, the k-means method is selected for the present studies. The details of k-means method present implementation are given below.

### 3.4.2 The Weather Data

For 50 years period, from 2001 to 2050, weather data are derived from the Coordinated Regional Climate Downscaling Experiment (CORDEX - http://cordex.org) provided from the

Earth System Grid Federation (ESGF) index nodes. Database can be accessed by the following link: http://cordex.org/data-access/esgf/

From the available Regional Climate Models (RCMs) which are participating in CORDEX, the INERIS-WRF331F was selected. Using the high horizontal resolution domain EUR 11 (about 10 km resolution) (ICARUS Report D3.1) this RCM provides high number of climate parameters at higher time frequency (daily). The moderate RCP4.5 scenario was selected. Following previous work (Serra et al., 1999; Austin et al., 2014; Makra et al., 2006; Sfetsos and Bartzis, 2007), the weather parameters considered, include (1) **the 2-meter temperature**, (2) **the daily temperature range** , (3) **the 2-meter relative humidity (%),** (4**) the surface pressure** , (5**) the precipitation** , (6) **the 10- meter U-component wind velocity** , (7) **the 10-meter V-component wind velocity**, (8) **the downward short-wave surface radiation** and (9) **the atmospheric boundary layer thickness** . Each of the above parameters has been averaged over the selected 50km x 50km city domain. All those variables were standardized to have zero mean and unity variance to avoid any bias from the individual parameter magnitude variety. For managing the netcdf files netCDF Operator (NCO) programm has been used. MATLAB software was used for exporting and editing and analysing the data.

### 3.4.3. Principal Component Analysis

The cluster analysis as described below need to be based on a number of uncorrelated variables Among the above-mentioned weather parameters some degree of correlation is expected. Principal component analysis (PCA) is a mathematical method that enable us to transform a number of (possibly) correlated parameters (such as the abovementioned weather parameters into a (smaller) number of uncorrelated variables called principal components (https://eclass.uoa.gr/modules/document/file.php/DI367/%CE%A5%CE%BB%CE%B9%CE%BA%CF%8C/PCA_method.pdf). PCA was applied to each city dataset which is composed by nine (9) columns (I,e, the above mentioned weather parameters) and ~18250 rows (each row corresponding to the observations of one day). VARIMAX rotation has been applied, which is a change of coordinates in principal component analysis (PCA) that maximizes the sum of the variances of the squared loadings. Thus, all the coefficients (squared correlation with factors) will be either large or near zero, with few intermediate values. The goal is to associate each variable to at most one factor (http://data-mining-tutorials.blogspot.com/2009/12/varimax-rotation-in-principal-component.html). PCA has been applied by using SPSS software. As an output, a new matrix is produced that includes again all the days of the study. Each day is now defined with the values of the selected principal components called factors or scores F (Preisendorfer and Mobley, 1988).

### 3.4.4. K- Means Cluster Analysis

In the k-means cluster analysis, a number of n vectors is partitioned to preselected k groups called clusters. The final grouping is done in such a way, that in every cluster, the sum of the squares of the distances of its vectors from the cluster centroid becomes minimal. Here, the number of vectors are the number of days under study. The vector that corresponds to each day consists of the values of the variables produced by the abovementioned PCA. For the present k-means clustering, the Lloyd's algorithm (Lloyd, 1982) has been applied. It has been applied by using the built in Matlab function.

The next step; is to define the optimal number of clusters. As an output, the Within Sum of Squares [WSS(k)] is calculated for each cluster's selection, defined as follows (Hoffmann and Schlunzen, 2013):

$$WSS(k) = \sum_{n=1}^{k} \sum_{x \in Ci} || \, x - zi \, || \, \hat{}2$$

where x denotes all data objects belonging to the cluster Ci; zi is the ith corresponding cluster centroids (CC).

As an example, the WSS(k) parameter for the city of Brno is shown as a function of the number of clusters (k) in Figure 3.1.

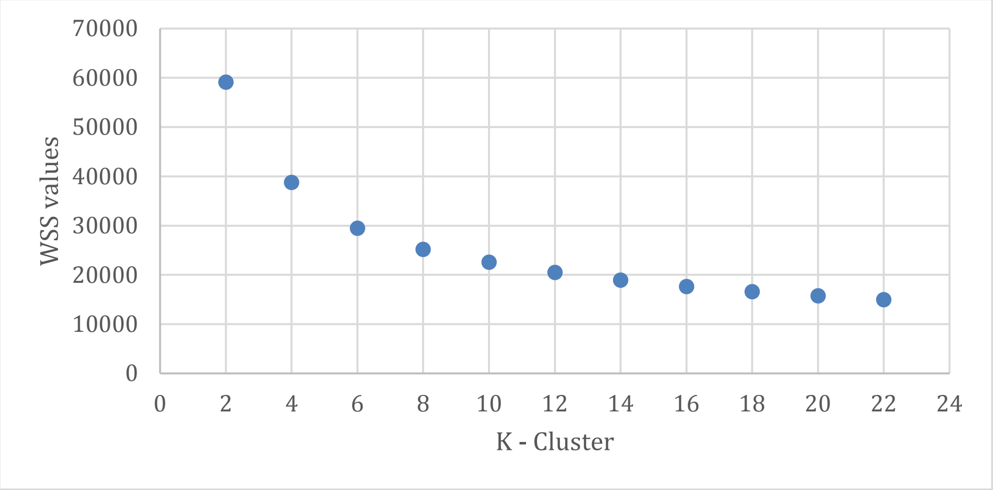


*Figure 3.1: WSS values vs k cluster solution*

It should be noted that WSS(k) decreases as the number of clusters increases. Figure 3.2 shows the corresponding fractional decrease defined as (Austin et al., 2014).

$$fractional\ decrease\ in\ WSS(k) = \frac{WSS = WSS(k) - WSS(k+1)}{WSS(k)}$$

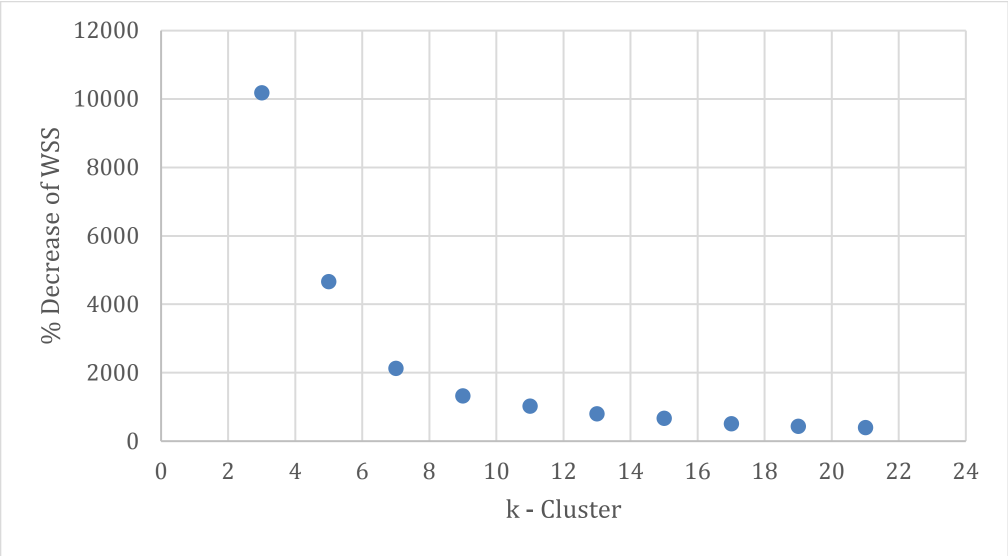


*Figure 3.2: The WSS parameter for the city of Brno*

The decrease slows significantly after k=8. This is a major criterion for selecting the final number of clusters (Austin e al., 2014) provided that the individual clusters have distinguishable differentiations at least with respect to weather patterns and air quality. Thus, for the city of Brno the final cluster number is taken equal to 8.

The same selection methodology was applied for the rest nine (9) cities. Table 3.2 gives the number of selected clusters for the ICARUS cities.

*Table 3.2: Clusters Numbers for the ICARUS cities*

| City | Number of clusters |
|---|---|
| Brno | 8 |
| Stuttgart | 10 |
| Basel | 8 |
| Athens | 10 |
| Thessaloniki | 8 |
| Milan | 8 |
| Madrid | 10 |
| Copenhagen - Roskilde | 8 |
| Ljubljana | 6 |

### 3.4.5 Clusters interpretation methodology

#### Clusters characterization

The cluster characteristization is mainly based on the weather parameters statistics (Average, SD, Min, Max) as well as wind patterns.

#### Clusters trends

Examine changes in 5-year period cluster frequencies of occurrence over the whole range of 50-years to identify relevant climatic trends.

#### Clusters and local heat waves

In Guerreiro et al. (2018) heat waves were defined as three consecutive days, where both the maximum and the minimum daily temperature exceed their respective 95th percentile from the historical summer data in 1951-2000 for months from May to September. Following this idea, in the present study, heat waves were defined as three consecutive days, where both the maximum and the minimum daily temperature exceed their respective 95th percentile from the period 2001-2050, using the set of the CORDEX summer data produced by INERIS-WRF331F model. The reasons for selecting this particular model were: (a) It provides one of the most complete model datasets in CORDEX database and (b) the simulation data provided are expected to be more coherent with the present detailed atmospheric modeling data that are produced by using the WRF-CHEM model belonging to the same family. Here, the heat wave days frequency occurrence per 5year period is estimated. Furthermore, heat waves occurrence vs clusters were examined to identify the specific clusters associated with heat waves occurrence.

#### Clusters and Air Quality

Collect existing air quality data ($NO_2$, $O_3$, $PM_{10}$) and associate them with the selected clusters. Identify the clusters with elevated concentration for each pollutant.

#### Representative Days

The next step is to identify the representative day(s) per cluster per the 5-year time period by selecting the day which has the closest distance from the cluster's centroid (Sfetsos et al., 2005) In order to perform air quality simulations and reveal hourly air quality levels for the three clusters that indicate elevated concentrations for $NO_2$, $O_3$ and $PM_{10}$ respectively representatives days were selected. Atmospheric modeling simulations, that include air concentration predictions on the respective representative days, were performed in the following 5year periods: 2016-2020, 2021-2025, 2031-2035)

## 3.5 The Atmospheric Modeling

### 3.5.1. The Models

Details concerning atmospheric modeling are given in ICARUS WP3 Milestone M3.2

WRF-Chem is the Weather Research and Forecasting (WRF) model coupled with Chemistry. The model simulates the emission, transport, mixing, and chemical transformation of trace gases and aerosols simultaneously with the meteorology. The model is used for investigation of regional-scale air quality, field program analysis, and cloud-scale interactions between clouds and chemistry. The WRF-Chem (version 3.6.1, August 2014) has been used for the present studies. The model overview with the available pre-processors is shown in Figure 3.3.


*Figure 3.3: The WRF-Chem modeling system overview*

The WRF-Chem model supports horizontal nesting (Figure 3.4) that allows resolution to be focused over a region of interest by introducing an additional grid (or grids) into the simulation. In the 3.6.1 version, only horizontal refinement is available: there is no vertical nesting option.

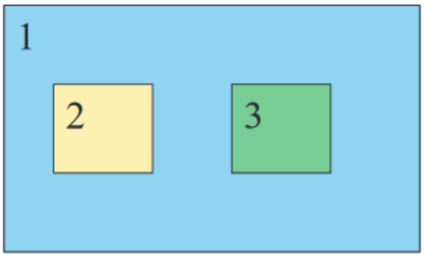


*Figure 3.4: Nest example*

### 3.5.2 The Grids

The option of two level multiple horizontal nesting has been adopted. An outer grid with dimensions 12x12km has been implemented over Europe as shown in Figure 3.5. The Grid Projection has been defined as Lambert conformal Conic with lat0 = 35° lat1=65° standard lat=52° standard lon= 10° consisting of 303 x 303 cells. On the urban scale nine (9) nests with dimensions 2x2km have been used consisting of 42x42 grid cells each. As a notice WRF-Chem assumes a spherical model of Earth with 6370000m radius.

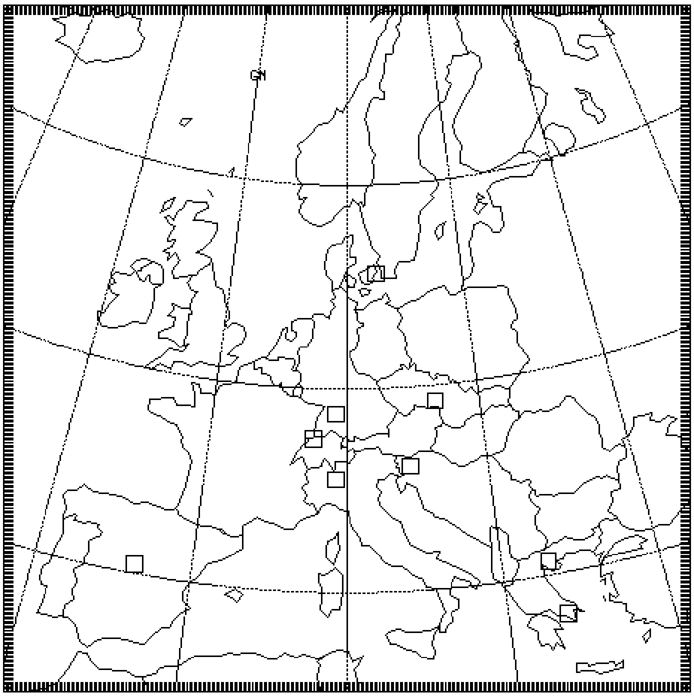

*Figure 3.5: The Grids. The vertical 27 - level grid extends from the surface to about 20 km*

## 3.6 The Emission Inventories

For the present analysis the following emission inventory data have been utilized:

EDGAR HTAP V2

It includes annual data for the year 2010 with 0.1x0.1 deg spatial resolution over Europe. It covers the pollutants $NO_X$, $NH_3$, $PM_{10}$, $PM_{2.5}$, $SO_2$, CO and NMVOC. HTAP V2 uses nationally reported emissions combined with regional scientific inventories in the format of sector-specific gridmaps. The gridmaps are complemented with EDGARv4.3 data for those regions where data are absent. The global gridmaps are a joint effort from US-EPA, the MICS-Asia group, EMEP/TNO, the REAS and the EDGAR group to serve in the first place the scientific community for hemispheric transport of air pollution. The static version is available on this EDGAR website, but also the GEIA data portal and the ECCAD server.

The data were downloaded from ftp://aftp.fsl.noaa.gov/divisions/taq/global_emissions/

according to WRF-Chem manual guidance.

More details can be found in http://edgar.jrc.ec.europa.eu/htap_v2/

The University of Stuttgart (USTUTT) High Resolution Emission Inventory Data

It includes annual data for years 2015, 2020, 2030, with 1x1km spatial resolution over Europe. This work has been performed under ICARUS WP2 Activities

It covers the pollutants $NO_X$, $NH_3$, $PM_{10}$, $PM_{2.5}$, $SO_2$, and NMVOC in five (5) sectors (agriculture, energy, industry, residential, transport). It consists of following Emission Inventories.

- One top down emission inventory covering all EU28 countries. The projection of the data is on the European Grid based on ETRS89 Lambert Azimuthal Equal Area coordinate reference system.
- Nine (9) bottom up emission inventories covering the nine (9) abovementioned ICARUS cities. Grid cell geographic coordinates are provided for each grid cell. The cities covered are Stuttgart, Basel and Brno. Grid cell geographic coordinate (latitude, longitude) are provided for each grid cell.

More details can be found in Deliverables D2.1 and D2.2.

## 3.7 Benzo(a)pyrene in PM

Benzo(a)pyrene (BaP) is the most widely investigated PAH as a marker for the carcinogenic risk (IARC, 2012) of PAHs in ambient air. The Air Quality European directive (EU, 2004) sets a target value for ambient air concentration of BaP in order to avoid, prevent and reduce harmful effects of PAHs on human health and the environment. Around 90% or more of BaP in ambient air is adsorbed onto aerosols and around 10% or less is in the gas phase (Guerreiro et al., 2016). The target value for BaP (measured in $PM_{10}$) for the protection of human health is set at 1 ng/m$^3$ (EU, 2004) as an annual mean. The World Health Organization (WHO) has not recommended a guideline value for BaP. The WHO reference level of 0.12 ng/m$^3$ was estimated assuming WHO unit risk (WHO, 2010) for lung cancer for PAH mixtures and an acceptable risk of additional lifetime cancer risk of approximately 1 in 100 000 (ETC/ACM, 2011).

BaP is a PAH mainly found in fine PM. The Air Quality Directive (EU, 2004) prescribes that BaP concentration measurements should be made in the $PM_{10}$ fraction. Despite this requirement, available data in any PM fraction were used in the current analysis. The justification is that most of the BaP is present in $PM_{2.5}$ and not in the coarser fraction of $PM_{10}$, and the gaseous fraction of the total BaP is quite small (EEA, 2016).

The BaP/PM ratios were produced from the available concentrations reported in various European peer-reviewed studies, as shown in Table 3.3. As it can be seen from the studies that report BaP in both $PM_{2.5}$ and $PM_{10}$, more than 93% of BaP (93-100% range) is present in the $PM_{2.5}$ fraction. Due to the above, cumulative distribution function (CDF) of the BaP/PM2.5 ratios was plotted in a diagram as shown in Figure 3.6. Probability distribution fitting was applied. Between gamma and normal distribution, the gamma distribution was found to best fit the data. The above analysis led to the following statistical data for the BaP/PM2.5 ratios:

Mean value: 8.2E-05

25% percentile: 2.3E-05

75% percentile: 11E-05

*Table 3.3: BaP and PM concentrations and BaP/PM ratios from various European studies*

| **Location** | **Sampling period** | **PM2.5 (μg/m³)** | **PM10 (μg/m³)** | **BaP in PM2.5 (ng/m³)** | **BaP in PM10 (ng/m³)** | **BaP/PM2.5** | **BaP/PM10** | **Reference** |
|---|---|---|---|---|---|---|---|---|
| Zabrze (Poland) urban background | oct-dec 2007 | 41.31 | 46.29 | 19.19 | 19.32 | 4.65E-04 | 4.17E-04 | W.R. Kozlowska et al., 2013 |
| Duisburg (Germany) urban background | autumn | 19 | 26 | 1.05 | 1.1 | 5.53E-05 | 4.23E-05 | K. Saarnio et al., 2008 |
| Prague (Czech Republic) urban background | winter | 30 | 36 | 3.03 | 3.15 | 1.01E-04 | 8.75E-05 | |
| Amsterdam (The Netherlands) urban background | winter | 27 | 36 | 0.33 | 0.35 | 1.22E-05 | 9.72E-06 | |
| Helsinki (Finland) urban backgroundsping | sping | 11 | 24 | 0.14 | 0.15 | 1.27E-05 | 6.25E-06 | |
| Barcelona (Spain) urban background | spring | 19 | 42 | 0.08 | 0.08 | 4.21E-06 | 1.90E-06 | |
| Athens (Greece) urban background | summer | 26 | 55 | 0.05 | 0.05 | 1.92E-06 | 9.09E-07 | |
| Taranto (Italy) Tamburi station crowded urban | winter | | 126 | | 5.63 | | 4.47E-05 | P. Di Filippo et al., 2010 |
| Taranto (Italy) Tamburi station crowded urban | summer | | 61 | | 0.83 | | 1.36E-05 | |
| Taranto (Italy) Statte station urban | winter | | 40 | | 0.76 | | 1.90E-05 | |
| Taranto (Italy) Statte station urban | summer | | 48 | | 0.29 | | 6.04E-06 | |
| Taranto (Italy) Palagiano station rural/background area | winter | | 68 | | 0.34 | | 5.00E-06 | |
| Taranto (Italy) Palagiano station rural/background area | summer | | 42 | | 0.13 | | 3.10E-06 | |

| | | | | | | | | |
|---|---|---|---|---|---|---|---|---|
| Zelzate (Belgium) industrial | sep 2006-sep 2007 | | 34.2 | | 0.66 | | 1.93E-05 | J. Vercauteren et al., 2011 |
| Borgerhout (Belgium) urban background | sep 2006-sep 2007 | | 33.7 | | 0.85 | | 2.52E-05 | |
| Aarschot (Belgium) rural background | sep 2006-sep 2007 | | 27.6 | | 0.61 | | 2.21E-05 | |
| Detached-house area 1 DH1 Vartiokylä (Finland) | 2009–2015 | 7.5 | | 0.6 | | 8.00E-05 | | H. Hellen et al., 2017 |
| Detached-house area 3 DH3 Päiväkumpu (Finland) | 2011 | 10.4 | | 1.2 | | 1.15E-04 | | |
| Detached-house area 4 DH4 Kattilalaakso (Finland) | 2012 | 8.2 | | 0.6 | | 7.32E-05 | | |
| Detached-house area 5 DH5 Kauniainen (Finland) | 2013 | 7.1 | | 0.4 | | 5.63E-05 | | |
| Detached-house area 6 DH6 Tapanila (Finland) | 2013 | 8.8 | | 1 | | 1.14E-04 | | |
| Detached-house area 7 DH7 Ruskeasanta (Finland) | 2014 | 10.8 | | 1 | | 9.26E-05 | | |
| Detached-house area 8 DH8 Lintuvaara (Finland) | 2015 | 7.1 | | 0.9 | | 1.27E-04 | | |
| Street canyon 2 SC2 Töölöntulli (Finland) | 2010 | 13 | | 0.3 | | 2.31E-05 | | |
| Street canyon 3 SC3 Mäkelänkatu (Finland) | 2015 | 8 | | 0.2 | | 2.50E-05 | | |
| Urban background UB Kallio (Finland) | 2007–2015 | 7.8 | | 0.3 | | 3.85E-05 | | |
| Rural background 1 RB1 Virolahti (Finland) | 2007–2015 | 6.1 | | 0.2 | | 3.28E-05 | | |
| Remote background RE Pallas (Finland) | 2009–2015 | 3.7 | | 0.03 | | 8.11E-06 | | |

| | | | | | | | | |
|---|---|---|---|---|---|---|---|---|
| Kaunas (Lithuania) location 1, urban traffic | jan-feb 2009 | 34.5 | | 6.2 | | 1.80E-04 | | L. Kliucininkas et al., 2011 |
| Kaunas (Lithuania) location 2, urban traffic | jan-feb 2009 | 36.7 | | 3.2 | | 8.72E-05 | | |
| Virolahti (Finland) regional background | winter 2006 | 6.3 | 8.2 | 0.69 | 0.73 | 1.10E-04 | | U. Makkonen et al., 2010 |

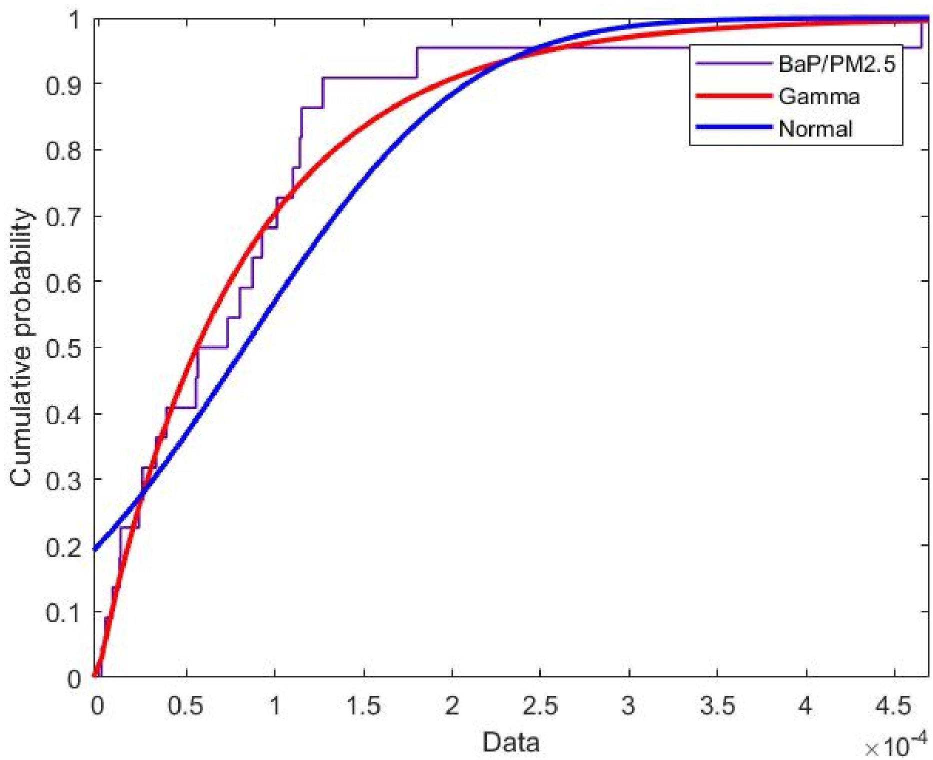


*Figure 3. 6: Cumulative distribution function of the BaP/PM2.5 ratios and distribution fitting*

## 3.8 The Emission Trends Influence

As it has been pointed out above, the air quality levels at a certain location, are affected not only from the weather patterns but also from the relevant emissions and their associated sources. The emission inventories are changing with respect to time reflecting the evolution of new technologies, the implementation of new European and national relevant policies, changes of life style etc. In the ICARUS Project, the USTUTT emission inventories derived for the years 2015,2020 and 2030 reflect such changes.

The emission inventory changes are expected to affect the air pollutant concentrations levels. In order to illustrate such an effect, the representative days for the clusters with elevated air pollutants concentrations in the period 2031-2035 have been simulated with the three available emission inventories: 2015,2020 and 2030. In this case, the air concentration differences will depend only on emission inventory differences.

## 3.9 Green House Gases (GHGs)

### 3.9.1. The Model

WRF-Chem is used for GHG Modeling. The domain has the same characteristics with the Europe domain used in the Air Quality Modeling. The grid used has dimensions of 304x304 cells with 12x12 km spacing covering Europe area.

The model was initiated with meteorological data from NCAR CESM Global Bias-Corrected CMIP5 Output to Support WRF/MPAS Research dataset using the RCP4.5 Future Scenario. The data have 6-hour temporal frequency and temporal range from 01-01-1951 to 31-12-2100.

Variables included are:

| | | | |
|---|---|---|---|
| Air Temperature | Boundary Layer Winds | Geopotential Height | Humidity |
| Sea Ice Concentration | Sea Level Pressure | Sea Surface Temperature | Skin Temperature |
| Snow Water Equivalent | Soil Moisture/Water Content | Soil Temperature | Surface Pressure |
| Surface Winds | Upper Air Temperature | Upper Level Winds | |

$CO_2$ and $CH_4$ anthropogenic emissions, provided by USTUTT, for the years 2015,2020 and 2030 are used as input data. WRF-Chem simulated $CO_2$ and $CH_4$ as gas tracers. The simulation duration is 48 hours including 24 hours spin up time.

Results are extracted from the grid cell (12x12 km) covering:

a. the center of each Icarus city region, and

b. the three remote GHG monitoring location given in Plateu Rosa (IT), Jungfraujoch (CH) and Hohenpeissenberg (D) in which hourly data for $CO_2$ and $CH_4$ exist (https://ds.data.jma.go.jp/gmd/wdcgg/)

### 3.9.2. The Approach

It is well known that the concentrations of the major greenhouse gases during the industrial era have been increased directly or indirectly due to human activities. As a result, their background concentrations in atmosphere have been already increased considerably. The adopted scenario to study the climatic change in the future have shown such this trend is likely to continue. For example, Figures 3.7 (a) and (b) show how the background concentrations over Europe for the main greenhouse gases $CO_2$ and $CH_4$ evolve in the period 2001-2050 under climatic scenario RCP4.5. (http://www.iiasa.ac.at/web-apps/tnt/RcpDb/dsd?Action=htmlpage&page=about)

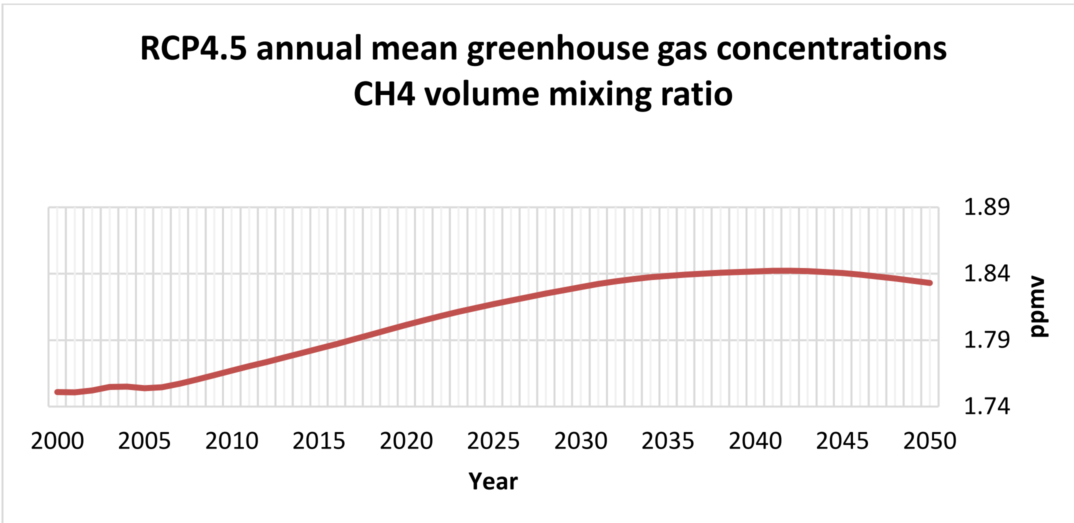


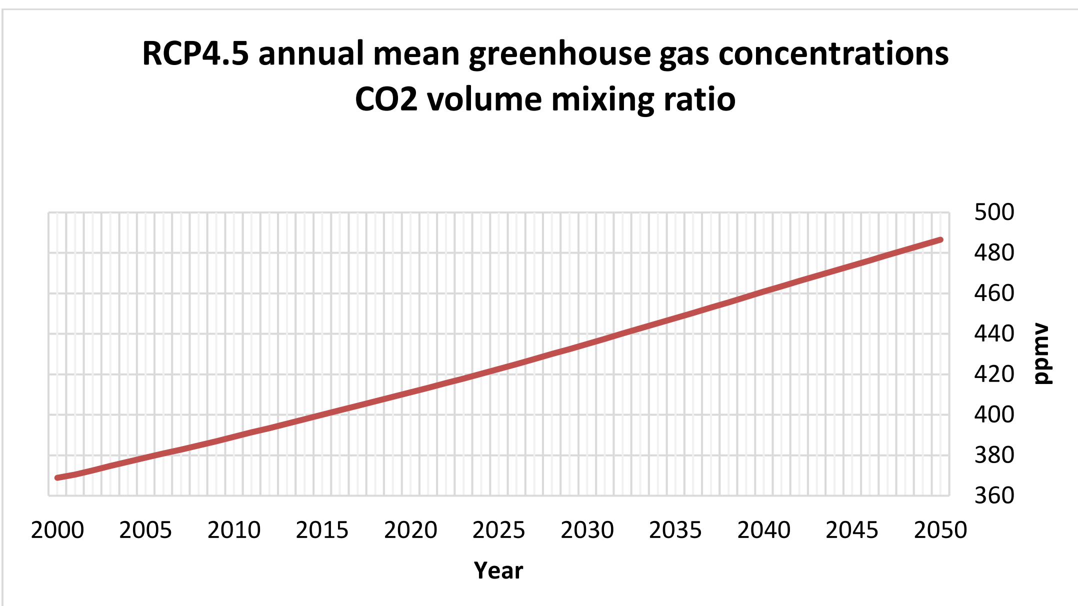


*Figure 3.7: RCP4.5 Climatic scenario: the $CO_2$ and $CH_4$ concentrations*

The GHG concentrations with respect to space and time are expected to deviate from the above-mentioned background concentrations mainly due to current anthropogenic emissions as well as meteorological local variability. The next question is how such deviations can be combined with the background concentrations to provide the real GHG concentration levels on local and hourly scale.

A series of daily simulations estimating the $CO_2$ and $CH_4$ concentration difference variability at the abovementioned selected sites have been performed and the results are shown in Figures 3.8 (a) and (b). The Plateau Rosa Station seems to represent reliably enough the background concentrations indicating no significant influence from the current anthropogenic emission rates.

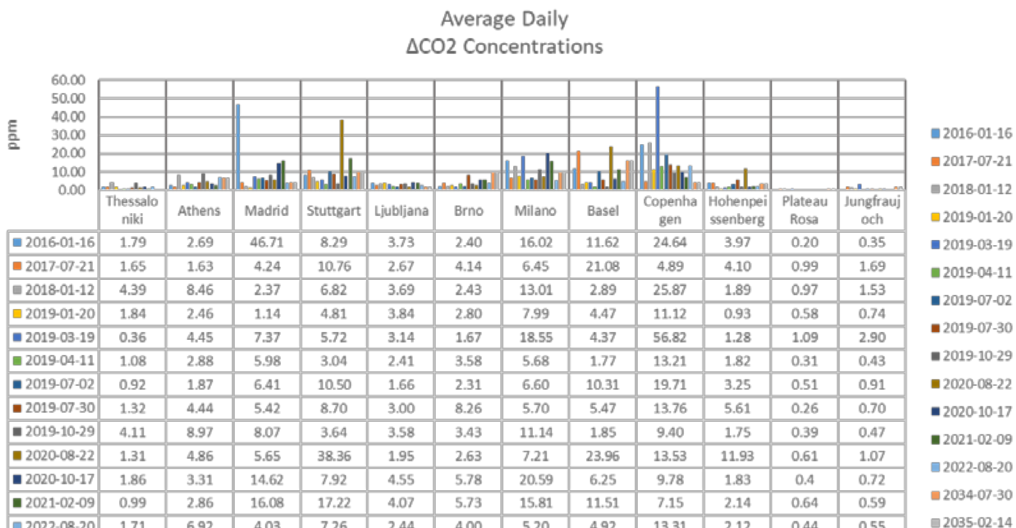


| | Thessaloniki | Athens | Madrid | Stuttgart | Ljubljana | Brno | Milano | Basel | Copenhagen | Hohenpeissenberg | Plateau Rosa | Jungfraujoch |
|---|---|---|---|---|---|---|---|---|---|---|---|---|
| 2016-01-16 | 1.79 | 2.69 | 46.71 | 8.29 | 3.73 | 2.40 | 16.02 | 11.62 | 24.64 | 3.97 | 0.20 | 0.35 |
| 2017-07-21 | 1.65 | 1.63 | 4.24 | 10.76 | 2.67 | 4.14 | 6.45 | 21.08 | 4.89 | 4.10 | 0.99 | 1.69 |
| 2018-01-12 | 4.39 | 8.46 | 2.37 | 6.82 | 3.69 | 2.43 | 13.01 | 2.89 | 25.87 | 1.89 | 0.97 | 1.53 |
| 2019-01-20 | 1.84 | 2.46 | 1.14 | 4.81 | 3.84 | 2.80 | 7.99 | 4.47 | 11.12 | 0.93 | 0.58 | 0.74 |
| 2019-03-19 | 0.36 | 4.45 | 7.37 | 5.72 | 3.14 | 1.67 | 18.55 | 4.37 | 56.82 | 1.28 | 1.09 | 2.90 |
| 2019-04-11 | 1.08 | 2.88 | 5.98 | 3.04 | 2.41 | 3.58 | 5.68 | 1.77 | 13.21 | 1.82 | 0.31 | 0.43 |
| 2019-07-02 | 0.92 | 1.87 | 6.41 | 10.50 | 1.66 | 2.31 | 6.60 | 10.31 | 19.71 | 3.25 | 0.51 | 0.91 |
| 2019-07-30 | 1.32 | 4.44 | 5.42 | 8.70 | 3.00 | 8.26 | 5.70 | 5.47 | 13.76 | 5.61 | 0.26 | 0.70 |
| 2019-10-29 | 4.11 | 8.97 | 8.07 | 3.64 | 3.58 | 3.43 | 11.14 | 1.85 | 9.40 | 1.75 | 0.39 | 0.47 |
| 2020-08-22 | 1.31 | 4.86 | 5.65 | 38.36 | 1.95 | 2.63 | 7.21 | 23.96 | 13.53 | 11.93 | 0.61 | 1.07 |
| 2020-10-17 | 1.86 | 3.31 | 14.62 | 7.92 | 4.55 | 5.78 | 20.59 | 6.25 | 9.78 | 1.83 | 0.4 | 0.72 |
| 2021-02-09 | 0.99 | 2.86 | 16.08 | 17.22 | 4.07 | 5.73 | 15.81 | 11.51 | 7.15 | 2.14 | 0.64 | 0.59 |
| 2022-08-20 | 1.71 | 6.92 | 4.03 | 7.26 | 2.44 | 4.00 | 5.20 | 4.92 | 13.31 | 2.12 | 0.44 | 0.55 |
| 2034-07-30 | 0.27 | 6.67 | 4.47 | 9.96 | 1.75 | 9.56 | 9.55 | 15.86 | 4.45 | 3.72 | 1.08 | 1.9 |
| 2035-02-14 | 0.27 | 6.67 | 4.47 | 9.96 | 1.75 | 9.56 | 9.55 | 15.86 | 4.45 | 3.72 | 1.08 | 1.9 |

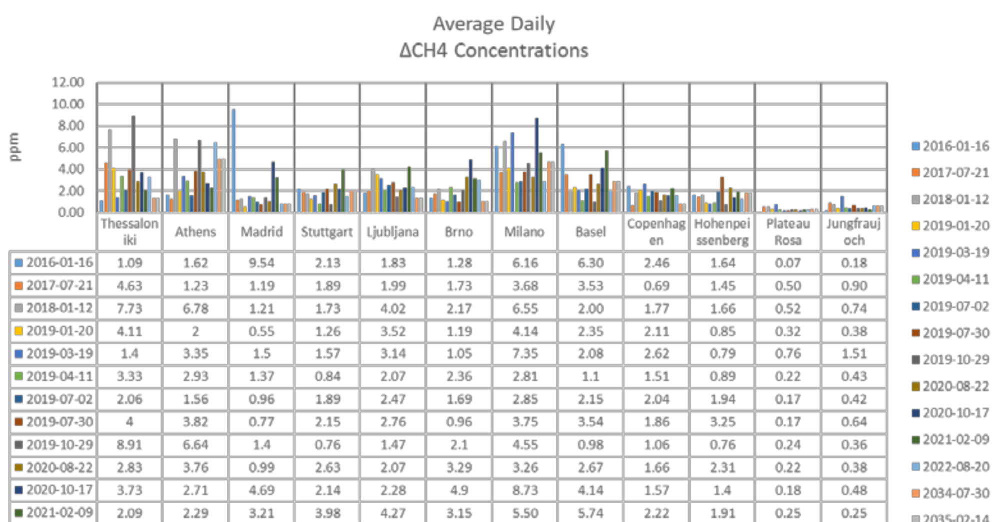


| | Thessaloniki | Athens | Madrid | Stuttgart | Ljubljana | Brno | Milano | Basel | Copenhagen | Hohenpeissenberg | Plateau Rosa | Jungfraujoch |
|---|---|---|---|---|---|---|---|---|---|---|---|---|
| 2016-01-16 | 1.09 | 1.62 | 9.54 | 2.13 | 1.83 | 1.28 | 6.16 | 6.30 | 2.46 | 1.64 | 0.07 | 0.18 |
| 2017-07-21 | 4.63 | 1.23 | 1.19 | 1.89 | 1.99 | 1.73 | 3.68 | 3.53 | 0.69 | 1.45 | 0.50 | 0.90 |
| 2018-01-12 | 7.73 | 6.78 | 1.21 | 1.73 | 4.02 | 2.17 | 6.55 | 2.00 | 1.77 | 1.66 | 0.52 | 0.74 |
| 2019-01-20 | 4.11 | 2 | 0.55 | 1.26 | 3.52 | 1.19 | 4.14 | 2.35 | 2.11 | 0.85 | 0.32 | 0.38 |
| 2019-03-19 | 1.4 | 3.35 | 1.5 | 1.57 | 3.14 | 1.05 | 7.35 | 2.08 | 2.62 | 0.79 | 0.76 | 1.51 |
| 2019-04-11 | 3.33 | 2.93 | 1.37 | 0.84 | 2.07 | 2.36 | 2.81 | 1.1 | 1.51 | 0.89 | 0.22 | 0.43 |
| 2019-07-02 | 2.06 | 1.56 | 0.96 | 1.89 | 2.47 | 1.69 | 2.85 | 2.15 | 2.04 | 1.94 | 0.17 | 0.42 |
| 2019-07-30 | 4 | 3.82 | 0.77 | 2.15 | 2.76 | 0.96 | 3.75 | 3.54 | 1.86 | 3.25 | 0.17 | 0.64 |
| 2019-10-29 | 8.91 | 6.64 | 1.4 | 0.76 | 1.47 | 2.1 | 4.55 | 0.98 | 1.06 | 0.76 | 0.24 | 0.36 |
| 2020-08-22 | 2.83 | 3.76 | 0.99 | 2.63 | 2.07 | 3.29 | 3.26 | 2.67 | 1.66 | 2.31 | 0.22 | 0.38 |
| 2020-10-17 | 3.73 | 2.71 | 4.69 | 2.14 | 2.28 | 4.9 | 8.73 | 4.14 | 1.57 | 1.4 | 0.18 | 0.48 |
| 2021-02-09 | 2.09 | 2.29 | 3.21 | 3.98 | 4.27 | 3.15 | 5.50 | 5.74 | 2.22 | 1.91 | 0.25 | 0.25 |
| 2022-08-20 | 3.30 | 6.49 | 0.81 | 1.52 | 2.38 | 2.99 | 2.85 | 2.03 | 1.60 | 1.26 | 0.25 | 0.58 |
| 2034-07-30 | 1.31 | 4.98 | 0.8 | 2.04 | 1.29 | 1.03 | 4.68 | 2.82 | 0.8 | 1.79 | 0.33 | 0.61 |
| 2035-02-14 | 1.31 | 4.98 | 0.8 | 2.04 | 1.29 | 1.03 | 4.68 | 2.82 | 0.8 | 1.79 | 0.33 | 0.61 |

*Figure 3.8: The current anthropogenic emissions contributions to $CO_2$ and $CH_4$ concentrations*

Such a result could help to investigate to what degree there is a need (a) for correction of background annual concentrations values based on the Plataeu Rosa historical data and (b) for adding temporal profile in terms of days/hours in the annual background concentrations when estimating local real concentrations. This can be done by looking at the Plateau Rosa observation data from the historical period.

Figures 3.9 (a) and (b) show the comparisons of $CO_2$ and $CH_4$ annual observation data during the period 1993-2017 with the RCP4.5 climatic scenario data.

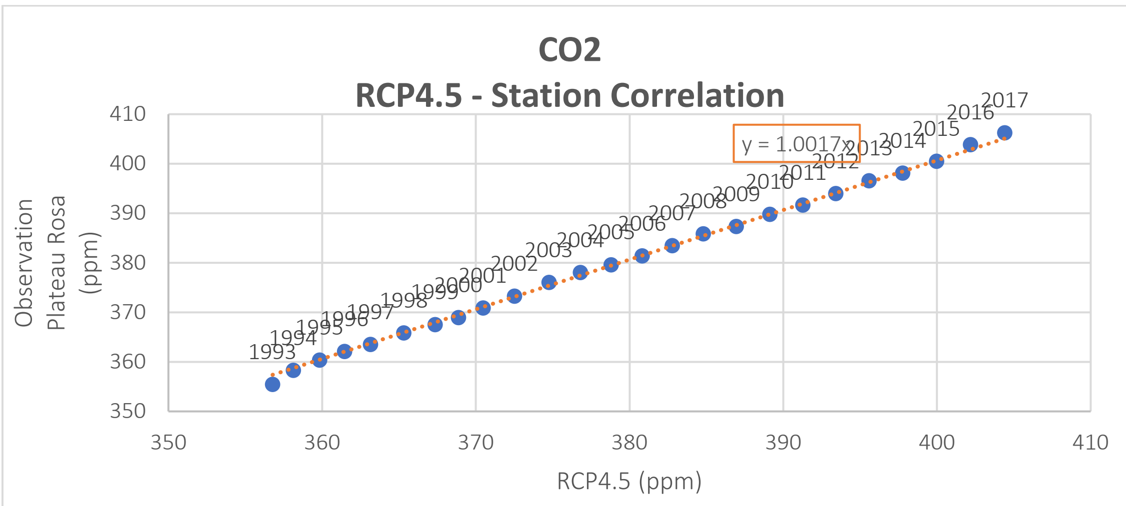


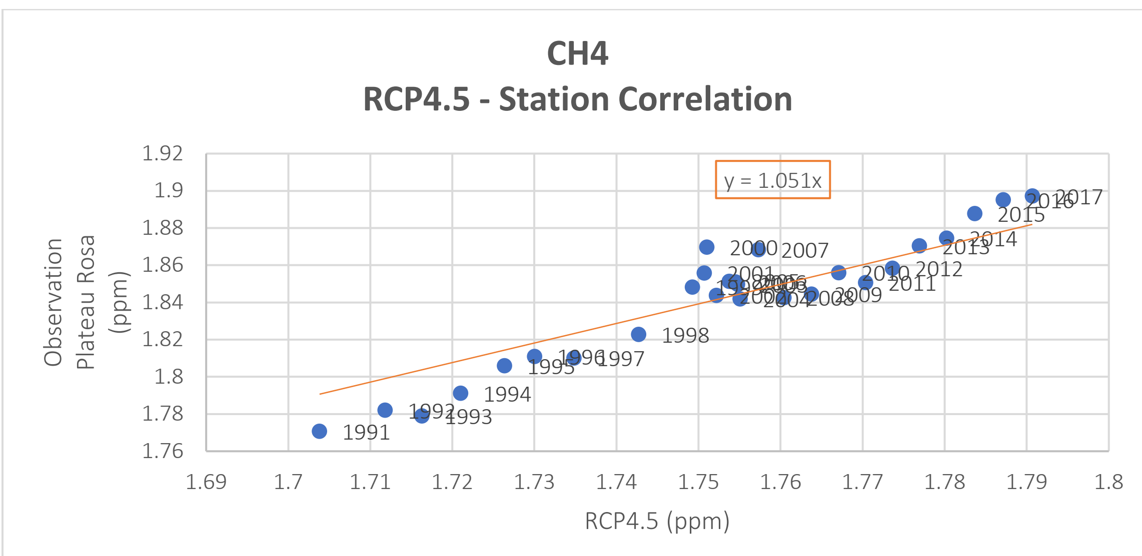


*Figure 3.9: The Plateau Rosa Station: $CO_2$ and $CH_4$ yearly concentrations . The observed vs the RCP4.5 climatic scenario data for the historical period (1993-2017)*

For $CO_2$ concentrations there is an almost perfect correlation. In the case of $CH_4$ it seems to exist a 5% underestimation which for the purposes of this study is considered rather insignificant.

Based on 2017 hourly observation data in Plateau Rosa station, the daily and diurnal profiles of $CO_2$ and $CH_4$ concentrations have been derived. The results are shown in Figures 3.10(a), (b) and Figures 3.11 (a), (b) respectively

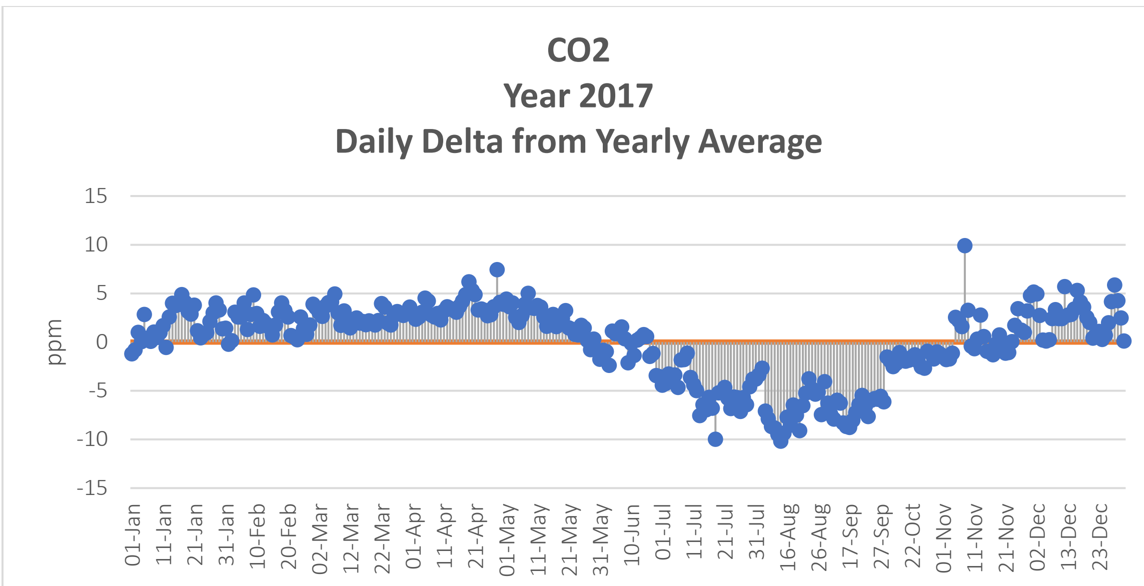


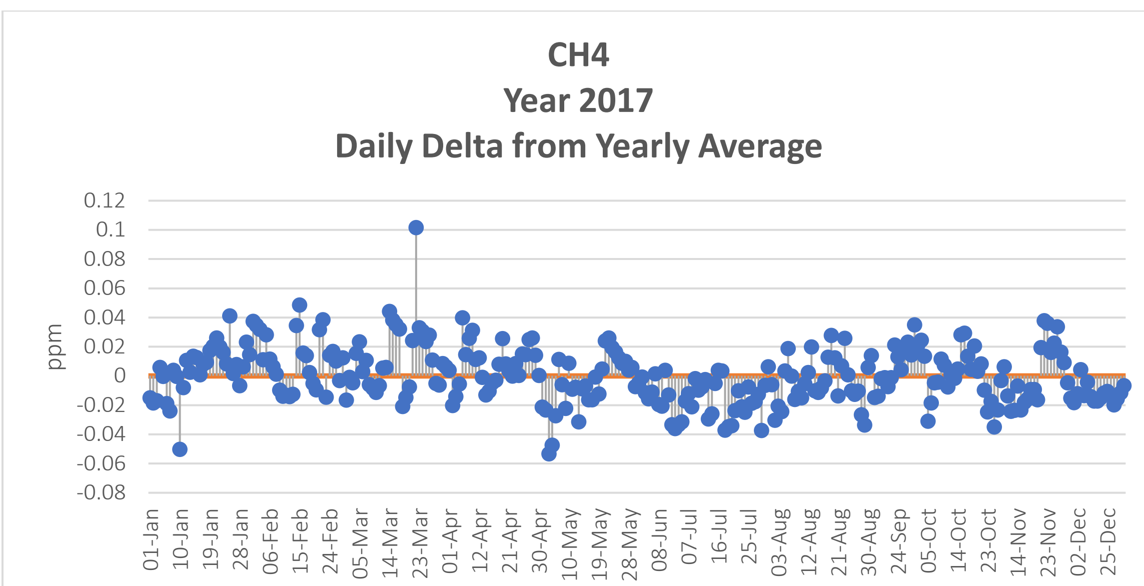


*Figure 3.10: The Plateau Rosa Station: The Daily Concentration variation profile for the year 2017*

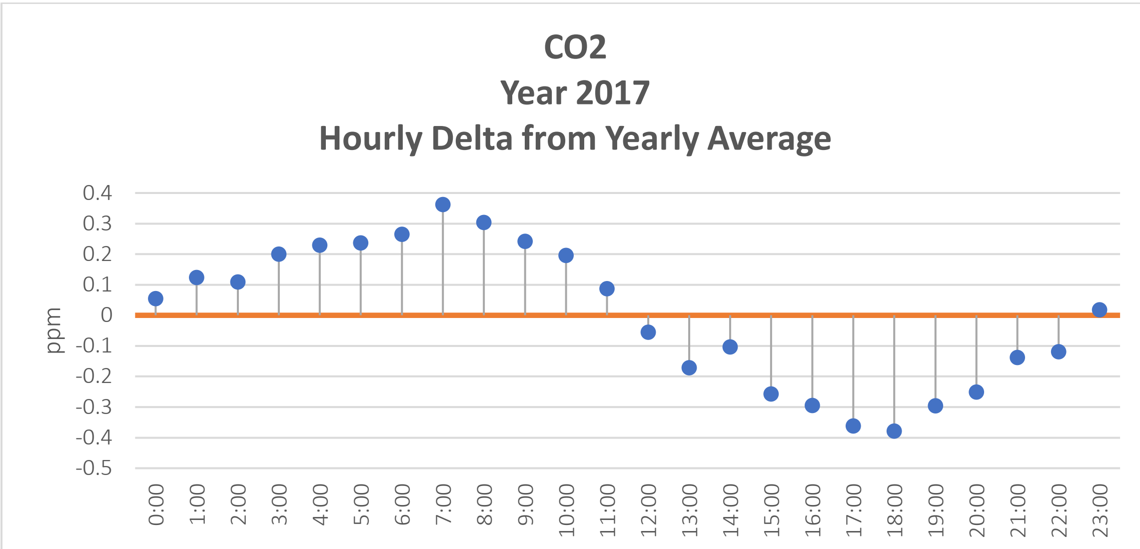


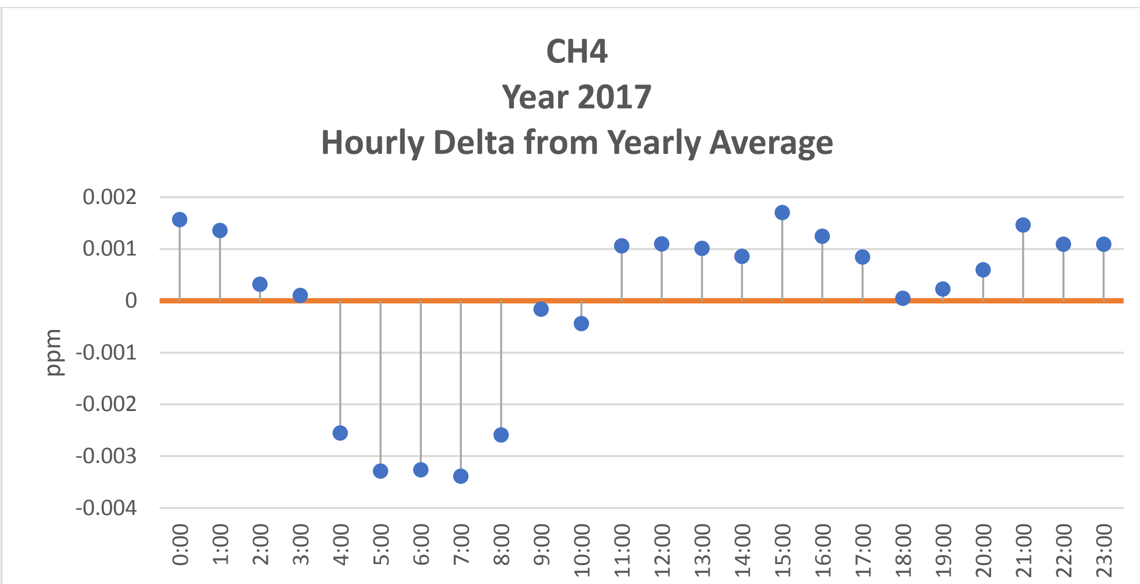


*Figure 3.11: The Plateau Rosa Station: Diurnal Concentration variation profile for the year 2017*

The variations observed usually do not exceed the 2.5% of the respective mean values and therefore are considered insignificant.

Thus, the annual background values given under RCP4.5 scenario and shown in Figures 3.7 (a) and (b) are taken as hourly background values in the present modeling for $CO_2$ and $CH_4$ local concentrations.

# 4. Results and Discussion

## 4.1 Air Quality data

We searched for historical air quality data for the period 2001-2015. The search was done through HEALS EDMS Database (https://heals.uowm.gr/). The original source of the derived data was EEA Database (https://www.eea.europa.eu/data-and-maps/data/airbase-the-european-air-quality-database-7). The selection of the station was done on the ground that is has the most complete data ($NO_2$, $O_3$, $PM_{10}$). If more than one station had available data for the 2001-2015 period, the averaged values for the area were calculated. In Table 4.1 are presented the location of the selected stations per city area.

*Table 4.1: Locations of the meteorological stations per city*

| City area | Meteorological station | Longitude | Latitude |
|---|---|---|---|
| Stuttgart | DEBW011 | 9.172506 | 48.825575 |
| Brno | CZ0BBND | 16.597271 | 49.205463 |
| Basel | CH0008A | 7.583270 | 47.541084 |
| | CH0029A | 7.594703 | 47.567019 |
| | CH0017A | 7.582075 | 47.565911 |
| Athens | GR0039A | 23.819418 | 37.995106 |
| | GR0030A | 23.647511 | 37.943287 |
| | GR0002A | 23.726843 | 37.978207 |
| | GR0035A | 23.776886 | 38.069633 |
| | GR0022A | 23.787357 | 38.030838 |
| Thessaloniki | GR0018A | 22.945288 | 40.633774 |
| | GR0019A | 22.959303 | 40.578917 |
| | GR0020A | 22.893438 | 40.673550 |
| | GR0046A | 22.802366 | 40.657845 |
| | GR0047A | 23.031681 | 40.588931 |

| | | | |
|---|---|---|---|
| Milan | IT0705A | 9.195833 | 45.462780 |
| | IT1017A | 9.247778 | 45.498890 |
| Madrid | ES1532A | -3.651389 | 40.388056 |
| | ES1426A | -3.645278 | 40.408056 |
| | ES0126A | -3.731944 | 40.394722 |
| Copenhagen - Roskilde | DK0034A | 12.571114 | 55.669167 |
| | DK0045A | 12.561400 | 55.700279 |
| | DK0030A | 12.553336 | 55.698334 |
| Ljubljana | SI0003A | 14.517222 | 46.065834 |

## 4.2 Stuttgart

### 4.2.1 PCA results

The PCA analysis applied to the Stuttgart data has led to the following results.

Three (3) principal components have been identified as factors for the cluster analysis. Principal Components (PC) explaining 70.96% of the total variance in the initial data. Table 4.2.1 shows the factors loadings after the varimax rotation and the physical interpretation of each PCs.

Factor 1 explains 32.70% of the total variance and contains the 2 temperature variables, mean, daily temperature range and the down ward short-wave radiation.

Factor 2 explains 22.41% of the total variance and contains the atmospheric boundary layer thickness, the U wind component and a negative sign of surface pressure.

Factor 3 explains 15.84% of the total variance and contains V wind component and a negative sign of Relative Humidity and precipitation.

*Table 4.2.1: The Principal Components results*

| Meteorological parameter | Principal Components | | |
|---|---|---|---|
| | 1 | 2 | 3 |
| Downward short-wave surface radiation | .886 | | |
| Temperature | .820 | | |
| Temperature Range | .763 | | |
| Atmospheric boundary layer thickness | | .818 | |
| Surface pressure | | -.700 | |
| U wind | | .641 | |
| RH | | | -.757 |
| Precipitation | | | -.717 |
| V wind | | | .694 |

### 4.2.2 Clustering results

#### Cluster description and trends

As explained in 3.4.4 the selected clusters of the city of Stuttgart are 10. In Figure 4.2.1 are shown the number of days per cluster, where clusters 4,5 and 9 have the most days and cluster 3, 7 and 8 have the less, especially the last one. The monthly distribution per cluster is presented in Table 4.2.2 and in Figure 4.2.2. By dividing the year in two periods, cold and warm, clusters 1,3,7,9 and 10 could be categorized in cold period and on the other hand clusters 2,4,5 and 8 in warm period. Cluster 6 seems to have days which spread during the whole year.


*Figure 4.2.1: Number of Days per cluster*

*Table 4.2.2: Monthly distribution per cluster*

| | | Month | | | | | | | | | | | |
|---|---|---|---|---|---|---|---|---|---|---|---|---|---|
| | | Jan | Feb | Mar | Apr | May | Jun | Jul | Aug | Sep | Oct | Nov | Dec |
| cluster10 | 1 | 411 | 336 | 222 | 50 | 9 | 2 | 0 | 0 | 53 | 264 | 318 | 341 |
| | 2 | 1 | 10 | 103 | 423 | 482 | 290 | 82 | 199 | 307 | 107 | 15 | 1 |
| | 3 | 242 | 174 | 155 | 143 | 56 | 17 | 4 | 16 | 73 | 152 | 221 | 235 |
| | 4 | 0 | 0 | 14 | 188 | 288 | 380 | 640 | 608 | 291 | 16 | 1 | 0 |
| | 5 | 0 | 0 | 7 | 53 | 305 | 509 | 570 | 513 | 179 | 4 | 0 | 0 |
| | 6 | 124 | 147 | 224 | 222 | 245 | 121 | 61 | 80 | 223 | 231 | 113 | 129 |
| | 7 | 194 | 195 | 181 | 125 | 42 | 12 | 2 | 9 | 41 | 145 | 200 | 268 |
| | 8 | 2 | 14 | 19 | 28 | 82 | 159 | 191 | 114 | 39 | 27 | 10 | 8 |
| | 9 | 460 | 366 | 249 | 62 | 12 | 5 | 0 | 2 | 79 | 259 | 416 | 472 |
| | 10 | 116 | 170 | 376 | 206 | 29 | 5 | 0 | 9 | 215 | 345 | 206 | 96 |

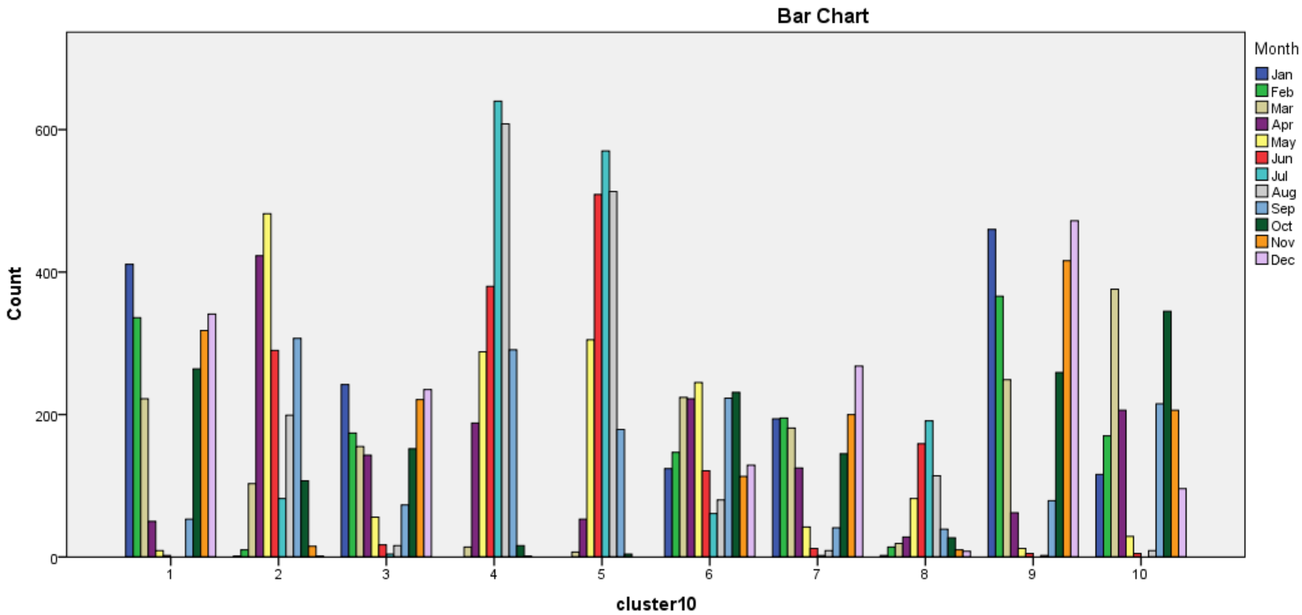


*Figure 4.2.2: Visualized bar chart of monthly distribution per cluster*

A trend analysis of the 5-year frequency of each cluster (Figure 4.2.3). There is an evidence that in clusters 5, 7 and 9 there is a linear increase in frequency occurrence through the ten 5-year periods. On the other hand, clusters 6 and 10 show a linear decrease in frequency occurrence. In the rest clusters no clear trends could be pointed out.

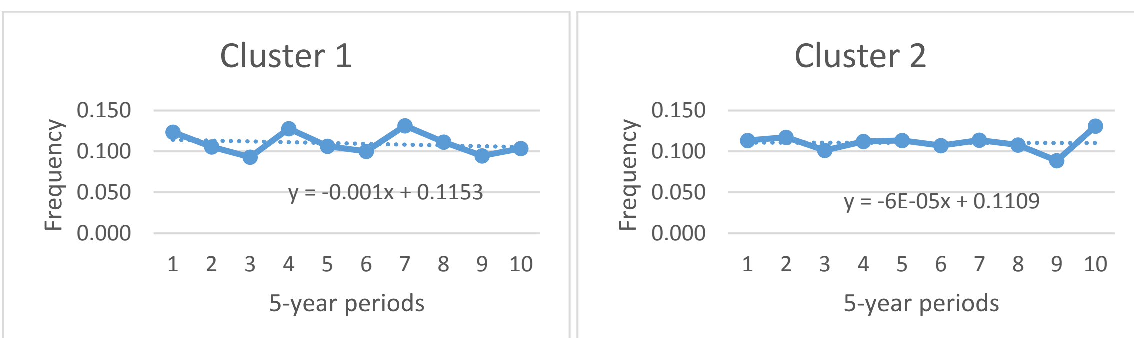

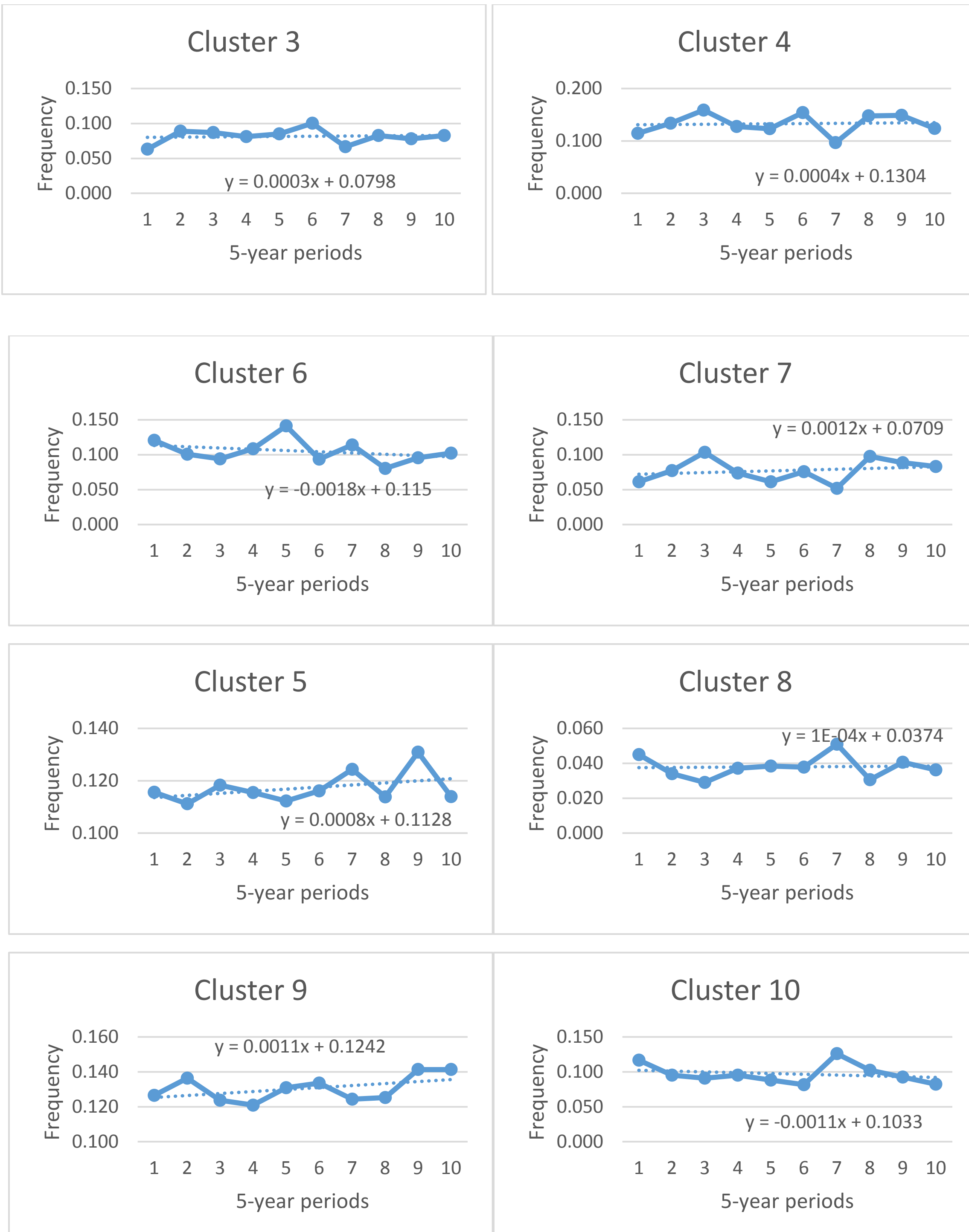


*Figure 4.2.3: Cluster 1-10 frequency trends*

## Cluster characterization

The clusters' implementation is based on the mean values of weather parameters which are displayed in Table 4.2.3.

From the cold period clusters 1 and 10 are characterized by low atmospheric boundary layer and higher surface pressure. Wind speed is almost equal but cluster 10 is a little bit warmer, where mean temperature and shortwave radiation are higher. Clusters 3,7 and 9 are described by high atmospheric boundary layer and lower surface pressure. All of them seems to have strong winds while 3 and 9 showed higher precipitation rate and higher relative humidity values. In warm period, clusters 4 and 5 are the warmest with the highest short-wave radiation. Cluster 8 has the higher precipitation and relative humidity. The atmospheric boundary level is higher in cluster 2, which seems to be the less warm cluster and lower in cluster 8.

*Table 4.2.3: Summary of the 10 clusters*

| | Clusters | | | | | | | | | |
|---|---|---|---|---|---|---|---|---|---|---|
| | 1 | 2 | 3 | 4 | 5 | 6 | 7 | 8 | 9 | 10 |
| Parameters | Mean (SD) | Mean (SD) | Mean (SD) | Mean (SD) | Mean (SD) | Mean (SD) | Mean (SD) | Mean (SD) | Mean (SD) | Mean (SD) |
| Temperature ( $^{o}$C) | 0,66 (5,31) | 10,34 (4,45) | 5,91 (3,72) | 18,16 (5,09) | 16,83 (4,81) | 6,3 (5,95) | 8,57 (4) | 14,97 (6,33) | 3,88 (3,8) | 6,77 (5,53) |
| Daily Temperature Range ( $^{o}$C) | 5,19 (2,04) | 6,99 (1,75) | 4,24 (1,77) | 10,94 (1,72) | 8,25 (1,72) | 4,56 (1,73) | 5,65 (2,22) | 5,42 (2,11) | 4,5 (1,86) | 9,17 (2,11) |
| Relative Humidity (%) | 87,63 (5,96) | 76,83 (5,01) | 80,78 (4,44) | 68,27 (7,23) | 81,62 (4,48) | 88,74 (4,21) | 67,14 (8,64) | 89,43 (4,22) | 81,64 (5,12) | 69,65 (9,73) |
| Surface Pressure (Pa) | 97437,4 (947,69) | 96175,69 (679,26) | 95303,29 (858,18) | 96853,21 (591,58) | 96530,95 (593,34) | 96209,83 (820,76) | 95905,83 (884,82) | 96001,88 (722,63) | 96387,93 (879,18) | 97494,13 (812,65) |
| Precipitation (kg/m2/s) | 0,000012 (0,000016) | 0,000034 (0,000031) | 0,000083 (0,000054) | 0,000007 (0,000014) | 0,000059 (0,000048) | 0,000065 (0,000045) | 0,000022 (0,000024) | 0,000238 (0,000099) | 0,000024 (0,000023) | 0,000003 (0,000009) |
| Downward Short Wave Radiation | 81,5 (42,44) | 214,12 (63,59) | 88,08 (62,56) | 300,26 (49,33) | 245,22 (51,3) | 97,34 (56,22) | 104,95 (71,23) | 147,5 (76,81) | 72,76 (40,15) | 152,53 (62,54) |
| u wind component (m/s) | 1,39 (2,59) | 4,01 (1,81) | 8,13 (2,23) | -1,25 (2,56) | 0,18 (2,25) | 2,76 (2,62) | 6,74 (2,41) | 1,29 (2,85) | 5,49 (2,13) | 0,64 (2,72) |
| v wind component (m/s) | -0,21 (1,6) | 0,56 (1,75) | 1,43 (2,08) | 0,23 (1,46) | -1,2 (1,4) | -1,79 (1,83) | 4,18 (1,61) | -2,15 (1,94) | 1,49 (1,72) | 1,34 (1,82) |
| V wind (m/s) | 2,92 (1,64) | 4,54 (1,47) | 8,55 (2,09) | 2,81 (1,55) | 2,6 (1,31) | 4,18 (1,88) | 8,23 (1,9) | 3,77 (1,99) | 6,05 (1,8) | 3,18 (1,66) |
| Atmospheric Boundary Layer Thickness (m) | 318,77 (133,77) | 748,26 (155,12) | 989,9 (205,57) | 645,15 (132,74) | 545,35 (126,1) | 477,05 (158,66) | 1042,52 (218,66) | 472,45 (154,46) | 670,55 (156,41) | 419,76 (162,07) |

In addition to the previous Table 4.2.3, Figure 4.2.4 presents the mean normalized (z-score) variables of each cluster, respectively showing the differences of the parameters per cluster.

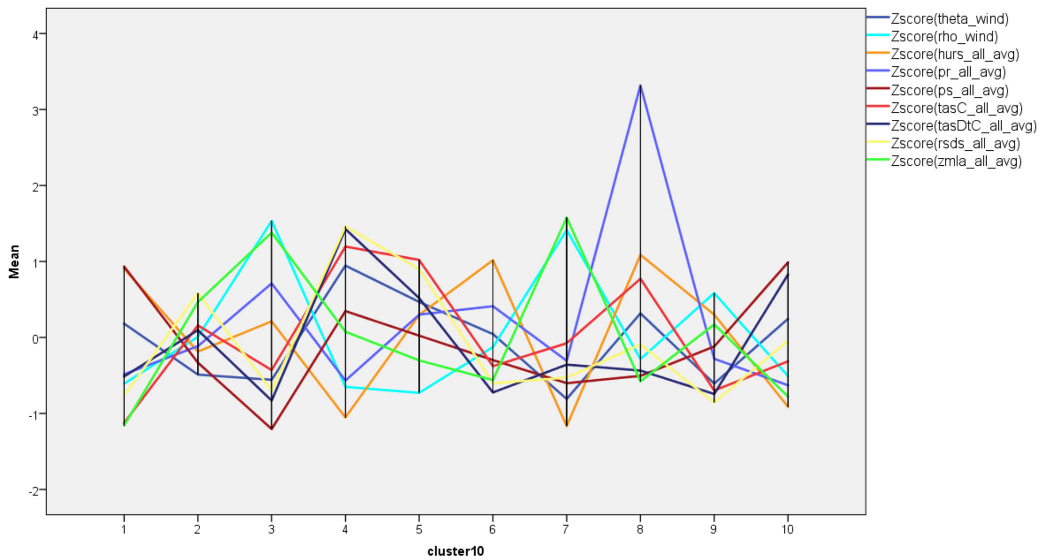


*Figure 4.2.4: Normalized variables (z-score) averaged for each cluster*

Daily, 10-meter from ground level, wind data were used to create the wind roses per each cluster as they are shown in Figures 4.2.5-4.2.14. Each wind direction distribution per cluster is presented in more details in Table 4.2.4.

Cluster 1: Around 40% of the daily wind directions were from the WSW, W and WNW direction with moderate wind speeds, mostly up to 6m/s. Weak wind speeds varied in the E direction.

Cluster 2: Around 60% of the daily wind directions were from the WSW and W direction with wind speeds, mostly up to 7m/s. Stronger winds up to 10m/s were recorded in WNW direction.

Cluster 3: Up to 70% of the daily wind directions were from the WSW and W direction with wind speeds, mostly up to 12m/s.

Cluster 4: Around 45% of the daily wind directions were from the ENE, E and ESE direction with moderate wind speeds, mostly up to 6m/s. Weak wind speeds varied in the W direction.

Cluster 5: Winds directions ranged from WSW to ENE directions. These directions don't necessarily indicate the prevailing wind in this cluster. Wind speeds were mostly up to 5m/s.

Cluster 6: Around 60% of the daily wind directions were from the W, WNW and NW direction with wind speeds, mostly up to 8m/s.

Cluster 7: 85% of the daily wind directions were from the WSW and SW direction with wind speeds, mostly up to 12m/s.

Cluster 8: Winds directions ranged from W to ENE directions. These directions don't necessarily indicate the prevailing wind in this cluster. Wind speeds were mostly up to 8m/s.

Cluster 9: Most of the winds came from W and WSW with speeds up to 12m/s.

Cluster 10: Up to 75% of the daily wind directions were from the WSW up to 10m/s and SW direction with wind speeds, mostly up to 7m/s. Weak wind speeds varied in the E to S direction.

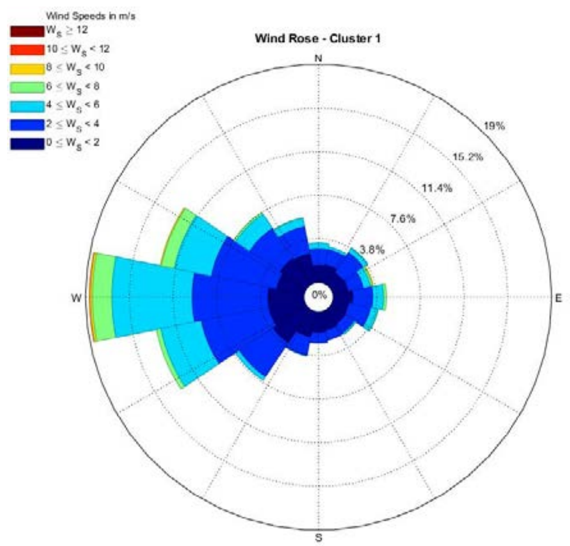


*Figure 4.2.5: Wind Rose -Cluster 1*

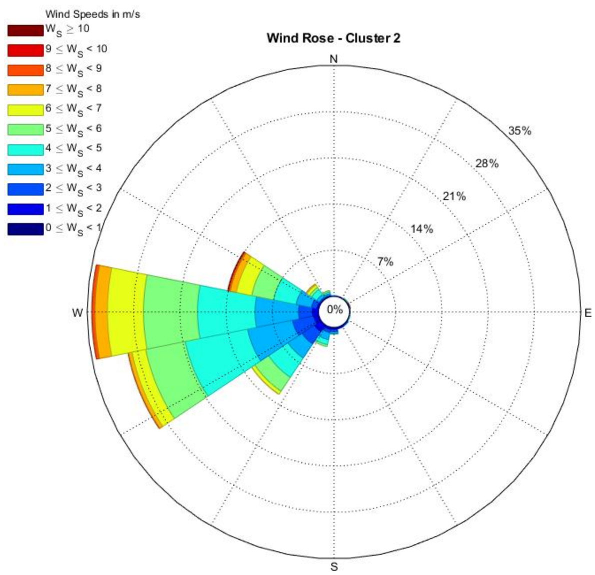


*Figure 4.2.6: Wind Rose - Cluster 2*

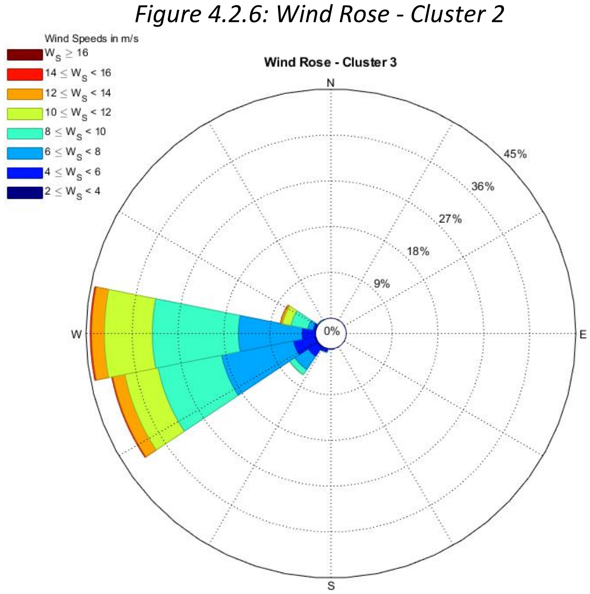


*Figure 4.2.7: Wind Rose - Cluster 3*

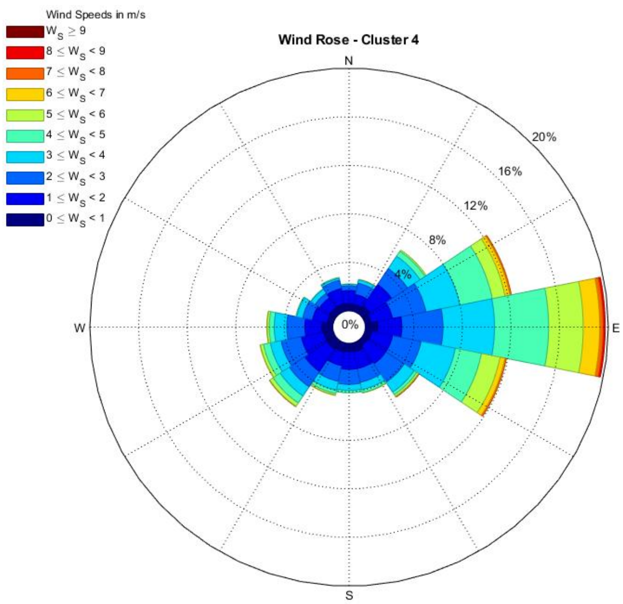


*Figure 4.2.8: Wind Rose - Cluster 4*

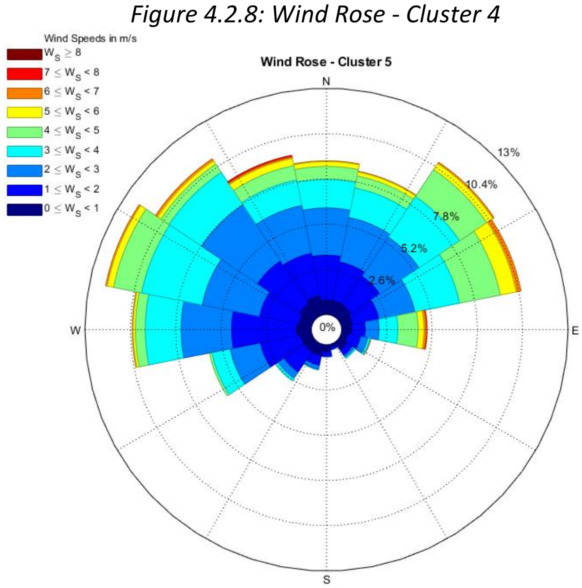


*Figure 4.2.9: Wind Rose - Cluster 5*

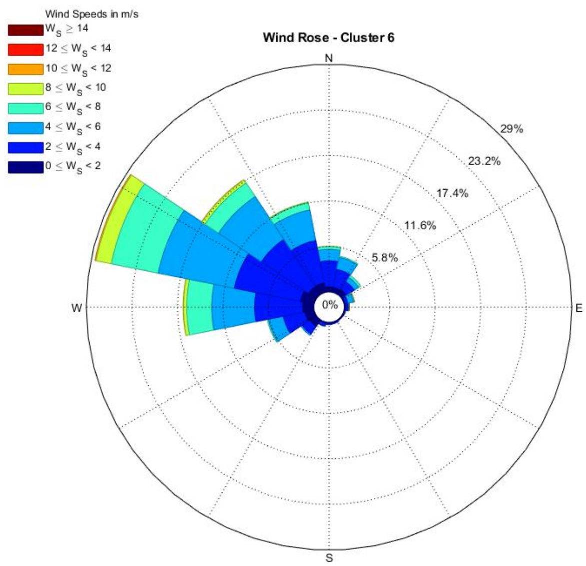


*Figure 4.2.10: Wind Rose - Cluster 6*

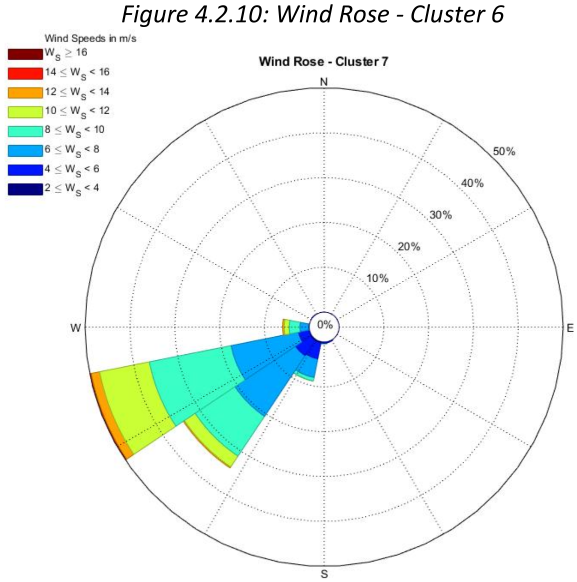


*Figure 4.2.11: Wind Rose - Cluster 7*

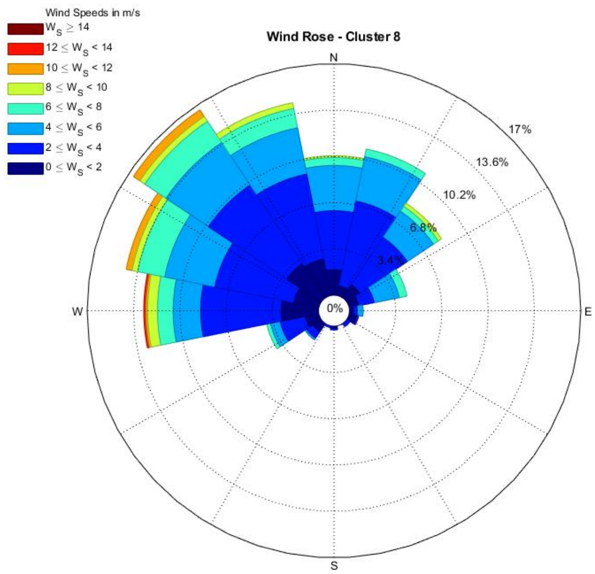


*Figure 4.2.12: Wind Rose - Cluster 8*

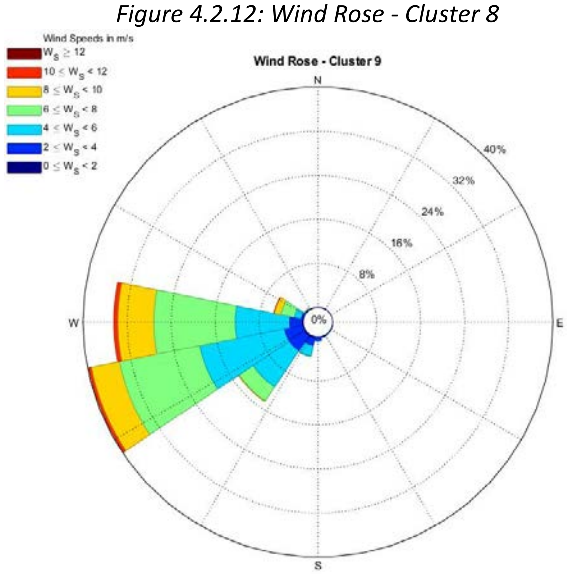


*Figure 4.2.13: Wind Rose - Cluster 9*

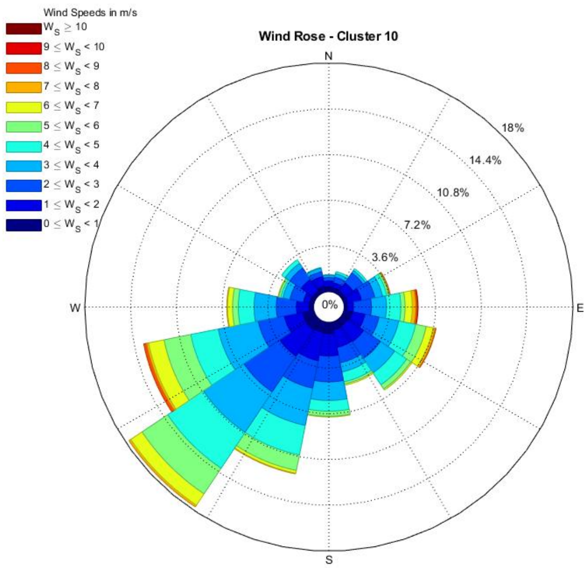


*Figure 4.2.14: Wind Rose - Cluster 10*

*Table 4.2.4: 16 Wind Direction distribution per cluster*

| | | | 16wind | | | | | | | | | | | | | | | | Total |
|---|---|---|---|---|---|---|---|---|---|---|---|---|---|---|---|---|---|---|---|
| | | | S | SSW | SW | WSW | W | WNW | NW | NNW | N | NNE | NE | ENE | E | ESE | SE | SSE | |
| cluster | 1 | Count | 55 | 79 | 149 | 263 | 374 | 256 | 153 | 116 | 69 | 64 | 78 | 72 | 93 | 81 | 53 | 51 | 2006 |
| | | % | 2,7% | 3,9% | 7,4% | 13,1% | 18,6% | 12,8% | 7,6% | 5,8% | 3,4% | 3,2% | 3,9% | 3,6% | 4,6% | 4,0% | 2,6% | 2,5% | 100,0% |
| | 2 | Count | 21 | 61 | 256 | 595 | 693 | 284 | 56 | 20 | 3 | 2 | 5 | 5 | 3 | 4 | 6 | 6 | 2020 |
| | | % | 1,0% | 3,0% | 12,7% | 29,5% | 34,3% | 14,1% | 2,8% | 1,0% | 0,1% | 0,1% | 0,2% | 0,2% | 0,1% | 0,2% | 0,3% | 0,3% | 100,0% |
| | 3 | Count | 2 | 12 | 101 | 608 | 656 | 106 | 3 | 0 | 0 | 0 | 0 | 0 | 0 | 0 | 0 | 0 | 1488 |
| | | % | 0,1% | 0,8% | 6,8% | 40,9% | 44,1% | 7,1% | 0,2% | 0,0% | 0,0% | 0,0% | 0,0% | 0,0% | 0,0% | 0,0% | 0,0% | 0,0% | 100,0% |
| | 4 | Count | 99 | 107 | 159 | 149 | 132 | 76 | 60 | 69 | 54 | 65 | 153 | 298 | 481 | 286 | 136 | 102 | 2426 |
| | | % | 4,1% | 4,4% | 6,6% | 6,1% | 5,4% | 3,1% | 2,5% | 2,8% | 2,2% | 2,7% | 6,3% | 12,3% | 19,8% | 11,8% | 5,6% | 4,2% | 100,0% |
| | 5 | Count | 15 | 32 | 57 | 128 | 220 | 258 | 234 | 200 | 189 | 180 | 229 | 225 | 105 | 37 | 24 | 7 | 2140 |
| | | % | 0,7% | 1,5% | 2,7% | 6,0% | 10,3% | 12,1% | 10,9% | 9,3% | 8,8% | 8,4% | 10,7% | 10,5% | 4,9% | 1,7% | 1,1% | 0,3% | 100,0% |
| | 6 | Count | 6 | 11 | 46 | 117 | 320 | 547 | 338 | 225 | 112 | 90 | 56 | 27 | 13 | 4 | 3 | 5 | 1920 |
| | | % | 0,3% | 0,6% | 2,4% | 6,1% | 16,7% | 28,5% | 17,6% | 11,7% | 5,8% | 4,7% | 2,9% | 1,4% | 0,7% | 0,2% | 0,2% | 0,3% | 100,0% |
| | 7 | Count | 6 | 127 | 487 | 706 | 84 | 0 | 1 | 0 | 0 | 0 | 0 | 0 | 0 | 0 | 0 | 3 | 1414 |
| | | % | 0,4% | 9,0% | 34,4% | 49,9% | 5,9% | 0,0% | 0,1% | 0,0% | 0,0% | 0,0% | 0,0% | 0,0% | 0,0% | 0,0% | 0,0% | 0,2% | 100,0% |
| | 8 | Count | 2 | 1 | 10 | 27 | 89 | 100 | 115 | 100 | 71 | 76 | 58 | 30 | 7 | 5 | 2 | 0 | 693 |
| | | % | 0,3% | 0,1% | 1,4% | 3,9% | 12,8% | 14,4% | 16,6% | 14,4% | 10,2% | 11,0% | 8,4% | 4,3% | 1,0% | 0,7% | 0,3% | 0,0% | 100,0% |
| | 9 | Count | 18 | 90 | 350 | 947 | 819 | 131 | 9 | 3 | 1 | 2 | 1 | 0 | 0 | 3 | 3 | 5 | 2382 |
| | | % | 0,8% | 3,8% | 14,7% | 39,8% | 34,4% | 5,5% | 0,4% | 0,1% | 0,0% | 0,1% | 0,0% | 0,0% | 0,0% | 0,1% | 0,1% | 0,2% | 100,0% |
| | 10 | Count | 132 | 216 | 314 | 242 | 121 | 51 | 58 | 35 | 24 | 29 | 43 | 66 | 103 | 131 | 118 | 90 | 1773 |
| | | % | 7,4% | 12,2% | 17,7% | 13,6% | 6,8% | 2,9% | 3,3% | 2,0% | 1,4% | 1,6% | 2,4% | 3,7% | 5,8% | 7,4% | 6,7% | 5,1% | 100,0% |
| Total | | Count | 356 | 736 | 1929 | 3782 | 3508 | 1809 | 1027 | 768 | 523 | 508 | 623 | 723 | 805 | 551 | 345 | 269 | 18262 |
| | | % | 1,9% | 4,0% | 10,6% | 20,7% | 19,2% | 9,9% | 5,6% | 4,2% | 2,9% | 2,8% | 3,4% | 4,0% | 4,4% | 3,0% | 1,9% | 1,5% | 100,0% |

## Clusters and local Heat Waves

In Figures 4.2.15 and 4.2.16 are presented the heat waves occurrence per 5-year period and per cluster. The 5-year period 2041-2045 shows the highest number of heat waves, while the next 5-year period shows a decrease. The most heat waves were associated with clusters 4 and 5 which correspond to clusters with days belong to warm period (see Table 4.2.2).

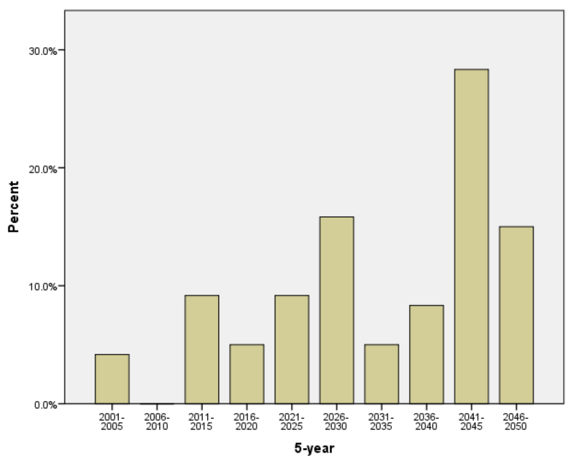


*Figure 4.2.15: Heat Waves per 5-year period*

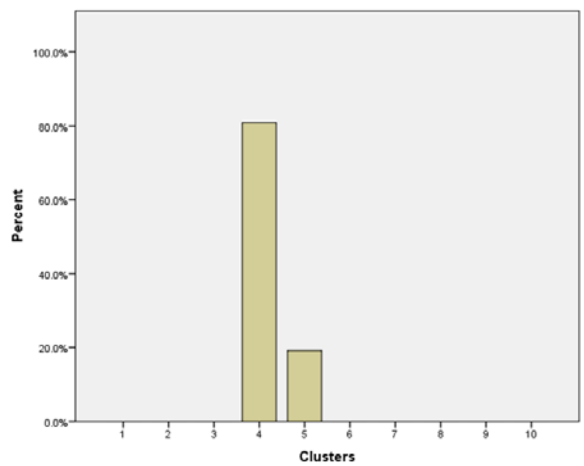


*Figure 4.2.16: Heat Waves per cluster*

## Clusters versus Air Quality level

As it can be seen in Table 4.1 one observation station has been used for the present analysis. The station descriptive statistics for $NO_2$, $O_3$ and $PM_{10}$ is given in Table 4.2.5.

*Table 4.2.5: Air pollutants descriptive statistics*

| | | NO2 | O3 | PM10 |
|---|---|---|---|---|
| Mean | | 43,7392 | 35,6998 | 25,8738 |
| Std. Deviation | | 17,65519 | 22,73449 | 15,60840 |
| Minimum | | 4,05 | 0,10 | 2,50 |
| Maximum | | 142,99 | 119,09 | 134,00 |
| Percentiles | 5 | 17,6490 | 2,7784 | 8,0982 |
| | 25 | 31,5415 | 16,8260 | 15,0000 |
| | 50 | 42,1890 | 35,0430 | 22,0000 |
| | 75 | 53,5210 | 51,3330 | 33,0000 |
| | 95 | 74,1955 | 74,9640 | 55,9768 |

Table 4.2.6 presents the pollutants' concentrations per cluster. Higher mean $NO_2$ concentrations are observed in clusters 1,7 and 9. Higher mean $O_3$ concentrations are observed in clusters 2,4,5 and 8. Higher mean $PM_{10}$ concentrations are observed in clusters 1,7 and 9.

*Table 4.2.6: Summary pollutant concentrations per cluster*

| | Clusters | | | | | | | | | |
|---|---|---|---|---|---|---|---|---|---|---|
| | 1 | 2 | 3 | 4 | 5 | 6 | 7 | 8 | 9 | 10 |
| Pollutants | Mean (SD) | Mean (SD) | Mean (SD) | Mean (SD) | Mean (SD) | Mean (SD) | Mean (SD) | Mean (SD) | Mean (SD) | Mean (SD) |
| PM10 (μg/m3) | 30,07 (18,08) | 22,49 (11,3) | 25,65 (15,55) | 20,97 (9,82) | 21,06 (9) | 26,96 (15,48) | 31,17 (19,47) | 20,19 (8,97) | 29,53 (19,19) | 28,2 (17,08) |
| O3 (μg/m3) | 23,56 (17,28) | 44,87 (17,79) | 25,09 (19,43) | 52,04 (20,15) | 55,65 (18,43) | 35,9 (22,63) | 20,71 (17,27) | 50,2 (19,15) | 21,47 (17,38) | 27,73 (16,02) |
| NO2 (μg/m3) | 47,6 (19,06) | 40,25 (14,02) | 46,86 (18,26) | 38,25 (14,14) | 36,97 (14,64) | 44,04 (17,6) | 49,81 (18,16) | 35,93 (13,63) | 49,46 (20,35) | 46,22 (17,38) |

The differences in concentrations per cluster are shown in Figures 4.2.17-4.2.19.

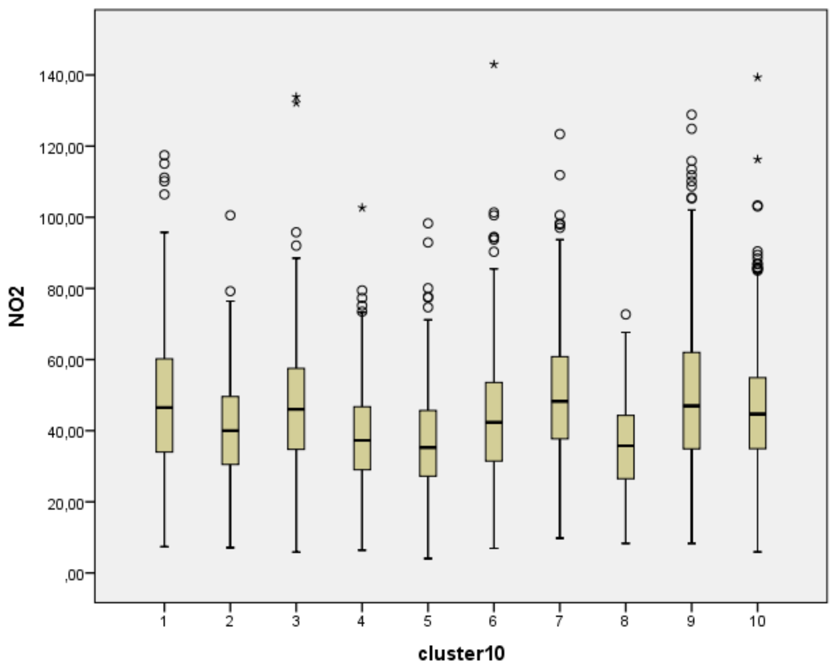


*Figure 4.2.17: $NO_2$ concentration statistics per cluster*

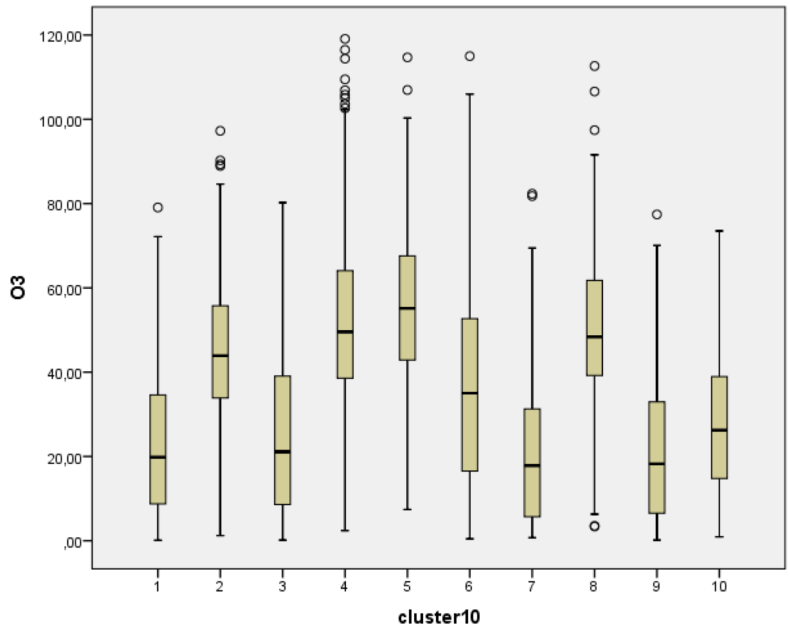


*Figure 4.2.18: $O_3$ concentration statistics per cluster*

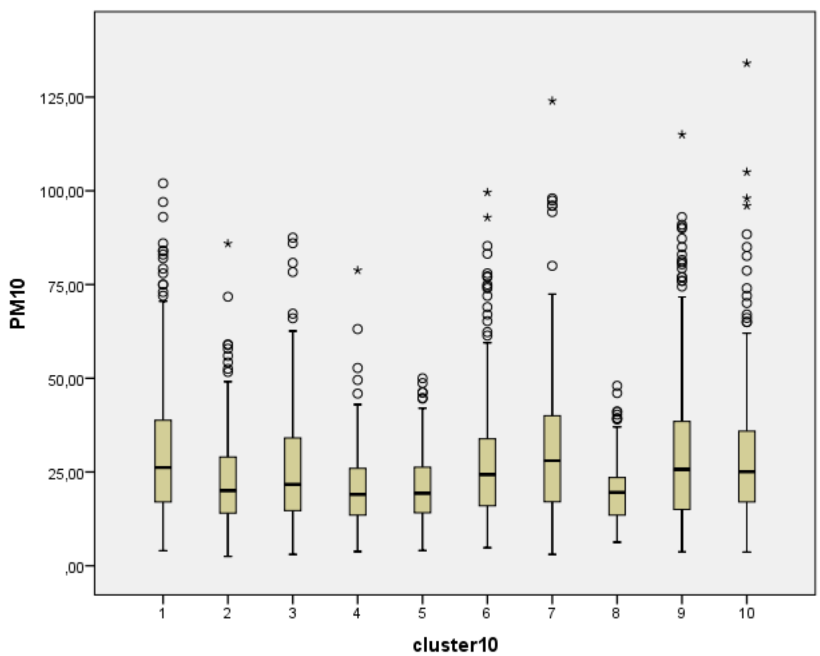


*Figure 4.2.19: $PM_{10}$ concentration statistics per cluster*

## Representative Days

In the following Table 4.2.7 are presented the selected RDs per 5-year period and per cluster.

*Table 4.2.7: Representative days per cluster and 5year period*

| Closest days to centroids per 5year per cluster | | | clusters | | | | | | | | | |
|---|---|---|---|---|---|---|---|---|---|---|---|---|
| | | | 1 | 2 | 3 | 4 | 5 | 6 | 7 | 8 | 9 | 10 |
| 5 year period | 2001-2005 | 1 | 2001/02/08 | 2001/06/07 | 2004/02/09 | 2002/06/14 | 2004/06/14 | 2001/03/07 | 2004/02/29 | 2005/09/05 | 2001/02/11 | 2003/03/20 |
| | 2006-2010 | 2 | 2006/11/08 | 2008/09/01 | 2009/12/23 | 2010/08/31 | 2008/06/20 | 2007/03/16 | 2010/10/11 | 2006/08/28 | 2007/11/21 | 2008/11/13 |
| | 2011-2015 | 3 | 2011/02/25 | 2015/05/07 | 2012/10/10 | 2011/08/17 | 2011/07/22 | 2012/10/14 | 2012/03/17 | 2015/06/10 | 2011/10/17 | 2011/03/15 |
| | 2016-2020 | 4 | 2019/02/12 | 2016/05/16 | 2018/11/15 | 2016/05/07 | 2020/08/22 | 2017/09/11 | 2020/10/17 | 2020/04/17 | 2020/03/05 | 2019/03/02 |
| | 2021-2025 | 5 | 2022/02/21 | 2023/04/30 | 2023/05/08 | 2023/08/07 | 2022/08/20 | 2022/03/17 | 2021/02/09 | 2023/05/20 | 2022/10/15 | 2022/11/11 |
| | 2026-2030 | 6 | 2028/03/13 | 2027/04/29 | 2029/12/07 | 2027/07/30 | 2030/06/05 | 2027/09/21 | 2029/11/10 | 2030/08/06 | 2028/10/26 | 2028/03/27 |
| | 2031-2035 | 7 | 2035/10/15 | 2033/04/22 | 2031/10/09 | 2033/08/18 | 2034/07/30 | 2033/03/22 | 2035/02/14 | 2035/06/13 | 2035/10/13 | 2031/03/13 |
| | 2036-2040 | 8 | 2039/11/13 | 2040/04/27 | 2036/03/05 | 2038/06/22 | 2037/08/18 | 2037/06/07 | 2036/10/12 | 2040/07/06 | 2039/10/27 | 2040/03/11 |
| | 2041-2045 | 9 | 2044/12/25 | 2045/04/26 | 2045/02/09 | 2041/09/06 | 2041/08/09 | 2045/09/21 | 2041/12/29 | 2044/09/07 | 2042/10/14 | 2043/03/27 |
| | 2046-2050 | 10 | 2049/12/21 | 2046/08/16 | 2049/03/03 | 2050/05/09 | 2046/07/12 | 2050/09/24 | 2050/01/31 | 2047/07/08 | 2048/03/18 | 2050/02/15 |

## Selected Clusters and RDs for modeling purposes

Selected RDs will be used to perform targeted weather and air quality simulations within each selected 5-year period estimating hourly/daily concentrations of the priority pollutants to assess the climatic effect on air quality evolution and the characteristics of air quality future episodes. The selection was based on 3-year periods (2016-2020, 2021-2025 and 2031-2035) and on the clusters with the most elevated concentrations of $PM_{10}$, $NO_2$ and $O_3$. In the case of Stuttgart, cluster 5 recorded the most elevated values of $O_3$ and cluster 7 for the case of $NO_2$ and $PM_{10}$. In Table 4.2.8 are presented the selected days which was used for modeling purposes.

*Table 4.2.8: RDs for modeling purposes*

| Period | Cluster 5 (O3) | Cluster 7 (NO2, PM) |
|---|---|---|
| 2016-2020 | 2020/08/22 | 2020/10/17 |
| 2021-2025 | 2022/08/20 | 2021/02/09 |
| 2031-2035 | 2034/07/30 | 2035/02/14 |

### 4.2.3 Air Quality Modeling results

#### 4.2.3.1 Overall results

In Figure 4.2.20 the daily average concentrations of $NO_2$, $O_3$, $PM_{10}$ and $PM_{2.5}$ for selected RDs are presented.

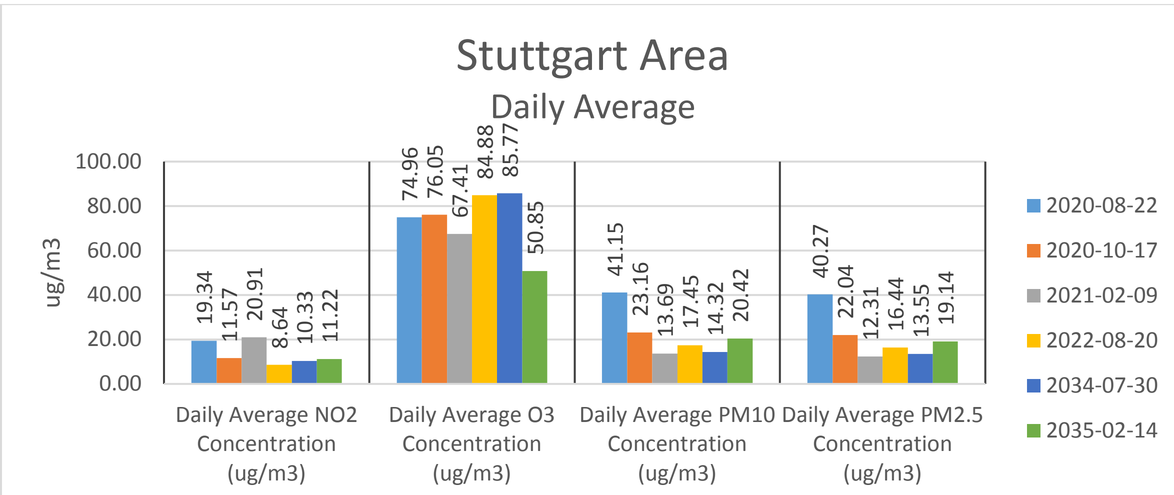


*Figure 4.2.20: Daily average concentrations*

In Figure 4.2.21 the obtained daily averaged concentrations are compared based on USTUTT and EGDAR HTAP emission inventories respectively. The results seem not to differ significantly.

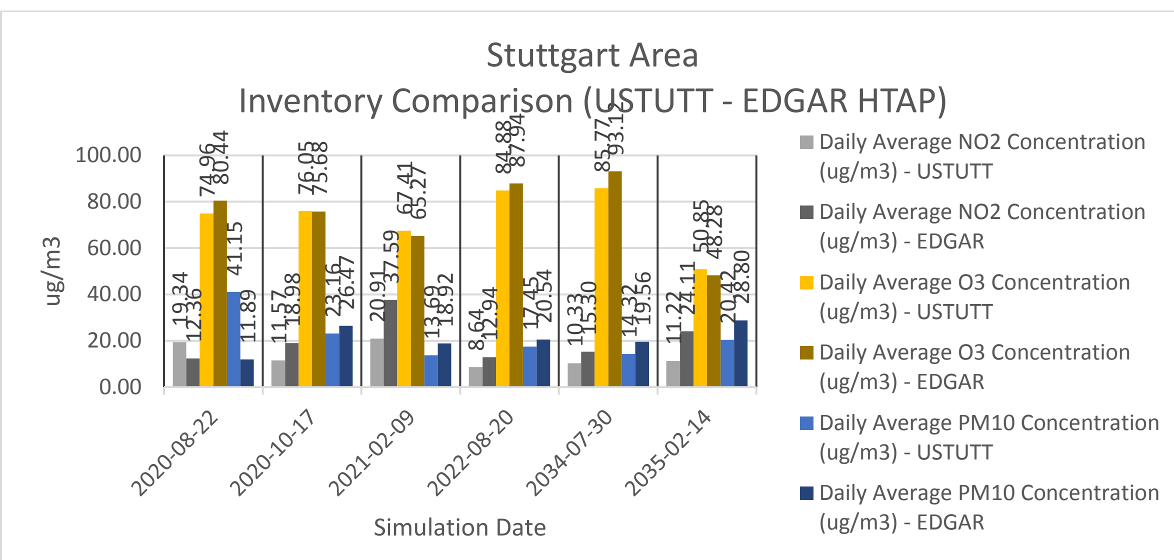


*Figure 4.2.21: Daily average concentrations – USTUTT vs EDGAR HTAP comparison*

#### 4.2.3.2 Clusters results

$NO_2$ Concentrations (Cluster 7)

In Figure 4.2.22, the results are presented in terms of concentrations average, daily maximum and hourly maximum. The diurnal variations are shown in Figure 4.2.23. Europe concentration maps, of the day with elevated average concentration, are presented in Figures 4.2.24.
The daily maximum concentrations seem to be very close or exceed the EU and WHO yearly limit of $40\mu g/m^3$. The maximum hourly concentrations being below the limit of $200\mu g/m^3$, show a decreasing trend.

$O_3$ Concentrations (Cluster 5)

In Figure 4.2.25, the results are presented in terms of concentrations average, daily maximum and hourly maximum. The diurnal variations are shown in Figure 4.2.26. Europe concentration maps, of the day with elevated average concentration, are presented in Figures 4.2.27.
The daily average concentrations show an increasing trend with maximum values very close to the WHO 8hr limit of $100\mu g/m^3$. The maximum hourly concentrations exceed this limit as well as the EU 8hr limit of $120\mu g/m^3$.

$PM_{10}$ Concentrations (Cluster 7)

In Figure 4.2.28, the results are presented in terms of concentrations average, daily maximum and hourly maximum. The diurnal variations are shown in Figure 4.2.29. Europe concentration maps, of the day with elevated average concentration, are presented in Figures 4.2.30.
The daily maximum concentrations show maximum values very close to the WHO yearly limit of $20\mu g/m^3$.

NO$_2$-Cluster 7

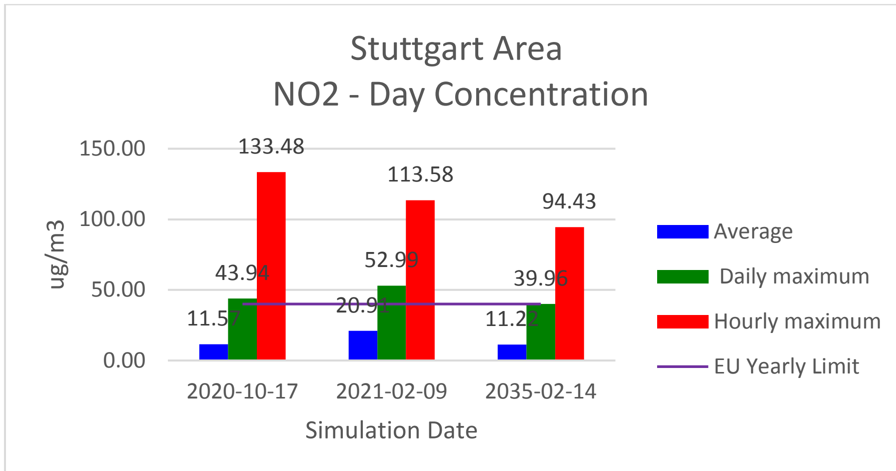


*Figure 4.2.22: NO$_2$ Day concentrations*

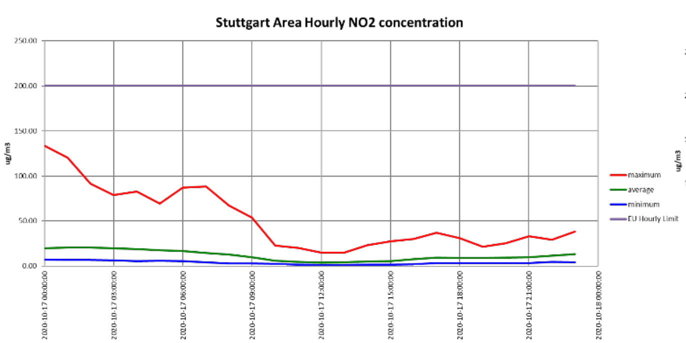


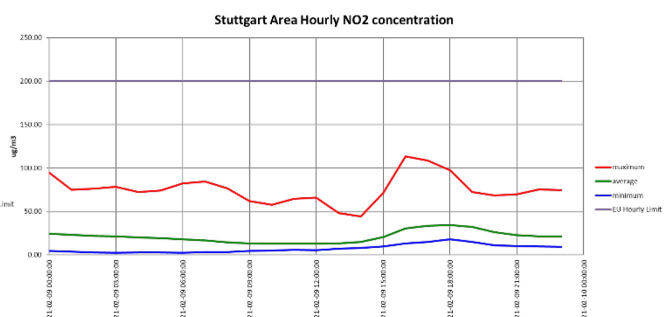


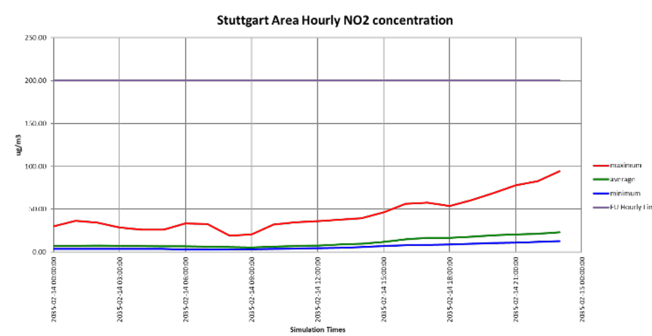


*Figure 4.2.23: Hourly NO$_2$ concentrations*

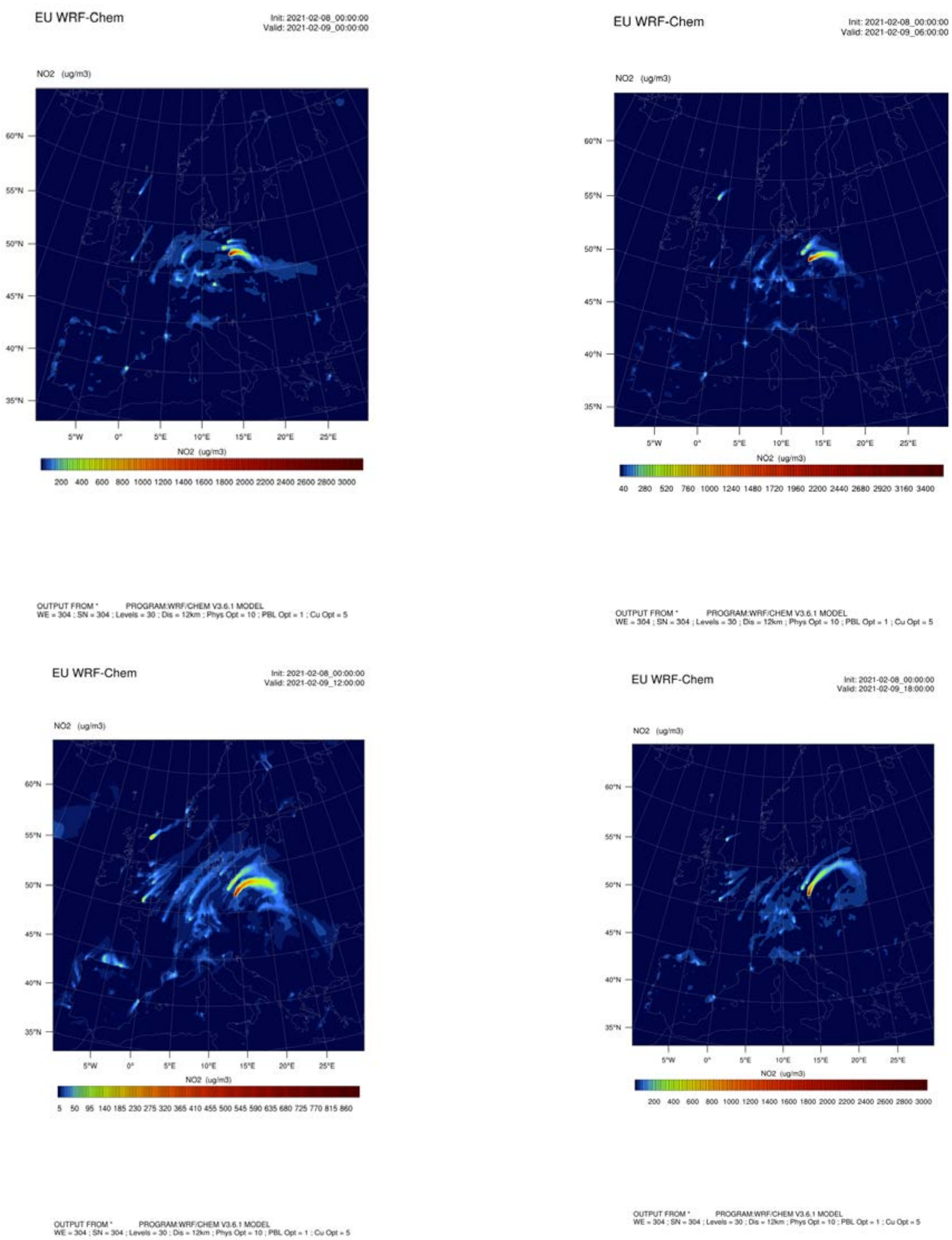


*Figure 4.2.24: $NO_2$ Europe maps*

O$_3$-Cluster 5

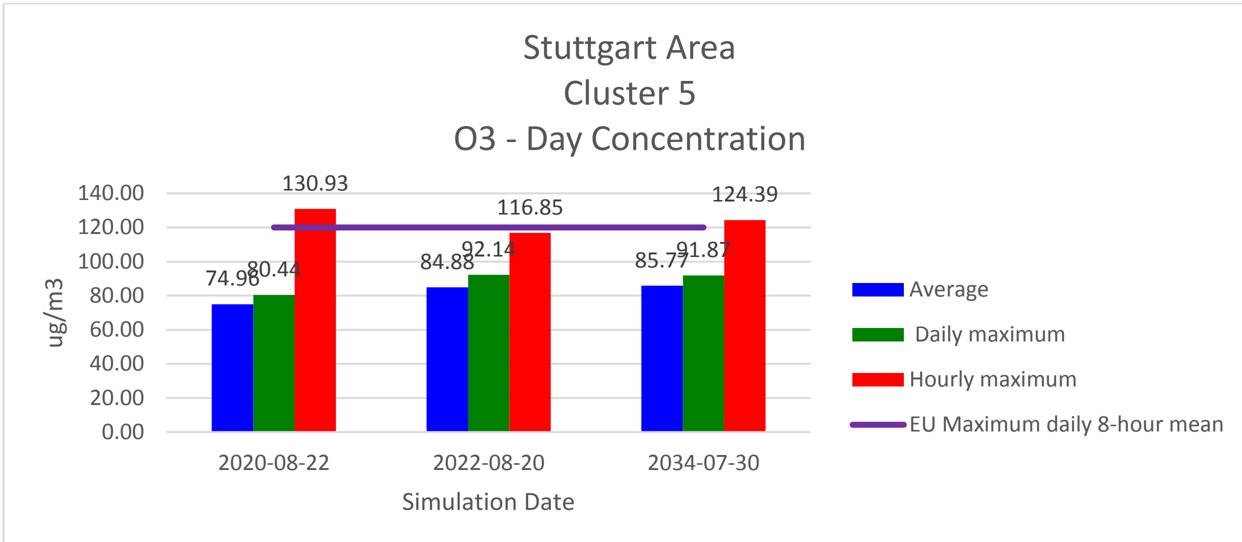


*Figure 4.2.25: O$_3$ Daily concentrations*

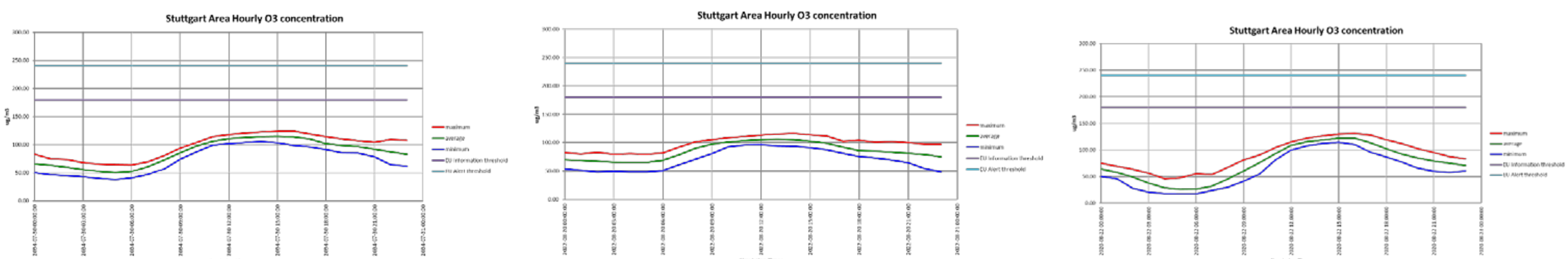


*Figure 4.2.26: O$_3$ Hourly concentrations*

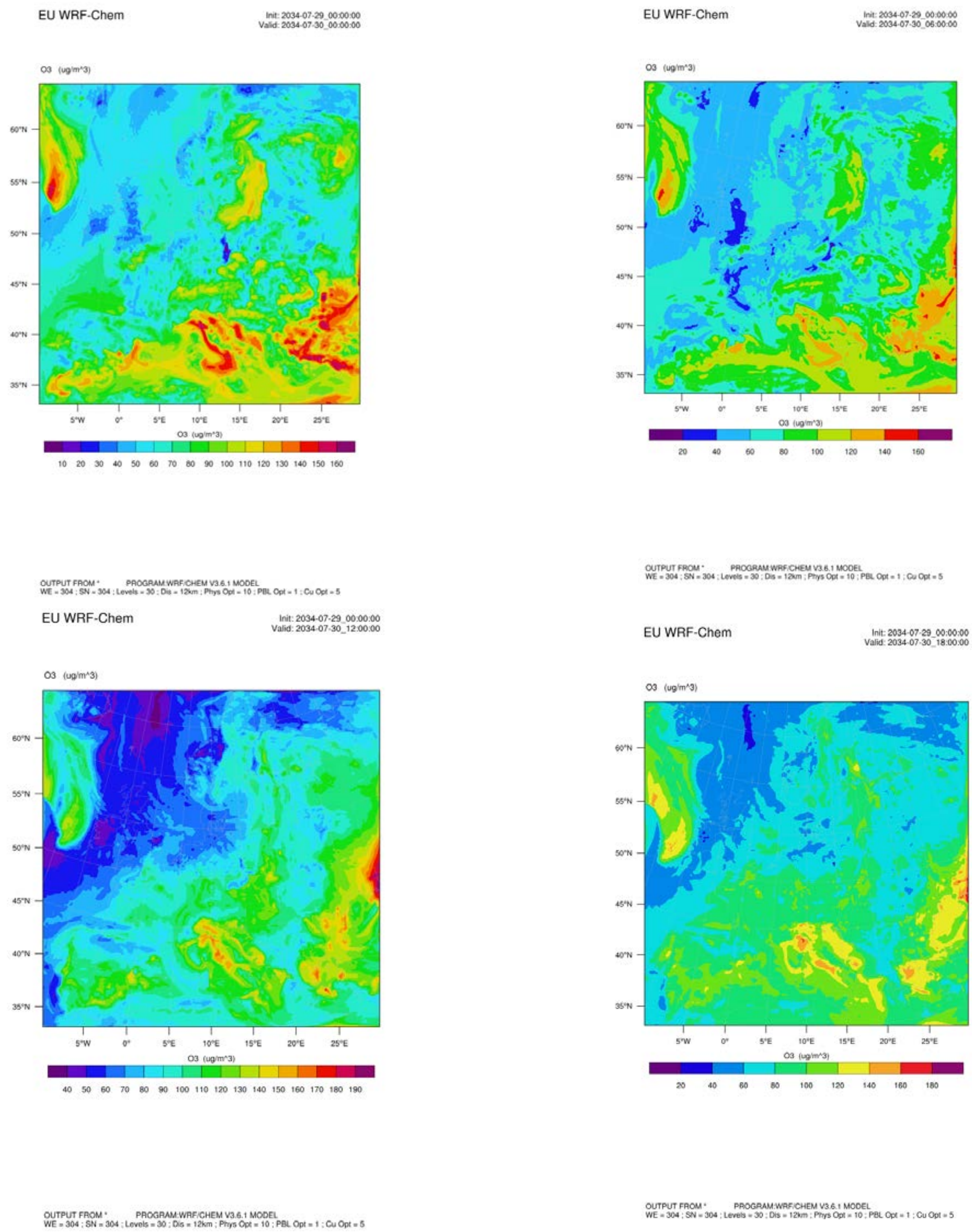


*Figure 4.2.27: $O_3$ Europe maps*

### $PM_{10}$-Cluster 7

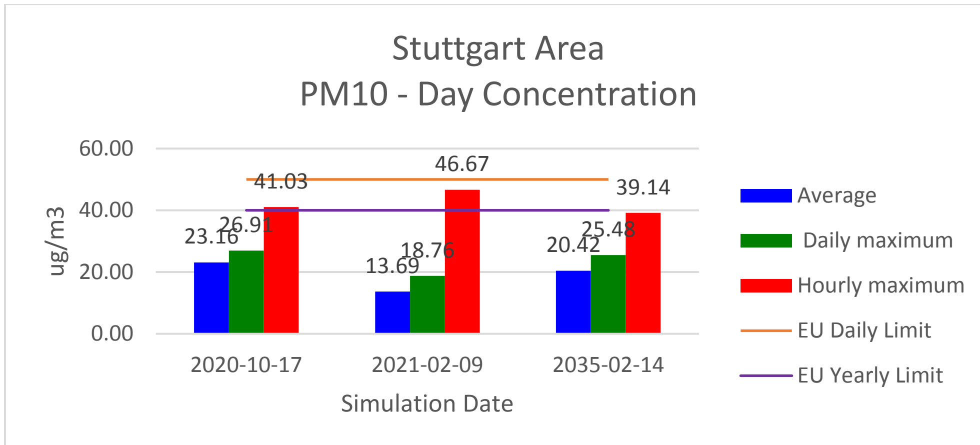


*Figure 4.2.28: $PM_{10}$ Day concentrations*

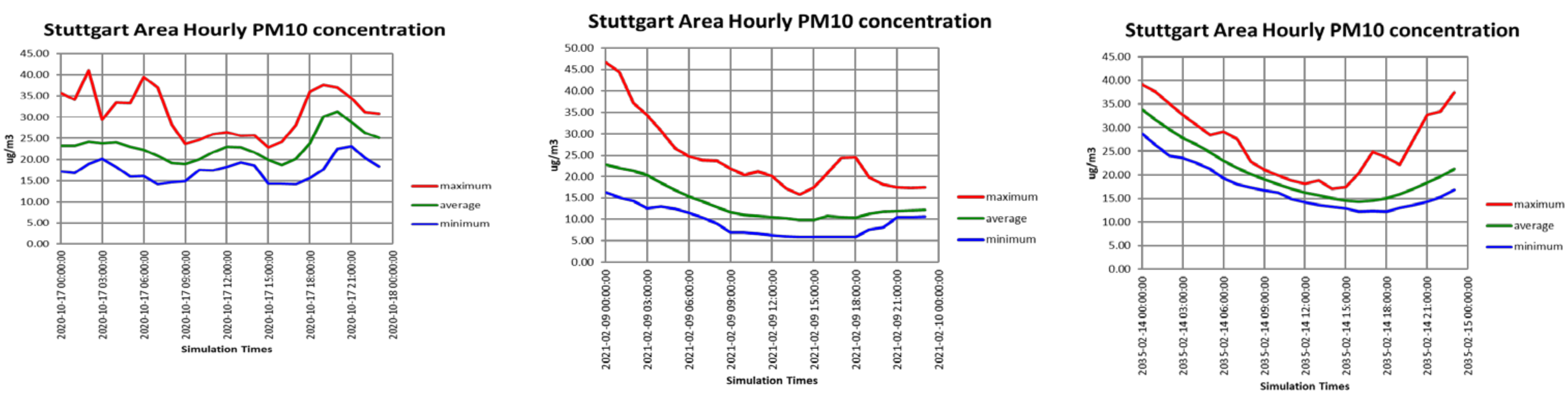


*Figure 4.2.29: $PM_{10}$ Hourly concentrations*

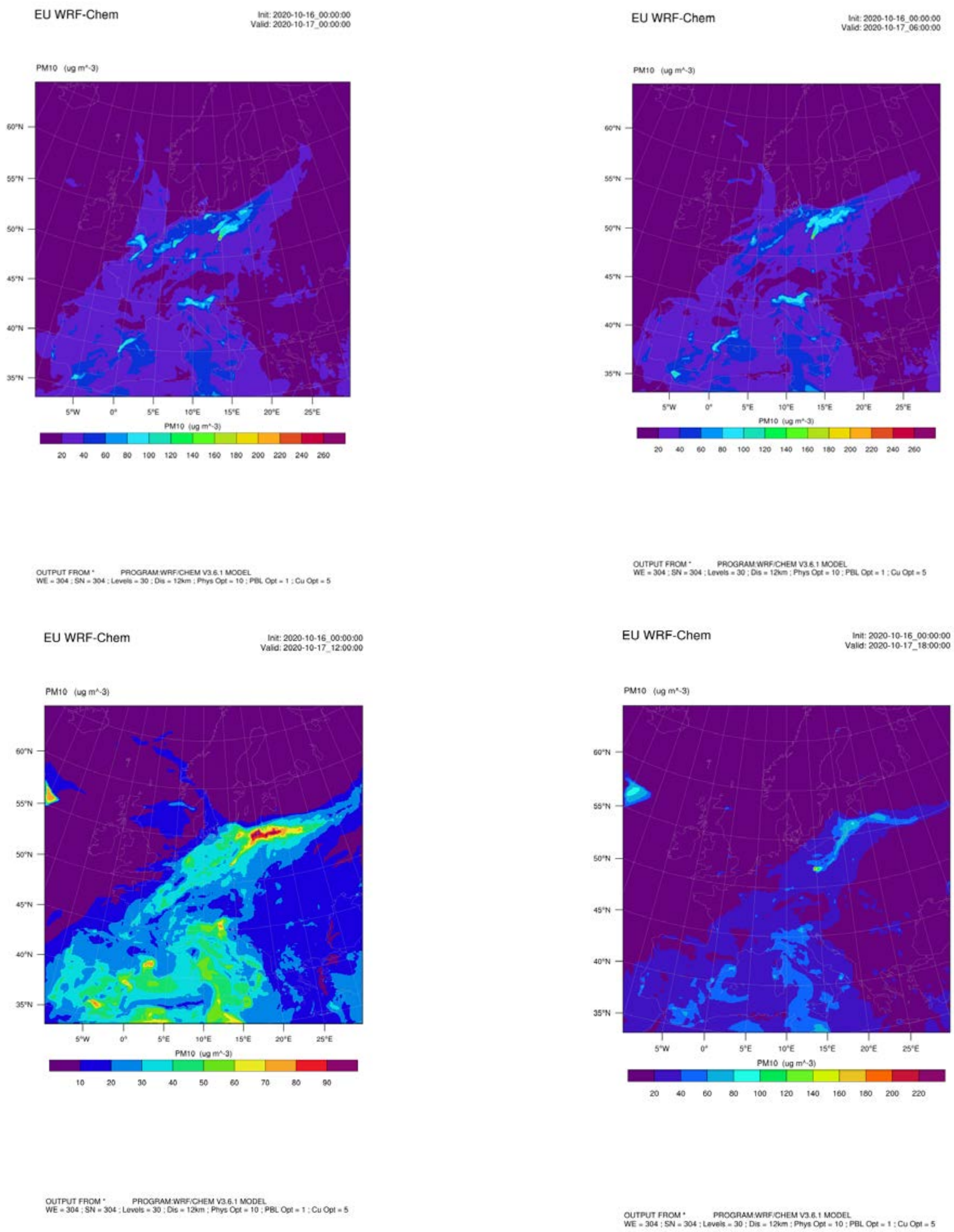


*Figure 4.2.30:PM$_{10}$ Europe maps*

PM$_{2.5}$ Concentrations (Cluster 7)

In Figure 4.2.31, the results are presented in terms of concentrations average, daily maximum and hourly maximum. Europe concentration maps are presented in Figures 4.2.33.
The daily maximum concentrations show maximum values well exceeding the WHO yearly limit of 10µg/m$^3$.

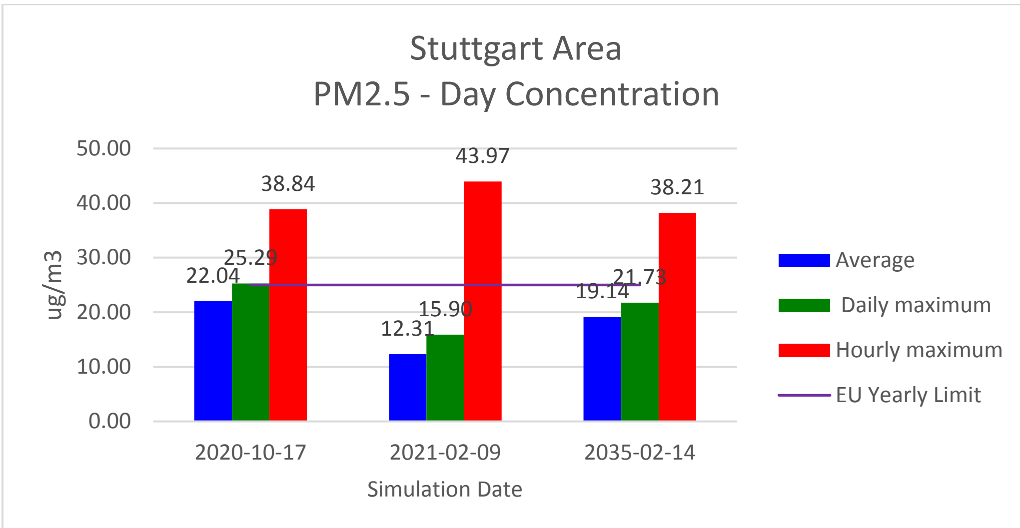


*Figure 4.2.31: PM$_{2.5}$ Day concentrations*

Figure 4.2.32 presents the estimated BaP daily concentrations contained in PM$_{2.5}$. All days are above WHO annual limit of 0.12ng/m$^3$ and close to the EU annual limit of 1ng/m$^3$.

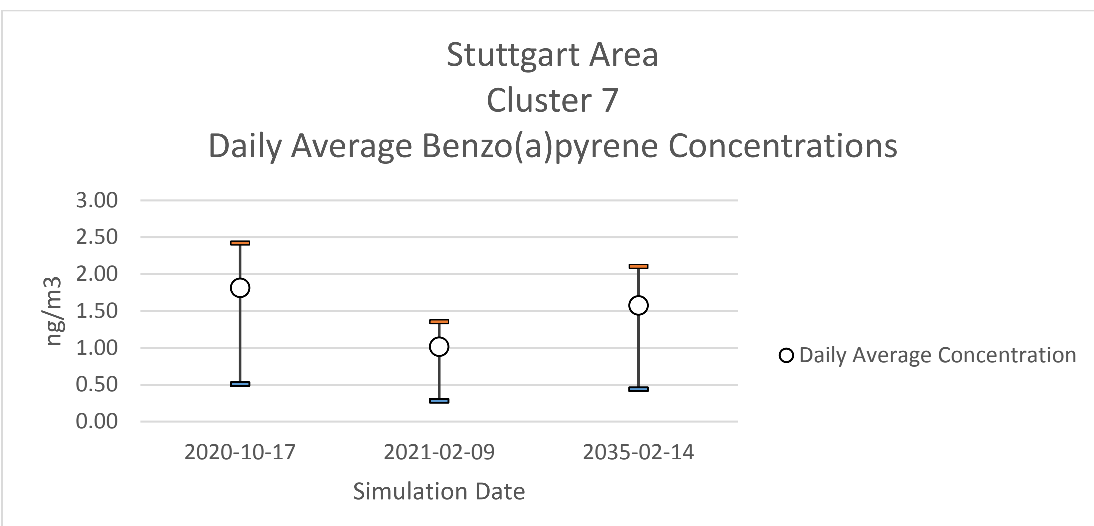


*Figure 4.2.32: BaP daily concentrations*

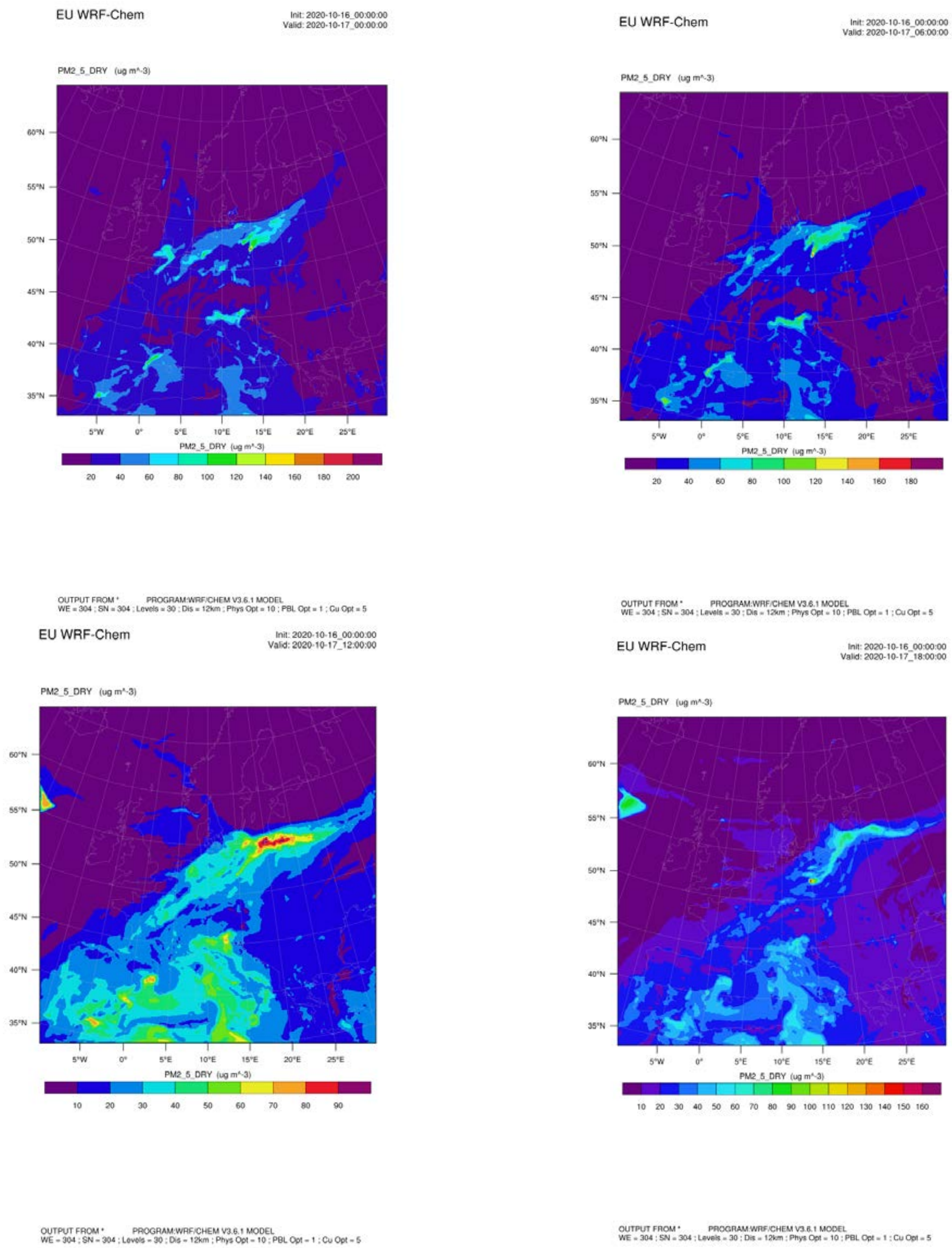


*Figure 4.2.33: PM$_{2.5}$ Europe maps*

### 4.2.3.3 The Emission Inventory effect

Figures 4.2.34, 4.2.35, 4.2.36 and 4.2.37 illustrate the emission inventory temporal change effect on $NO_2$, $O_3$, $PM_{10}$ and $PM_{2.5}$ concentration levels respectively. There is a clearly decreasing trend in all pollutants indicating the positive effect on emission reductions intervention.

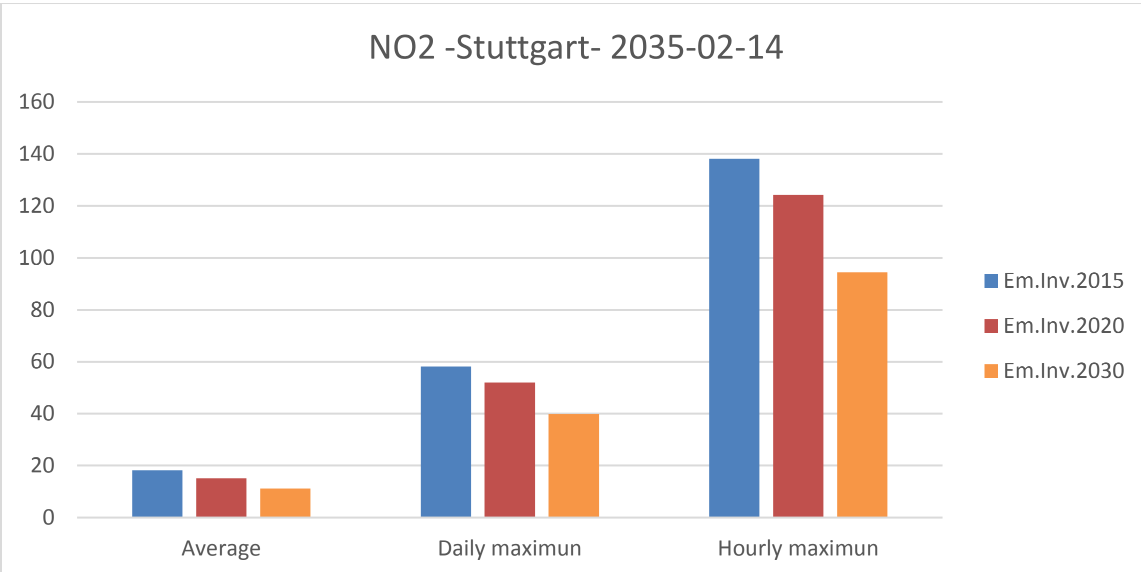


*Figure 4.2.34: $NO_2$ emission inventory comparison*

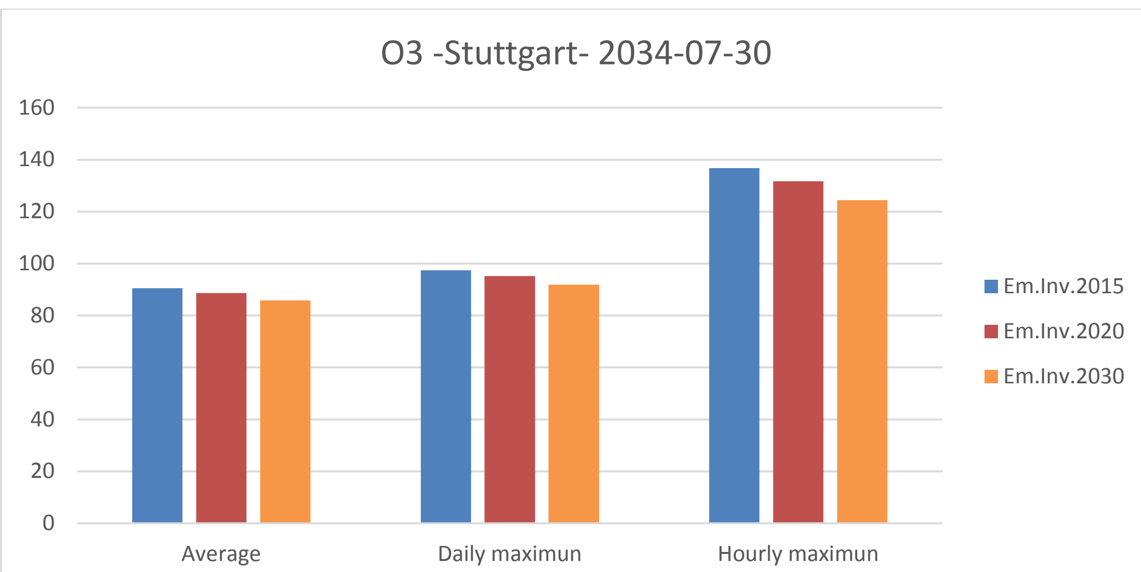


*Figure 4.2.35: $O_3$ emission inventory comparison*

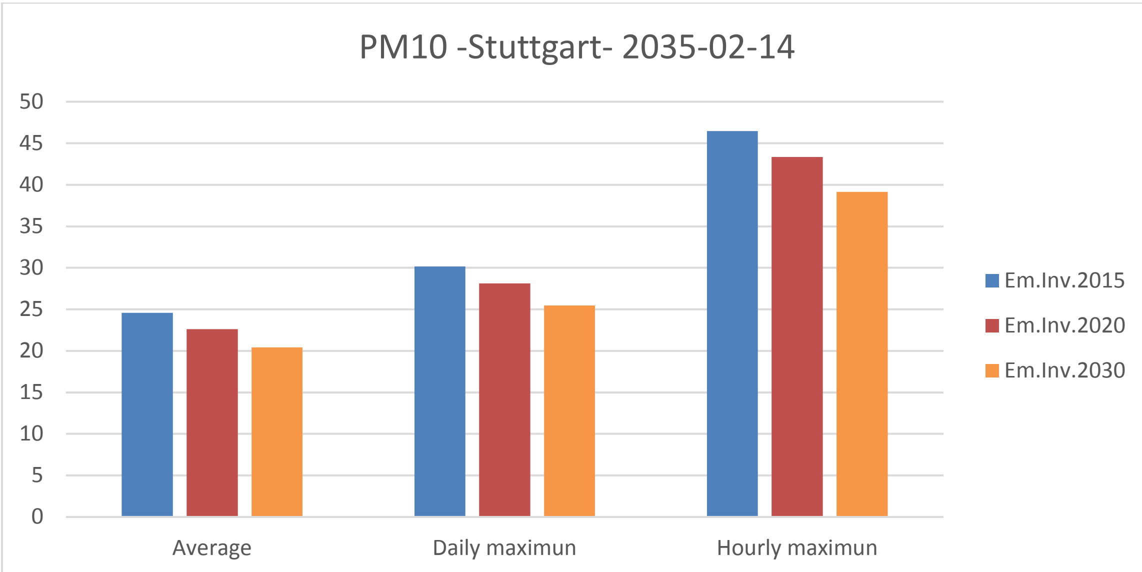


*Figure 4.2.36: $PM_{10}$ emission inventory comparison*

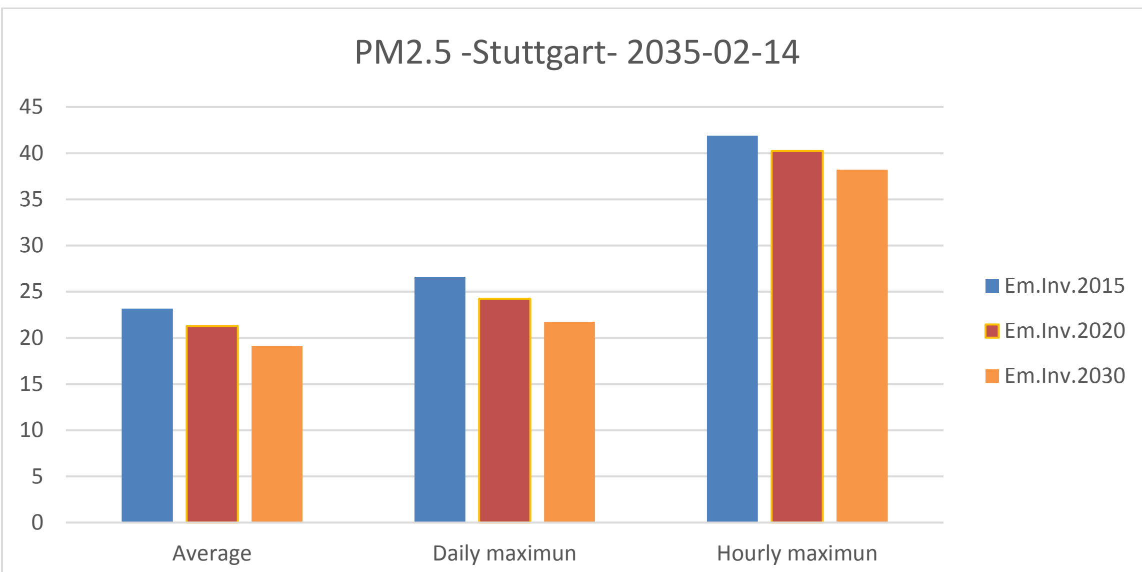


*Figure 4.2.37: $PM_{2.5}$ emission inventory comparison*

### 4.2.4 The GHGs Modeling results

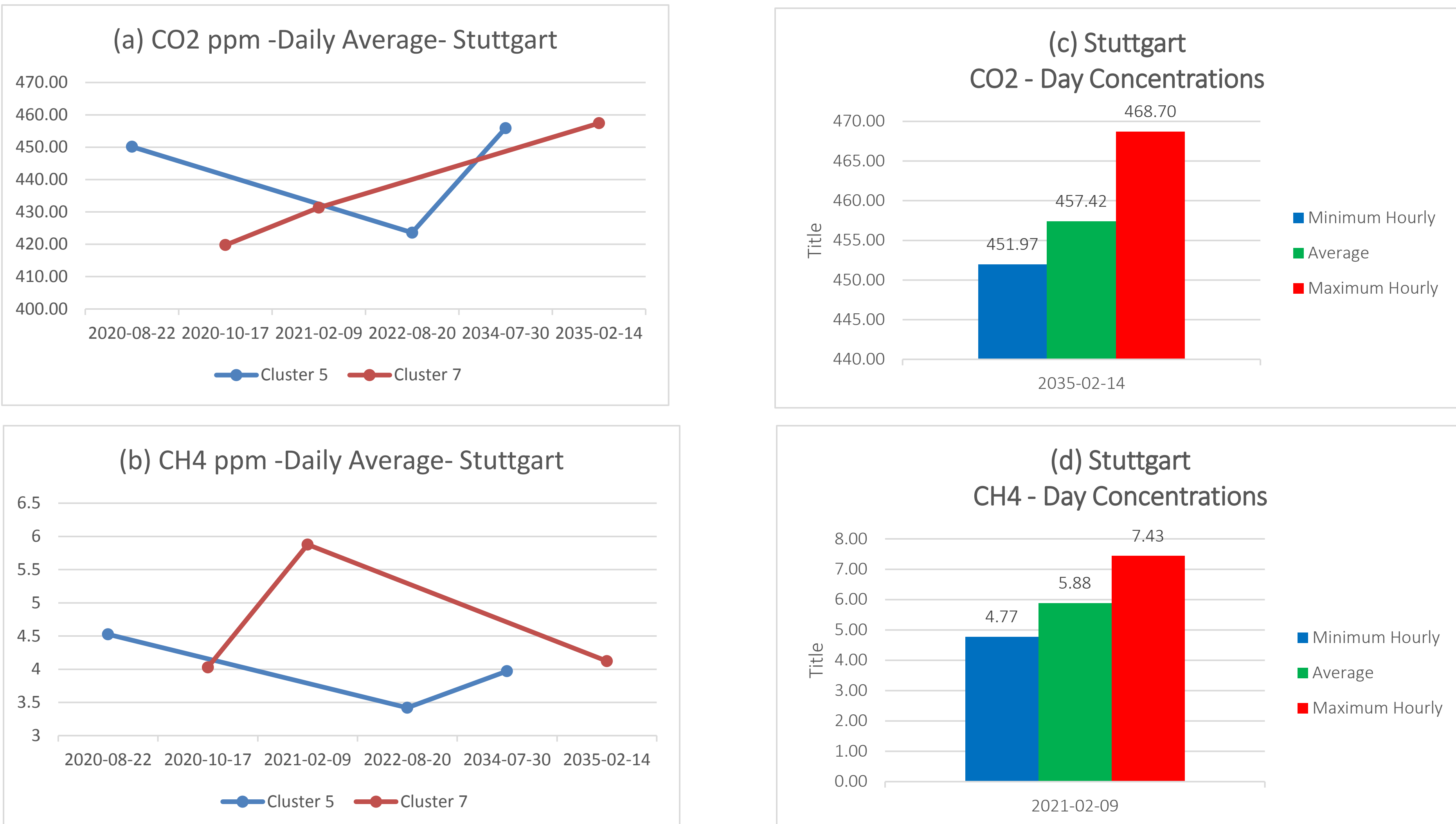


*Figure 4.2.38: (a),(b) $CO_2$ and $CH_4$ Daily average concentrations . (c),(d) $CO_2$ and $CH_4$ concentrations of the most polluted day*

### 4.2.5 Conclusions

For Stuttgart greater area, Clusters 1,3,7,9 and 10 could be categorized in cold period and on the other hand clusters 2,4,5 and 8 in warm period.

In clusters 5, 7 and 9 there is an increasing trend in frequency occurrence through the ten 5-year periods. On the other hand, clusters 6 and 10 show a linear decrease.

The 5-year period 2041-2045 shows the highest number of heat waves, while the next 5-year period shows a decrease. The most heat waves were associated with clusters 4 and 5 which correspond to clusters with days belong to warm period.

Cluster 7 is characterized with elevated $NO_2$ and PM concentrations whereas cluster 5 with elevated $O_3$ concentrations.

$NO_2$ daily maximum concentrations seem to be very close or exceed the EU and WHO yearly limit of 40μg/m$^3$. The maximum hourly concentrations being below the limit of 200μg/m$^3$, show a decreasing trend.

$O_3$ daily average concentrations show an increasing trend with maximum values very close to the WHO 8hr limit of 100μg/m$^3$. The maximum hourly concentrations exceed this limit as well as the EU 8hr limit of 120μg/m$^3$.

$PM_{10}$ daily maximum concentrations show maximum values very close to the WHO yearly limit of 20μg/m$^3$.

$PM_{2.5}$ daily maximum concentrations show maximum values well exceeding the WHO yearly limit of 10μg/m$^3$.

For all days BaP daily concentrations are above WHO annual limit of 0.12ng/m$^3$ and close to the EU annual limit of 1ng/m$^3$.

There is a clearly decreasing trend in all pollutants indicating the positive effect on emission reductions intervention.

## 4.3 Brno

### 4.3.1 PCA results

The PCA analysis applied to Brno data has led to the following results.

Four (4) principal components have been identified as factors for the cluster analysis (Table 4.3.1). Principal Components (PC) explaining 70.96% of the total variance in the initial data.

Factor 1 explains 32.23% of the total variance and contains the 2 temperature variables, mean, daily temperature range, the down ward short-wave radiation and the RH.

Factor 2 explains 21.07% of the total variance and contains the atmospheric boundary layer thickness and the U wind component.

Factor 3 explains 15.70% of the total variance and contains precipitation and a negative sign of surface pressure.

Factor 4 explains 11.53% of the total variance and contains V wind component.

*Table 4.3.1: The Principal Components results*

| Meteorological parameter | Principal Components | | | |
|---|---|---|---|---|
| | 1 | 2 | 3 | 4 |
| Downward short-wave surface radiation | .894 | | | |
| Temperature | .859 | | | |
| Temperature Range | .755 | | | |
| RH | -.607 | | | |
| Atmospheric boundary layer thickness | | .837 | | |
| U wind | | .746 | | |
| Precipitation | | | .869 | |
| Surface pressure | | | -.653 | |
| V wind | | | | .947 |

### 4.3.2 Clustering results

#### Cluster description and trends

As explained in 3.4.4 the selected clusters of the city of Brno are 8. In Figure 4.3.1 are shown the number of days per cluster, where clusters 4 and 5 have the most days and cluster 2,3 and 8 have the less, especially the last one. The monthly distribution per cluster is presented in Table 4.3.2 and in Figure 4.3.2. By dividing the year in two periods, cold and warm, clusters 1,2,6,7 and 8 could be categorized in cold period and on the other hand clusters 3,4 and 5 in warm period.


*Figure 4.3.1: Number of Days per cluster*

*Table 4.3.2: Monthly distribution per cluster*

| | | Month | | | | | | | | | | | | Total |
|---|---|---|---|---|---|---|---|---|---|---|---|---|---|---|
| | | Jan | Feb | Mar | Apr | May | Jun | Jul | Aug | Sep | Oct | Nov | Dec | |
| Cluster8 | 1 | 270 | 314 | 418 | 208 | 130 | 47 | 12 | 16 | 156 | 296 | 281 | 246 | 2394 |
| | 2 | 348 | 283 | 237 | 23 | 2 | 0 | 0 | 0 | 53 | 286 | 293 | 282 | 1807 |
| | 3 | 27 | 25 | 60 | 88 | 248 | 364 | 264 | 147 | 122 | 80 | 50 | 22 | 1497 |
| | 4 | 0 | 0 | 37 | 290 | 557 | 680 | 747 | 559 | 295 | 22 | 0 | 0 | 3187 |
| | 5 | 2 | 28 | 123 | 296 | 309 | 306 | 499 | 744 | 527 | 187 | 13 | 0 | 3034 |
| | 6 | 245 | 226 | 291 | 356 | 183 | 64 | 14 | 51 | 156 | 224 | 202 | 263 | 2275 |
| | 7 | 495 | 319 | 173 | 55 | 37 | 6 | 5 | 9 | 66 | 231 | 432 | 500 | 2328 |
| | 8 | 163 | 217 | 211 | 184 | 84 | 33 | 9 | 24 | 125 | 224 | 229 | 237 | 1740 |
| Total | | 1550 | 1412 | 1550 | 1500 | 1550 | 1500 | 1550 | 1550 | 1500 | 1550 | 1500 | 1550 | 18262 |

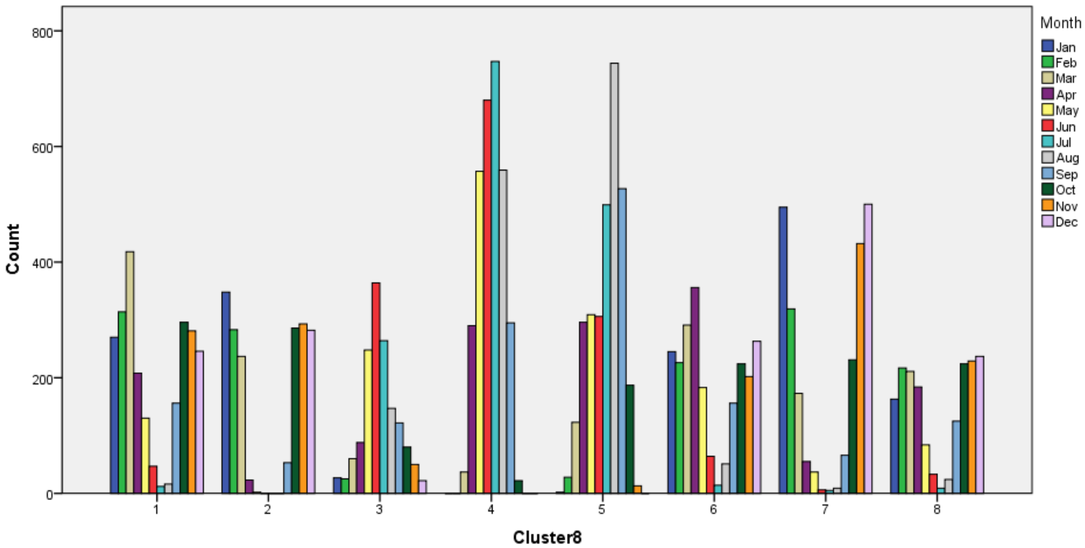


*Figure 4.3.2: Visualized bar chart of monthly distribution per cluster*

A trend analysis of the 5-year frequency of each cluster (Figure 4.3.3). There is an evidence that in cluster 4 there is a linear increase in frequency occurrence through the ten 5-year periods and a slight increase in 1 and 5. On the other hand, clusters 3 and 7 show a slight decrease in frequency occurrence. In the rest clusters no clear trends could be pointed out.

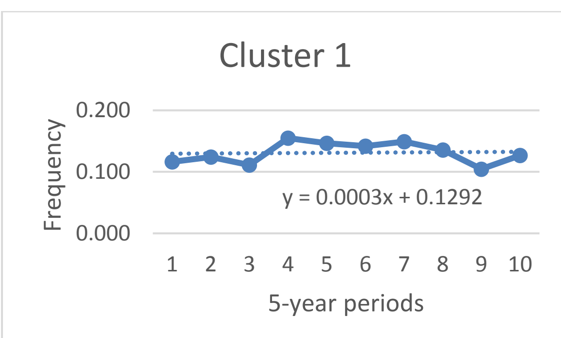


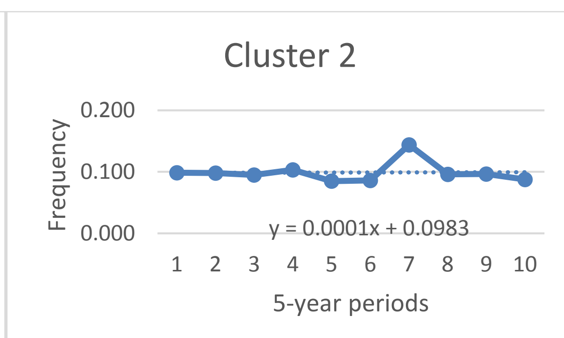


*Figure 4.3.3: Cluster 1-8 frequency trends*

## Cluster characterization

The clusters' implementation is based on the mean values of weather parameters which are displayed in Table 4.3.3.

*Table 4.3.3: Summary of the 8 clusters*

| | Cluster | | | | | | | |
|---|---|---|---|---|---|---|---|---|
| | 1 | 2 | 3 | 4 | 5 | 6 | 7 | 8 |
| | Mean (SD) | Mean (SD) | Mean (SD) | Mean (SD) | Mean (SD) | Mean (SD) | Mean (SD) | Mean (SD) |
| Temperature ( ºC) | 3,19 (5,95) | 1,77 (6,56) | 15,11 (6,77) | 17,06 (5,84) | 18,32 (6,39) | 6,22 (4,78) | 2,75 (5,59) | 8,04 (5,2) |
| Daily Temperature Range (ºC) | 4,86 (1,63) | 6,82 (2,62) | 6,59 (2,45) | 8,84 (1,85) | 11,82 (2,07) | 5,55 (1,9) | 5,93 (2,4) | 7,81 (2,61) |
| Relative Humidity (%) | 73 (7,83) | 77,5 (11,95) | 82,38 (5,82) | 66,51 (8,64) | 61,16 (10,66) | 66,9 (7,37) | 84,1 (8,16) | 70,32 (8,8) |
| Surface Pressure (Pa) | 97919,86 (859,95) | 99014,24 (686,17) | 96817,84 (747,68) | 97856,13 (642,16) | 97867,16 (653,22) | 96864,81 (772,6) | 97325,27 (739,48) | 96565,64 (803,26) |
| Precipitation (kg/m2/s) | 0,000009 (0,000019) | 0,000003 (0,000009) | 0,000172 (0,000082) | 0,000013 (0,000022) | 0,00001 (0,00002) | 0,000012 (0,000019) | 0,000026 (0,000031) | 0,000027 (0,000033) |
| Downward Short Wave Radiation | 123,41 (66,04) | 98,73 (52,31) | 175,48 (93,41) | 288,16 (55,55) | 268,71 (63,92) | 148,56 (86,63) | 69,4 (41,83) | 115,23 (74,1) |
| u wind component (m/s) | 3 (2,55) | -0,32 (2,21) | -1,08 (2,35) | -0,81 (2,44) | -0,91 (1,88) | 6,22 (2,05) | 0,21 (2,38) | 1,96 (2,43) |
| v wind component (m/s) | -4,47 (2,19) | -0,57 (2,36) | -0,6 (3,08) | -3,17 (1,59) | 1,44 (1,93) | -1,66 (2,16) | 1,55 (2,29) | 3,54 (2,44) |
| V wind (m/s) | 6,07 (1,87) | 2,91 (1,57) | 3,57 (1,95) | 4,13 (1,47) | 2,84 (1,45) | 6,78 (2,1) | 3,23 (1,69) | 4,98 (1,85) |
| Atmospheric Boundary Layer Thickness (m) | 726,81 (180,29) | 334,43 (142,99) | 536,41 (146,11) | 781,17 (148,25) | 684,56 (160,33) | 1023,34 (208,16) | 381,33 (138,9) | 715,74 (187,28) |

In addition to the previous Table 4.3.3, Figure 4.3.4 presents the mean normalized (z-score) variables of each cluster, respectively showing the differences of the parameters per cluster.

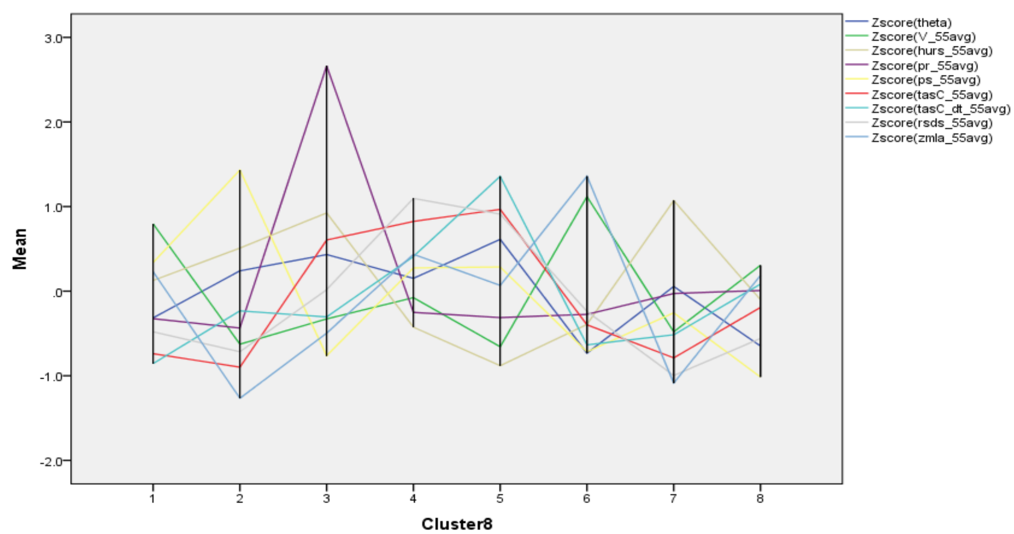


*Figure 4.3.4: Normalized variables (z-score) averaged for each cluster*

Daily, 10-meter from ground level, wind data were used to create the wind roses per each cluster as they are shown in Figures 4.3.5-4.3.12. Each wind direction distribution per cluster is presented in more details in Table 4.3.4.

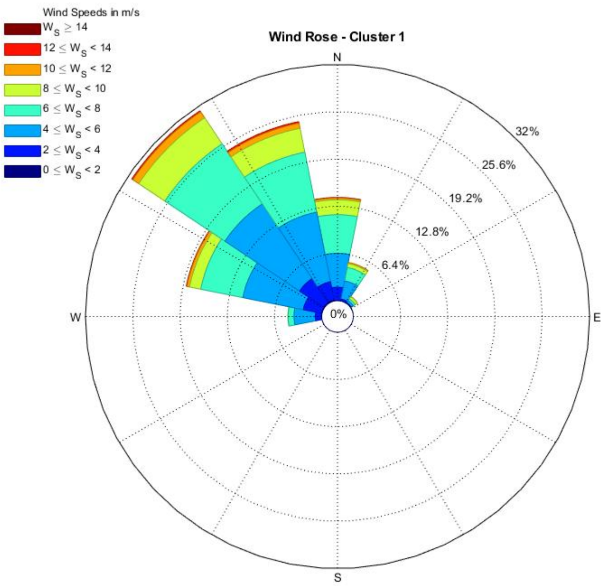


*Figure 4.3.5: Wind Rose - Cluster 1*

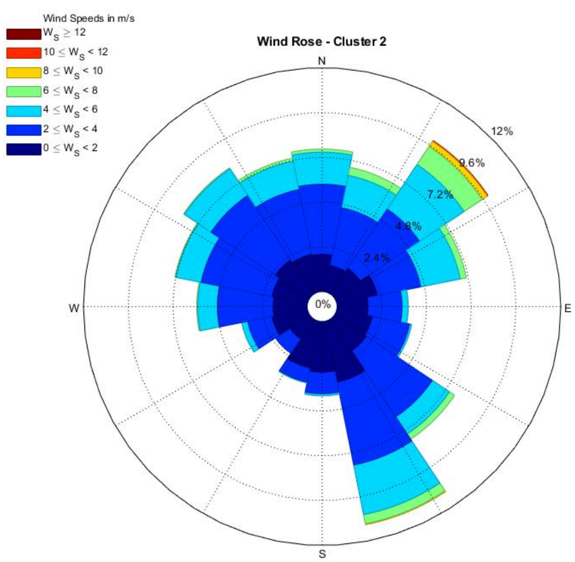


*Figure 4.3.6: Wind Rose - Cluster 2*

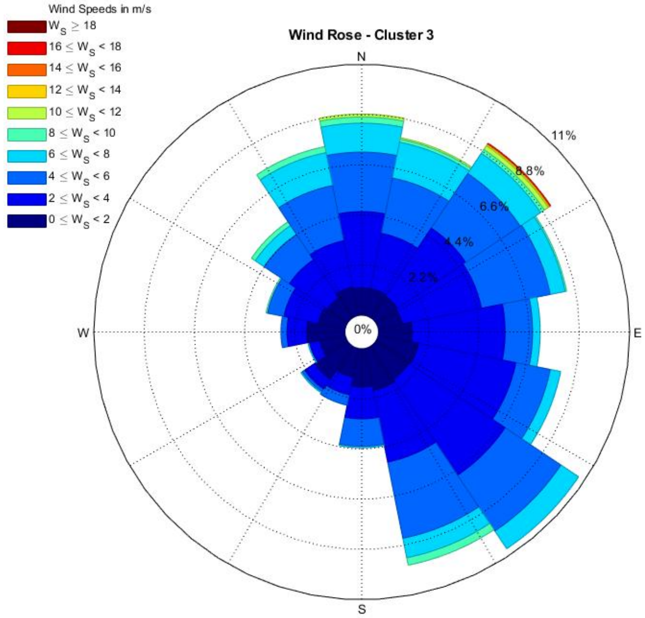


*Figure 4.3.7: Wind Rose - Cluster 3*

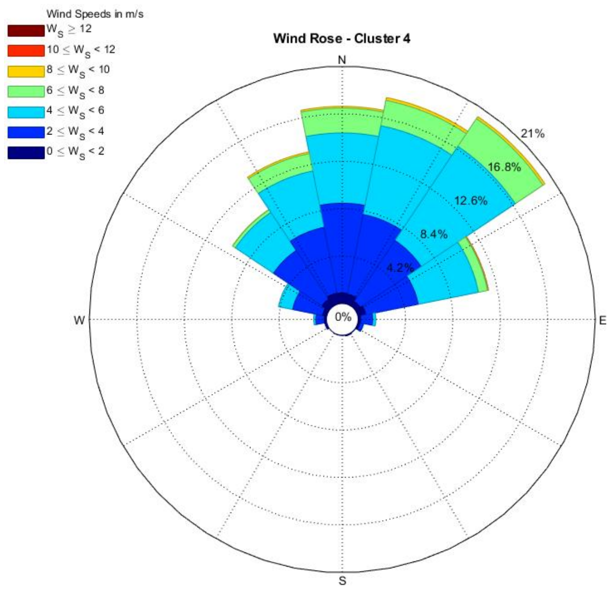


*Figure 4.3.8: Wind Rose - Cluster 4*

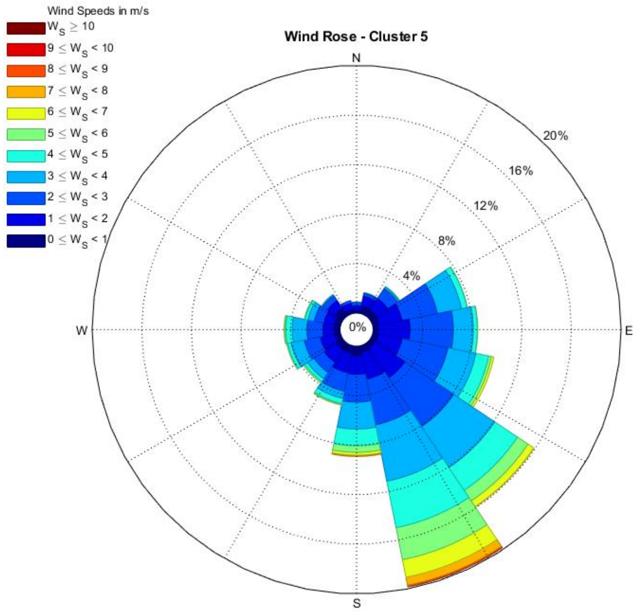


*Figure 4.3.9: Wind Rose - Cluster 5*

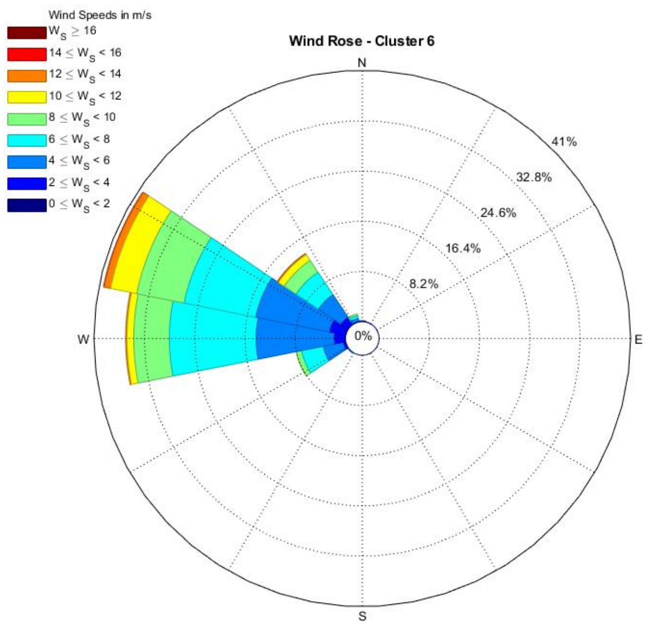


*Figure 4.3.10: Wind Rose - Cluster 6*

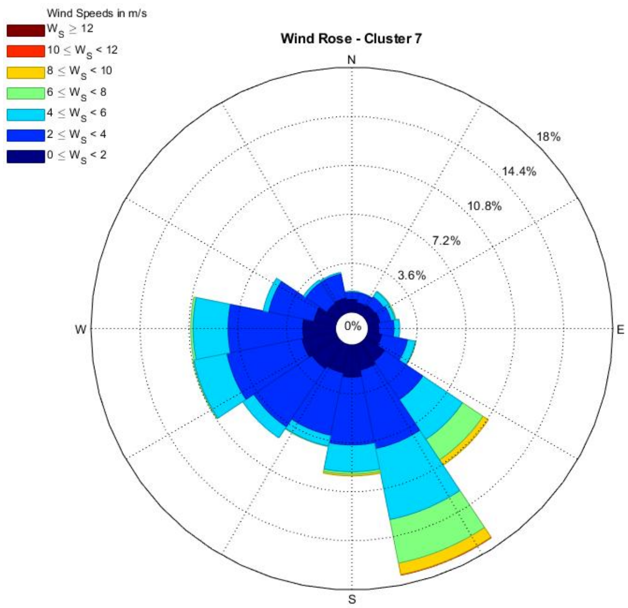


*Figure 4.3.11: Wind Rose - Cluster 7*

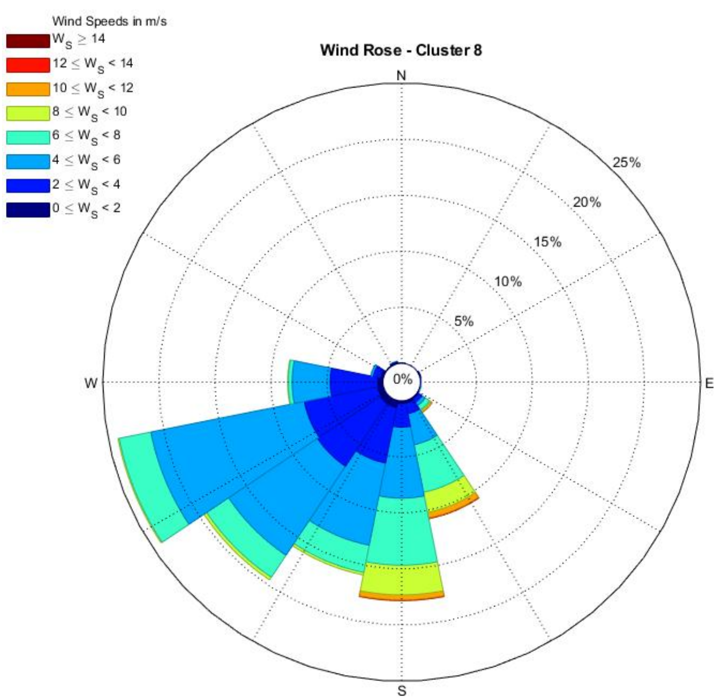


*Figure 4.3.12: Wind Rose - Cluster 8*

*Table 4.3.4: Wind Direction distribution per cluster*

| | | | Wind16 | | | | | | | | | | | | | | | | Total |
|---|---|---|---|---|---|---|---|---|---|---|---|---|---|---|---|---|---|---|---|
| | | | S | SSW | SW | WSW | W | WNW | NW | NNW | N | NNE | NE | ENE | E | ESE | SE | SSE | |
| Cluster | 1 | Count | 0 | 0 | 0 | 0 | 110 | 449 | 751 | 593 | 335 | 128 | 27 | 1 | 0 | 0 | 0 | 0 | 2394 |
| | | % within Cluster8 | 0.0% | 0.0% | 0.0% | 0.0% | 4.6% | 18.8% | 31.4% | 24.8% | 14.0% | 5.3% | 1.1% | 0.0% | 0.0% | 0.0% | 0.0% | 0.0% | 100.0% |
| | 2 | Count | 72 | 61 | 40 | 65 | 107 | 131 | 147 | 132 | 138 | 123 | 179 | 128 | 69 | 74 | 140 | 201 | 1807 |
| | | % within Cluster8 | 4.0% | 3.4% | 2.2% | 3.6% | 5.9% | 7.2% | 8.1% | 7.3% | 7.6% | 6.8% | 9.9% | 7.1% | 3.8% | 4.1% | 7.7% | 11.1% | 100.0% |
| | 3 | Count | 65 | 38 | 37 | 25 | 42 | 53 | 76 | 113 | 132 | 119 | 138 | 126 | 106 | 122 | 160 | 145 | 1497 |
| | | % within Cluster8 | 4.3% | 2.5% | 2.5% | 1.7% | 2.8% | 3.5% | 5.1% | 7.5% | 8.8% | 7.9% | 9.2% | 8.4% | 7.1% | 8.1% | 10.7% | 9.7% | 100.0% |
| | 4 | Count | 1 | 1 | 0 | 6 | 36 | 139 | 328 | 437 | 556 | 593 | 643 | 376 | 50 | 17 | 1 | 3 | 3187 |
| | | % within Cluster8 | 0.0% | 0.0% | 0.0% | 0.2% | 1.1% | 4.4% | 10.3% | 13.7% | 17.4% | 18.6% | 20.2% | 11.8% | 1.6% | 0.5% | 0.0% | 0.1% | 100.0% |
| | 5 | Count | 270 | 148 | 116 | 134 | 137 | 90 | 63 | 32 | 27 | 52 | 87 | 236 | 256 | 302 | 482 | 602 | 3034 |
| | | % within Cluster8 | 8.9% | 4.9% | 3.8% | 4.4% | 4.5% | 3.0% | 2.1% | 1.1% | 0.9% | 1.7% | 2.9% | 7.8% | 8.4% | 10.0% | 15.9% | 19.8% | 100.0% |
| | 6 | Count | 0 | 0 | 3 | 188 | 815 | 916 | 317 | 31 | 4 | 1 | 0 | 0 | 0 | 0 | 0 | 0 | 2275 |
| | | % within Cluster8 | 0.0% | 0.0% | 0.1% | 8.3% | 35.8% | 40.3% | 13.9% | 1.4% | 0.2% | 0.0% | 0.0% | 0.0% | 0.0% | 0.0% | 0.0% | 0.0% | 100.0% |
| | 7 | Count | 224 | 178 | 197 | 250 | 248 | 127 | 72 | 70 | 36 | 35 | 49 | 49 | 54 | 84 | 253 | 402 | 2328 |
| | | % within Cluster8 | 9.6% | 7.6% | 8.5% | 10.7% | 10.7% | 5.5% | 3.1% | 3.0% | 1.5% | 1.5% | 2.1% | 2.1% | 2.3% | 3.6% | 10.9% | 17.3% | 100.0% |
| | 8 | Count | 310 | 276 | 340 | 420 | 148 | 20 | 1 | 4 | 1 | 0 | 0 | 2 | 1 | 2 | 28 | 187 | 1740 |
| | | % within Cluster8 | 17.8% | 15.9% | 19.5% | 24.1% | 8.5% | 1.1% | 0.1% | 0.2% | 0.1% | 0.0% | 0.0% | 0.1% | 0.1% | 0.1% | 1.6% | 10.7% | 100.0% |
| Total | | Count | 942 | 702 | 733 | 1088 | 1643 | 1925 | 1755 | 1412 | 1229 | 1051 | 1123 | 918 | 536 | 601 | 1064 | 1540 | 18262 |
| | | % within Cluster8 | 5.2% | 3.8% | 4.0% | 6.0% | 9.0% | 10.5% | 9.6% | 7.7% | 6.7% | 5.8% | 6.1% | 5.0% | 2.9% | 3.3% | 5.8% | 8.4% | 100.0% |

## Clusters and local Heat Waves

In Figures 4.3.13 and 4.3.14 are presented the heat waves occurrence per 5-year period and per cluster. The 5-year period 2041-2045 shows the highest number of heat waves. The most heat waves were associated with clusters 4 and especially 5 which correspond to clusters with days belong to warm period (see Table 4.3.2).

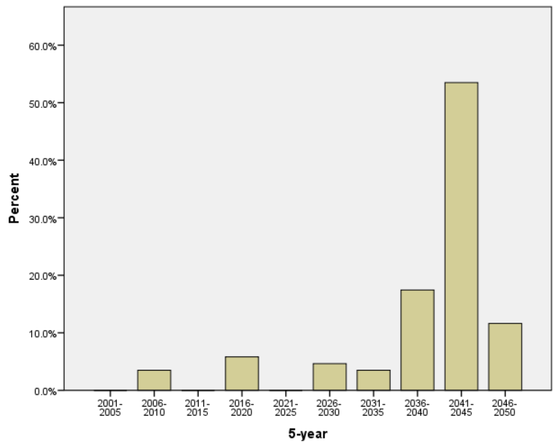


*Figure 4.3.13: Heat Waves per 5-year period*

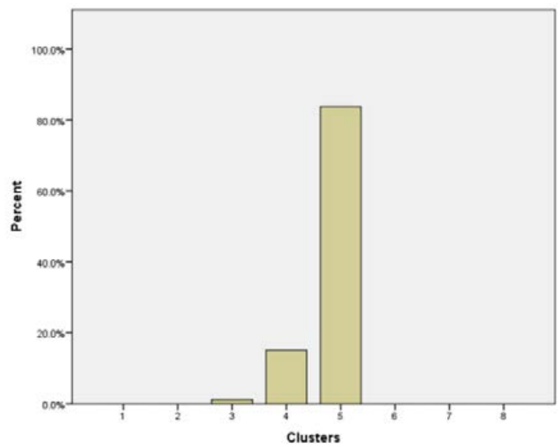


*Figure 4.3.14: Heat Waves per cluster*

## Clusters versus Air Quality level

As it can be seen in Table 4.1 one observation station has been used for the present analysis. The station descriptive statistics for $NO_2$, $O_3$ and $PM_{10}$ is given in Table 4.3.5.

*Table 4.3.5: Air pollutants descriptive statistics*

| | | NO2 | O3 | PM10 |
|---|---|---|---|---|
| Mean | | 43.6719 | 35.4442 | 39.4942 |
| Std. Deviation | | 12.82162 | 20.61489 | 21.83015 |
| Minimum | | 10.84 | 1.11 | 2.71 |
| Maximum | | 112.58 | 104.58 | 254.79 |
| Percentiles | 5 | 23.6700 | 5.4812 | 15.7293 |
| | 25 | 35.0480 | 16.9140 | 25.2500 |
| | 50 | 43.5230 | 34.4800 | 34.3330 |
| | 75 | 51.3320 | 50.7980 | 48.0208 |
| | 95 | 64.7406 | 70.2378 | 81.2815 |

Table 4.2.6 presents the pollutants' concentrations per cluster. Higher mean $NO_2$ concentrations are observed in clusters 1,2 and 7. Higher mean $O_3$ concentrations are observed in clusters 3,4 and 5. Higher mean $PM_{10}$ concentrations are observed in clusters 1,2 and 7.

*Table 4.3.6: Summary pollutant concentrations per cluster*

| | Cluster | | | | | | | |
|---|---|---|---|---|---|---|---|---|
| | 1 | 2 | 3 | 4 | 5 | 6 | 7 | 8 |
| | Mean (SD) | Mean (SD) | Mean (SD) | Mean (SD) | Mean (SD) | Mean (SD) | Mean (SD) | Mean (SD) |
| PM10 (μg/m3) | 45,81 (22,95) | 47,44 (26,64) | 32,65 (13,84) | 29,42 (10,89) | 32,4 (13,19) | 41,59 (20,87) | 48,39 (28,56) | 44,22 (25,24) |
| O3 (μg/m3) | 29,21 (18,58) | 24,08 (14,49) | 46,43 (18,08) | 51,77 (15,92) | 47,89 (17,09) | 30,9 (18,38) | 19,8 (13,89) | 26,1 (18,55) |
| NO2 (μg/m3) | 47,38 (13,17) | 47,61 (14,39) | 41,17 (9,93) | 37,72 (10,14) | 39,47 (10,55) | 46,13 (12,68) | 47,36 (13,54) | 45,91 (13,49) |

The differences in concentrations per cluster are shown in Figures 4.3.15-4.3.17.

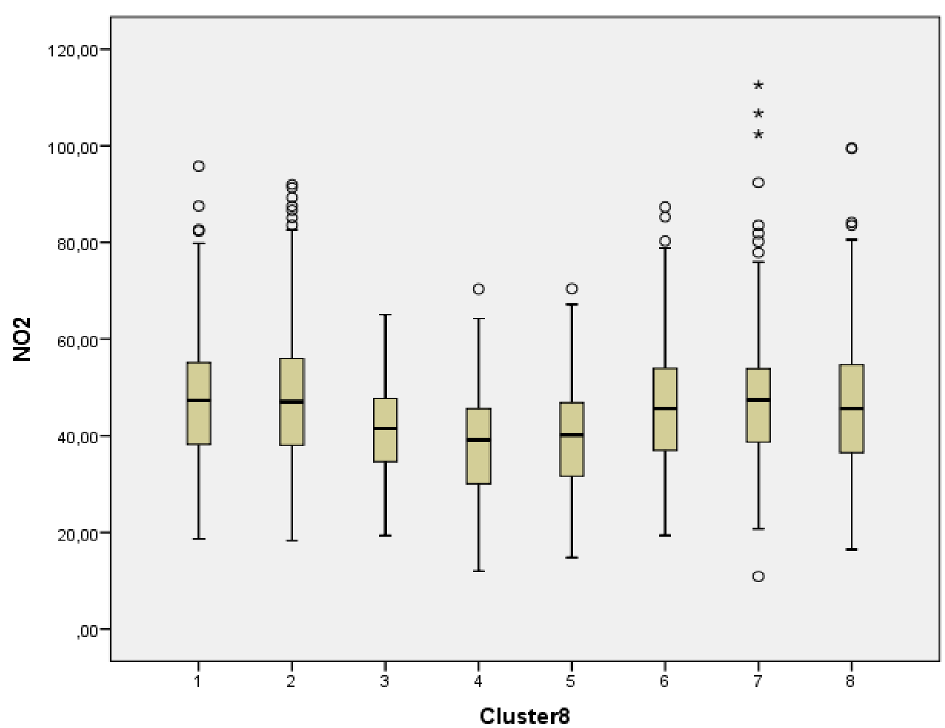


*Figure 4.3.15: $NO_2$ concentration statistics per cluster*

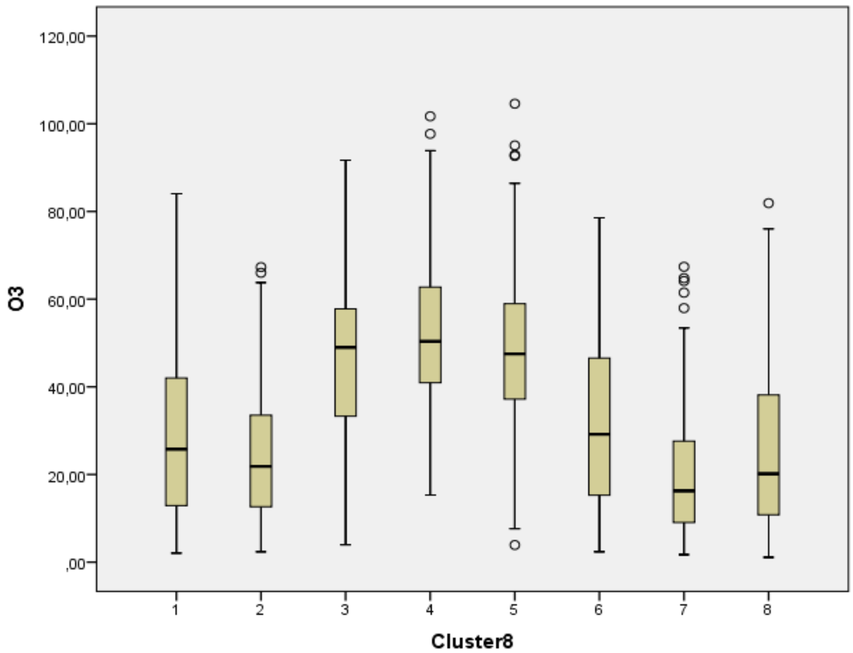


*Figure 4.3.16: $O_3$ concentration statistics per cluster*

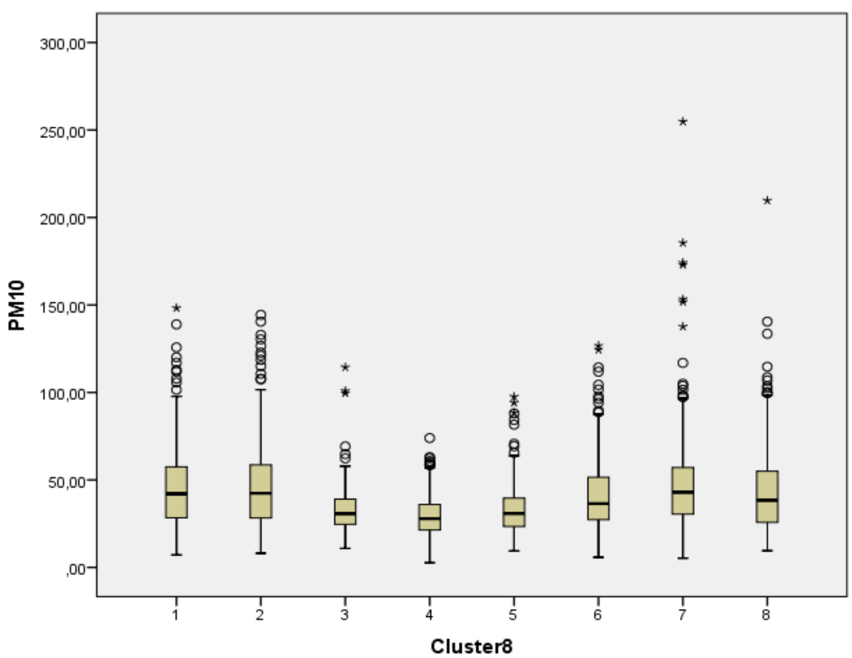


*Figure 4.3.17: $PM_{10}$ concentration statistics per cluster*

## Representative Days

In the following Table 4.3.7 are presented the selected RDs per 5-year period and per cluster.

*Table 4.3.7: Representative days per cluster and 5year period*

| Closest days to centroids per 5year per cluster | | | clusters | | | | | | | |
|---|---|---|---|---|---|---|---|---|---|---|
| | | | 1 | 2 | 3 | 4 | 5 | 6 | 7 | 8 |
| 5 year period | 2001-2005 | 1 | 2001/03/08 | 2005/02/01 | 2002/08/02 | 2004/06/27 | 2003/06/27 | 2003/03/17 | 2001/10/21 | 2004/02/21 |
| | 2006-2010 | 2 | 2009/10/26 | 2006/11/18 | 2008/08/05 | 2010/08/25 | 2006/09/03 | 2010/11/06 | 2007/11/12 | 2010/10/24 |
| | 2011-2015 | 3 | 2012/02/01 | 2015/02/20 | 2011/06/08 | 2011/06/12 | 2012/05/13 | 2011/03/17 | 2014/02/12 | 2014/10/12 |
| | 2016-2020 | 4 | 2018/02/16 | 2016/01/16 | 2017/06/04 | 2017/07/21 | 2020/09/09 | 2018/03/08 | 2019/11/04 | 2020/10/10 |
| | 2021-2025 | 5 | 2023/10/27 | 2022/02/25 | 2022/08/16 | 2021/09/03 | 2022/06/11 | 2024/02/28 | 2023/11/05 | 2025/03/08 |
| | 2026-2030 | 6 | 2028/02/29 | 2027/02/26 | 2030/05/15 | 2030/07/13 | 2029/08/26 | 2027/09/21 | 2028/12/05 | 2026/10/09 |
| | 2031-2035 | 7 | 2035/04/07 | 2031/02/17 | 2035/04/29 | 2033/07/20 | 2031/05/20 | 2034/09/27 | 2034/02/24 | 2034/11/05 |
| | 2036-2040 | 8 | 2038/12/29 | 2039/11/09 | 2040/05/25 | 2036/05/29 | 2036/06/10 | 2036/10/16 | 2037/11/27 | 2036/03/16 |
| | 2041-2045 | 9 | 2045/02/21 | 2043/02/15 | 2044/08/20 | 2044/08/29 | 2044/09/07 | 2042/03/31 | 2045/11/21 | 2041/04/07 |
| | 2046-2050 | 10 | 2050/12/18 | 2049/11/02 | 2049/09/19 | 2048/07/30 | 2049/09/14 | 2048/10/05 | 2049/02/27 | 2049/10/01 |

## Selected Clusters and RDs for modeling purposes

Selected RDs will be used to perform targeted weather and air quality simulations within each selected 5-year period estimating hourly/daily concentrations of the priority pollutants to assess the climatic effect on air quality evolution and the characteristics of air quality future episodes. The selection was based on 3-year periods (2016-2020, 2021-2025 and 2031-2035) and on the clusters with the most elevated concentrations of $PM_{10}$, $NO_2$ and $O_3$. In the case of Brno, cluster 2 recorded the most elevated values of $NO_2$, cluster 4 for the case of $O_3$ and cluster 7 for the case of $PM_{10}$. In Table 4.3.8 are presented the selected days which was used for modeling purposes.

*Table 4.3.8: RDs for modeling purposes*

| **Period** | **Cluster 2 (NO2)** | **Cluster 4 (O3)** | **Cluster 7 (PM)** |
|---|---|---|---|
| 2016-2020 | 2016-01-16 | 2017-07-21 | 2019-11-04 |
| 2021-2025 | 2022-02-25 | 2021-09-03 | 2023-11-05 |
| 2031-2035 | 2031-02-17 | 2033-07-20 | 2034-02-24 |

### 4.3.3 Air Quality Modeling results

#### 4.3.3.1 Overall results

In Figure 4.3.18 the daily average concentrations of $NO_2$, $O_3$, $PM_{10}$ and $PM_{2.5}$ for selected RDs are presented.

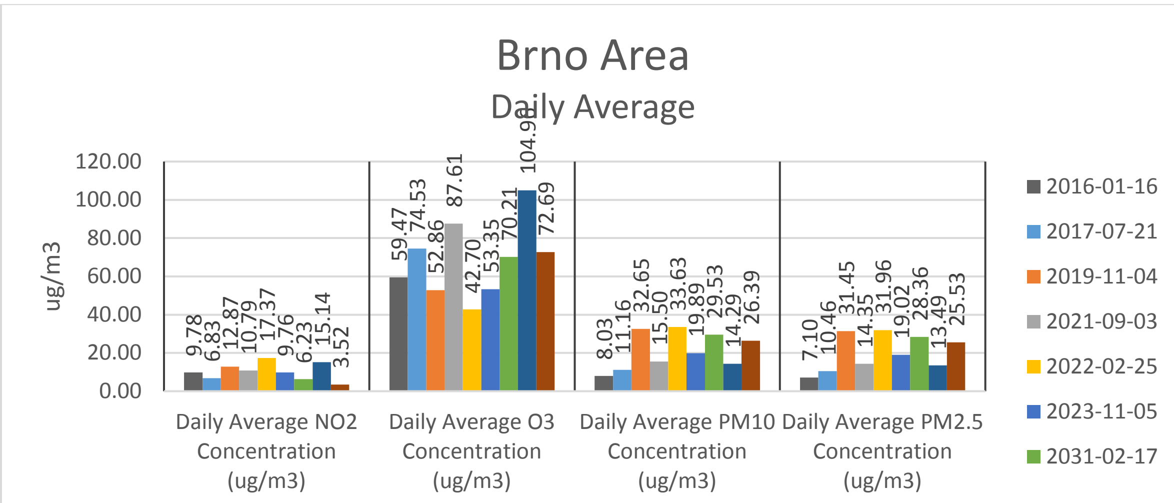


*Figure 4.3.18: Daily average concentrations*

In Figure 4.3.19 the obtained daily averaged concentrations are compared based on USTUTT and EGDAR HTAP emission inventories respectively. The results seem not to differ significantly.

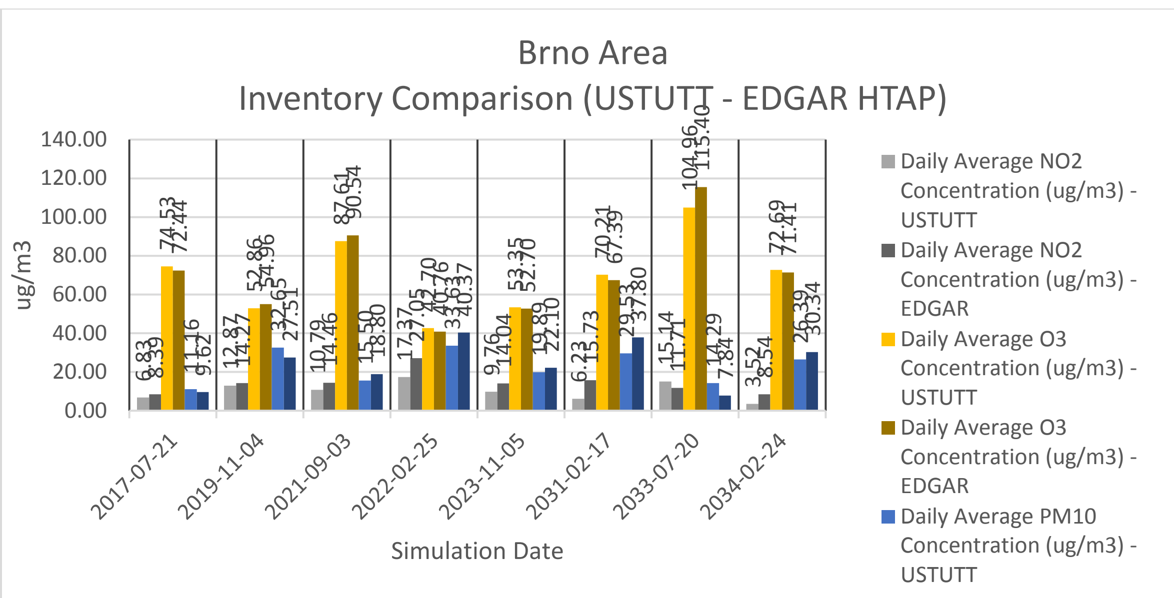


*Figure 4.3.19: Daily average concentrations – USTUTT vs EDGAR HTAP comparison*

#### 4.3.3.2 Clusters results

NO2 Concentrations (Cluster 2)

In Figure 4.3.20, the results are presented in terms of concentrations average, daily maximum and hourly maximum. The diurnal variations are shown in Figure 4.3.21.
The daily maximum concentrations seem to be lower than the EU and WHO yearly limit except one day which is close to 40μg/m$^3$. The maximum hourly concentrations are below the limit of 200μg/m$^3$.

$O_3$ Concentrations (Cluster 4)

In Figure 4.3.22, the results are presented in terms of concentrations average, daily maximum and hourly maximum. The diurnal variations are shown in Figure 4.3.23.
Concentrations show an increasing trend with maximum values exceeding the WHO 8hr limit of 100μg/m$^3$. The maximum hourly concentrations exceed this limit as well as the EU 8hr limit of 120μg/m$^3$.

PM10 Concentrations (Cluster 7)

In Figure 4.3.24, the results are presented in terms of concentrations average, daily maximum and hourly maximum. The diurnal variations are shown in Figure 4.3.25.
The daily maximum concentrations show maximum values exceed the WHO yearly limit of 20μg/m$^3$, however all concentrations are below the daily WHO limit of 50 μg/m$^3$.

### $NO_2$-Cluster 2

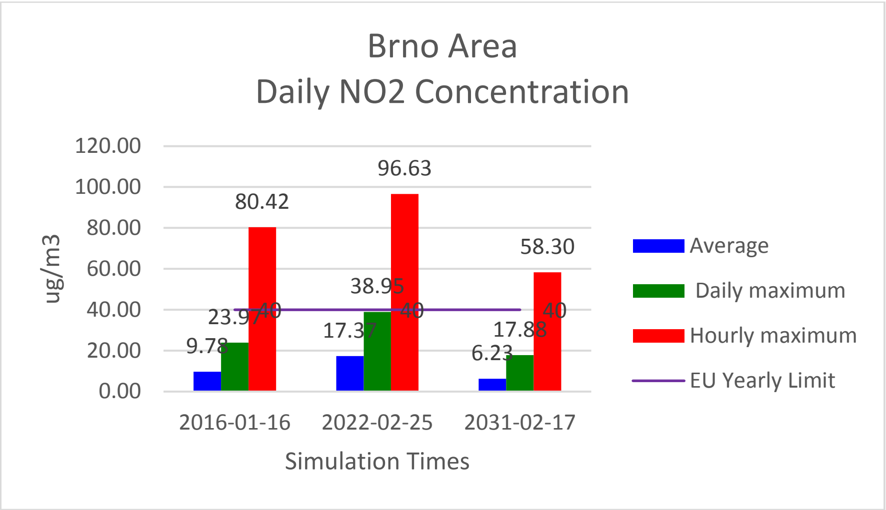


*Figure 4.3.20: Daily $NO_2$ concentrations*

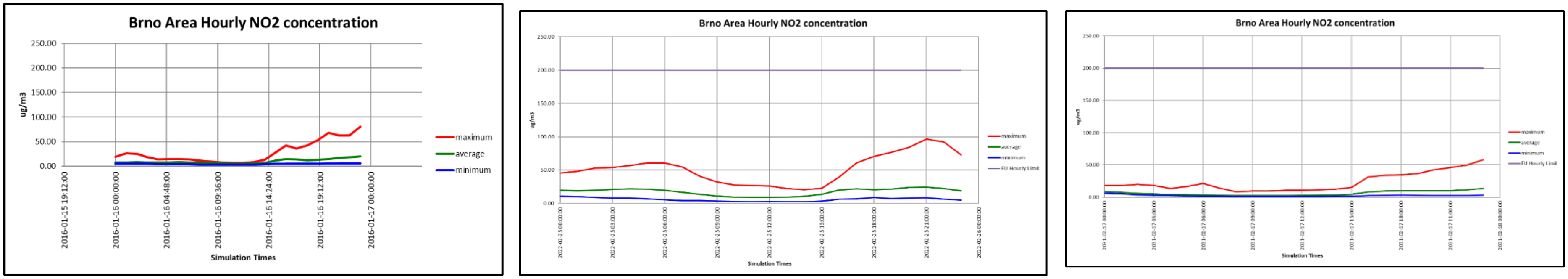


*Figure 4.3.21: Hourly $NO_2$ concentrations*

### $O_3$-Cluster 4

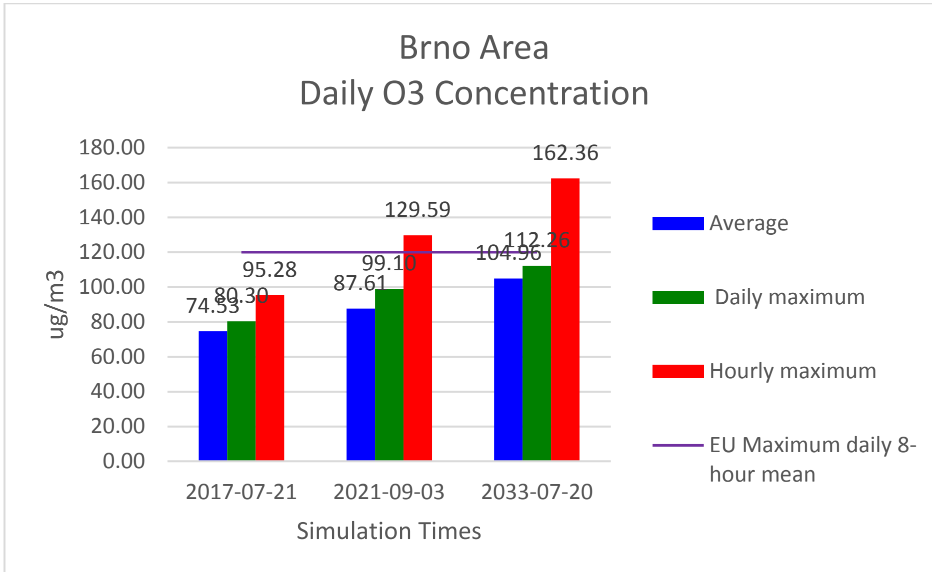


*Figure 4.3.22: $O_3$ Daily concentrations*

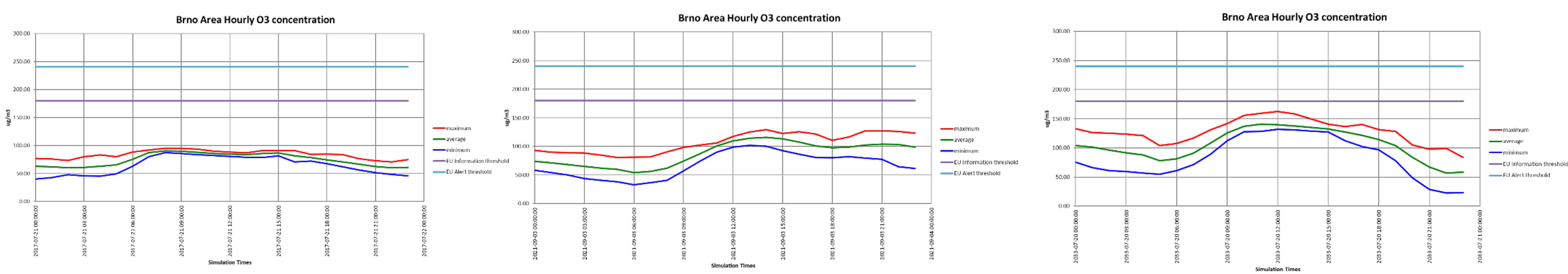


*Figure 4.3.23: $O_3$ Hourly concentrations*

PM$_{10}$-Cluster 7

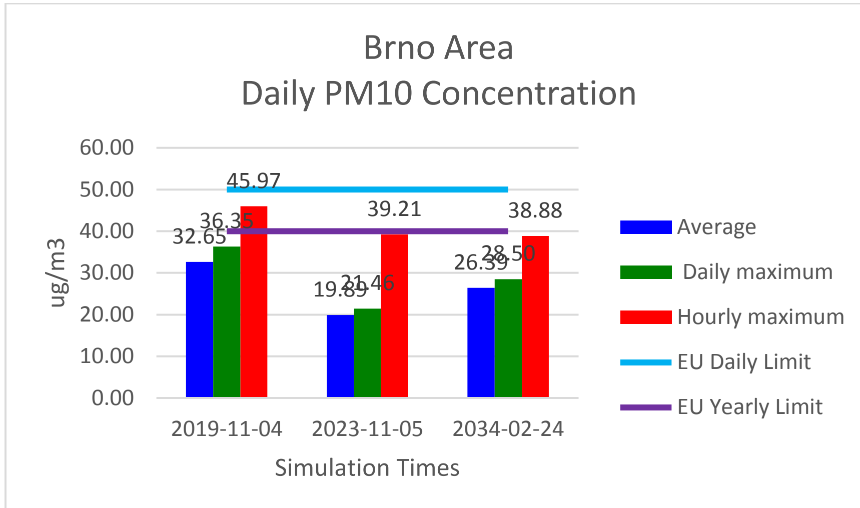


*Figure 4.3.24: PM$_{10}$ Daily concentrations*

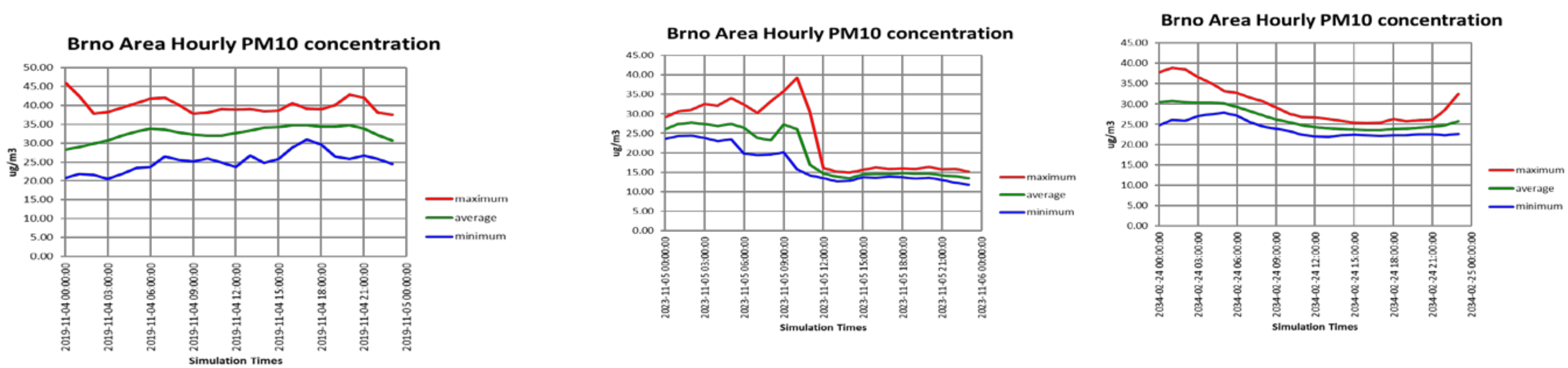


*Figure 4.3.25: PM$_{10}$ Hourly concentrations*

PM$_{2.5}$ Concentrations (Cluster 7)

In Figure 4.3.26, the results are presented in terms of concentrations average, daily maximum and hourly maximum.
The daily maximum concentrations show maximum values well exceeding the WHO yearly limit of 10μg/m$^3$, also are close/over the daily WHO limit of 25μg/m$^3$.

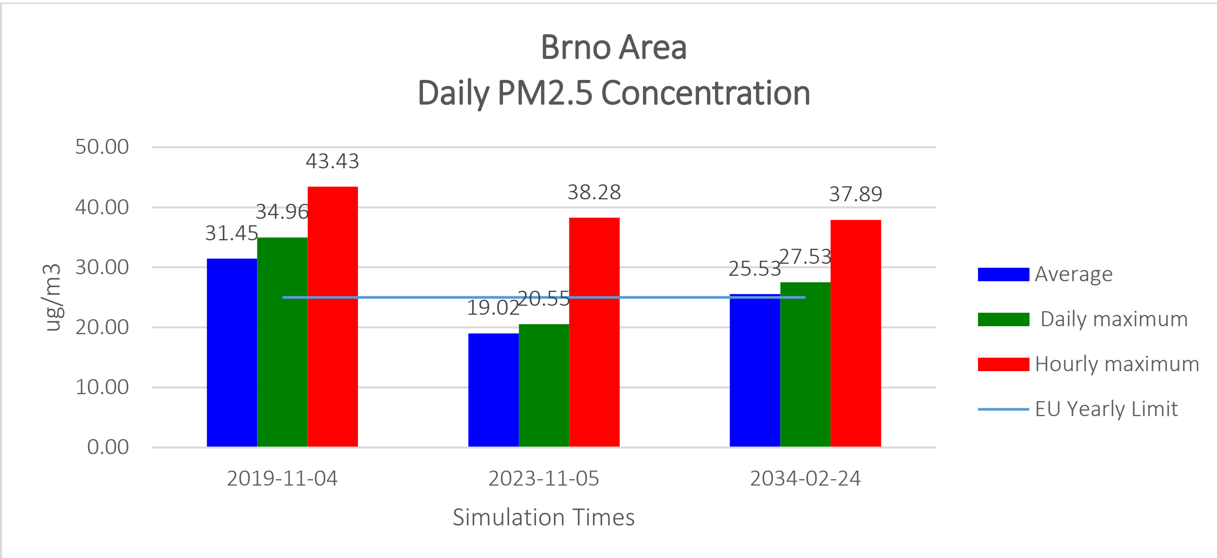


*Figure 4.3.26: PM$_{2.5}$ Daily concentrations*

Figure 4.3.27 presents the estimated BaP daily concentrations contained in PM$_{2.5}$. All days are above WHO annual limit of 0.12ng/m$^3$ and to the EU annual limit of 1ng/m$^3$.

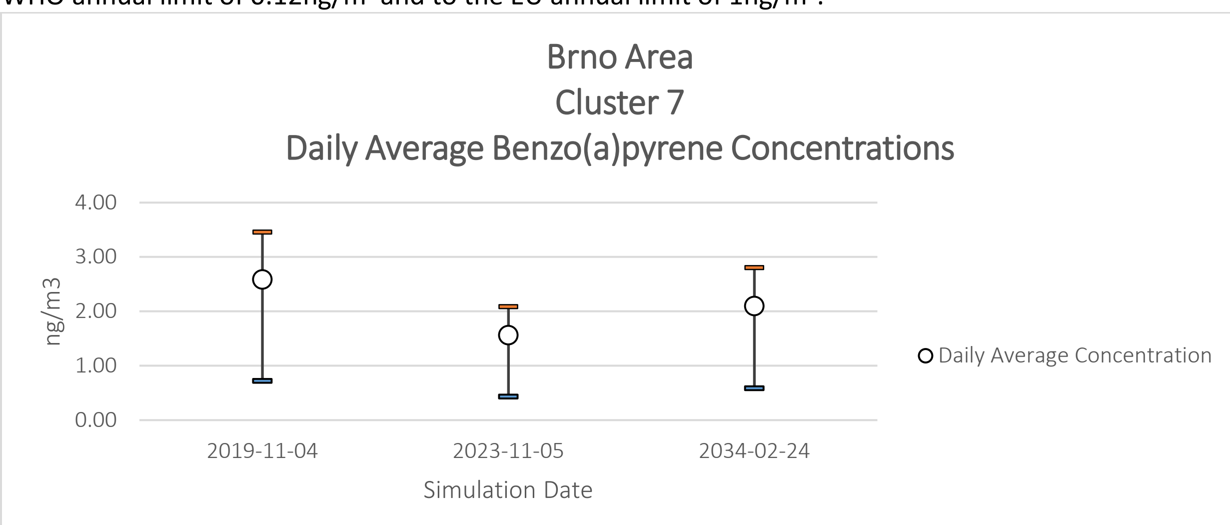


*Figure 4.3.27: BaP Daily concentrations*

#### 4.3.3.3 The Emission Inventory effect

Figures 4.3.28, 4.3.29, 4.3.30 and 4.3.31 illustrate the emission inventory temporal change effect on $NO_2$, $O_3$, $PM_{10}$ and $PM_{2.5}$ concentration levels respectively. There is a clearly decreasing trend in $NO_2$ and slight decrease in $O_3$, on the other hand, slight increases are observed in $PM_{10}$ and $PM_{2.5}$.

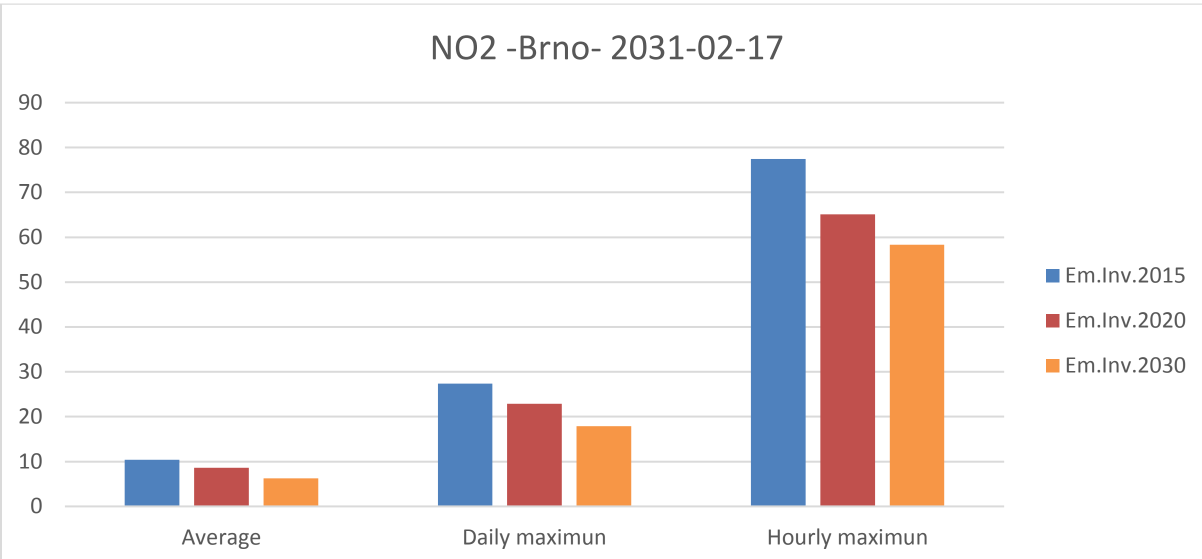


*Figure 4.3.28: $NO_2$ emission inventory comparison*

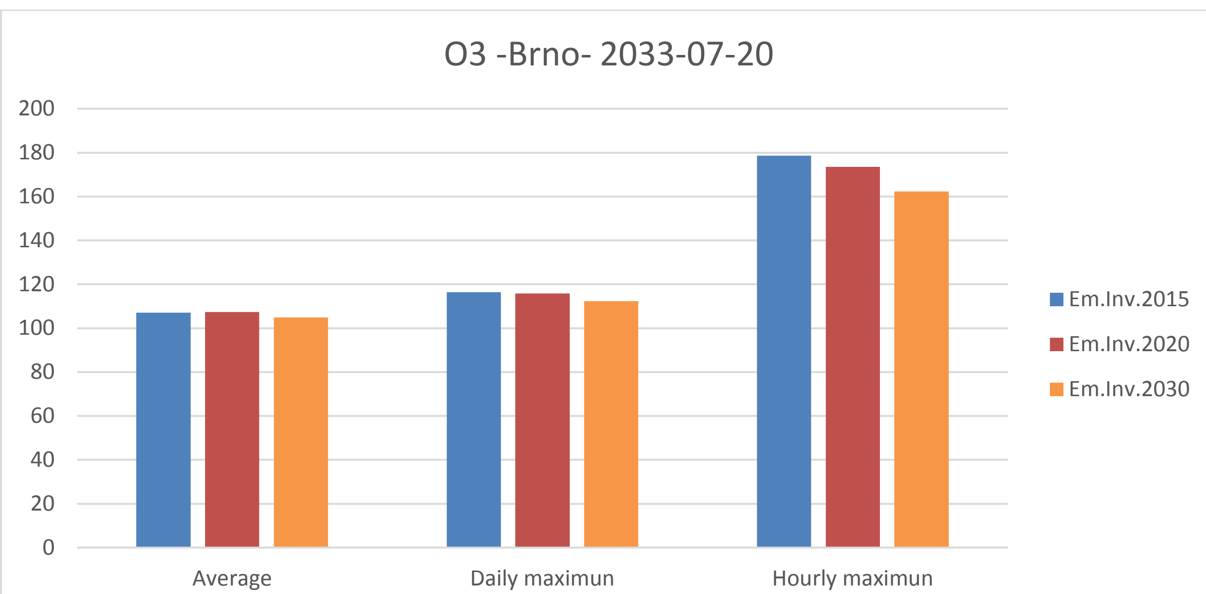


*Figure 4.3.29: $O_3$ emission inventory comparison*

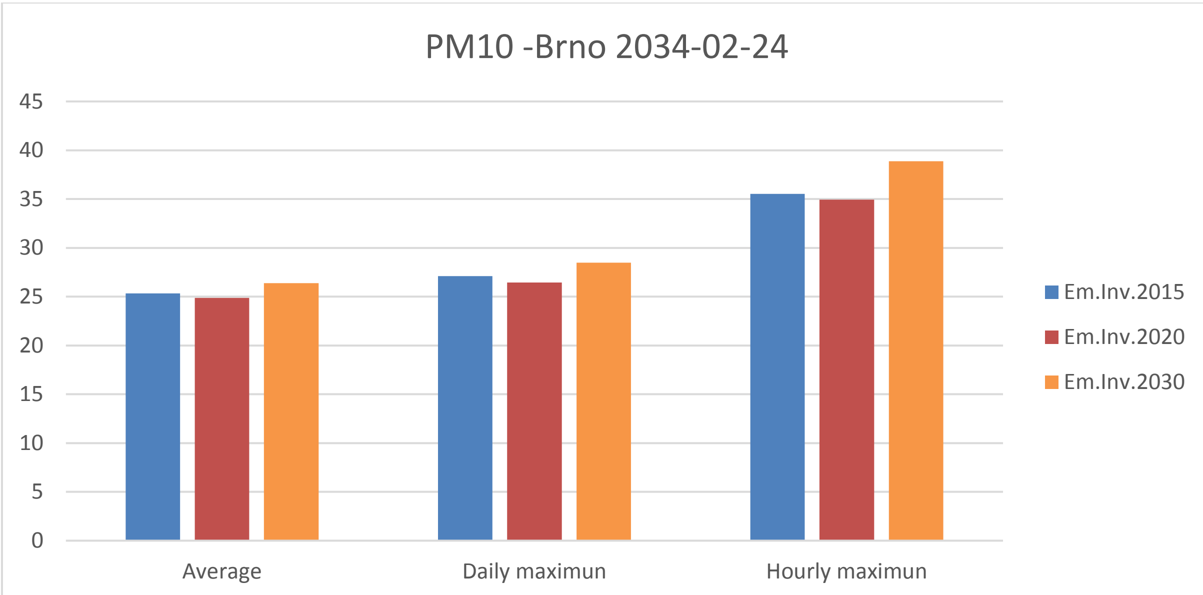


*Figure 4.3.30: $PM_{10}$ emission inventory comparison*

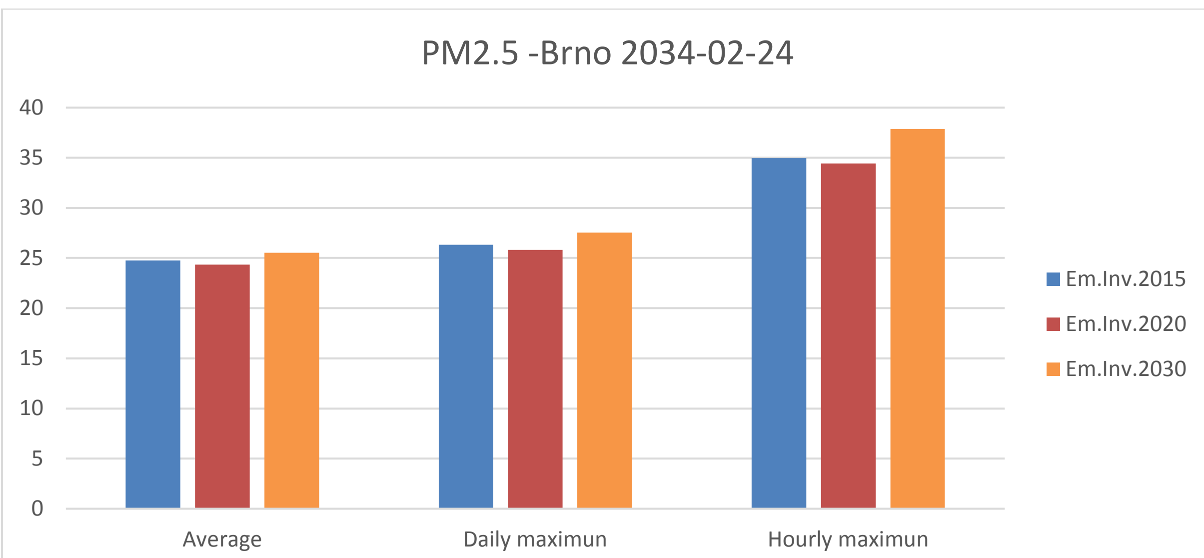


*Figure 4.3.31: $PM_{2.5}$ emission inventory comparison*

### 4.3.4 The GHGs Modeling results

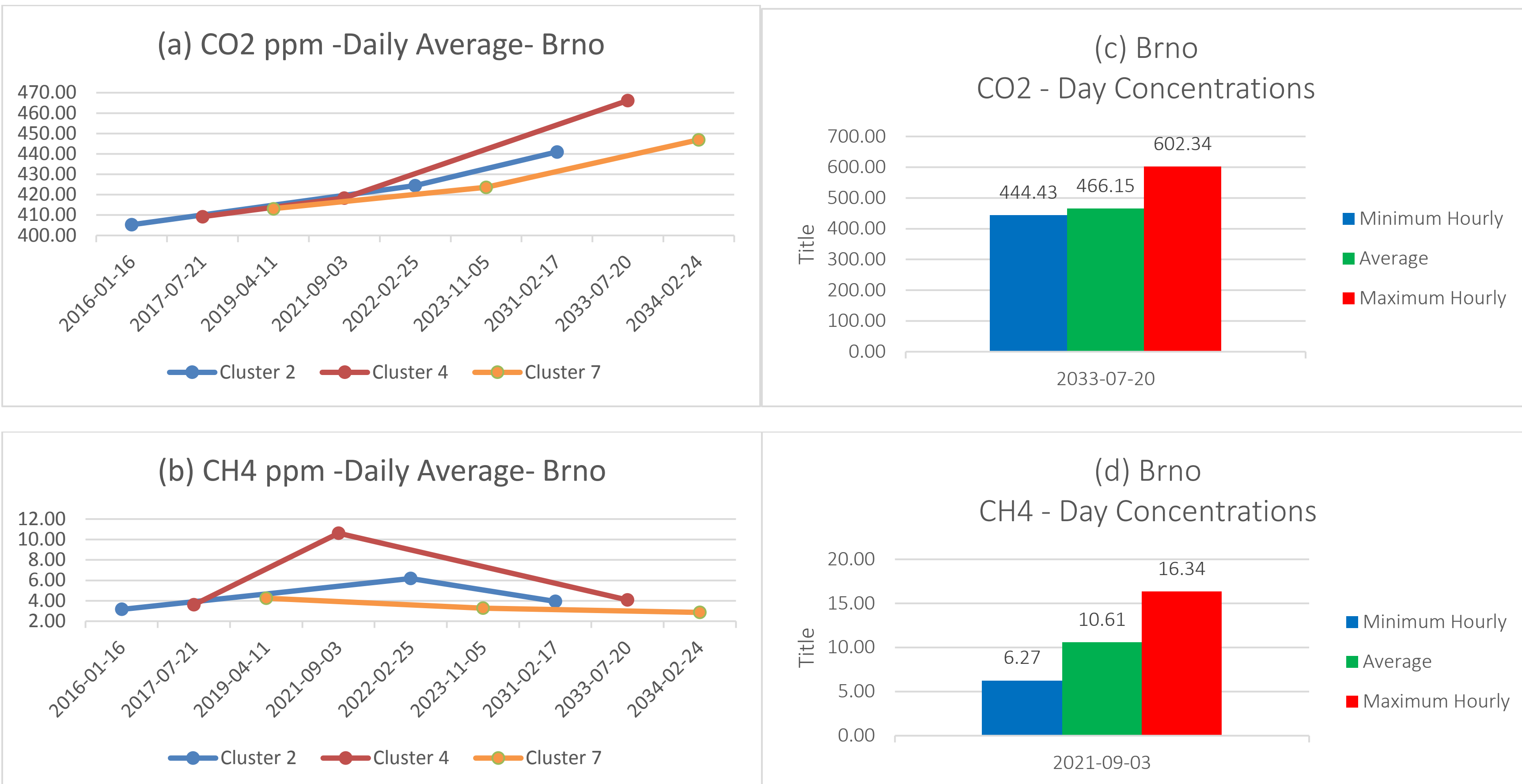


*Figure 4.3.32: (a),(b) $CO_2$ and $CH_4$ Daily average concentrations . (c),(d) $CO_2$ and $CH_4$ concentrations of the most polluted day*

### 4.3.5 Conclusions

For Brno greater area, clusters 1,2,6,7 and 8 could be categorized in cold period and on the other hand clusters 3,4 and 5 in warm period.

In cluster 4 there is a linear increase in frequency occurrence through the ten 5-year periods and a slight increase in 1 and 5. On the other hand, clusters 3 and 7 show a slight decrease.

The 5-year period 2041-2045 shows the highest number of heat waves. The most heat waves were associated with clusters 4 and especially 5 which correspond to clusters with days belong to warm period

Cluster 2 is characterized with elevated $NO_2$ concentrations, cluster 4 with elevated $O_3$ concentrations and cluster 7 with elevated PM concentrations.

$NO_2$ daily maximum concentrations seem to be lower than the EU and WHO yearly limit except one day which is close to 40μg/m$^3$. The maximum hourly concentrations are below the limit of 200μg/m$^3$.

$O_3$ concentrations show an increasing trend with maximum values exceeding the WHO 8hr limit of 100μg/m$^3$. The maximum hourly concentrations exceed this limit as well as the EU 8hr limit of 120μg/m$^3$.

$PM_{10}$ daily maximum concentrations show maximum values exceed the WHO yearly limit of 20μg/m$^3$, however all concentrations are below the daily WHO limit of 50 μg/m$^3$.

$PM_{2.5}$ daily maximum concentrations show maximum values well exceeding the WHO yearly limit of 10μg/m$^3$, also are close/over the daily WHO limit of 25μg/m$^3$.

For all days BaP daily concentrations are above WHO annual limit of 0.12ng/m$^3$ and EU annual limit of 1ng/m$^3$.

Emission reductions intervention shows a decreasing trend in $NO_2$ and slight decrease in $O_3$, on the other hand, slight increases are observed in $PM_{10}$ and $PM_{2.5}$

## 4.4 Basel

### 4.4.1 PCA results

The PCA analysis applied to the Basel data has led to the following results.

Three (3) principal components have been identified as factors for the cluster analysis (Table 4.4.1). Principal Components (PC) explaining 72.65% of the total variance in the initial data.

Factor 1 explains 34.54% of the total variance and contains the 2 temperature variables, mean, daily temperature range and the down ward short-wave radiation.

Factor 2 explains 22.08% of the total variance and contains the atmospheric boundary layer thickness, the U and V wind component and a negative sign of RH.

Factor 3 explains 16.03% of the total variance and contains precipitation and a negative sign of surface pressure.

*Table 4.4.1: The Principal Components results*

| Meteorological parameter | Principal Components | | |
|---|---|---|---|
| | 1 | 2 | 3 |
| Downward short-wave surface radiation | .875 | | |
| Temperature | .812 | | |
| Temperature Range | .742 | | |
| V wind | | .813 | |
| Atmospheric boundary layer thickness | | .804 | |
| U wind | | .645 | |
| RH | | -.622 | |
| Precipitation | | | .799 |
| Surface pressure | | | -.666 |

### 4.4.2 Clustering results

#### Cluster description and trends

As explained in 3.4.4 the selected clusters of the city of Basel are 8. In Figure 4.4.1 are shown the number of days per cluster, where clusters 1,2 and 5 have the most days and cluster 6 and 8 have the less. The monthly distribution per cluster is presented in Table 4.4.2 and in Figure 4.4.2. By dividing the year in two periods, cold and warm, clusters 1,4,6 and 7 could be categorized in cold period and on the other hand clusters 2,5 and 8 in warm period.

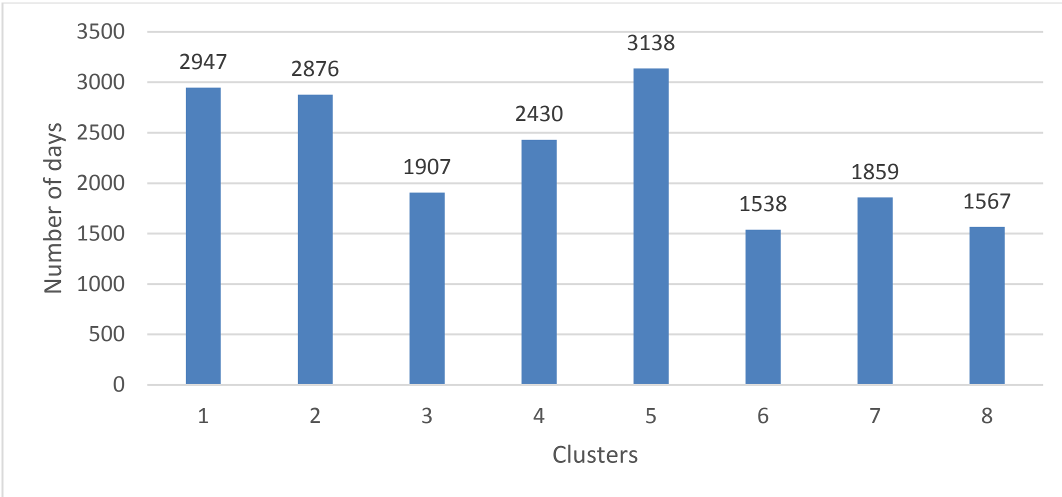


*Figure 4.4.1: Number of Days per cluster*

*Table 4.4.2: Monthly distribution per cluster*

| Count | | | | | | | | | | | | | | |
|---|---|---|---|---|---|---|---|---|---|---|---|---|---|---|
| | | Month | | | | | | | | | | | | Total |
| | | Jan | Feb | Mar | Apr | May | Jun | Jul | Aug | Sep | Oct | Nov | Dec | |
| Cluster8 | 1 | 489 | 381 | 369 | 212 | 80 | 20 | 4 | 4 | 144 | 334 | 425 | 485 | 2947 |
| | 2 | 0 | 0 | 5 | 145 | 340 | 522 | 820 | 754 | 282 | 8 | 0 | 0 | 2876 |
| | 3 | 151 | 211 | 385 | 272 | 25 | 0 | 0 | 3 | 165 | 351 | 214 | 130 | 1907 |
| | 4 | 459 | 379 | 275 | 72 | 20 | 8 | 6 | 1 | 85 | 343 | 397 | 385 | 2430 |
| | 5 | 0 | 4 | 89 | 373 | 703 | 551 | 291 | 476 | 541 | 99 | 11 | 0 | 3138 |
| | 6 | 234 | 227 | 206 | 132 | 37 | 6 | 1 | 9 | 34 | 131 | 220 | 301 | 1538 |
| | 7 | 210 | 180 | 171 | 233 | 147 | 67 | 18 | 38 | 136 | 212 | 212 | 235 | 1859 |
| | 8 | 7 | 30 | 50 | 61 | 198 | 326 | 410 | 265 | 113 | 72 | 21 | 14 | 1567 |
| Total | | 1550 | 1412 | 1550 | 1500 | 1550 | 1500 | 1550 | 1550 | 1500 | 1550 | 1500 | 1550 | 18262 |

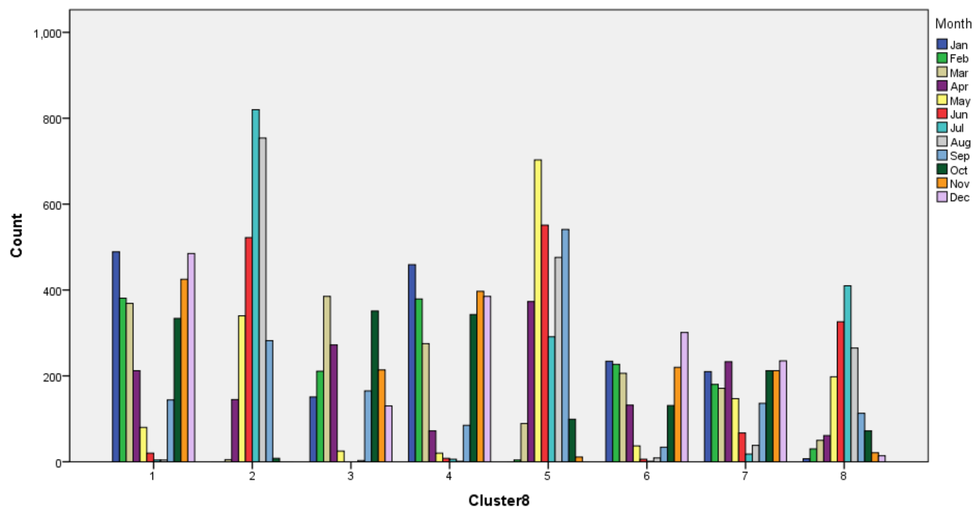


*Figure 4.4.2: Visualized bar chart of monthly distribution per cluster*

A trend analysis of the 5-year frequency of each cluster (Figure 4.4.3). There is an evidence that in clusters 1, 2 and 6 there is a linear increase in frequency occurrence through the ten 5-year periods. On the other hand, clusters 3,4 and 5 show a linear decrease in frequency occurrence. In the rest clusters no clear trends could be pointed out.

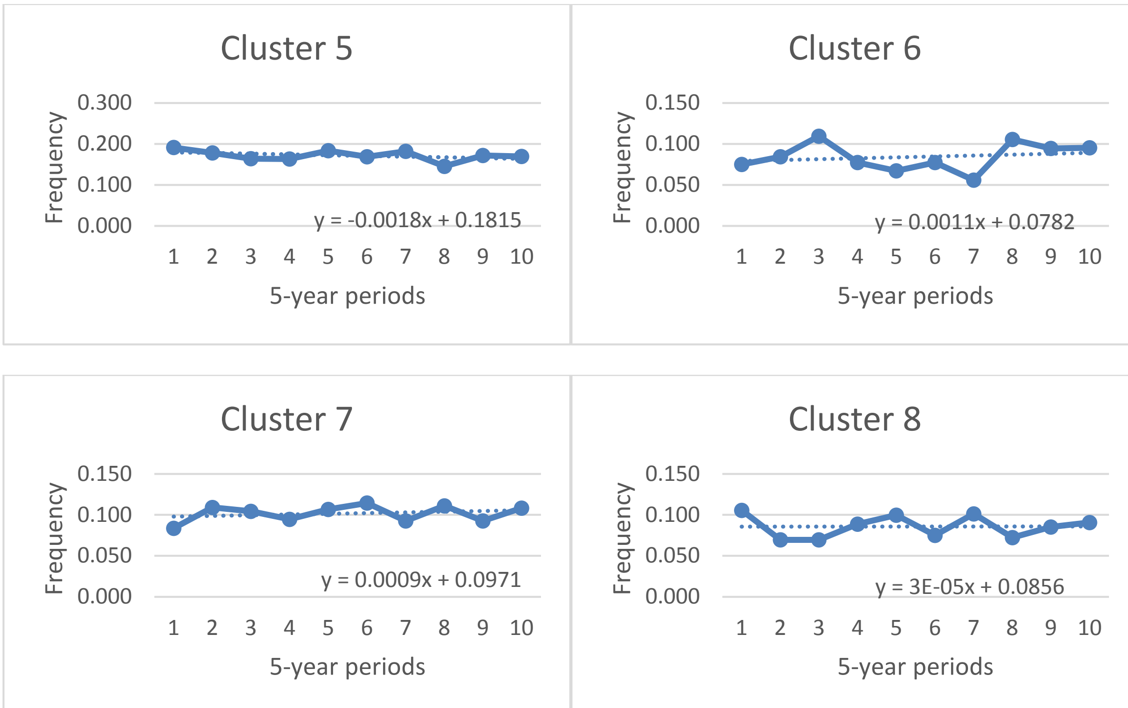


*Figure 4.4.3: Cluster 1-8 frequency trends*

## Cluster characterization

The clusters' implementation is based on the mean values of weather parameters which are displayed in Table 4.4.3.

*Table 4.4.3: Summary of the 8 clusters*

| | Cluster | | | | | | | |
|---|---|---|---|---|---|---|---|---|
| | 1 | 2 | 3 | 4 | 5 | 6 | 7 | 8 |
| | Mean (SD) | Mean (SD) | Mean (SD) | Mean (SD) | Mean (SD) | Mean (SD) | Mean (SD) | Mean (SD) |
| Temperature ( °C) | 3,8 (3,89) | 17,66 (4,68) | 6,58 (5,11) | 0,85 (5,38) | 11,53 (5,23) | 8,34 (3,95) | 6,98 (3,96) | 13,96 (6,19) |
| Daily Temperature Range ( °C) | 4,45 (1,87) | 10,74 (1,63) | 9,51 (2,19) | 5,62 (2,08) | 7,39 (1,6) | 5,94 (2,38) | 4,74 (1,87) | 5,55 (2,01) |
| Relative Humidity (%) | 85,33 (4,93) | 73,74 (6,98) | 67,68 (9,48) | 87,53 (5,95) | 83,26 (4,48) | 67,42 (9,34) | 81,59 (4,72) | 90 (3,82) |

| | | | | | | | | |
|---|---|---|---|---|---|---|---|---|
| Surface Pressure (Pa) | 95144,41 (838,91) | 95548,54 (582,77) | 96337,35 (792,5) | 96107,75 (930,32) | 95334,38 (636,25) | 94915,94 (853,46) | 94326,93 (807,27) | 94940,19 (683,83) |
| Precipitation (kg/m2/s) | 0,000053 (0,00004) | 0,000019 (0,00003) | 0,000005 (0,000013) | 0,000018 (0,000025) | 0,000041 (0,000035) | 0,000034 (0,000035) | 0,000108 (0,000063) | 0,000167 (0,000092) |
| Downward Short Wave Radiation | 80,59 (49,59) | 301,53 (43,72) | 156,2 (67,15) | 92,72 (45,59) | 219,63 (55,44) | 103,39 (67,92) | 108,03 (75,3) | 162,97 (80,37) |
| u wind component (m/s) | 5,54 (2,14) | -0,51 (2,15) | 0,87 (2,65) | 1,16 (2,56) | 1,87 (2,31) | 7,3 (2,27) | 7,5 (2,4) | 0,99 (2,43) |
| v wind component (m/s) | 0,73 (1,78) | -0,41 (1,32) | 1,22 (1,58) | -0,54 (1,62) | -0,9 (1,52) | 4,37 (1,77) | 1,83 (1,78) | -1,94 (1,67) |
| V wind (m/s) | 5,93 (1,95) | 2,26 (1,31) | 3,03 (1,61) | 2,92 (1,52) | 3,19 (1,33) | 8,72 (2,16) | 7,95 (2,3) | 3,37 (1,44) |
| Atmospheric Boundary Layer Thickness (m) | 616,92 (166) | 551,24 (116,16) | 405,48 (169,96) | 309,9 (126,23) | 535,06 (137,26) | 1028,45 (227,52) | 930,2 (203,37) | 428,19 (122,1) |

In addition to the previous Table 4.4.3, Figure 4.4.4 presents the mean normalized (z-score) variables of each cluster, respectively showing the differences of the parameters per cluster.

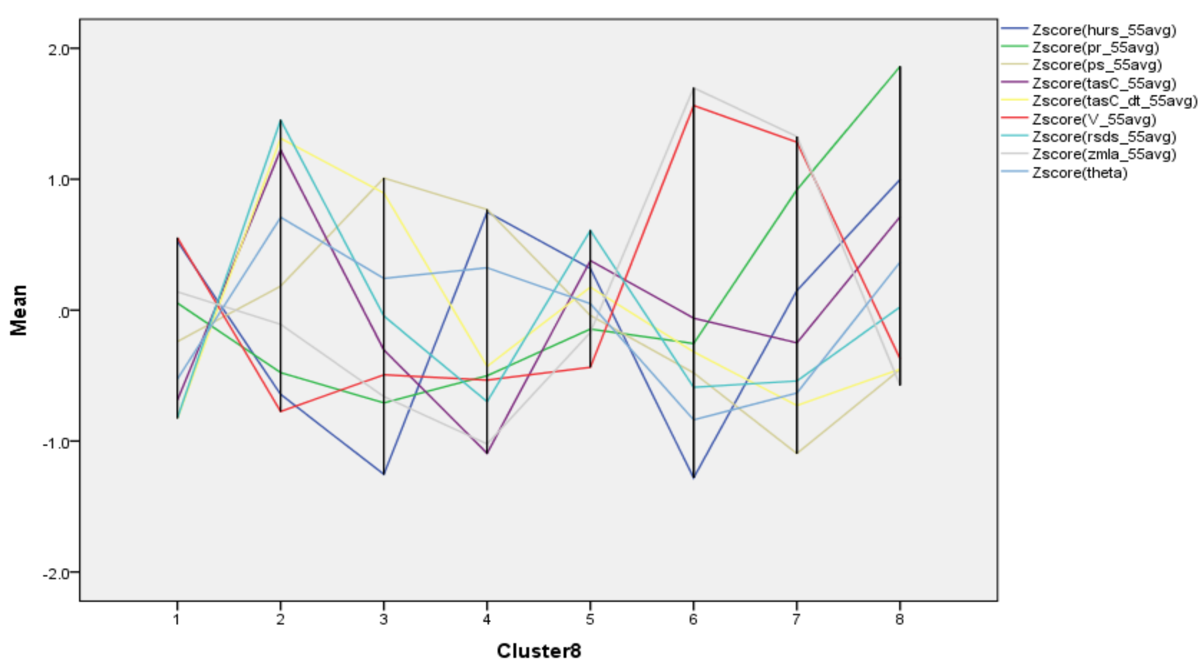


*Figure 4.4.4: Normalized variables (z-score) averaged for each cluster*

Daily, 10-meter from ground level, wind data were used to create the wind roses per each cluster as they are shown in Figures 4.4.5-4.2.12. Each wind direction distribution per cluster is presented in more details in Table 4.4.4.

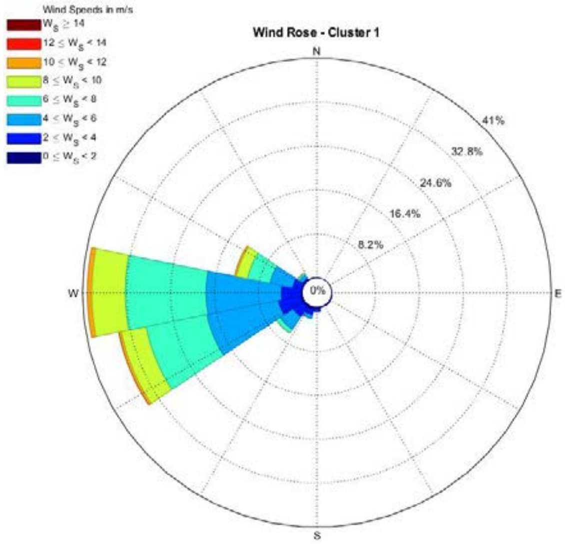


*Figure 4.4.5: Wind Rose - Cluster 1*

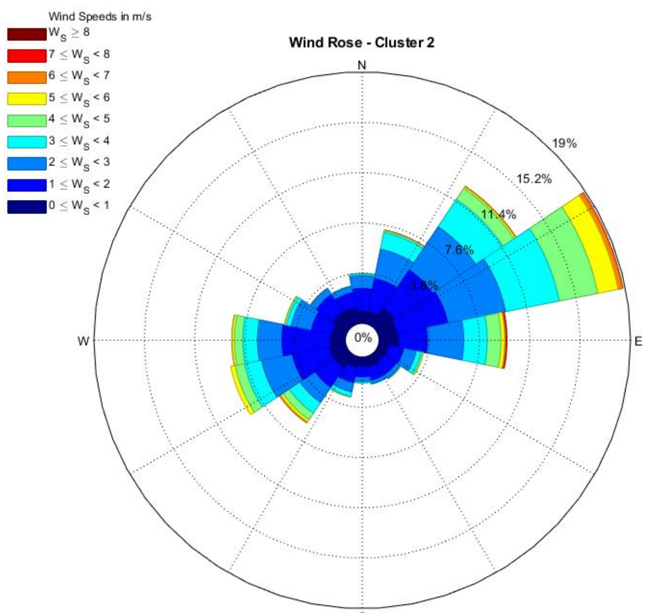


*Figure 4.4.6: Wind Rose - Cluster 2*

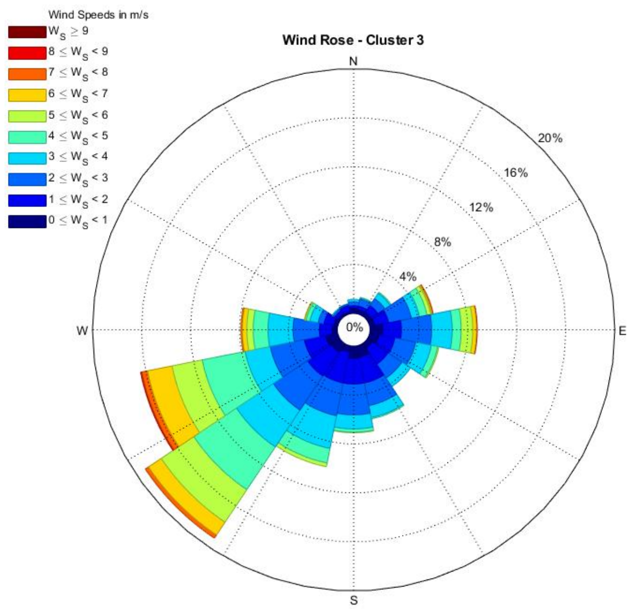


*Figure 4.4.7: Wind Rose - Cluster 3*

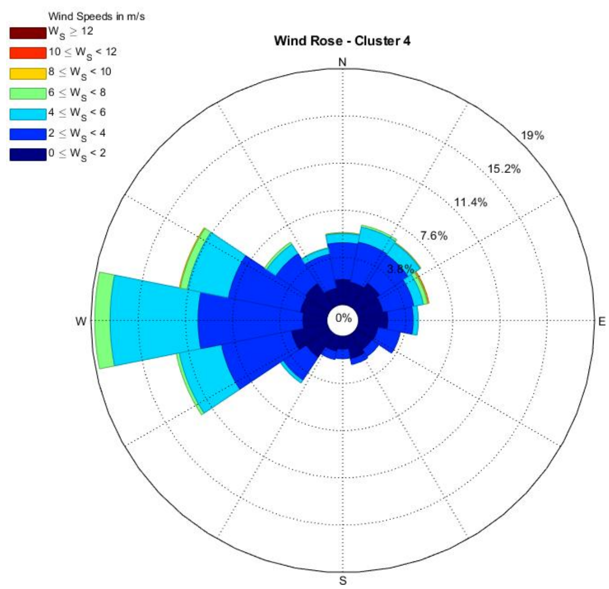


*Figure 4.4.8: Wind Rose - Cluster 4*

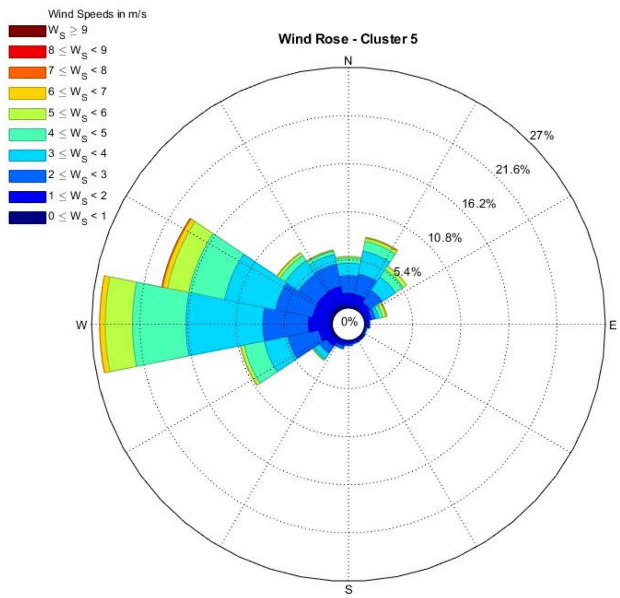


*Figure 4.4.9: Wind Rose - Cluster 5*

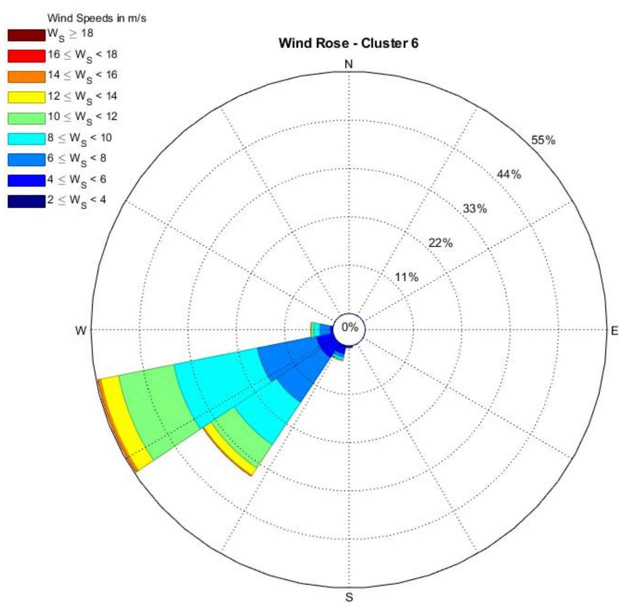


*Figure 4.4.10: Wind Rose - Cluster 6*

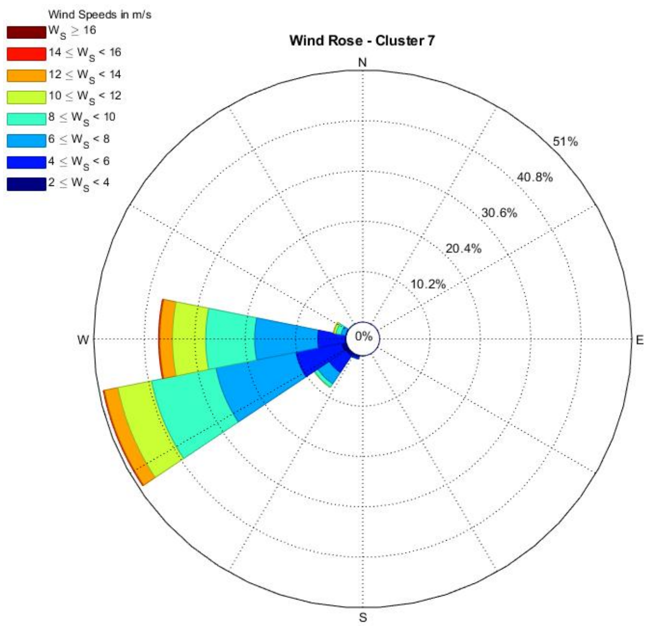


*Figure 4.4.11: Wind Rose - Cluster 7*

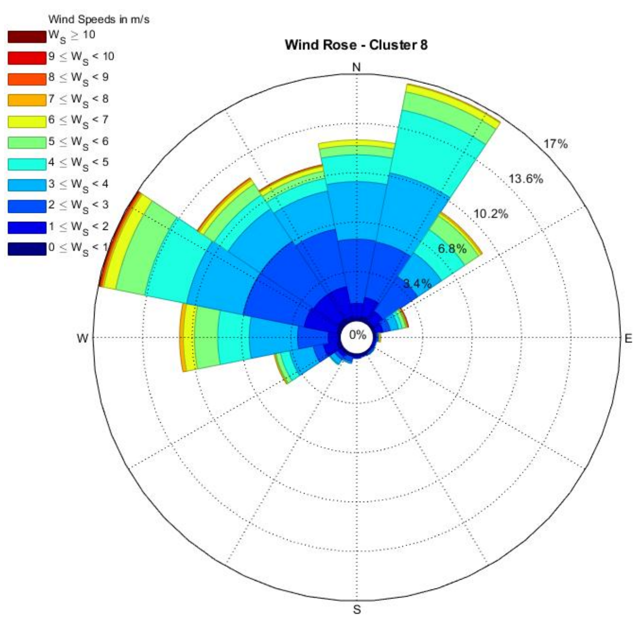


*Figure 4.4.12: Wind Rose - Cluster 8*

*Table 4.4.4: 16 Wind Direction distribution per cluster*

| | | | Wind16 | | | | | | | | | | | | | | | | Total |
|---|---|---|---|---|---|---|---|---|---|---|---|---|---|---|---|---|---|---|---|
| | | | S | SSW | SW | WSW | W | WNW | NW | NNW | N | NNE | NE | ENE | E | ESE | SE | SSE | |
| Cluster8 | 1 | Count | 25 | 65 | 189 | 1031 | 1182 | 381 | 49 | 4 | 2 | 0 | 0 | 1 | 2 | 5 | 7 | 4 | 2947 |
| | | % within Cluster8 | 0.8% | 2.2% | 6.4% | 35.0% | 40.1% | 12.9% | 1.7% | 0.1% | 0.1% | 0.0% | 0.0% | 0.0% | 0.1% | 0.2% | 0.2% | 0.1% | 100.0% |
| | 2 | Count | 57 | 90 | 180 | 255 | 247 | 136 | 100 | 84 | 109 | 208 | 366 | 541 | 278 | 99 | 65 | 61 | 2876 |
| | | % within Cluster8 | 2.0% | 3.1% | 6.3% | 8.9% | 8.6% | 4.7% | 3.5% | 2.9% | 3.8% | 7.2% | 12.7% | 18.8% | 9.7% | 3.4% | 2.3% | 2.1% | 100.0% |
| | 3 | Count | 135 | 192 | 365 | 313 | 150 | 53 | 15 | 16 | 22 | 26 | 45 | 101 | 167 | 110 | 81 | 116 | 1907 |
| | | % within Cluster8 | 7.1% | 10.1% | 19.1% | 16.4% | 7.9% | 2.8% | 0.8% | 0.8% | 1.2% | 1.4% | 2.4% | 5.3% | 8.8% | 5.8% | 4.2% | 6.1% | 100.0% |
| | 4 | Count | 44 | 47 | 116 | 301 | 454 | 295 | 153 | 114 | 141 | 159 | 153 | 141 | 117 | 84 | 54 | 57 | 2430 |
| | | % within Cluster8 | 1.8% | 1.9% | 4.8% | 12.4% | 18.7% | 12.1% | 6.3% | 4.7% | 5.8% | 6.5% | 6.3% | 5.8% | 4.8% | 3.5% | 2.2% | 2.3% | 100.0% |
| | 5 | Count | 20 | 33 | 97 | 331 | 819 | 613 | 247 | 210 | 182 | 255 | 190 | 82 | 20 | 11 | 13 | 15 | 3138 |
| | | % within Cluster8 | 0.6% | 1.1% | 3.1% | 10.5% | 26.1% | 19.5% | 7.9% | 6.7% | 5.8% | 8.1% | 6.1% | 2.6% | 0.6% | 0.4% | 0.4% | 0.5% | 100.0% |
| | 6 | Count | 7 | 55 | 559 | 839 | 78 | 0 | 0 | 0 | 0 | 0 | 0 | 0 | 0 | 0 | 0 | 0 | 1538 |
| | | % within Cluster8 | 0.5% | 3.6% | 36.3% | 54.6% | 5.1% | 0.0% | 0.0% | 0.0% | 0.0% | 0.0% | 0.0% | 0.0% | 0.0% | 0.0% | 0.0% | 0.0% | 100.0% |
| | 7 | Count | 1 | 15 | 157 | 931 | 704 | 50 | 1 | 0 | 0 | 0 | 0 | 0 | 0 | 0 | 0 | 0 | 1859 |
| | | % within Cluster8 | 0.1% | 0.8% | 8.4% | 50.1% | 37.9% | 2.7% | 0.1% | 0.0% | 0.0% | 0.0% | 0.0% | 0.0% | 0.0% | 0.0% | 0.0% | 0.0% | 100.0% |
| | 8 | Count | 5 | 11 | 18 | 73 | 173 | 265 | 189 | 172 | 195 | 261 | 145 | 39 | 8 | 4 | 5 | 4 | 1567 |
| | | % within Cluster8 | 0.3% | 0.7% | 1.1% | 4.7% | 11.0% | 16.9% | 12.1% | 11.0% | 12.4% | 16.7% | 9.3% | 2.5% | 0.5% | 0.3% | 0.3% | 0.3% | 100.0% |
| Total | | Count | 294 | 508 | 1681 | 4074 | 3807 | 1793 | 754 | 600 | 651 | 909 | 899 | 905 | 592 | 313 | 225 | 257 | 18262 |
| | | % within Cluster8 | 1.6% | 2.8% | 9.2% | 22.3% | 20.8% | 9.8% | 4.1% | 3.3% | 3.6% | 5.0% | 4.9% | 5.0% | 3.2% | 1.7% | 1.2% | 1.4% | 100.0% |

## Clusters and local Heat Waves

In Figures 4.4.13 and 4.4.14 are presented the heat waves occurrence per 5-year period and per cluster. The 5-year period 2041-2045 shows the highest number of heat waves, while the next 5-year period shows a decrease. The most heat waves were associated with cluster 2 which correspond to cluster with days belong to warm period (see Table 4.4.2).

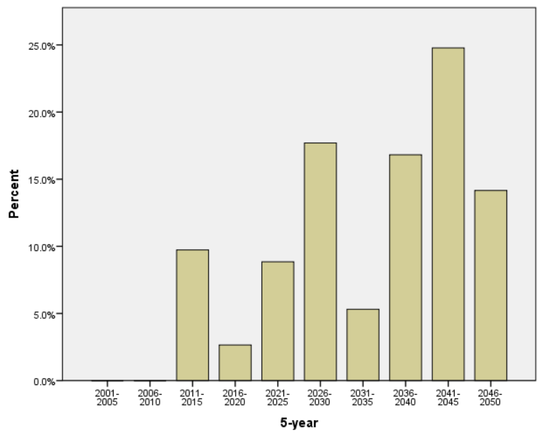


*Figure 4.4.15: Heat Waves per 5-year period*

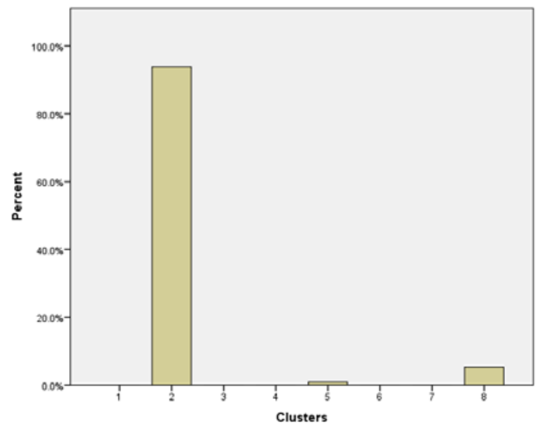


*Figure 4.4.14: Heat Waves per cluster*

## Clusters versus Air Quality level

As it can be seen in Table 4.1 three observation stations have been used for the present analysis. The descriptive statistics for $NO_2$, $O_3$ and $PM_{10}$ is given in Table 4.4.5.

*Table 4.4.5: Air pollutants descriptive statistics*

| | | NO2 | O3 | PM10 |
|---|---|---|---|---|
| Mean | | 40.1989 | 44.4874 | 23.4915 |
| Std. Deviation | | 12.10542 | 26.61284 | 13.10173 |
| Minimum | | 2.95 | 0.79 | 2.75 |
| Maximum | | 101.91 | 140.15 | 120.53 |
| Percentiles | 5 | 21.4872 | 4.3018 | 8.5000 |
| | 25 | 32.0507 | 21.1645 | 14.3000 |
| | 50 | 39.9335 | 46.0875 | 20.5667 |
| | 75 | 48.0404 | 63.4708 | 29.4333 |
| | 95 | 59.9837 | 87.3321 | 49.2358 |

Table 4.4.6 presents the pollutants' concentrations per cluster. Higher mean $NO_2$ concentrations are observed in clusters 1,4 and 6. Higher mean $O_3$ concentrations are observed in clusters 2,5 and 8. Higher mean $PM_{10}$ concentrations are observed in clusters 1,4 and 6.

*Table 4.4.6: Summary pollutant concentrations per cluster*

| | Cluster | | | | | | | |
|---|---|---|---|---|---|---|---|---|
| | 1 | 2 | 3 | 4 | 5 | 6 | 7 | 8 |
| | Mean (SD) | Mean (SD) | Mean (SD) | Mean (SD) | Mean (SD) | Mean (SD) | Mean (SD) | Mean (SD) |
| PM10 (μg/m3) | 27,24 (15,22) | 18,81 (7,26) | 24,9 (13,92) | 27,82 (16,53) | 19,69 (8,4) | 26,43 (15,55) | 24,14 (12,65) | 20,35 (9,63) |
| O3 (μg/m3) | 29,61 (22,68) | 65,68 (20,63) | 35,5 (20,65) | 29,56 (22,01) | 59,94 (20,07) | 30,36 (22,48) | 37,11 (25,38) | 60,48 (23,52) |
| NO2 (μg/m3) | 43,46 (12,39) | 35,99 (10,45) | 41,82 (12,49) | 42,75 (12,97) | 37,59 (10,99) | 42,79 (12,5) | 41,41 (11,54) | 36,84 (10,79) |

The differences in concentrations per cluster are shown in Figures 4.4.15-4.2.17.

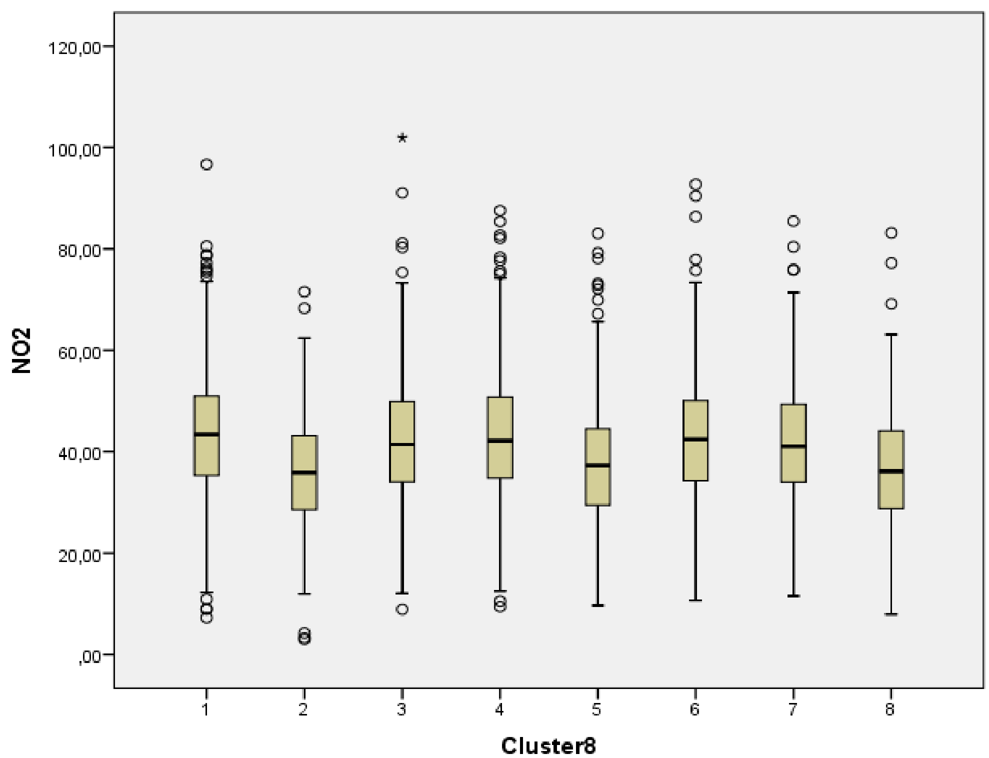


*Figure 4.4.15: $NO_2$ concentration statistics per cluster*

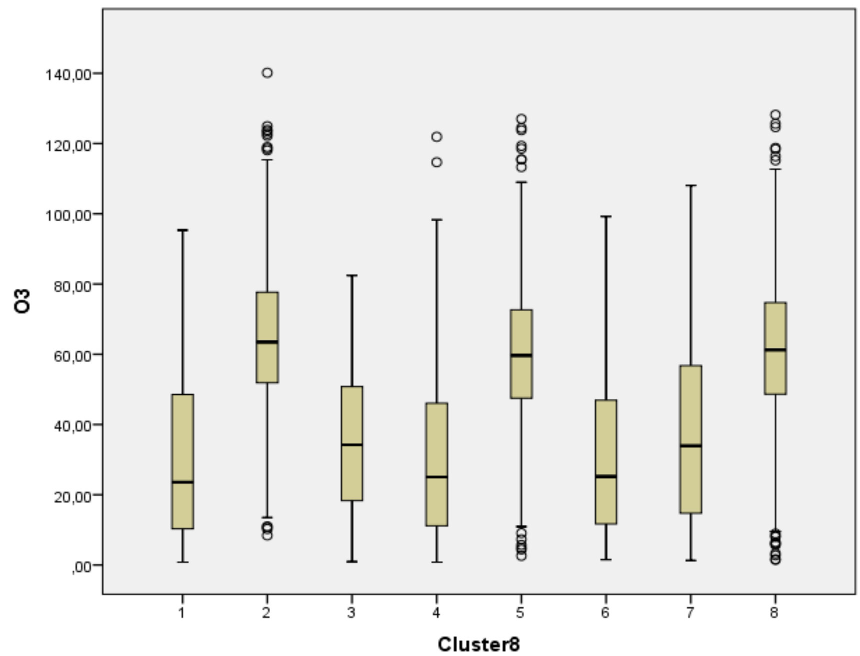


*Figure 4.4.16: $O_3$ concentration statistics per cluster*

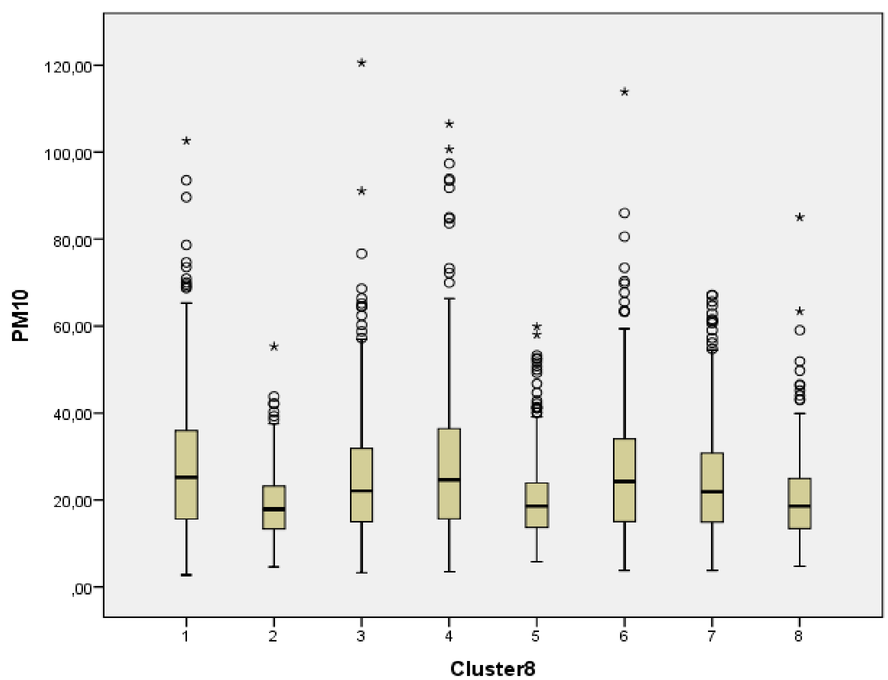


*Figure 4.4.17: $PM_{10}$ concentration statistics per cluster*

## Representative Days

In the following Table 4.4.7 are presented the selected RDs per 5-year period and per cluster.

*Table 4.4.7: Representative days per cluster and 5year period*

| Closest days to centroids per 5year per cluster | | | clusters | | | | | | | |
|---|---|---|---|---|---|---|---|---|---|---|
| | | | 1 | 2 | 3 | 4 | 5 | 6 | 7 | 8 |
| 5 year period | 2001-2005 | 1 | 2004/02/12 | 2002/07/11 | 2004/11/10 | 2001/02/16 | 2005/06/10 | 2003/11/03 | 2004/11/18 | 2005/08/06 |
| | 2006-2010 | 2 | 2009/11/13 | 2008/07/21 | 2008/01/02 | 2007/10/30 | 2010/05/13 | 2007/11/05 | 2009/04/11 | 2010/08/27 |
| | 2011-2015 | 3 | 2011/02/28 | 2013/07/09 | 2013/10/04 | 2011/02/25 | 2011/06/11 | 2012/03/20 | 2013/12/01 | 2015/09/17 |
| | 2016-2020 | 4 | 2018/09/13 | 2018/08/15 | 2019/10/28 | 2017/02/20 | 2017/06/20 | 2020/10/17 | 2016/01/30 | 2020/05/05 |
| | 2021-2025 | 5 | 2021/11/01 | 2023/05/27 | 2021/12/14 | 2024/03/21 | 2022/06/22 | 2021/10/29 | 2025/10/15 | 2025/07/03 |
| | 2026-2030 | 6 | 2028/01/23 | 2026/06/27 | 2026/10/18 | 2030/02/18 | 2029/08/19 | 2029/03/04 | 2029/03/18 | 2030/08/14 |
| | 2031-2035 | 7 | 2031/10/28 | 2035/06/09 | 2035/10/28 | 2035/02/07 | 2031/05/02 | 2032/12/26 | 2031/10/08 | 2035/05/23 |
| | 2036-2040 | 8 | 2036/02/29 | 2040/08/17 | 2039/11/04 | 2039/10/04 | 2038/05/29 | 2038/11/06 | 2037/03/25 | 2036/06/16 |
| | 2041-2045 | 9 | 2045/02/10 | 2041/09/06 | 2041/03/14 | 2045/12/10 | 2044/05/04 | 2044/10/12 | 2041/03/18 | 2045/06/27 |
| | 2046-2050 | 10 | 2046/02/02 | 2050/05/09 | 2048/03/04 | 2046/03/10 | 2046/08/14 | 2048/02/08 | 2048/04/12 | 2046/08/11 |

## Selected Clusters and RDs for modeling purposes

Selected RDs will be used to perform targeted weather and air quality simulations within each selected 5-year period estimating hourly/daily concentrations of the priority pollutants to assess the climatic effect on air quality evolution and the characteristics of air quality future episodes. The selection was based on 3-year periods (2016-2020, 2021-2025 and 2031-2035) and on the clusters with the most elevated concentrations of $PM_{10}$, $NO_2$ and $O_3$. In the case of Basel, cluster 1 recorded the most elevated values of $NO_2$, cluster 2 for the case of $O_3$ and cluster 4 for the case of $PM_{10}$. In Table 4.4.8 are presented the selected days which was used for modeling purposes.

*Table 4.4.8: RDs for modeling purposes*

| **Period** | **Cluster 1 (NO2)** | **Cluster 2 (O3)** | **Cluster 4 (PM)** |
|---|---|---|---|
| 2016-2020 | 2018-09-13 | 2018-08-15 | 2017-02-20 |
| 2021-2025 | 2021-11-01 | 2023-05-27 | 2024-03-21 |
| 2031-2035 | 2031-10-28 | 2035-06-09 | 2035-02-07 |

### 4.4.3 Air Quality Modeling results

#### 4.4.3.1 Overall results

In Figure 4.4.18 the daily average concentrations of $NO_2$, $O_3$, $PM_{10}$ and $PM_{2.5}$ for selected RDs are presented.

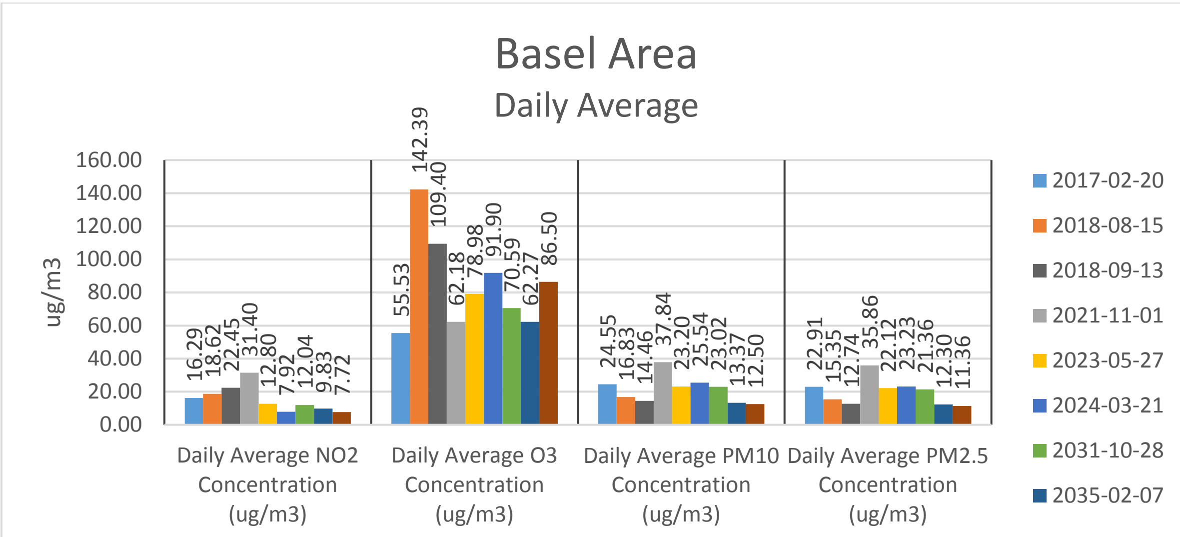


*Figure 4.4.18: Daily average concentrations*

In Figure 4.4.19 the obtained daily averaged concentrations are compared based on USTUTT and EGDAR HTAP emission inventories respectively. The results seem not to differ significantly.

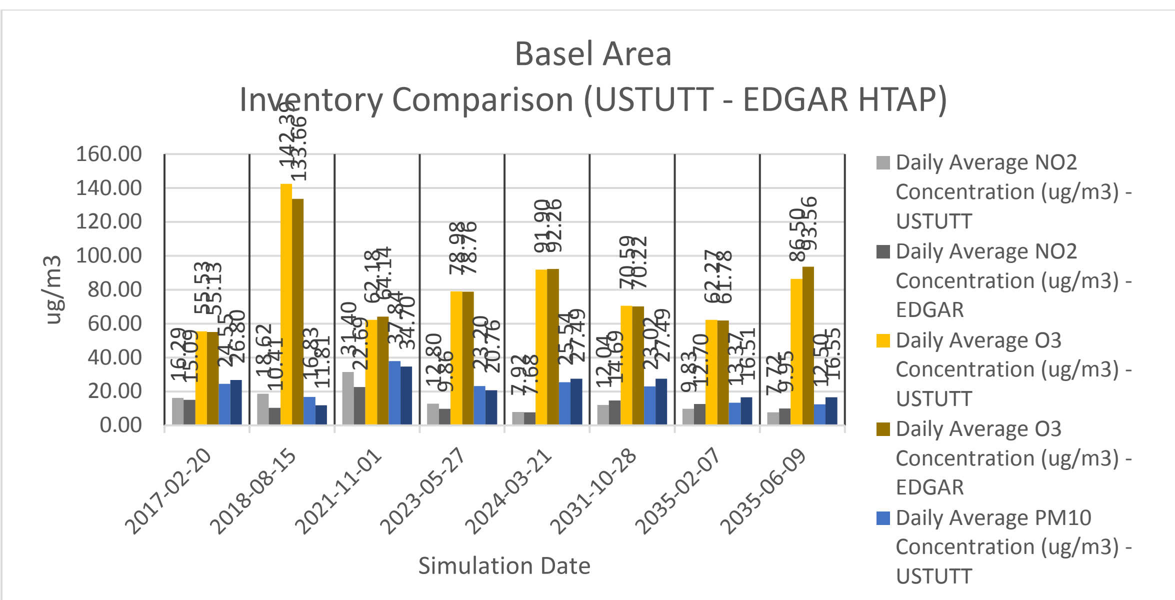


*Figure 4.4.19: Daily average concentrations – USTUTT vs EDGAR HTAP comparison*

#### 4.4.3.2 Clusters results

NO2 Concentrations (Cluster 1)

In Figure 4.4.20, the results are presented in terms of concentrations average, daily maximum and hourly maximum. The diurnal variations are shown in Figure 4.4.21.
Concentrations show a decreasing trend. The daily maximum concentrations exceed the EU and WHO yearly limit of 40μg/m$^3$. The maximum hourly concentrations showing a clear decreasing trend where in 2031 are below the limit of 200μg/m$^3$.

$O_3$ Concentrations (Cluster 2)

In Figure 4.4.22, the results are presented in terms of concentrations average, daily maximum and hourly maximum. The diurnal variations are shown in Figure 4.4.23.
Concentrations show a decreasing trend with maximum values exceeding the WHO 8hr limit of 100μg/m$^3$. The maximum hourly concentrations are close and sometimes above the WHO and the EU 8hr limit of 120μg/m$^3$.

PM10 Concentrations (Cluster 4)

In Figure 4.4.24, the results are presented in terms of concentrations average, daily maximum and hourly maximum. The diurnal variations are shown in Figure 4.4.25.
The daily maximum concentrations exceed the WHO yearly limit of 20μg/m$^3$, however all concentrations are below the daily WHO limit of 50μg/m$^3$ and there is a clear decreasing trend.

NO$_2$-Cluster 1

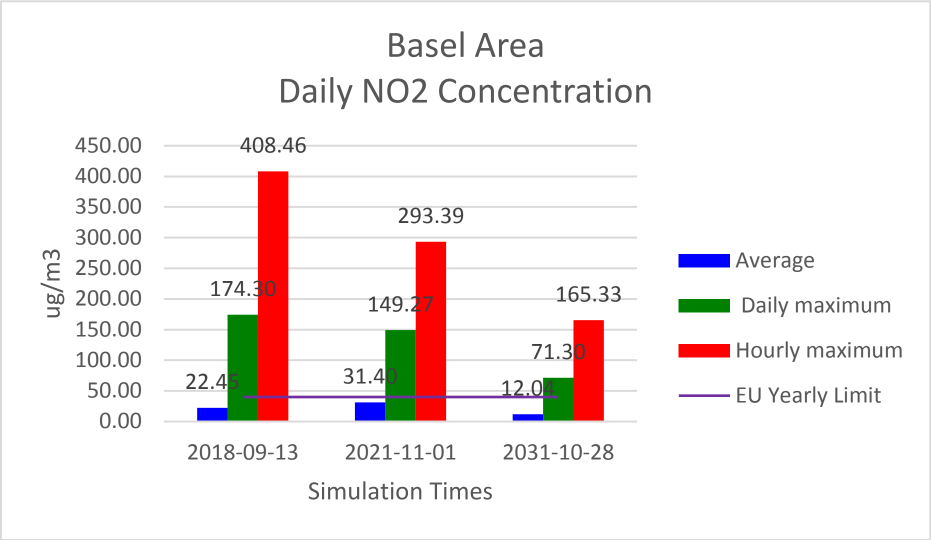


*Figure 4.4.20: NO$_2$ Day concentrations*

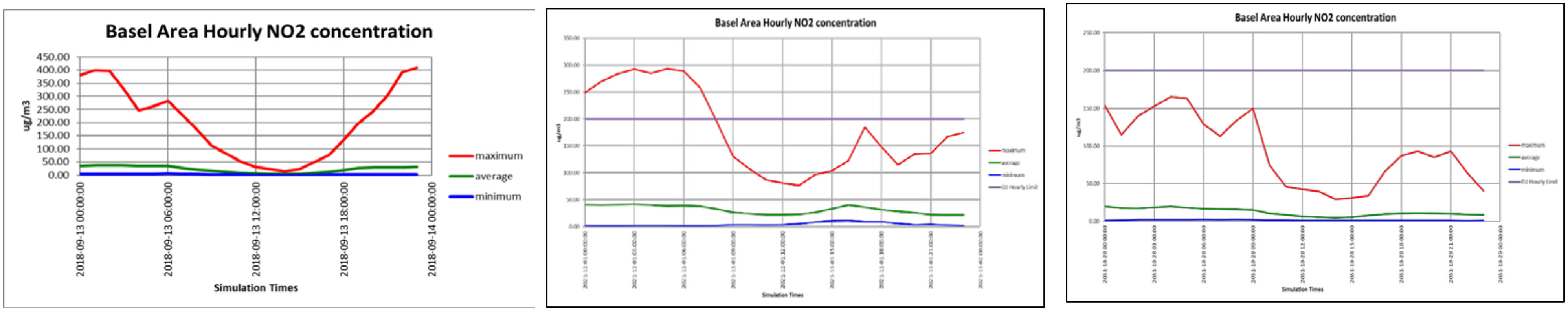


*Figure 4.4.21: Hourly NO$_2$ concentrations*

### $O_3$-Cluster 2

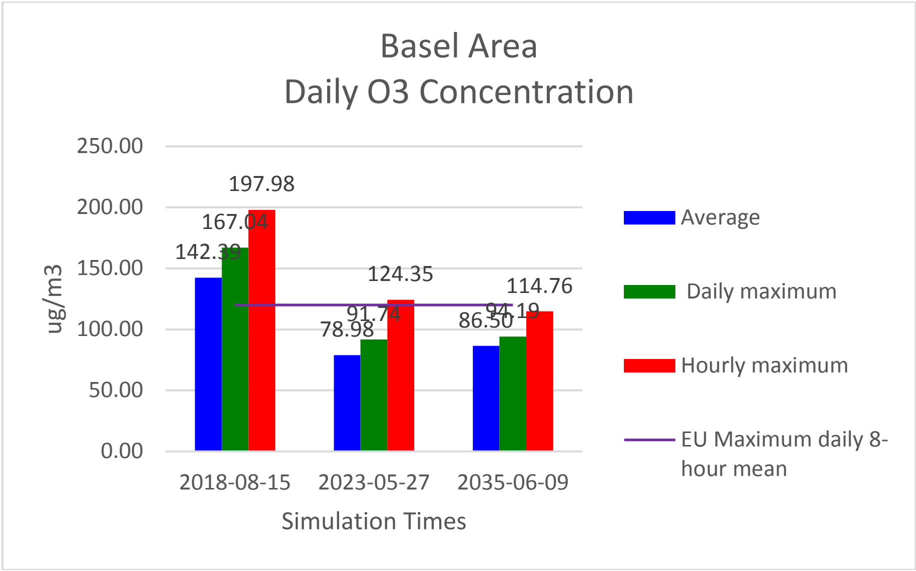


*Figure 4.4.22: $O_3$ Daily concentrations*

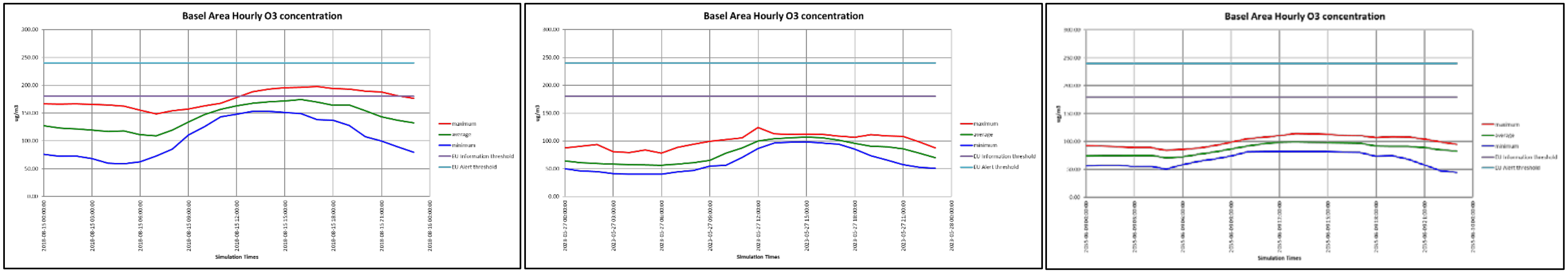


*Figure 4.4.23: $O_3$ Hourly concentrations*

### $PM_{10}$-Cluster 4

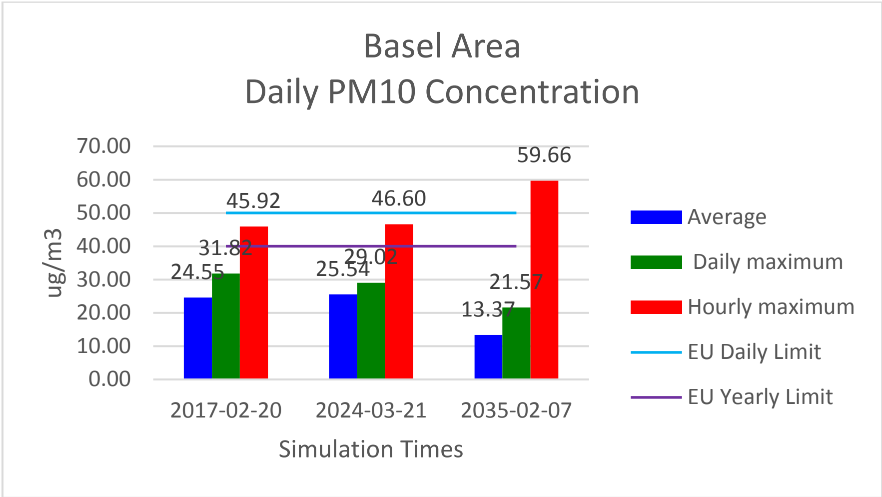


*Figure 4.4.24: $PM_{10}$ Daily concentrations*

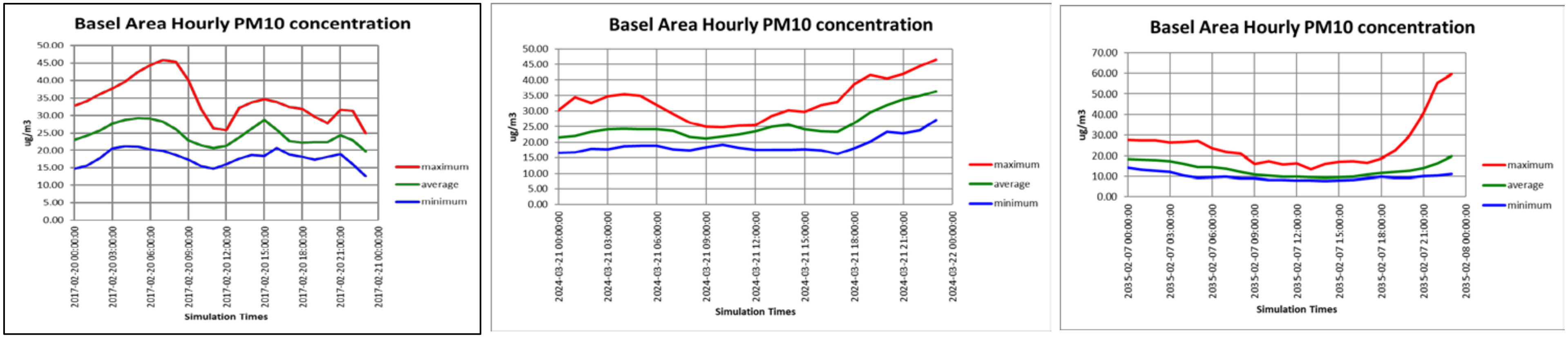


*Figure 4.4.25: $PM_{10}$ Hourly concentrations*

$PM_{2.5}$ Concentrations (Cluster 4)

In Figure 4.4.26, the results are presented in terms of concentrations average, daily maximum and hourly maximum.
The daily maximum concentrations exceed the WHO yearly limit of 10μg/m$^3$ following a decreasing trend.

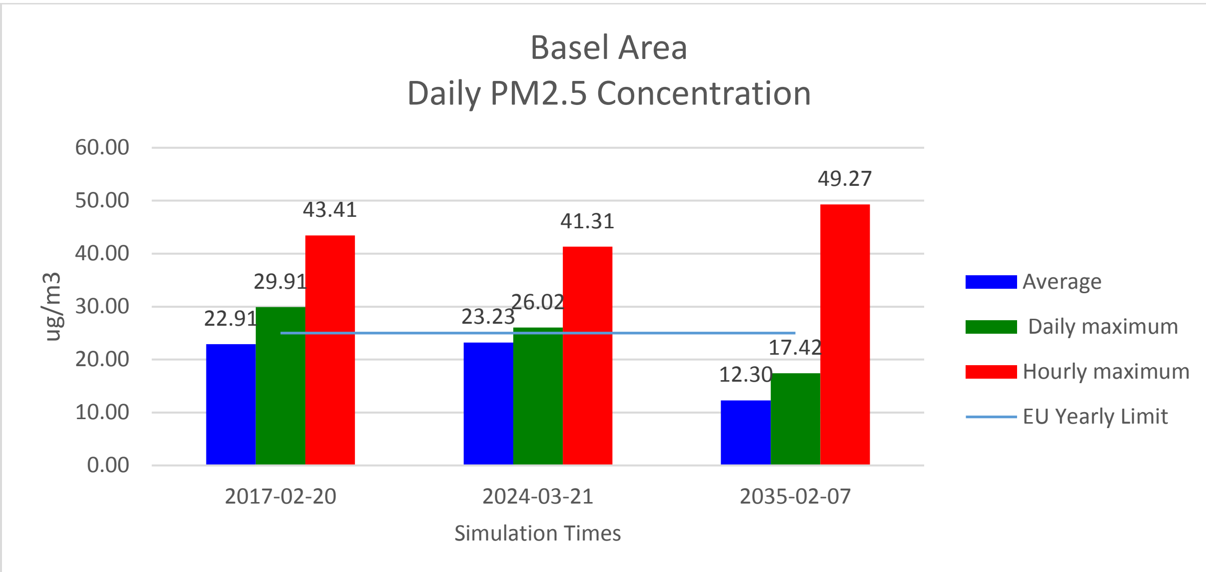


*Figure 4.4.26: $PM_{2.5}$ Day concentrations*

Figure 4.4.27 presents the estimated BaP daily concentrations contained in $PM_{2.5}$. All days are above WHO annual limit of 0.12ng/m$^3$ and only one day is on the EU annual limit of 1ng/m$^3$.

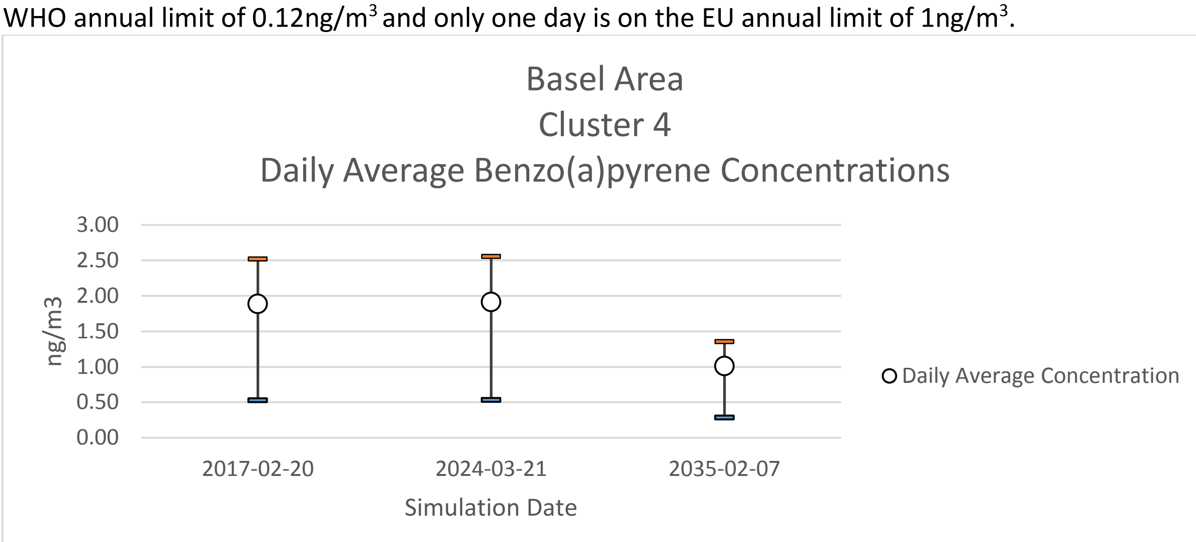


*Figure 4.4.27: BaP daily concentrations*

### 4.4.3.3 The Emission Inventory effect

Figures 4.4.28, 4.3.29, 4.3.30 and 4.3.31 illustrate the emission inventory temporal change effect on $NO_2$, $O_3$, $PM_{10}$ and $PM_{2.5}$ concentration levels respectively. There is a clearly decreasing trend in all pollutants indicating the positive effect on emission reductions intervention.

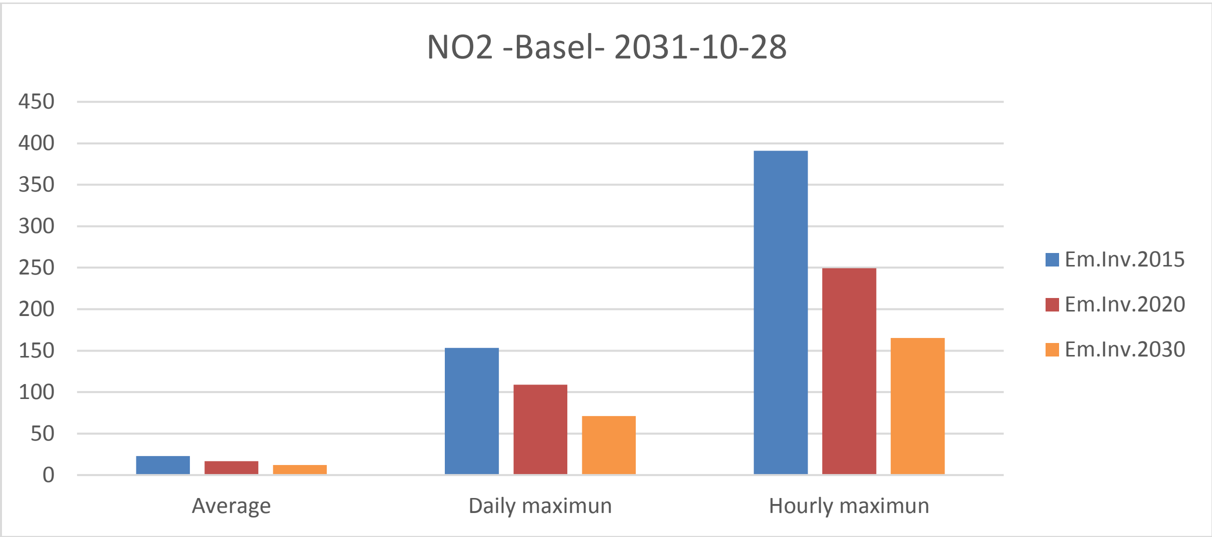


*Figure 4.4.28: $NO_2$ emission inventory comparison*

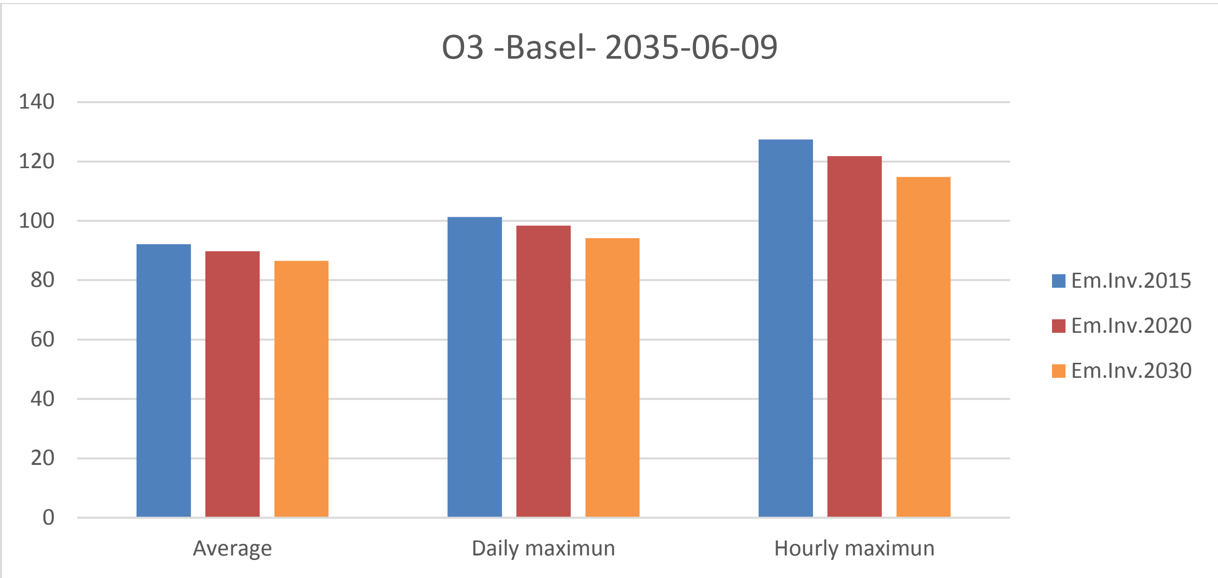


*Figure 4.4.29: $O_3$ emission inventory comparison*

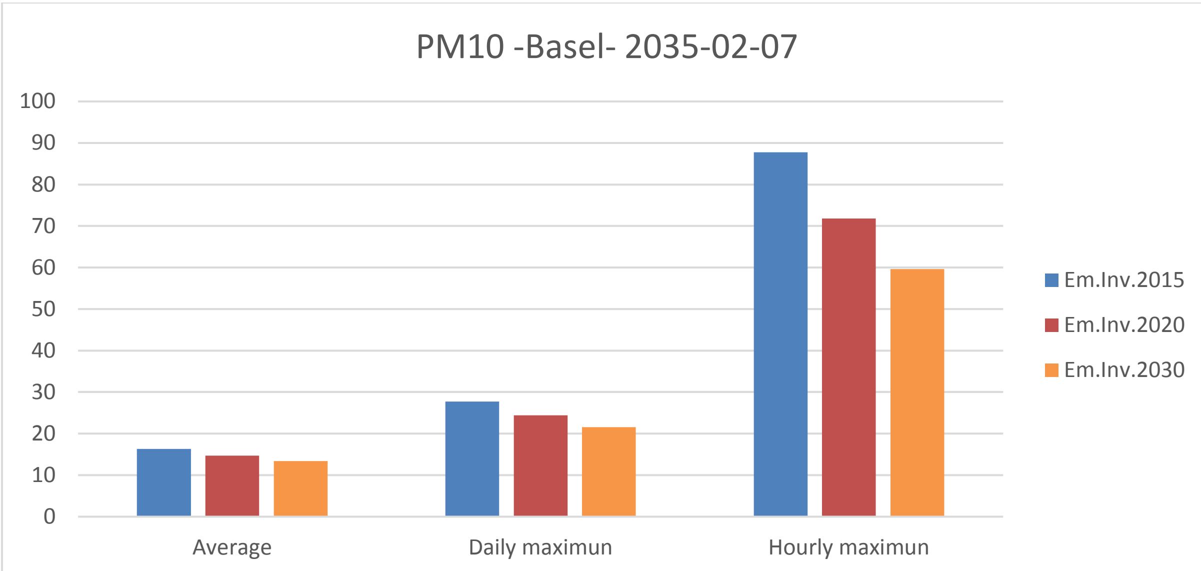


*Figure 4.4.30: $PM_{10}$ emission inventory comparison*

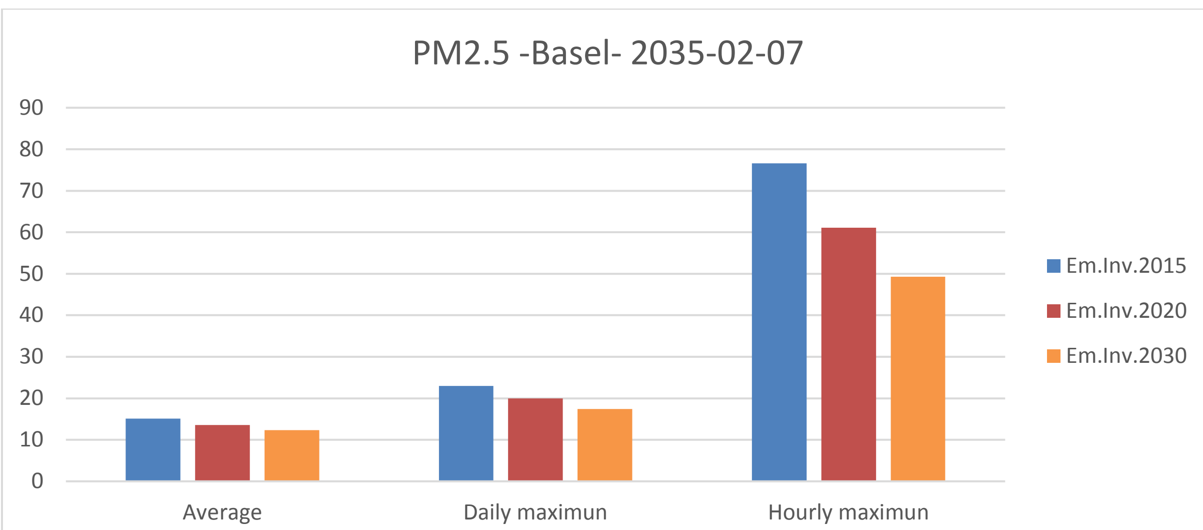


*Figure 4.4.31: $PM_{2.5}$ emission inventory comparison*

### 4.4.4 The GHGs Modeling results

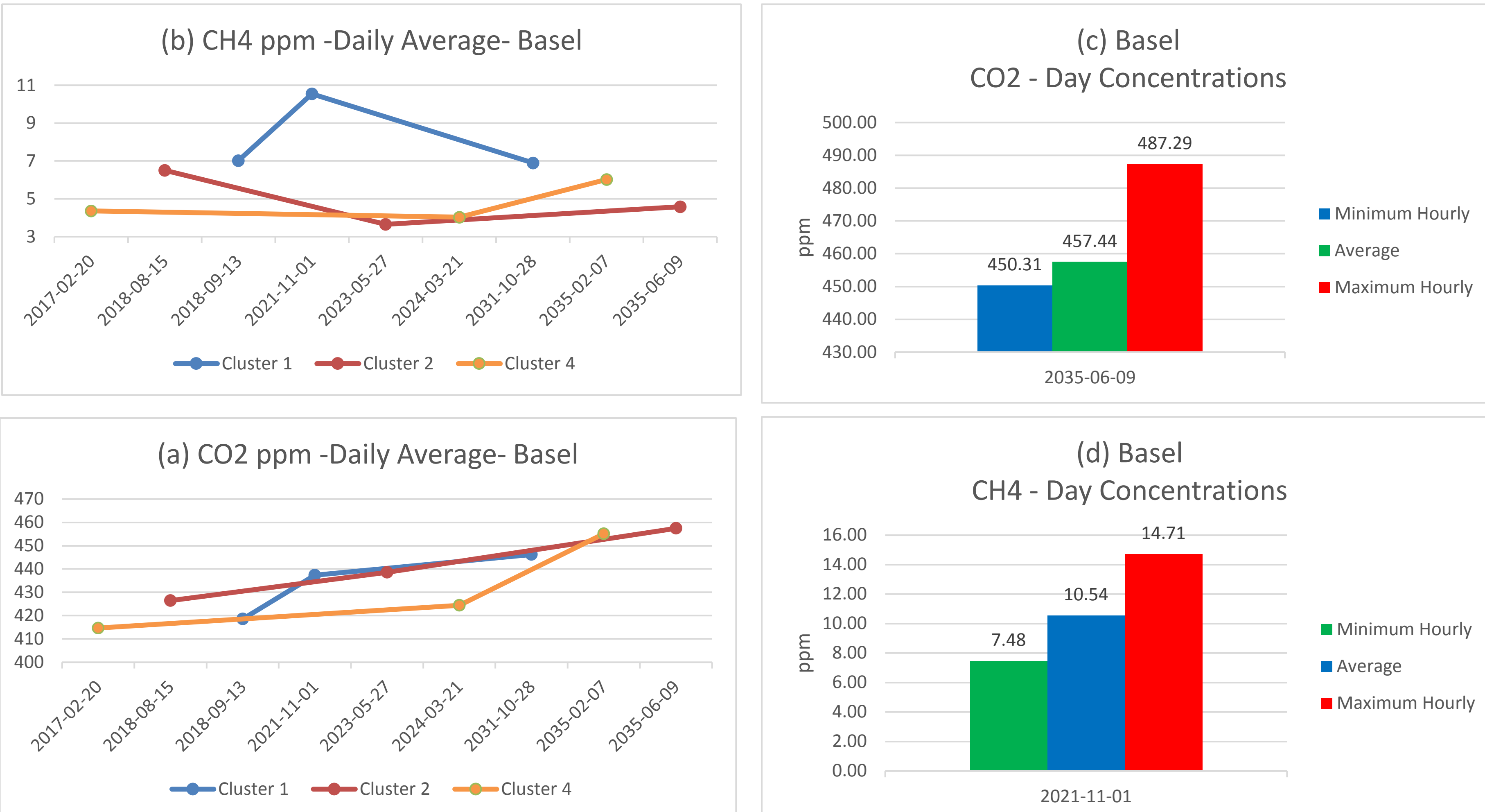


*Figure 4.4.32: (a),(b) $CO_2$ and $CH_4$ Daily average concentrations . (c),(d) $CO_2$ and $CH_4$ concentrations of the most polluted day*

### 4.4.5 Conclusions

For Basel greater area, clusters 1,4,6 and 7 could be categorized in cold period and on the other hand clusters 2,5 and 8 in warm period.

In clusters 1, 2 and 6 there is a linear increase in frequency occurrence through the ten 5-year periods. On the other hand, clusters 3,4 and 5 show a linear decrease in frequency occurrence.

The 5-year period 2041-2045 shows the highest number of heat waves, while the next 5-year period shows a decrease. The most heat waves were associated with cluster 2 which correspond to cluster with days belong to warm period.

Cluster 1 is characterized with elevated $NO_2$ concentrations, cluster 2 with elevated $O_3$ concentrations and cluster 4 with elevated PM concentrations.

$NO_2$ concentrations show a decreasing trend. The daily maximum concentrations exceed the EU and WHO yearly limit of 40μg/m$^3$. The maximum hourly concentrations showing a clear decreasing trend where in 2031 are below the limit of 200μg/m$^3$.

$O_3$ concentrations show a decreasing trend with maximum values exceeding the WHO 8hr limit of 100μg/m$^3$. The maximum hourly concentrations are close and sometimes above the WHO and the EU 8hr limit of 120μg/m$^3$.

$PM_{10}$ daily maximum concentrations exceed the WHO yearly limit of 20μg/m$^3$, however all concentrations are below the daily WHO limit of 50μg/m$^3$ and there is a clear decreasing trend.

$PM_{2.5}$ daily maximum concentrations exceed the WHO yearly limit of 10μg/m$^3$ following a decreasing trend.

All days are above WHO annual limit of 0.12ng/m$^3$ and only one day is on the EU annual limit of 1ng/m$^3$.

There is a clearly decreasing trend in all pollutants indicating the positive effect on emission reductions intervention.

## 4.5 Athens

### 4.5.1 PCA results

The PCA analysis applied to Athens data has led to the following results.

Four (4) principal components have been identified as factors for the cluster analysis (Table 4.5.1). Principal Components (PC) explaining 79.78% of the total variance in the initial data.

Factor 1 explains 28.70% of the total variance and contains mean daily temperature and the down ward short-wave radiation.

Factor 2 explains 18.68% of the total variance and contains RH, precipitation and a negative sign of daily temperature range.

Factor 3 explains 16.49% of the total variance and contains the atmospheric boundary layer thickness.

Factor 4 explains 15.90% of the total variance and contains U and V wind component.

*Table 4.5.1: The Principal Components results*

| Meteorological parameters | Principal Components | | | |
|---|---|---|---|---|
| | 1 | 2 | 3 | 4 |
| Temperature | .898 | | | |
| Downward short-wave surface radiation | .859 | | | |
| Surface pressure | | | | |
| RH | | .762 | | |
| Precipitation | | .755 | | |
| Temperature Range | | -.611 | | |
| Atmospheric boundary layer thickness | | | -.917 | |
| U wind | | | | .768 |
| V wind | | | | .765 |

### 4.5.2 Clustering results

<u>Cluster description and trends</u>

As explained in 3.4.4 the selected clusters of the city of Athens are 10. In Figure 4.5.1 are shown the number of days per cluster, where cluster 5 have the most days and cluster 3,8 and 9 have the less. The monthly distribution per cluster is presented in Table 4.5.2 and in Figure 4.5.2. By dividing the year in two periods, cold and warm, clusters 1,2,3,6 and 10 could be categorized in cold period and on the other hand clusters 4,5,7 and 9 in warm period.

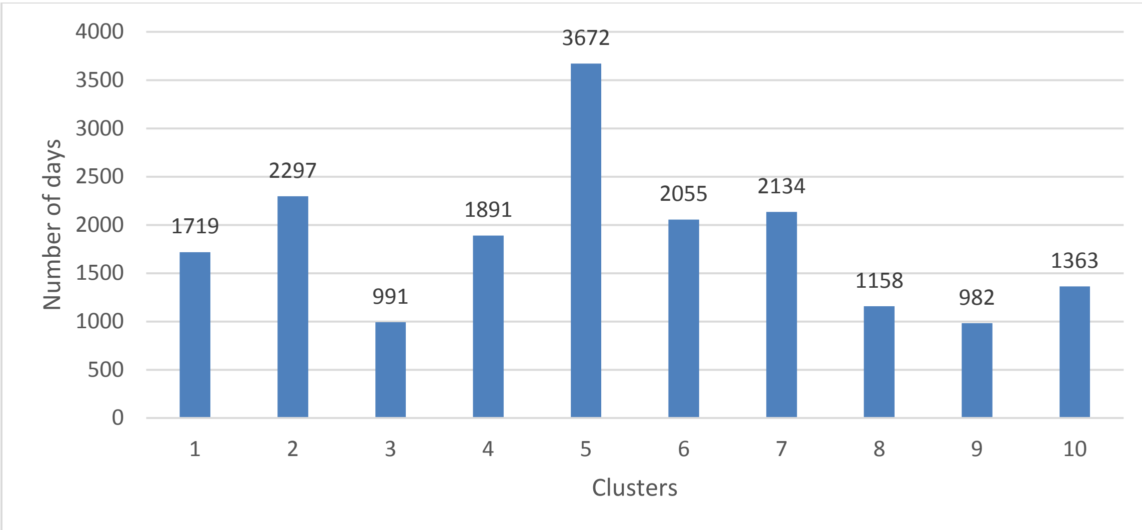


*Figure 4.5.1: Number of Days per cluster*

*Table 4.5.2: Monthly distribution per cluster*

| | | Month | | | | | | | | | | | | Total |
|---|---|---|---|---|---|---|---|---|---|---|---|---|---|---|
| | | Jan | Feb | Mar | Apr | May | Jun | Jul | Aug | Sep | Oct | Nov | Dec | |
| Clusters | 1 | 255 | 166 | 154 | 103 | 27 | 3 | 0 | 0 | 36 | 331 | 324 | 320 | 1719 |
| | 2 | 412 | 400 | 368 | 150 | 1 | 0 | 0 | 0 | 12 | 239 | 327 | 388 | 2297 |
| | 3 | 173 | 176 | 199 | 99 | 16 | 0 | 0 | 0 | 8 | 72 | 118 | 130 | 991 |
| | 4 | 0 | 0 | 6 | 52 | 63 | 109 | 514 | 780 | 341 | 26 | 0 | 0 | 1891 |
| | 5 | 0 | 1 | 37 | 307 | 570 | 708 | 616 | 599 | 711 | 123 | 0 | 0 | 3672 |
| | 6 | 335 | 283 | 266 | 132 | 65 | 5 | 1 | 0 | 29 | 250 | 322 | 367 | 2055 |
| | 7 | 1 | 7 | 73 | 338 | 549 | 496 | 250 | 129 | 224 | 66 | 1 | 0 | 2134 |
| | 8 | 127 | 148 | 190 | 158 | 169 | 50 | 13 | 6 | 43 | 68 | 81 | 105 | 1158 |
| | 9 | 65 | 48 | 73 | 64 | 85 | 129 | 156 | 36 | 61 | 113 | 99 | 53 | 982 |
| | 10 | 182 | 183 | 184 | 97 | 5 | 0 | 0 | 0 | 35 | 262 | 228 | 187 | 1363 |
| Total | | 1550 | 1412 | 1550 | 1500 | 1550 | 1500 | 1550 | 1550 | 1500 | 1550 | 1500 | 1550 | 18262 |

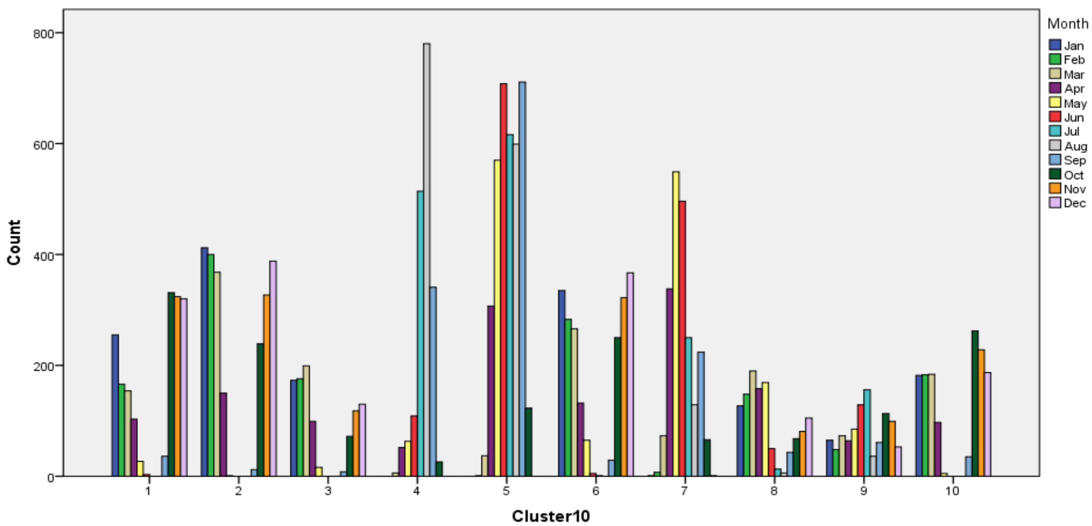


*Figure 4.5.2: Visualized bar chart of monthly distribution per cluster*

A trend analysis of the 5-year frequency of each cluster (Figure 4.5.3). There is an evidence that in clusters 4 and 10 there is a linear increase in frequency occurrence through the ten 5-year periods. On the other hand, clusters 3,8 and 9 show a linear decrease in frequency occurrence. In the rest clusters no clear trends could be pointed out.

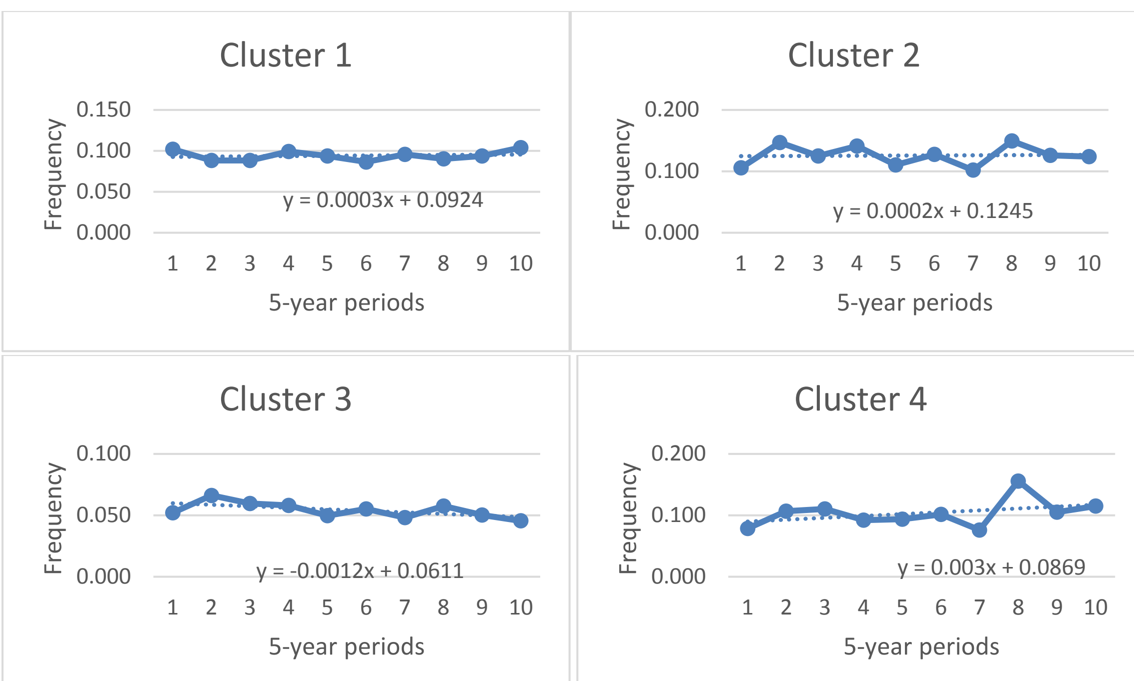

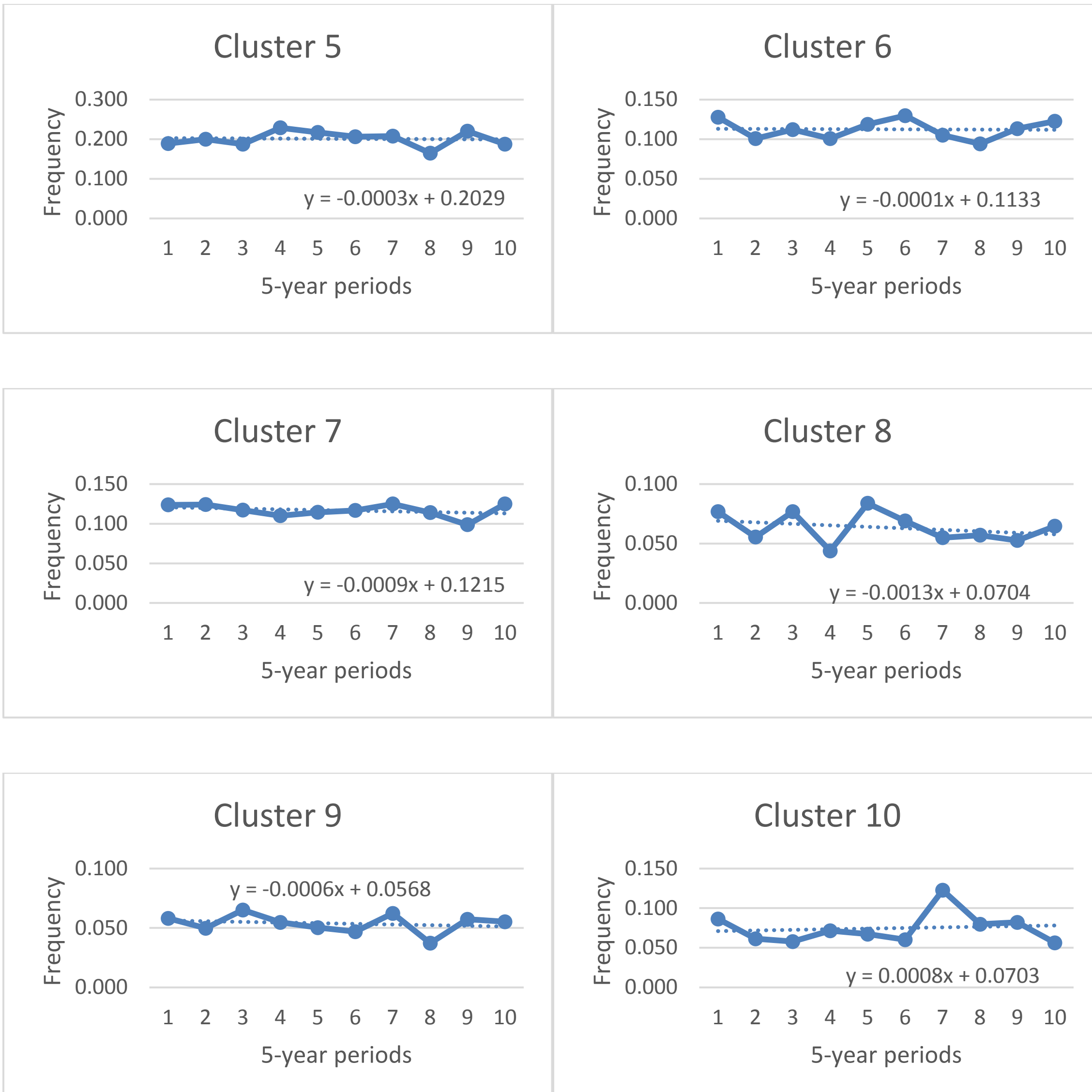


*Figure 4.5.3: Cluster 1-10 frequency trends*

## Cluster characterization

The clusters' implementation is based on the mean values of weather parameters which are displayed in Table 4.5.3.

*Table 4.5.3: Summary of the 10 clusters*

| | Cluster | | | | | | | | | |
|---|---|---|---|---|---|---|---|---|---|---|
| | 1 | 2 | 3 | 4 | 5 | 6 | 7 | 8 | 9 | 10 |
| | Mean (SD) | Mean (SD) | Mean (SD) | Mean (SD) | Mean (SD) | Mean (SD) | Mean (SD) | Mean (SD) | Mean (SD) | Mean (SD) |
| Temperature ( ºC) | 13,61 (3,63) | 11,47 (3,8) | 8,1 (4,19) | 25,17 (3,43) | 22,8 (4,13) | 13,47 (3,46) | 20,47 (4,91) | 13,84 (4,27) | 17,67 (5,63) | 10,05 (4,84) |
| Daily Temperature Range ( ºC) | 5,29 (1,13) | 6,78 (1,18) | 5,09 (1,1) | 5,89 (0,88) | 6,9 (0,97) | 5,07 (1,33) | 7,07 (0,93) | 5,16 (1,28) | 4,22 (1,21) | 3,81 (1,08) |
| Relative Humidity (%) | 82,13 (6,04) | 64,37 (7,4) | 55,3 (6,9) | 62,09 (6,62) | 67,77 (7,82) | 74,64 (5,33) | 62,01 (5,78) | 64,73 (5,67) | 82,71 (5,64) | 73,61 (7,71) |
| Surface Pressure (Pa) | 100132,93 (575,12) | 100451,41 (545,89) | 99780,74 (617,08) | 99317,54 (396,46) | 99227,34 (434,55) | 99200,18 (535,71) | 98981,53 (429,06) | 98555,29 (520,3) | 98898,67 (601,41) | 100358,36 (725,45) |
| Precipitation (kg/m2/s) | 0,00001 (0,000021) | 0,000001 (0,000003) | 0,000003 (0,000009) | 0,000003 (0,000012) | 0,000006 (0,000015) | 0,000014 (0,000024) | 0,000005 (0,000012) | 0,000011 (0,000019) | 0,000143 (0,000093) | 0,000011 (0,000024) |
| Downward Short Wave Radiation | 148,87 (57,27) | 173,38 (58,32) | 193,87 (68,11) | 318,73 (32,77) | 311,34 (41,67) | 147,56 (62,21) | 321,06 (43,11) | 217,68 (89,36) | 191,71 (94,96) | 160,5 (60,85) |
| u wind component (m/s) | 0,05 (1,65) | 2,53 (2,04) | 3,6 (2,27) | -1,58 (1,35) | 0,37 (1,42) | 3,36 (1,74) | 4,62 (1,62) | 6,82 (1,81) | -0,61 (2,55) | -1,42 (1,84) |
| v wind component (m/s) | 1,82 (2,92) | -0,89 (2,13) | -5,46 (2,46) | -6,96 (1,89) | 0,97 (2,43) | 3,47 (3,76) | 0,23 (2,75) | 1,8 (4,03) | 2,12 (4,96) | -7,09 (2,47) |
| V wind (m/s) | 3,26 (1,97) | 3,57 (1,77) | 7,05 (2,04) | 7,24 (1,99) | 2,56 (1,56) | 5,97 (2,19) | 5,36 (1,7) | 8,16 (1,65) | 5,14 (3,08) | 7,53 (2,25) |
| Atmospheric Boundary Layer Thickness (m) | 278,28 (98,89) | 316,5 (114,14) | 743,16 (200,49) | 717,47 (171,56) | 370,72 (86,75) | 498,93 (128,29) | 616,6 (145,43) | 850,24 (175,89) | 508,91 (174,34) | 609,37 (180,29) |

In addition to the previous Table 4.5.3, Figure 4.5.4 presents the mean normalized (z-score) variables of each cluster, respectively showing the differences of the parameters per cluster.

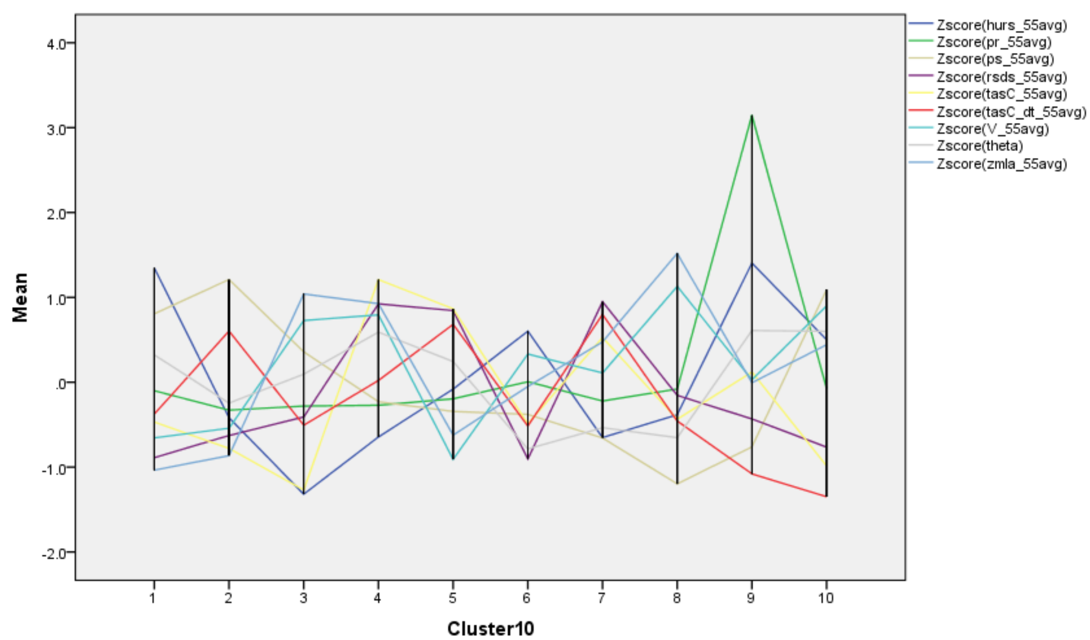


*Figure 4.5.4: Normalized variables (z-score) averaged for each cluster*

Daily, 10-meter from ground level, wind data were used to create the wind roses per each cluster as they are shown in Figures 4.5.5-4.5.14. Each wind direction distribution per cluster is presented in more details in Table 4.5.4.

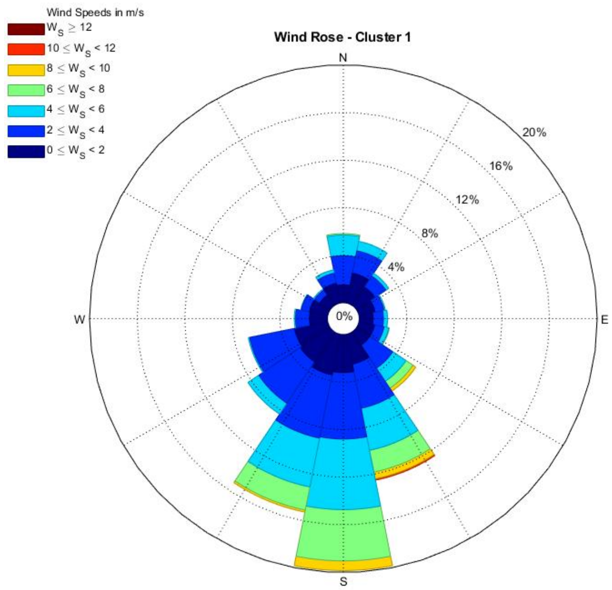


*Figure 4.5.5: Wind Rose - Cluster 1*

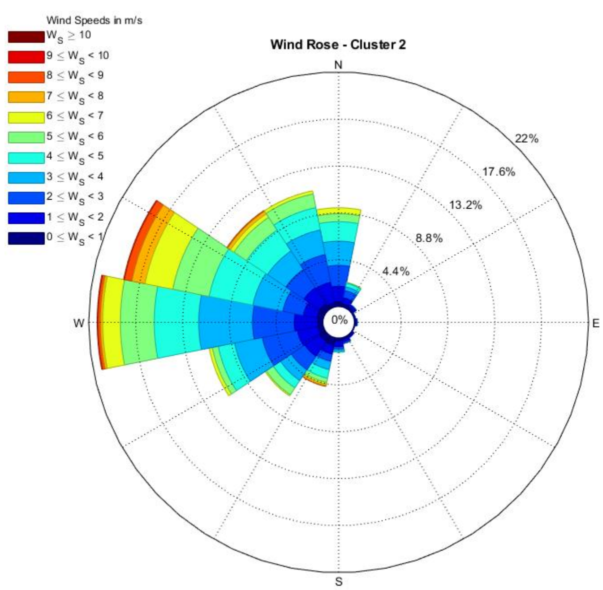


*Figure 4.5.6: Wind Rose - Cluster 2*

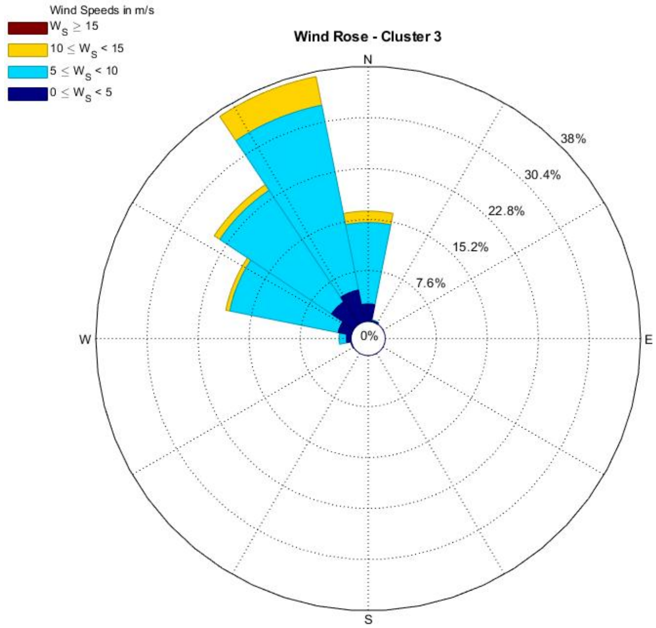


*Figure 4.5.7: Wind Rose - Cluster 3*

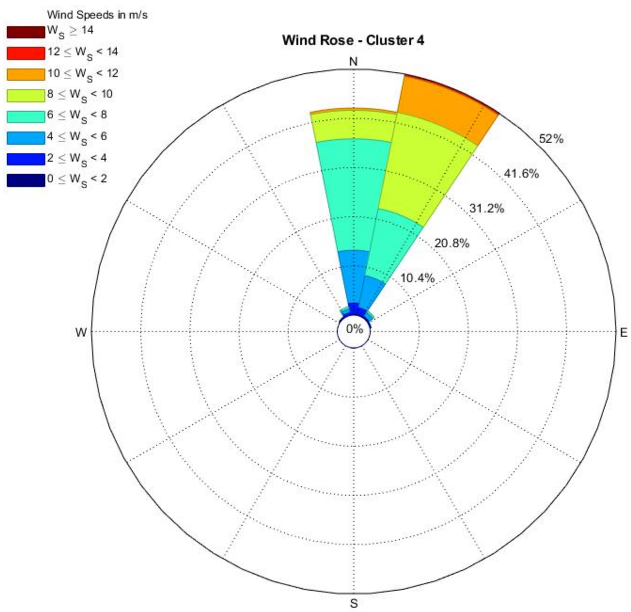


*Figure 4.5.8: Wind Rose - Cluster 4*

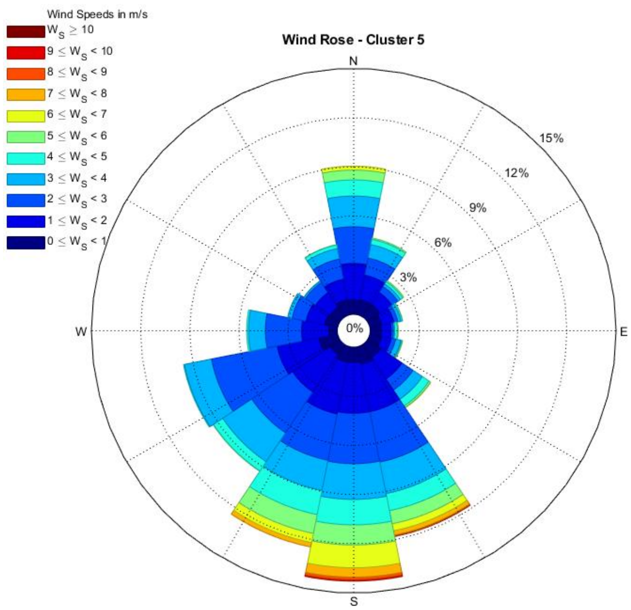


*Figure 4.5.9: Wind Rose - Cluster 5*

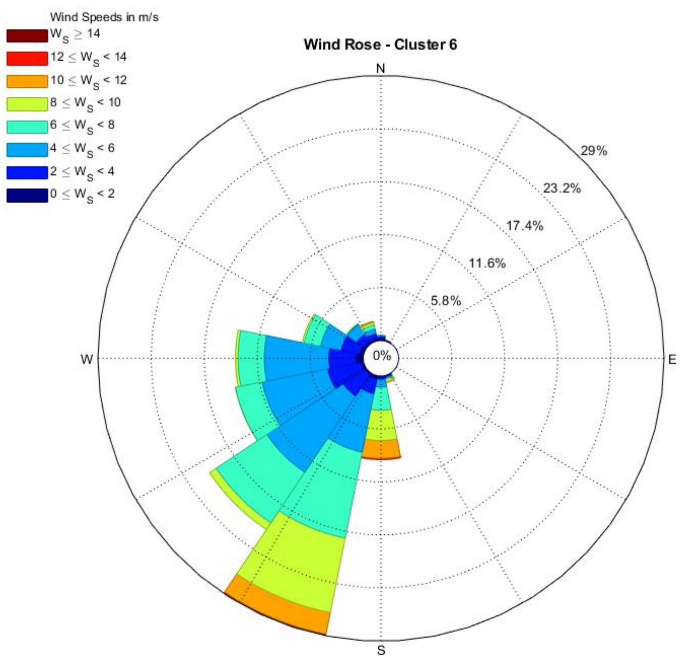


*Figure 4.5.10: Wind Rose - Cluster 6*

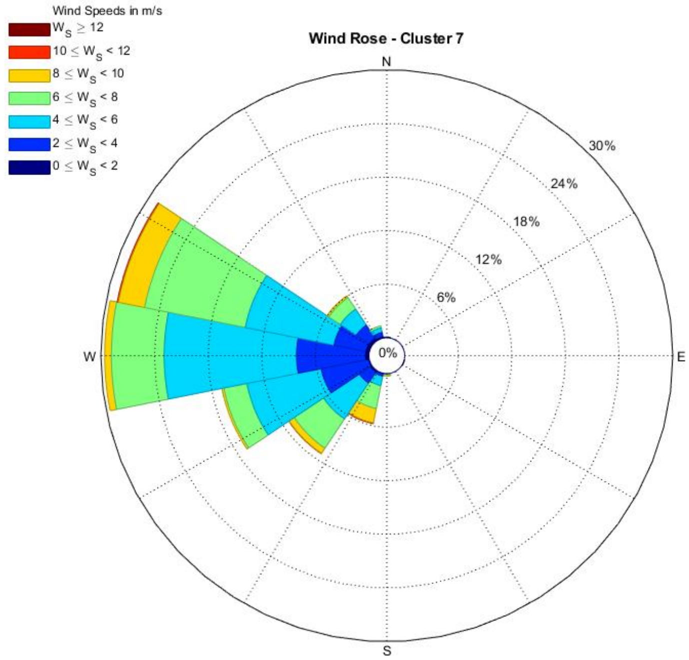


*Figure 4.5.11: Wind Rose - Cluster 7*

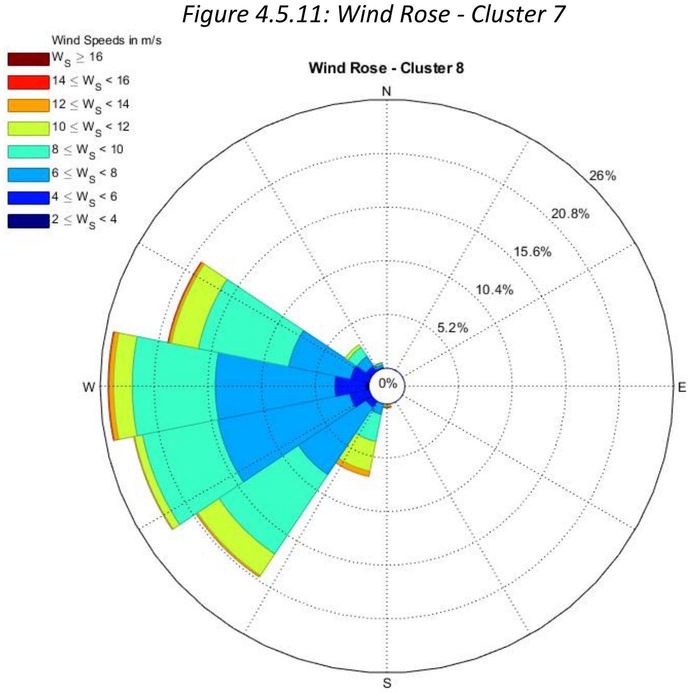


*Figure 4.5.12: Wind Rose - Cluster 8*

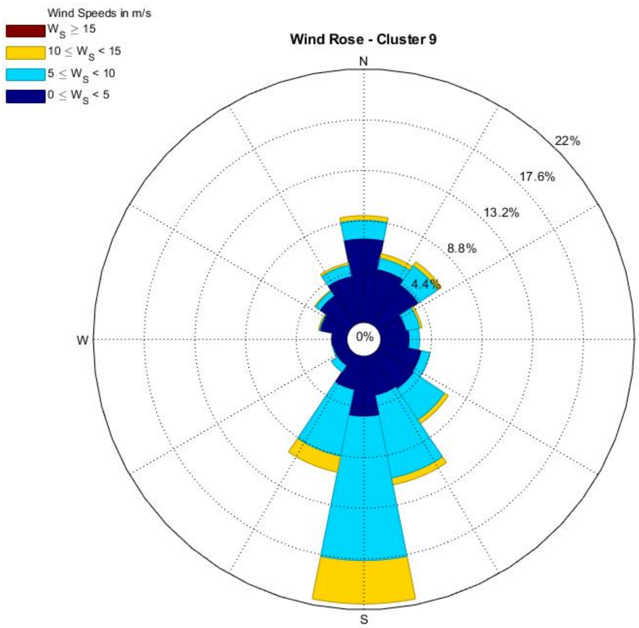


*Figure 4.5.13: Wind Rose - Cluster 9*

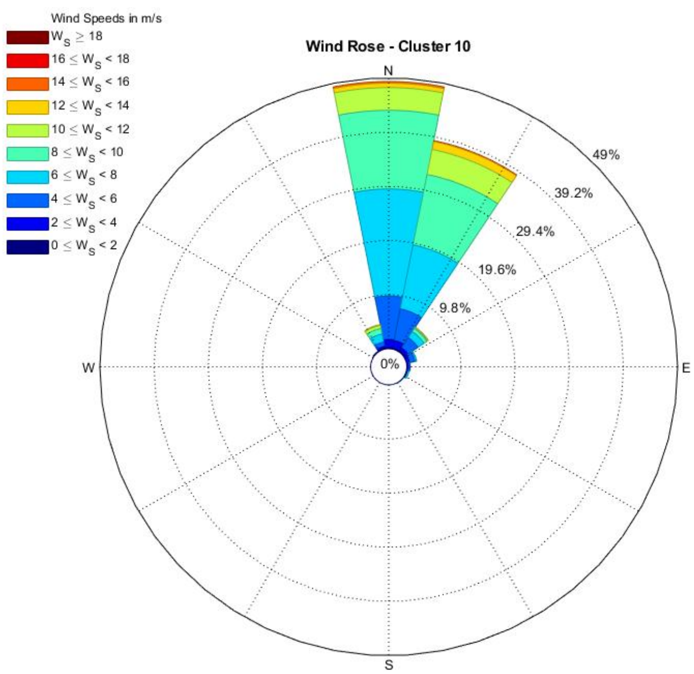


*Figure 4.5.14: Wind Rose - Cluster 10*

*Table 4.5.4: 16 Wind Direction distribution per cluster*

| | | | Wind16 | | | | | | | | | | | | | | | | Total |
|---|---|---|---|---|---|---|---|---|---|---|---|---|---|---|---|---|---|---|---|
| | | | S | SSW | SW | WSW | W | WNW | NW | NNW | N | NNE | NE | ENE | E | ESE | SE | SSE | |
| Cluster10 | 1 | Count | 341 | 262 | 143 | 117 | 48 | 40 | 29 | 49 | 100 | 91 | 56 | 39 | 41 | 45 | 103 | 215 | 1719 |
| | | % within Cluster10 | 19.8% | 15.2% | 8.3% | 6.8% | 2.8% | 2.3% | 1.7% | 2.9% | 5.8% | 5.3% | 3.3% | 2.3% | 2.4% | 2.6% | 6.0% | 12.5% | 100.0% |
| | 2 | Count | 31 | 107 | 157 | 251 | 487 | 439 | 256 | 255 | 213 | 54 | 13 | 4 | 7 | 2 | 7 | 14 | 2297 |
| | | % within Cluster10 | 1.3% | 4.7% | 6.8% | 10.9% | 21.2% | 19.1% | 11.1% | 11.1% | 9.3% | 2.4% | .6% | .2% | .3% | .1% | .3% | .6% | 100.0% |
| | 3 | Count | 0 | 0 | 0 | 1 | 18 | 189 | 248 | 369 | 163 | 3 | 0 | 0 | 0 | 0 | 0 | 0 | 991 |
| | | % within Cluster10 | 0.0% | 0.0% | 0.0% | .1% | 1.8% | 19.1% | 25.0% | 37.2% | 16.4% | .3% | 0.0% | 0.0% | 0.0% | 0.0% | 0.0% | 0.0% | 100.0% |
| | 4 | Count | 1 | 0 | 0 | 0 | 0 | 0 | 5 | 35 | 827 | 983 | 34 | 6 | 0 | 0 | 0 | 0 | 1891 |
| | | % within Cluster10 | .1% | 0.0% | 0.0% | 0.0% | 0.0% | 0.0% | .3% | 1.9% | 43.7% | 52.0% | 1.8% | .3% | 0.0% | 0.0% | 0.0% | 0.0% | 100.0% |
| | 5 | Count | 524 | 457 | 342 | 352 | 203 | 114 | 98 | 160 | 332 | 175 | 98 | 75 | 63 | 75 | 171 | 433 | 3672 |
| | | % within Cluster10 | 14.3% | 12.4% | 9.3% | 9.6% | 5.5% | 3.1% | 2.7% | 4.4% | 9.0% | 4.8% | 2.7% | 2.0% | 1.7% | 2.0% | 4.7% | 11.8% | 100.0% |
| | 6 | Count | 188 | 594 | 423 | 294 | 287 | 140 | 54 | 45 | 12 | 2 | 0 | 0 | 0 | 0 | 0 | 16 | 2055 |
| | | % within Cluster10 | 9.1% | 28.9% | 20.6% | 14.3% | 14.0% | 6.8% | 2.6% | 2.2% | .6% | .1% | 0.0% | 0.0% | 0.0% | 0.0% | 0.0% | .8% | 100.0% |
| | 7 | Count | 6 | 123 | 239 | 359 | 631 | 614 | 129 | 30 | 2 | 0 | 0 | 0 | 0 | 1 | 0 | 0 | 2134 |
| | | % within Cluster10 | .3% | 5.8% | 11.2% | 16.8% | 29.6% | 28.8% | 6.0% | 1.4% | .1% | 0.0% | 0.0% | 0.0% | 0.0% | .0% | 0.0% | 0.0% | 100.0% |
| | 8 | Count | 4 | 83 | 237 | 269 | 292 | 230 | 36 | 7 | 0 | 0 | 0 | 0 | 0 | 0 | 0 | 0 | 1158 |
| | | % within Cluster10 | .3% | 7.2% | 20.5% | 23.2% | 25.2% | 19.9% | 3.1% | .6% | 0.0% | 0.0% | 0.0% | 0.0% | 0.0% | 0.0% | 0.0% | 0.0% | 100.0% |
| | 9 | Count | 211 | 101 | 19 | 13 | 13 | 25 | 36 | 52 | 91 | 60 | 65 | 36 | 33 | 43 | 72 | 112 | 982 |
| | | % within Cluster10 | 21.5% | 10.3% | 1.9% | 1.3% | 1.3% | 2.5% | 3.7% | 5.3% | 9.3% | 6.1% | 6.6% | 3.7% | 3.4% | 4.4% | 7.3% | 11.4% | 100.0% |
| | 10 | Count | 0 | 0 | 0 | 0 | 0 | 0 | 2 | 62 | 659 | 524 | 73 | 26 | 9 | 7 | 1 | 0 | 1363 |
| | | % within Cluster10 | 0.0% | 0.0% | 0.0% | 0.0% | 0.0% | 0.0% | .1% | 4.5% | 48.3% | 38.4% | 5.4% | 1.9% | .7% | .5% | .1% | 0.0% | 100.0% |
| Total | | Count | 1306 | 1727 | 1560 | 1656 | 1979 | 1791 | 893 | 1064 | 2399 | 1892 | 339 | 186 | 153 | 173 | 354 | 790 | 18262 |
| | | % within Cluster10 | 7.2% | 9.5% | 8.5% | 9.1% | 10.8% | 9.8% | 4.9% | 5.8% | 13.1% | 10.4% | 1.9% | 1.0% | .8% | .9% | 1.9% | 4.3% | 100.0% |

## Clusters and local Heat Waves

In Figures 4.5.15 and 4.5.16 are presented the heat waves occurrence per 5-year period and per cluster. Heat waves occurrence shows an increased rate. The 5-year period 2046-2050 shows the highest number of heat waves. The most heat waves were associated with clusters 4 and 5 which correspond to clusters with days belong to warm period (see Table 4.5.2).

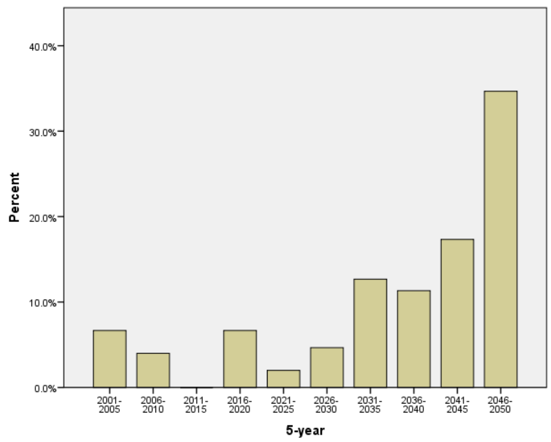


*Figure 4.5.15: Heat Waves per 5-year period*

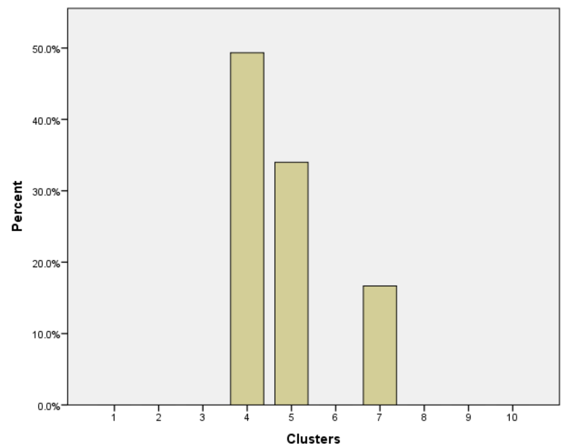


*Figure 4.5.16: Heat Waves per cluster*

## Clusters versus Air Quality level

As it can be seen in Table 4.1 five observation stations have been used for the present analysis. The descriptive statistics for $NO_2$, $O_3$ and $PM_{10}$ is given in Table 4.5.5.

*Table 4.5.5: Air pollutants descriptive statistics*

| | | MEAN_NO2 | MEAN_O3 | MEAN_PM10 |
|---|---|---|---|---|
| Mean | | 39.5219 | 56.2581 | 45.0176 |
| Std. Deviation | | 13.99865 | 21.96799 | 21.66797 |
| Minimum | | 5.87 | 4.24 | 5.96 |
| Maximum | | 96.50 | 120.17 | 387.75 |
| Percentiles | 5 | 18.6391 | 21.7433 | 20.5000 |
| | 25 | 29.1753 | 38.3834 | 31.0000 |
| | 50 | 38.3750 | 56.3608 | 40.8774 |
| | 75 | 48.4668 | 72.7603 | 54.0105 |
| | 95 | 64.1800 | 91.7876 | 81.8562 |

Table 4.5.6 presents the pollutants' concentrations per cluster. Higher mean $NO_2$ concentrations are observed in clusters 6,8 and 10. Higher mean $O_3$ concentrations are observed in clusters 4 and 5. Higher mean $PM_{10}$ concentrations are observed in clusters 3 and 6.

*Table 4.5.6: Summary pollutant concentrations per cluster*

| | Cluster | | | | | | | | | |
|---|---|---|---|---|---|---|---|---|---|---|
| | 1 | 2 | 3 | 4 | 5 | 6 | 7 | 8 | 9 | 10 |
| | Mean (SD) | Mean (SD) | Mean (SD) | Mean (SD) | Mean (SD) | Mean (SD) | Mean (SD) | Mean (SD) | Mean (SD) | Mean (SD) |
| PM10 (µg/m3) | 44.03 (20.51) | 46.61 (27.41) | 48.54 (27.77) | 41.79 (16.3) | 44.16 (16.99) | 47.21 (26.8) | 44.43 (18.05) | 46.13 (22.57) | 43.16 (16.94) | 45.49 (22.27) |
| O3 (µg/m3) | 41,12 (16,26) | 40,91 (16,11) | 43,7 (16,42) | 76,37 (14,62) | 72,48 (15,26) | 42,57 (17,43) | 70,04 (15,93) | 50,21 (18,96) | 59,1 (21,71) | 43,98 (16,18) |
| NO2 (µg/m3) | 40,41 (13,81) | 40,71 (13,86) | 40,46 (14,64) | 34,64 (13,69) | 37,61 (13,14) | 40,96 (14,34) | 40,85 (13,58) | 41,67 (14,4) | 38,51 (13,22) | 41,56 (14,96) |

The differences in concentrations per cluster are shown in Figures 4.5.17-4.5.19.

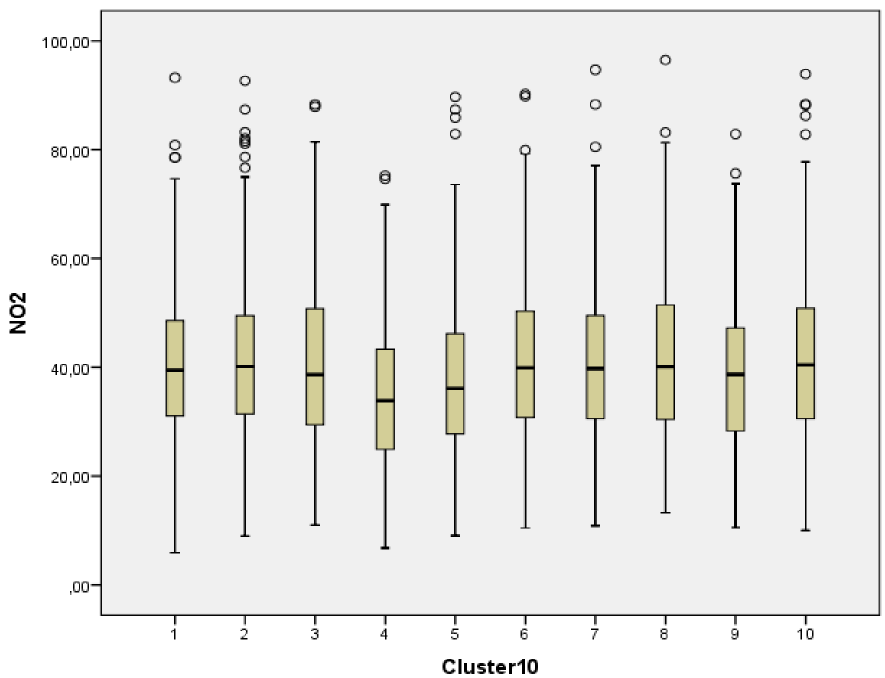


*Figure 4.5.17: $NO_2$ concentration statistics per cluster*

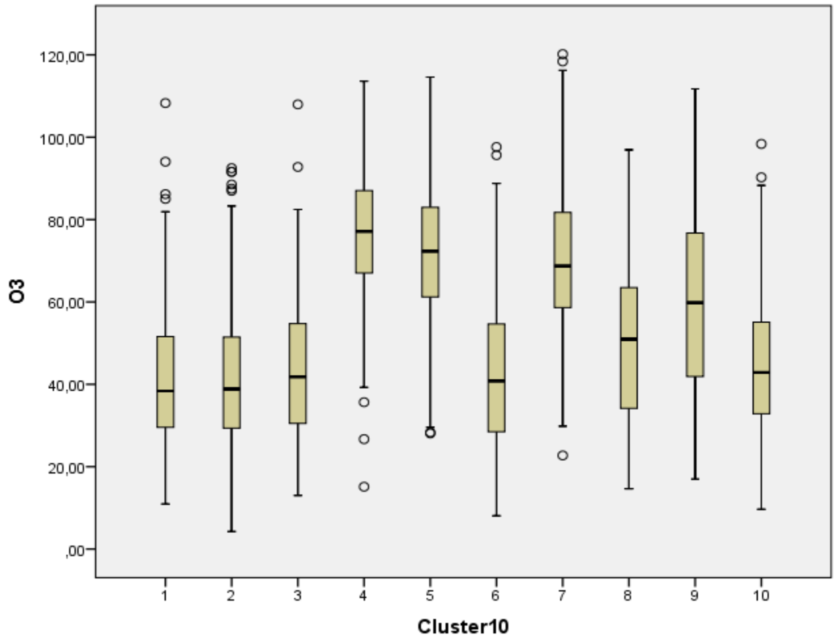


*Figure 4.5.18: $O_3$ concentration statistics per cluster*

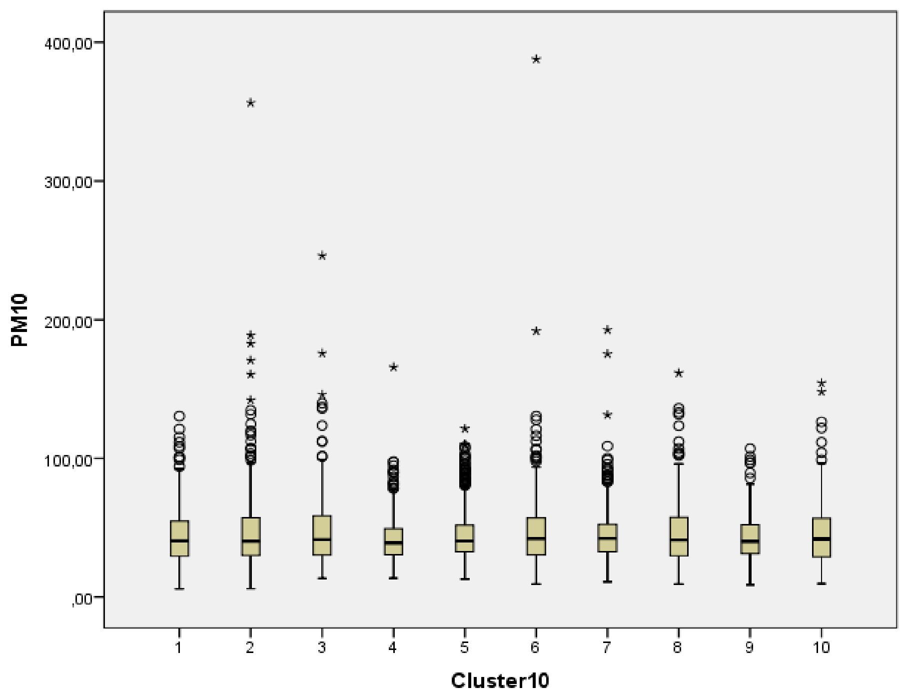


*Figure 4.5.19: $PM_{10}$ concentration statistics per cluster*

### Representative Days

In the following Table 4.5.7 are presented the selected RDs per 5-year period and per cluster.

*Table 4.5.7: Representative days per cluster and 5year period*

| Closest days to centroids per 5year per cluster | | | clusters | | | | | | | | | |
|---|---|---|---|---|---|---|---|---|---|---|---|---|
| | | | 1 | 2 | 3 | 4 | 5 | 6 | 7 | 8 | 9 | 10 |
| 5 year period | 2001-2005 | 1 | 2003-03-07 | 2003-11-16 | 2005-03-24 | 2005-08-17 | 2002-06-26 | 2005-11-21 | 2005-05-30 | 2003-03-29 | 2005-06-28 | 2002-03-08 |
| | 2006-2010 | 2 | 2009-11-16 | 2008-11-20 | 2008-11-02 | 2006-08-09 | 2008-08-25 | 2009-11-25 | 2006-05-22 | 2006-03-25 | 2006-04-06 | 2006-10-22 |
| | 2011-2015 | 3 | 2012-03-14 | 2011-02-07 | 2011-02-12 | 2015-07-21 | 2012-09-15 | 2011-11-06 | 2012-06-04 | 2012-04-04 | 2015-02-14 | 2011-03-07 |
| | 2016-2020 | 4 | 2019-11-01 | 2018-12-21 | 2019-01-20 | 2019-07-07 | 2018-06-29 | 2016-11-22 | 2016-05-11 | 2019-03-19 | 2019-03-12 | 2019-10-28 |
| | 2021-2025 | 5 | 2025-12-24 | 2022-12-27 | 2023-01-10 | 2022-08-22 | 2024-09-01 | 2023-02-03 | 2023-06-04 | 2024-03-13 | 2021-10-15 | 2022-10-29 |
| | 2026-2030 | 6 | 2027-11-05 | 2026-02-02 | 2029-10-15 | 2028-07-14 | 2029-09-15 | 2026-03-07 | 2029-06-04 | 2028-04-15 | 2030-03-26 | 2026-02-12 |
| | 2031-2035 | 7 | 2035-12-03 | 2035-11-20 | 2033-12-16 | 2033-09-03 | 2035-06-03 | 2034-11-30 | 2033-09-14 | 2032-04-21 | 2033-10-23 | 2035-03-16 |
| | 2036-2040 | 8 | 2038-11-23 | 2036-12-01 | 2038-02-22 | 2037-08-06 | 2036-06-05 | 2038-02-08 | 2037-06-26 | 2036-03-02 | 2036-10-26 | 2039-11-11 |
| | 2041-2045 | 9 | 2041-02-23 | 2041-11-12 | 2041-01-25 | 2041-08-13 | 2042-07-01 | 2041-03-16 | 2044-05-25 | 2044-02-22 | 2042-04-17 | 2043-11-07 |
| | 2046-2050 | 10 | 2046-12-09 | 2046-02-01 | 2050-01-29 | 2048-06-22 | 2047-05-30 | 2047-11-15 | 2046-05-25 | 2048-03-17 | 2049-04-17 | 2049-03-16 |

### Selected Clusters and RDs for modeling purposes

Selected RDs will be used to perform targeted weather and air quality simulations within each selected 5-year period estimating hourly/daily concentrations of the priority pollutants to assess the climatic effect on air quality evolution and the characteristics of air quality future episodes. The selection was based on 3-year periods (2016-2020, 2021-2025 and 2031-2035) and on the clusters with the most elevated concentrations of $PM_{10}$, $NO_2$ and $O_3$. In the case of Athens, cluster 8 recorded the most elevated values of $NO_2$, cluster 4 for the case of $O_3$ and cluster 3 for the case of $PM_{10}$. In Table 4.5.8 are presented the selected days which was used for modeling purposes.

*Table 4.5.8: RDs for modeling purposes*

| **Period** | **Cluster 3 (PM)** | **Cluster 4 (O3)** | **Cluster 8 (NO2)** |
|---|---|---|---|
| 2016-2020 | 2019-01-20 | 2019-07-07 | 2019-03-19 |
| 2021-2025 | 2023-01-10 | 2022-08-22 | 2024-03-13 |
| 2031-2035 | 2033-12-16 | 2033-09-03 | 2032-04-21 |

### 4.5.3 Air Quality Modeling results

#### 4.5.3.1 Overall results

In Figure 4.5.20 the daily average concentrations of $NO_2$, $O_3$, $PM_{10}$ and $PM_{2.5}$ for selected RDs are presented.

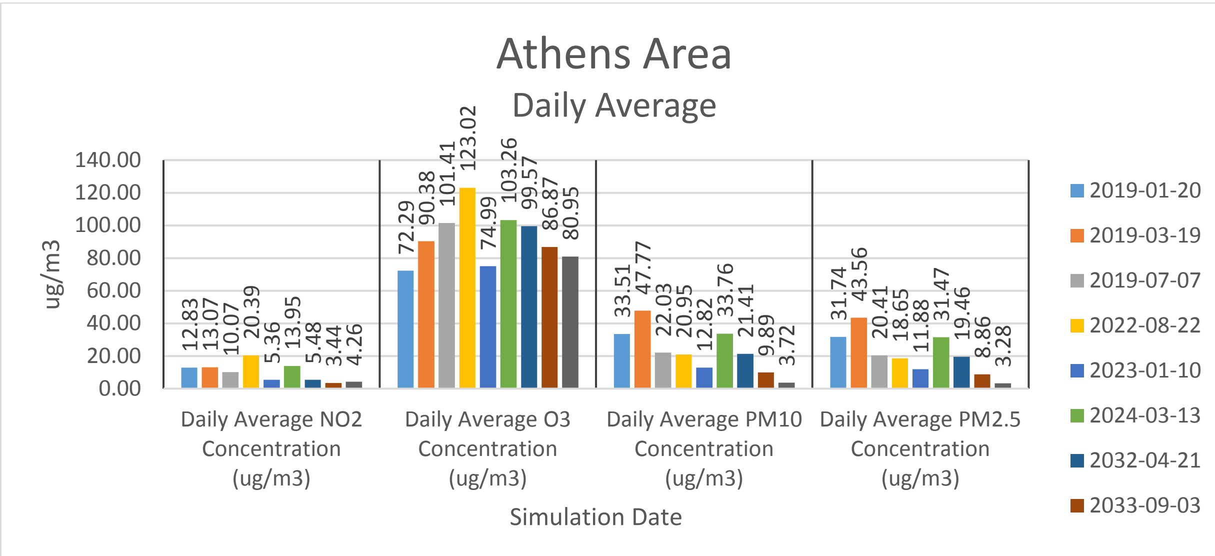


*Figure 4.5.20: Daily average concentrations*

In Figure 4.5.19 the obtained daily averaged concentrations are compared based on USTUTT and EGDAR HTAP emission inventories respectively. The results seem not to differ significantly.

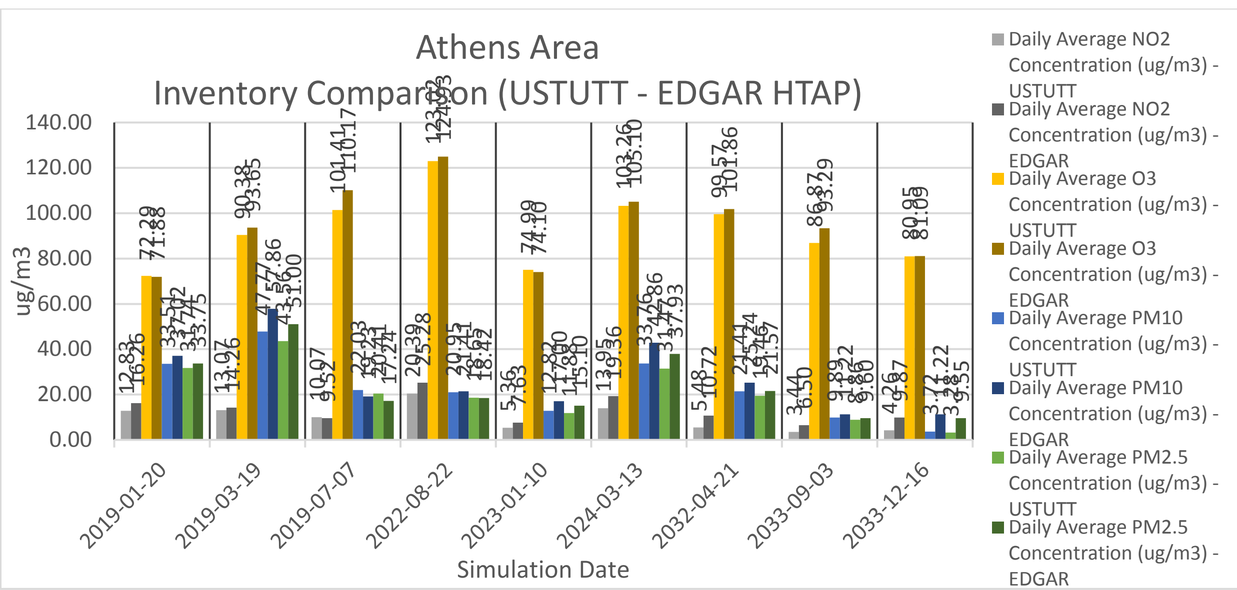


*Figure 4.5.21: Daily average concentrations – USTUTT vs EDGAR HTAP comparison*

#### 4.5.3.2 Clusters results

$NO_2$ Concentrations (Cluster 8)

In Figure 4.5.22, the results are presented in terms of concentrations average, daily maximum and hourly maximum. The diurnal variations are shown in Figure 4.5.23.
Concentrations show a decreasing trend. There is one day in which the daily maximum concentration is below the EU and WHO yearly limit of 40μg/m$^3$. The maximum hourly concentrations are below the limit of 200μg/m$^3$.

$O_3$ Concentrations (Cluster 4)

In Figure 4.5.24, the results are presented in terms of concentrations average, daily maximum and hourly maximum. The diurnal variations are shown in Figure 4.5.25.
The picture is mixed. Only in one day the daily maximum concentration is below WHO 8hr limit of 100μg/m$^3$. All maximum hourly concentrations are above the WHO limit.

$PM_{10}$ Concentrations (Cluster 3)

In Figure 4.5.26, the results are presented in terms of concentrations average, daily maximum and hourly maximum. The diurnal variations are shown in Figure 4.5.27.
The daily maximum concentrations in one day exceed the WHO yearly limit of 20μg/m$^3$, however all concentrations are below the daily WHO limit of 50μg/m$^3$ and there is a clear decreasing trend.

## $NO_2$-Cluster 8

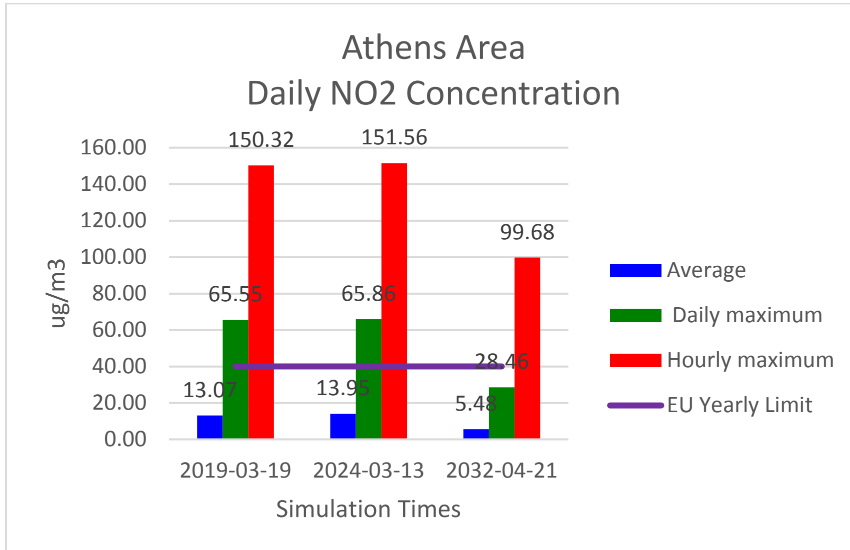


*Figure 4.5.22: $NO_2$ Day concentrations*

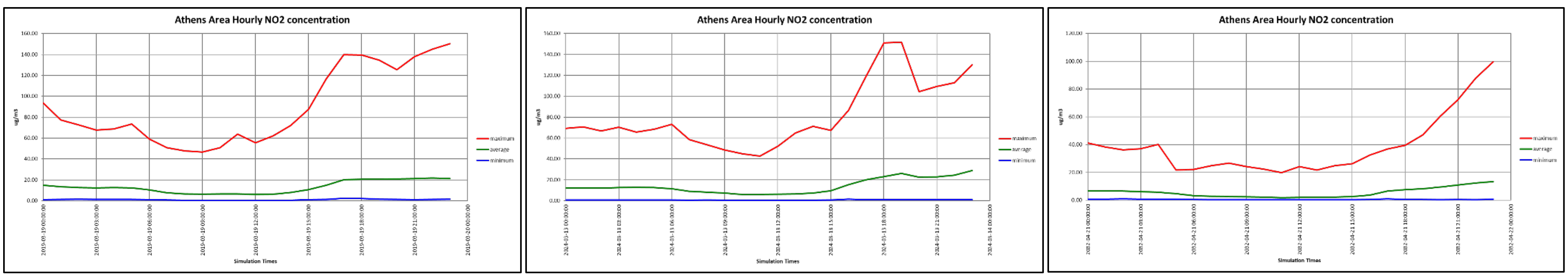


*Figure 4.5.23: Hourly $NO_2$ concentrations*

### $O_3$-Cluster 4

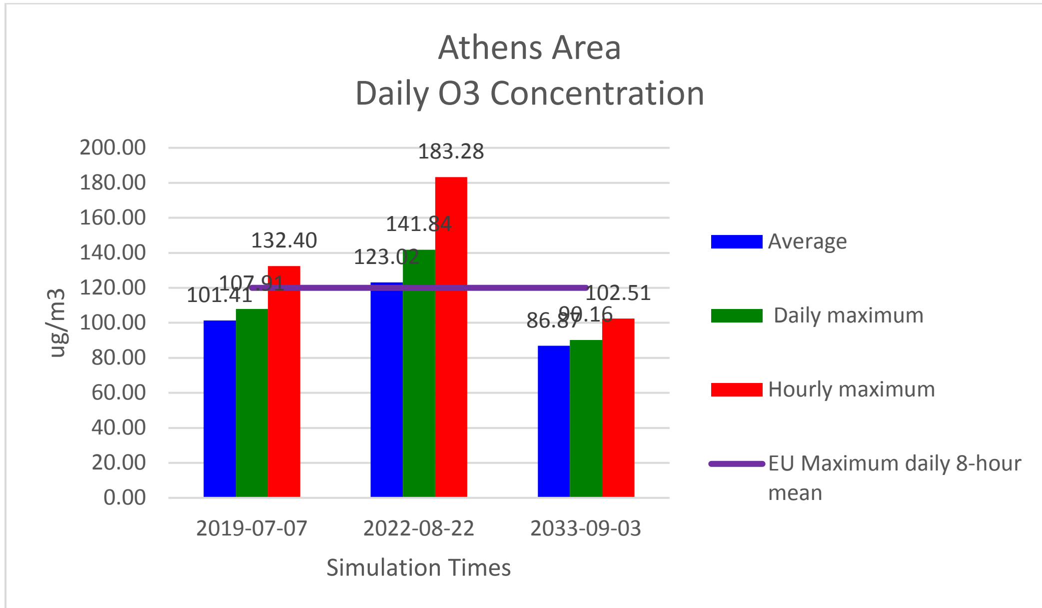


*Figure 4.5.24: $O_3$ Daily concentrations*

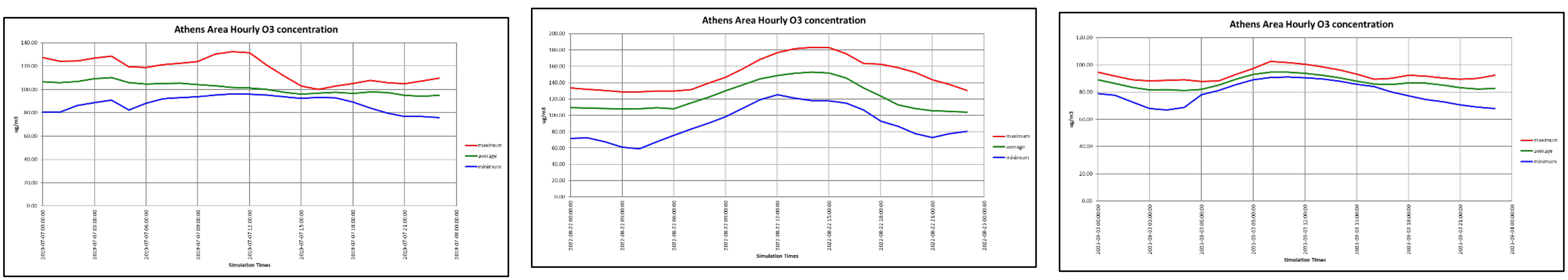


Figure 4.5.25: $O_3$ Hourly concentrations

PM$_{10}$-Cluster 3

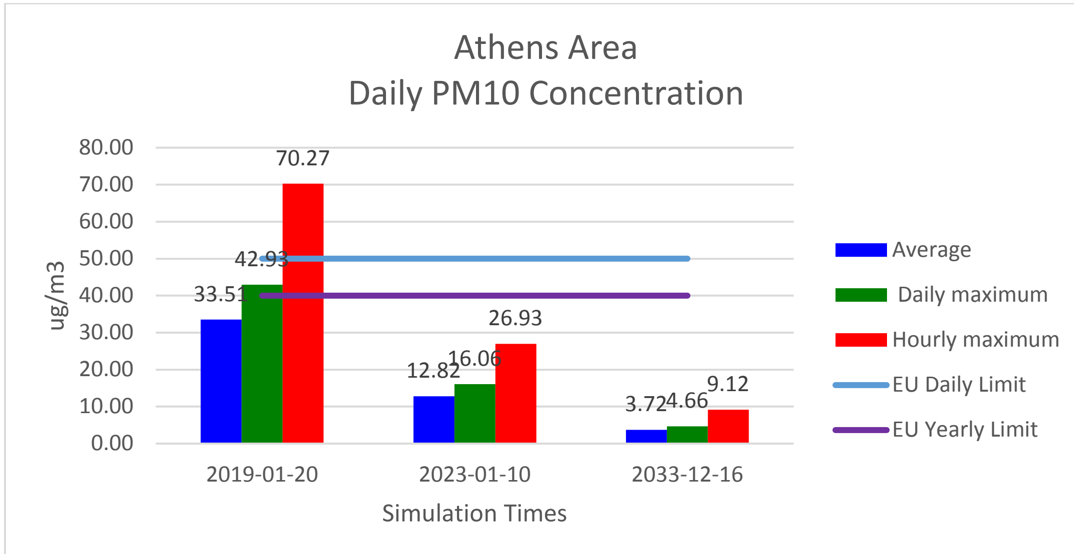


*Figure 4.5.26: PM$_{10}$ Daily concentrations*

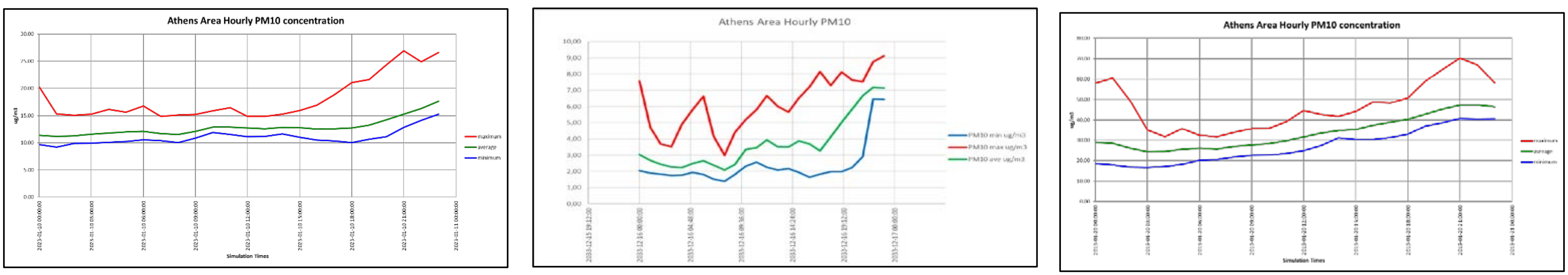


*Figure 4.5.27: PM$_{10}$ Hourly concentrations*

PM$_{2.5}$ Concentrations (Cluster 3)

In Figure 4.5.28, the results are presented in terms of concentrations average, daily maximum and hourly maximum.

The pollutants' concentrations are following a decreasing trend. The daily maximum concentrations are below the WHO yearly limit of 10μg/m$^3$ in two days.

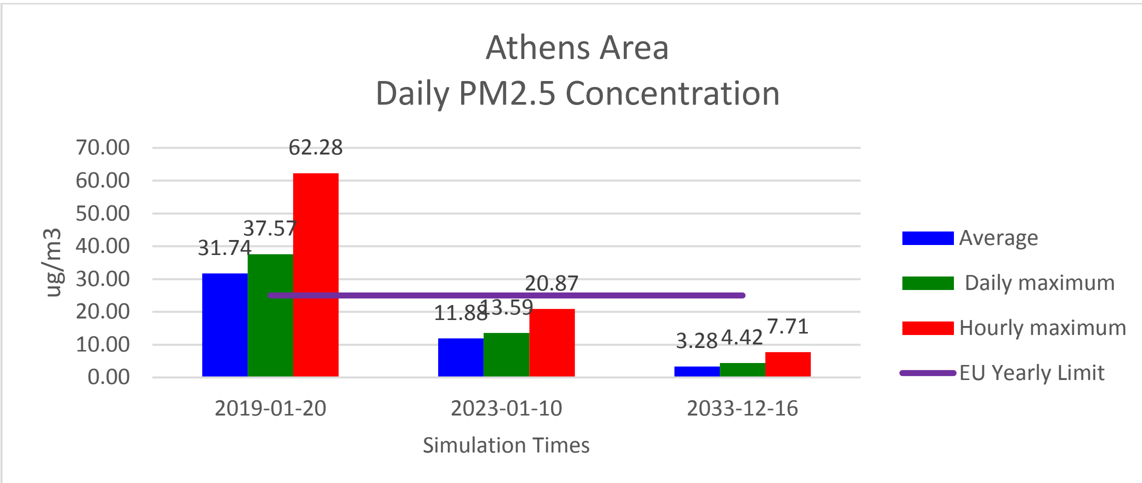


*Figure 4.5.28: PM$_{2.5}$ Day concentrations*

Figure 4.5.29 presents the estimated BaP daily concentrations contained in PM$_{2.5}$. There is a clear decreasing trend. All days are above WHO annual limit of 0.12ng/m$^3$ however one day almost reaches the WHO limit and two days are on and below the EU annual limit of 1ng/m$^3$.

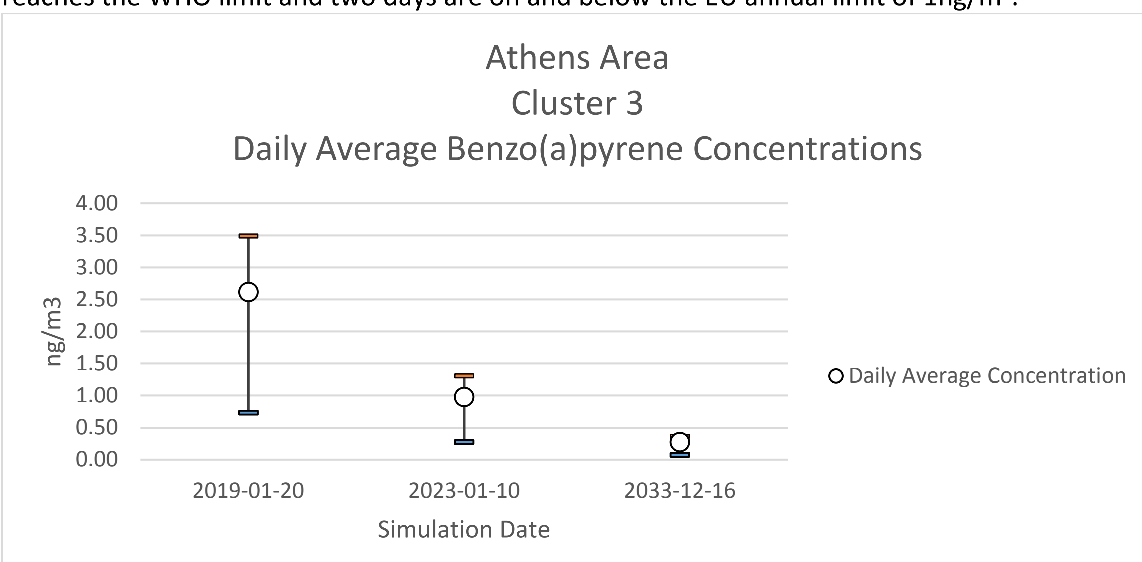


*Figure 4.5.29: BaP daily concentrations*

### 4.5.3.3 The Emission Inventory effect

Figures 4.5.30, 4.5.31, 4.5.32 and 4.5.33 illustrate the emission inventory temporal change effect on $NO_2$, $O_3$, $PM_{10}$ and $PM_{2.5}$ concentration levels respectively. There is a decreasing trend in $NO_2$ and PM concentrations and a slight decrease in $O_3$ indicating the positive effect on emission reductions intervention; a quality check of the emission inventory could clarify more the outcome.

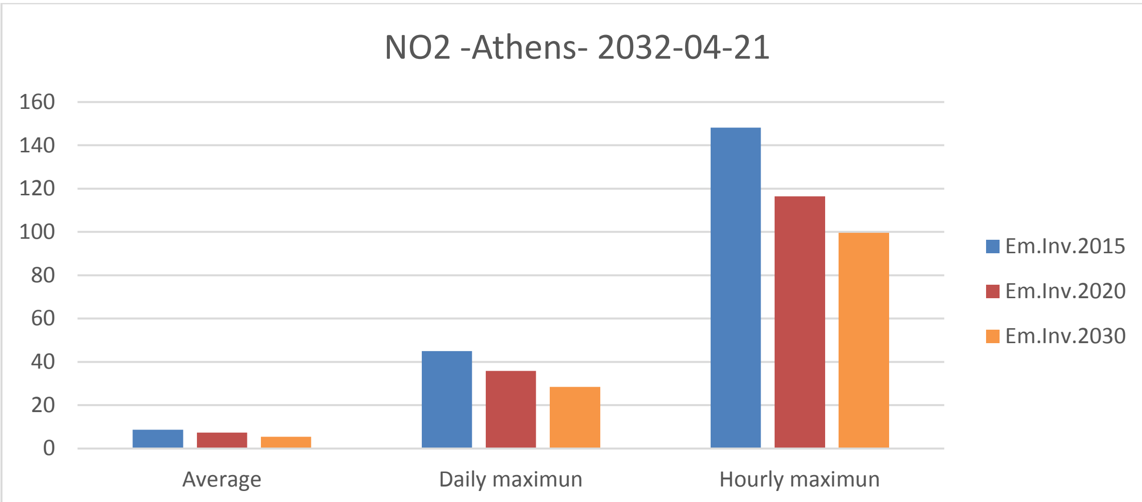


*Figure 4.5.30: $NO_2$ emission inventory comparison*

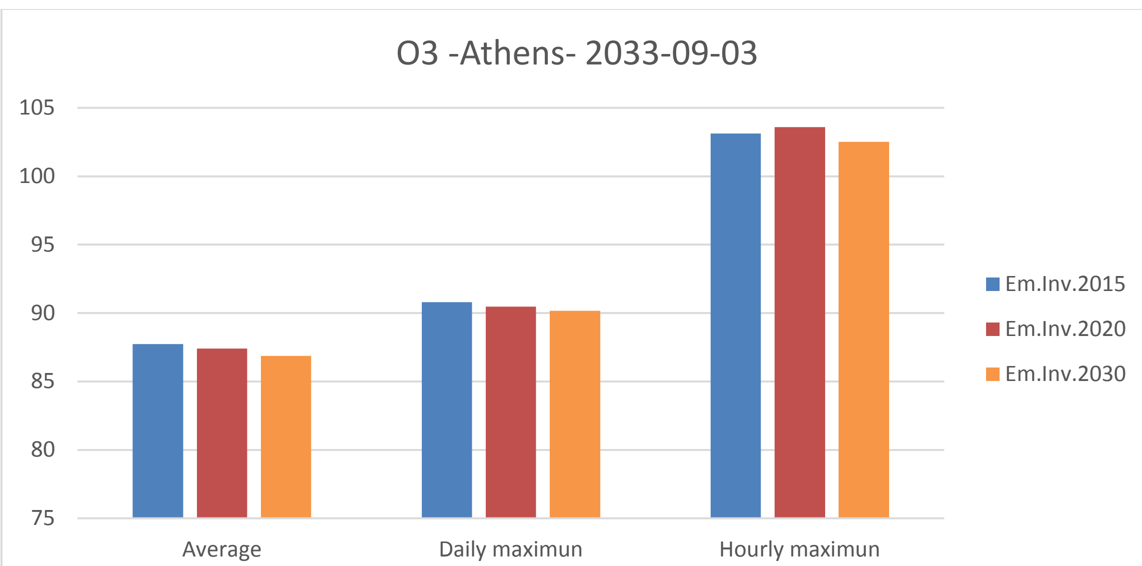


*Figure 4.5.31: $O_3$ emission inventory comparison*

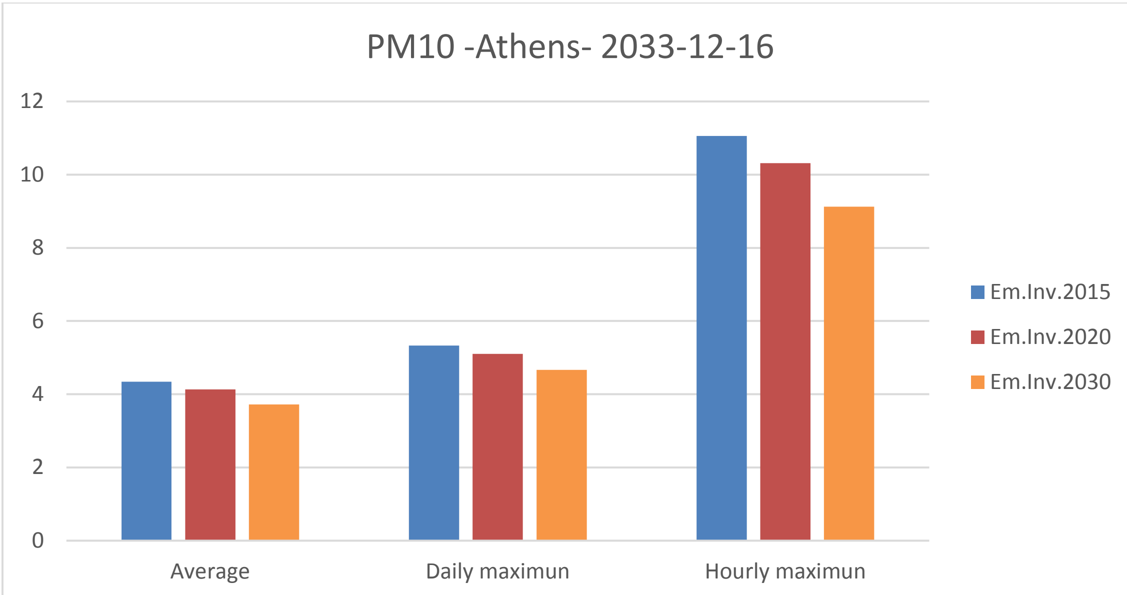


*Figure 4.5.32: $PM_{10}$ emission inventory comparison*

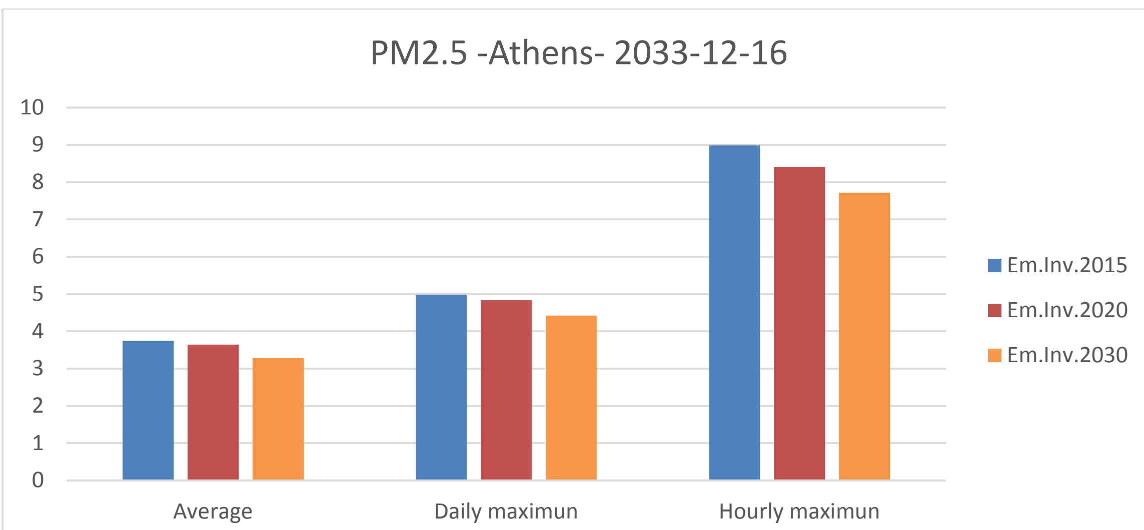


*Figure 4.5.33: $PM_{2.5}$ emission inventory comparison*

### 4.5.4 The GHGs Modeling result

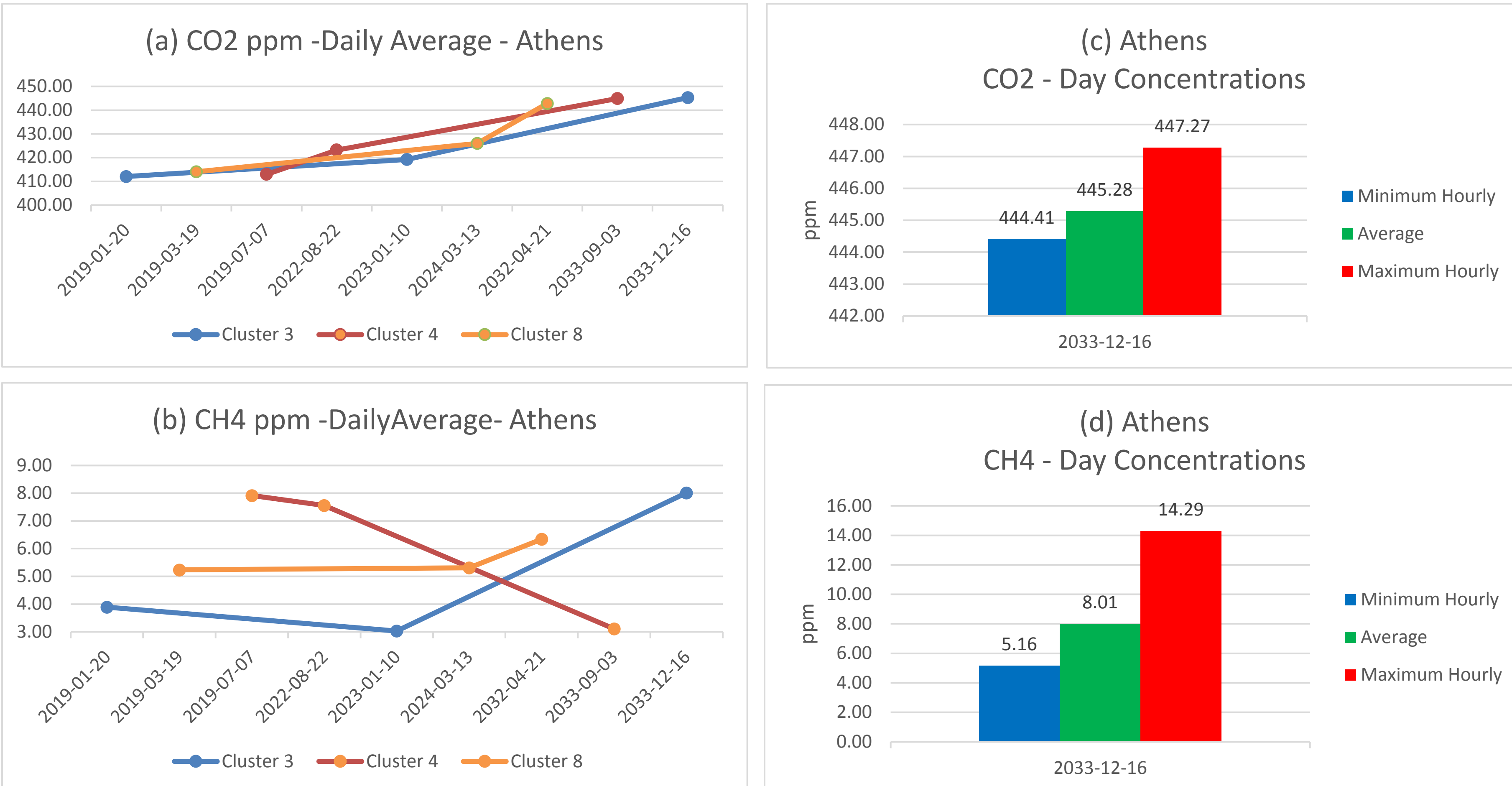


*Figure 4.5.34: (a),(b) $CO_2$ and $CH_4$ Daily average concentrations . (c),(d) $CO_2$ and $CH_4$ concentrations of the most polluted day*

### 4.5.5 Conclusions

For Athens greater area, clusters 1,2,3,6 and 10 could be categorized in cold period and on the other hand clusters 4,5,7 and 9 in warm period.

In clusters 4 and 10 there is a linear increase in frequency occurrence through the ten 5-year periods. On the other hand, clusters 3,8 and 9 show a linear decrease in frequency occurrence.

Heat waves occurrence shows an increased rate. The 5-year period 2046-2050 shows the highest number of heat waves. The most heat waves were associated with clusters 4 and 5 which correspond to clusters with days belong to warm period.

Cluster 8 is characterized with elevated $NO_2$ concentrations, cluster 4 with elevated $O_3$ concentrations and cluster 3 with elevated PM concentrations.

$NO_2$ concentrations show a decreasing trend. There is one day in which the daily maximum concentration is below the EU and WHO yearly limit of 40μg/m$^3$. The maximum hourly concentrations are below the limit of 200μg/m$^3$.

For $O_3$ concentrations the picture is mixed. Only in one day the daily maximum concentration is below WHO 8hr limit of 100μg/m$^3$. All maximum hourly concentrations are above the WHO limit.

$PM_{10}$ daily maximum concentrations in one day exceed the WHO yearly limit of 20μg/m$^3$, however all concentrations are below the daily WHO limit of 50μg/m$^3$ and there is a clear decreasing trend.

$PM_{2.5}$ concentrations are following a decreasing trend. The daily maximum concentrations are below the WHO yearly limit of 10μg/m$^3$ in two days.

For BaP concentrations, there is a clear decreasing trend. All days are above WHO annual limit of 0.12ng/m$^3$ however one day almost reaches the WHO limit and two days are on and below the EU annual limit of 1ng/m$^3$.

There is a decreasing trend in $NO_2$ and PM concentrations and a slight decrease in $O_3$ indicating the positive effect on emission reductions intervention; a quality check of the emission inventory could clarify more the outcome.

## 4.6 Thessaloniki

### 4.6.1 PCA results

The PCA analysis applied to the Thessaloniki data has led to the following results.

Three (3) principal components have been identified as factors for the cluster analysis (Table 4.6.1). Principal Components (PC) explaining 73.71% of the total variance in the initial data.

Factor 1 explains 34.23% of the total variance and contains the mean daily temperature, down ward short-wave radiation, atmospheric boundary layer thickness precipitation and a negative sign of surface pressure.

Factor 2 explains 23.12% of the total variance and contains the, the U and V wind component.

Factor 3 explains 16.34% of the total variance and contains the mean daily temperature range and a negative sign of precipitation and RH.

Table 4.6.1: The Principal Components results

| | Component | | |
|---|---|---|---|
| | 1 | 2 | 3 |
| Downward short-wave surface radiation | .858 | | |
| Temperature | .817 | | |
| Atmospheric boundary layer thickness | .741 | | |
| Surface pressure | -.633 | | |
| U wind | | -.861 | |
| V wind | | .773 | |
| Precipitation | | | -.790 |
| Temperature Range | | | .665 |
| RH | | | -.635 |

### 4.6.2 Clustering results

#### Cluster description and trends

As explained in 3.4.4 the selected clusters of the city of Thessaloniki are 8. In Figure 4.6.1 are shown the number of days per cluster, where clusters 1,8 have the most days and cluster 4 and 5 have the less. The monthly distribution per cluster is presented in Table 4.6.2 and in Figure 4.6.2. By dividing the year in two periods, cold and warm, clusters 3,5,6 and 8 could be categorized in cold period and on the other hand clusters 1,2 and 7 in warm period.

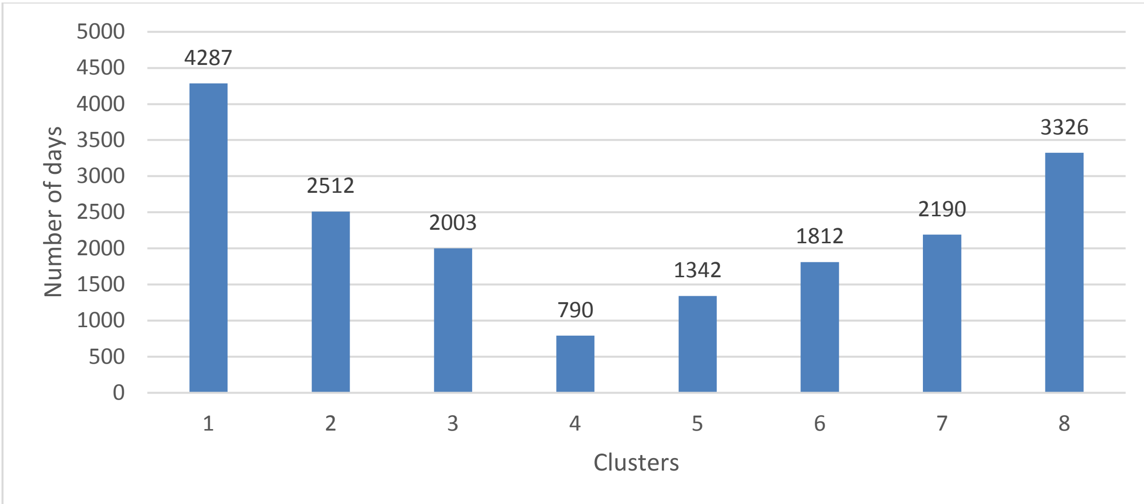


*Figure 4.6.1: Number of Days per cluster*

*Table 4.6.2: Monthly distribution per cluster*

| | | Month | | | | | | | | | | | | Total |
|---|---|---|---|---|---|---|---|---|---|---|---|---|---|---|
| | | Jan | Feb | Mar | Apr | May | Jun | Jul | Aug | Sep | Oct | Nov | Dec | |
| Cluster 8 | 1 | 0 | 22 | 114 | 426 | 458 | 505 | 694 | 1100 | 852 | 115 | 1 | 0 | 4287 |
| | 2 | 30 | 76 | 122 | 212 | 354 | 454 | 482 | 236 | 268 | 194 | 60 | 24 | 2512 |
| | 3 | 415 | 327 | 289 | 50 | 1 | 0 | 0 | 0 | 16 | 208 | 313 | 384 | 2003 |
| | 4 | 44 | 42 | 70 | 70 | 77 | 138 | 136 | 33 | 30 | 61 | 47 | 42 | 790 |
| | 5 | 180 | 217 | 289 | 173 | 83 | 13 | 1 | 5 | 37 | 90 | 127 | 127 | 1342 |
| | 6 | 385 | 207 | 165 | 71 | 14 | 1 | 0 | 1 | 17 | 197 | 341 | 413 | 1812 |
| | 7 | 6 | 36 | 124 | 393 | 554 | 389 | 237 | 175 | 200 | 56 | 17 | 3 | 2190 |
| | 8 | 490 | 485 | 377 | 105 | 9 | 0 | 0 | 0 | 80 | 629 | 594 | 557 | 3326 |
| Total | | 1550 | 1412 | 1550 | 1500 | 1550 | 1500 | 1550 | 1550 | 1500 | 1550 | 1500 | 1550 | 18262 |

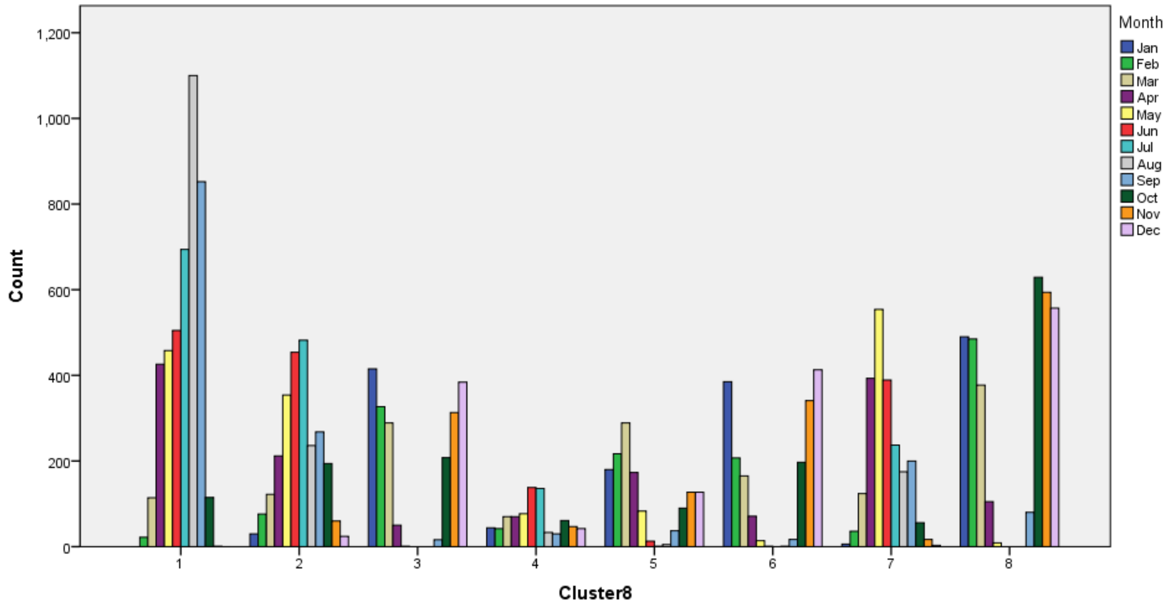


*Figure 4.6.2: Visualized bar chart of monthly distribution per cluster*

A trend analysis of the 5-year frequency of each cluster (Figure 4.6.3). There is an evidence that in clusters 1,7 and 8 there is a linear increase in frequency occurrence through the ten 5-year periods. On the other hand, clusters 3 and 4 show a linear decrease in frequency occurrence. In the rest clusters no clear trends could be pointed out.

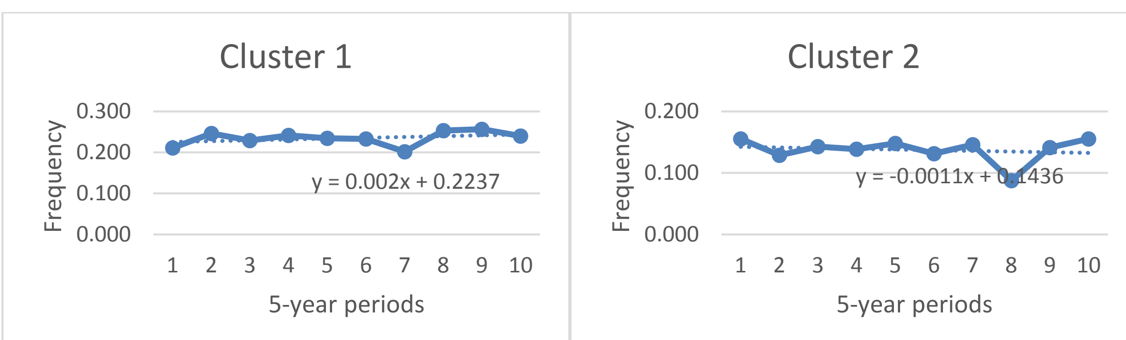

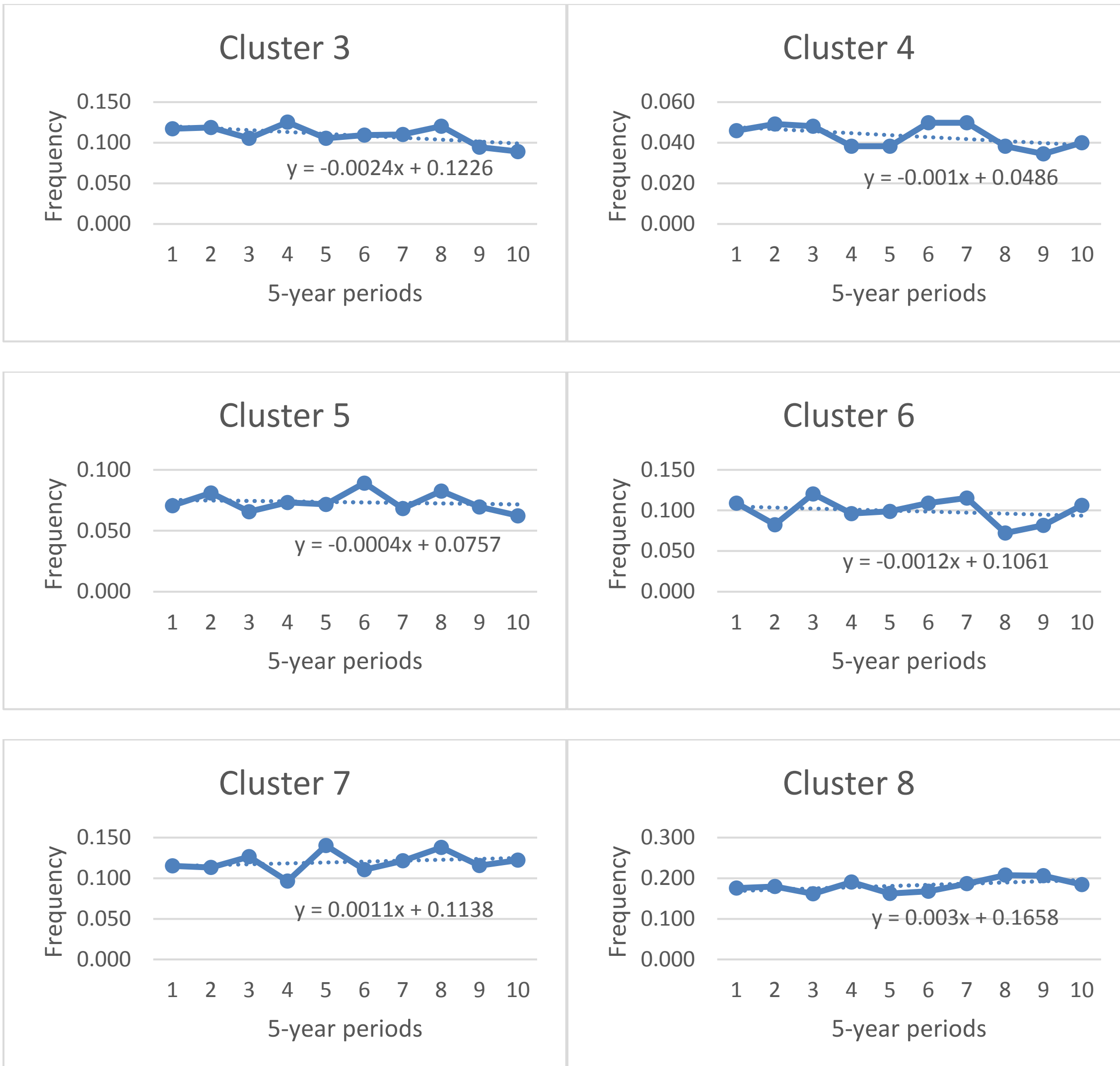


*Figure 4.6.3: Cluster 1-8 frequency trends*

## Cluster characterization

The clusters' implementation is based on the mean values of weather parameters which are displayed in Table 4.6.3.

*Table 4.6.3: Summary of the 8 clusters*

| | Cluster | | | | | | | |
|---|---|---|---|---|---|---|---|---|
| | 1 | 2 | 3 | 4 | 5 | 6 | 7 | 8 |
| | Mean (SD) | Mean (SD) | Mean (SD) | Mean (SD) | Mean (SD) | Mean (SD) | Mean (SD) | Mean (SD) |
| Temperature ( ºC) | 23,41 (4,96) | 20,52 (5,54) | 7,45 (5,02) | 16,3 (7,2) | 8,09 (5,29) | 9,67 (4,48) | 19,33 (5,78) | 10,66 (4,91) |
| Daily Temperature Range ( ºC) | 12,11 (1,5) | 9,22 (1,5) | 8,35 (1,91) | 6,21 (1,88) | 7,2 (1,7) | 6,67 (1,82) | 11,31 (1,68) | 10,11 (1,71) |
| Relative Humidity (%) | 50,35 (7,63) | 63,63 (7,04) | 51,48 (9,08) | 77,68 (6,79) | 48,08 (9,03) | 74,38 (9,52) | 48,32 (7,19) | 58,57 (10,37) |
| Surface Pressure (Pa) | 99532,96 (482,58) | 98952,19 (548,3) | 100095,21 (766,9) | 98856,65 (658,2) | 99151,84 (787,98) | 99686,72 (793,53) | 99003,77 (569,2) | 100607,47 (680,25) |
| Precipitation (kg/m2/s) | 0,000003 (0,000006) | 0,000039 (0,000038) | 0,000003 (0,000009) | 0,000192 (0,000103) | 0,000008 (0,000019) | 0,000027 (0,000033) | 0,000006 (0,000011) | 0,000001 (0,000004) |
| Downward Short Wave Radiation | 303,84 (45,23) | 260,26 (73,78) | 146,35 (55,42) | 170,96 (96,52) | 192,51 (77,38) | 96,25 (48,48) | 306,42 (55,67) | 149,46 (53,77) |
| u wind component (m/s) | -0,45 (0,98) | -0,57 (1,24) | 1,54 (0,91) | -1,73 (2,01) | 3,4 (1,41) | -1,01 (1,39) | 2 (1,21) | -0,37 (0,8) |
| v wind component (m/s) | 0,97 (1,46) | 1,57 (2,13) | -2,61 (2,14) | 0,4 (2,44) | -4,59 (2,77) | 1,38 (2,29) | -1,16 (2,39) | 0,71 (1,41) |
| V wind (m/s) | 1,7 (1,16) | 2,35 (1,82) | 3,49 (1,56) | 2,93 (2,12) | 6,3 (1,63) | 2,56 (1,89) | 3,27 (1,33) | 1,44 (1,1) |
| Atmospheric Boundary Layer Thickness (m) | 710,86 (167,55) | 666,95 (145,54) | 549,23 (159,36) | 508,23 (150,57) | 950,08 (266,96) | 357,61 (146,65) | 948,41 (165,97) | 310,26 (138,69) |

In addition to the previous Table 4.6.3, Figure 4.6.4 presents the mean normalized (z-score) variables of each cluster, respectively showing the differences of the parameters per cluster.

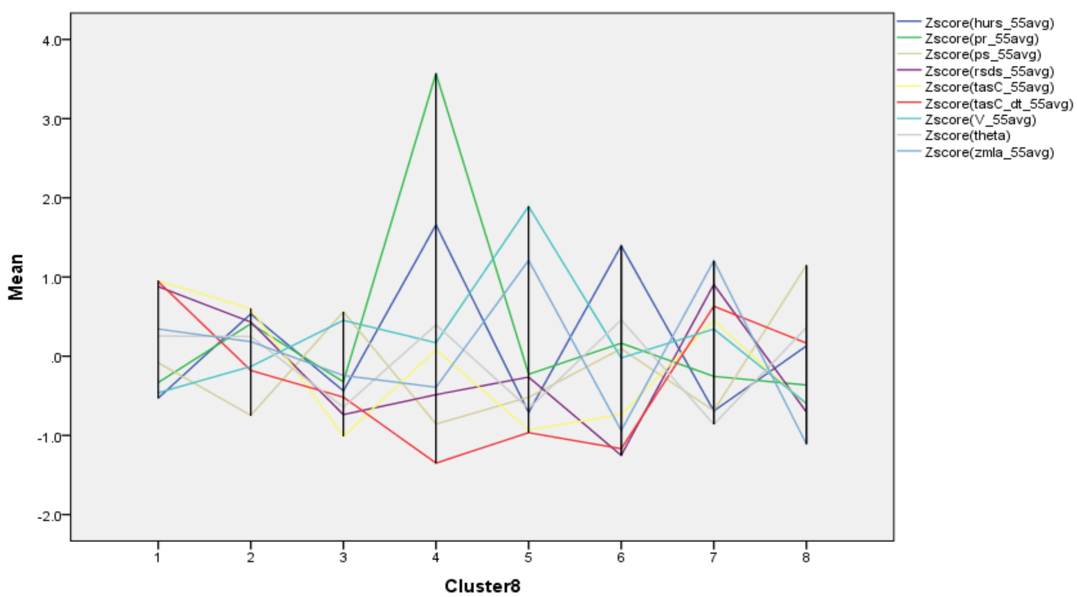


*Figure 4.6.4: Normalized variables (z-score) averaged for each cluster*

Daily, 10-meter from ground level, wind data were used to create the wind roses per each cluster as they are shown in Figures 4.6.5-4.5.12. Each wind direction distribution per cluster is presented in more details in Table 4.6.4.

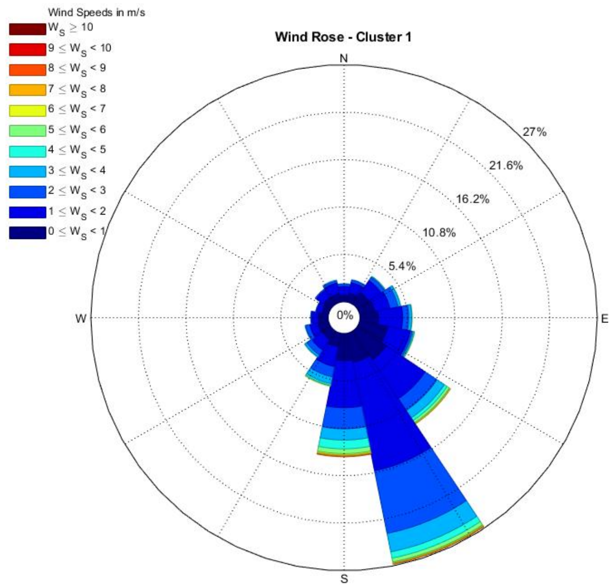


*Figure 4.6.5: Wind Rose - Cluster 1*

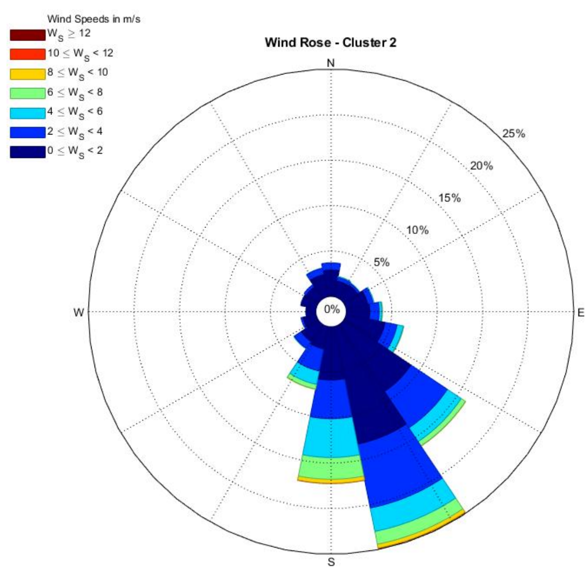


*Figure 4.6.6: Wind Rose - Cluster 2*

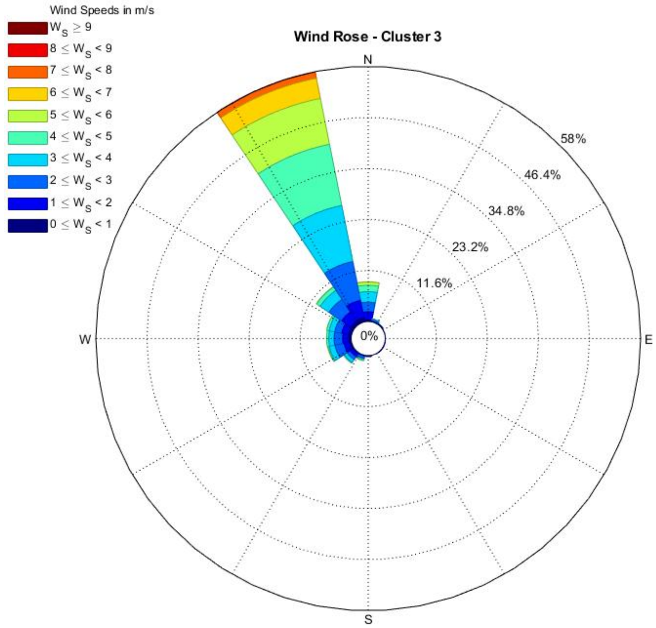


*Figure 4.6.7: Wind Rose - Cluster 3*

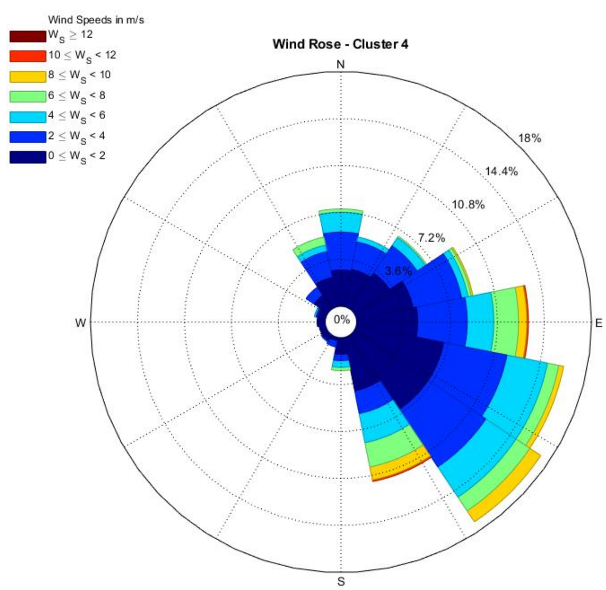


*Figure 4.6.8: Wind Rose - Cluster 4*

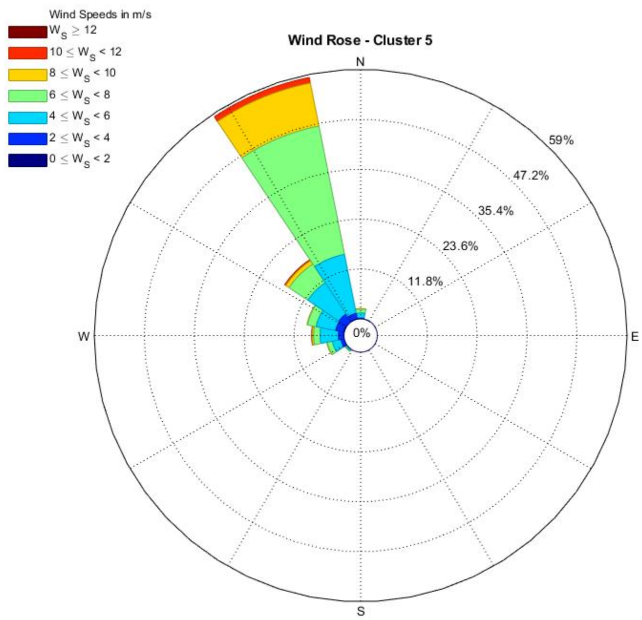


*Figure 4.6.9: Wind Rose - Cluster 5*

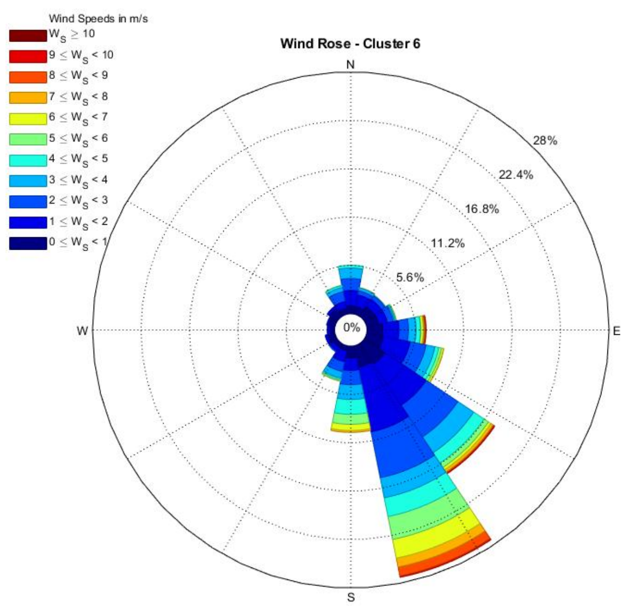


*Figure 4.6.10: Wind Rose - Cluster 6*

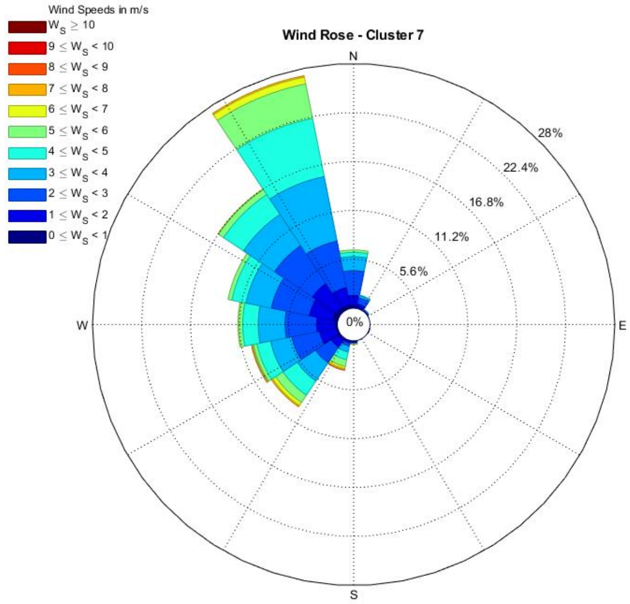


*Figure 4.6.11: Wind Rose - Cluster 7*

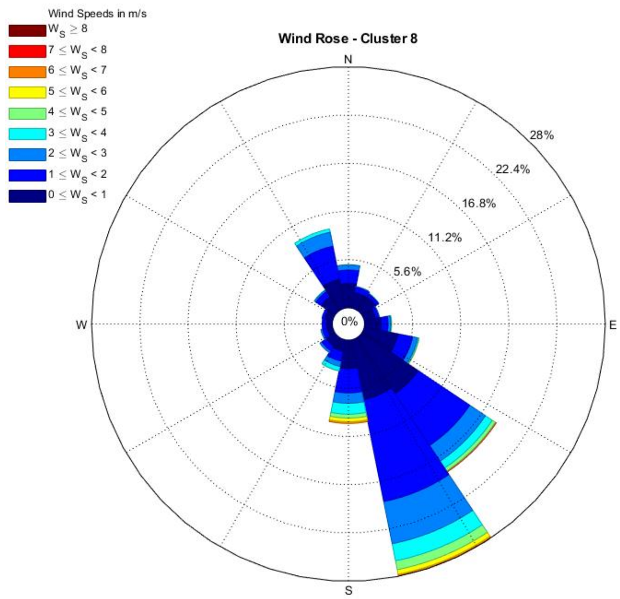


*Figure 4.6.12: Wind Rose - Cluster 8*

*Table 4.6.4: 16 Wind Direction distribution per cluster*

| | | | Wind16 | | | | | | | | | | | | | | | | Total |
|---|---|---|---|---|---|---|---|---|---|---|---|---|---|---|---|---|---|---|---|
| | | | S | SSW | SW | WSW | W | WNW | NW | NNW | N | NNE | NE | ENE | E | ESE | SE | SSE | |
| Cluster8 | 1 | Count | 601 | 264 | 155 | 117 | 86 | 65 | 92 | 110 | 89 | 112 | 166 | 205 | 255 | 274 | 547 | 1149 | 4287 |
| | | % within Cluster8 | 14.0% | 6.2% | 3.6% | 2.7% | 2.0% | 1.5% | 2.1% | 2.6% | 2.1% | 2.6% | 3.9% | 4.8% | 5.9% | 6.4% | 12.8% | 26.8% | 100.0% |
| | 2 | Count | 433 | 177 | 82 | 43 | 28 | 44 | 48 | 81 | 93 | 57 | 54 | 79 | 100 | 163 | 405 | 625 | 2512 |
| | | % within Cluster8 | 17.2% | 7.0% | 3.3% | 1.7% | 1.1% | 1.8% | 1.9% | 3.2% | 3.7% | 2.3% | 2.1% | 3.1% | 4.0% | 6.5% | 16.1% | 24.9% | 100.0% |
| | 3 | Count | 5 | 26 | 58 | 111 | 112 | 116 | 207 | 1161 | 181 | 15 | 5 | 1 | 1 | 2 | 2 | 0 | 2003 |
| | | % within Cluster8 | .2% | 1.3% | 2.9% | 5.5% | 5.6% | 5.8% | 10.3% | 58.0% | 9.0% | .7% | .2% | .0% | .0% | .1% | .1% | 0.0% | 100.0% |
| | 4 | Count | 20 | 6 | 5 | 4 | 5 | 7 | 16 | 43 | 59 | 43 | 53 | 72 | 104 | 128 | 136 | 89 | 790 |
| | | % within Cluster8 | 2.5% | .8% | .6% | .5% | .6% | .9% | 2.0% | 5.4% | 7.5% | 5.4% | 6.7% | 9.1% | 13.2% | 16.2% | 17.2% | 11.3% | 100.0% |
| | 5 | Count | 0 | 0 | 8 | 57 | 103 | 121 | 237 | 782 | 33 | 1 | 0 | 0 | 0 | 0 | 0 | 0 | 1342 |
| | | % within Cluster8 | 0.0% | 0.0% | .6% | 4.2% | 7.7% | 9.0% | 17.7% | 58.3% | 2.5% | .1% | 0.0% | 0.0% | 0.0% | 0.0% | 0.0% | 0.0% | 100.0% |
| | 6 | Count | 181 | 76 | 22 | 21 | 16 | 18 | 26 | 62 | 102 | 57 | 54 | 64 | 124 | 165 | 329 | 495 | 1812 |
| | | % within Cluster8 | 10.0% | 4.2% | 1.2% | 1.2% | .9% | 1.0% | 1.4% | 3.4% | 5.6% | 3.1% | 3.0% | 3.5% | 6.8% | 9.1% | 18.2% | 27.3% | 100.0% |
| | 7 | Count | 9 | 76 | 207 | 220 | 249 | 280 | 368 | 595 | 146 | 34 | 5 | 0 | 0 | 1 | 0 | 0 | 2190 |
| | | % within Cluster8 | .4% | 3.5% | 9.5% | 10.0% | 11.4% | 12.8% | 16.8% | 27.2% | 6.7% | 1.6% | .2% | 0.0% | 0.0% | .0% | 0.0% | 0.0% | 100.0% |
| | 8 | Count | 322 | 123 | 71 | 47 | 40 | 43 | 97 | 312 | 167 | 86 | 80 | 61 | 105 | 217 | 625 | 930 | 3326 |
| | | % within Cluster8 | 9.7% | 3.7% | 2.1% | 1.4% | 1.2% | 1.3% | 2.9% | 9.4% | 5.0% | 2.6% | 2.4% | 1.8% | 3.2% | 6.5% | 18.8% | 28.0% | 100.0% |
| Total | | Count | 1571 | 748 | 608 | 620 | 639 | 694 | 1091 | 3146 | 870 | 405 | 417 | 482 | 689 | 950 | 2044 | 3288 | 18262 |
| | | % within Cluster8 | 8.6% | 4.1% | 3.3% | 3.4% | 3.5% | 3.8% | 6.0% | 17.2% | 4.8% | 2.2% | 2.3% | 2.6% | 3.8% | 5.2% | 11.2% | 18.0% | 100.0% |

#### 3.4.5.1 Clusters and local Heat Waves

In Figures 4.6.13 and 4.6.14 are presented the heat waves occurrence per 5-year period and per cluster. Heat wave occurrence show an increasing rate after 2031.The 5-year period 2046-2050 shows the highest number of heat waves. The most heat waves were associated with cluster 1 which correspond to cluster with days belong to warm period (see Table 4.6.2).

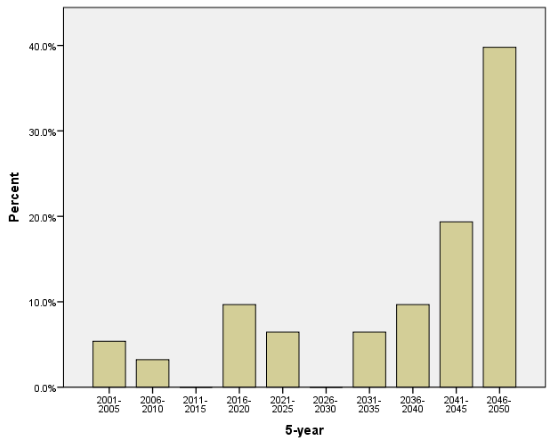


*Figure 4.6.13: Heat Waves per 5-year period*

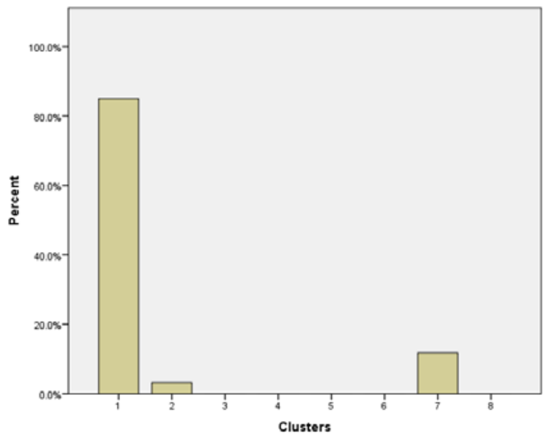


*Figure 4.6.14: Heat Waves per cluster*

#### 3.4.5.2 Clusters versus Air Quality level

As it can be seen in Table 4.1 five observation stations have been used for the present analysis. The descriptive statistics for $NO_2$, $O_3$ and $PM_{10}$ is given in Table 4.6.5.

*Table 4.6.5: Air pollutants descriptive statistics*

| | | MEAN_NO2 | MEAN_O3 | MEAN_PM10 |
|---|---|---|---|---|
| Mean | | 31.7384 | 57.2316 | 45.6042 |
| Std. Deviation | | 13.29536 | 25.84842 | 21.34237 |
| Minimum | | 5.65 | 3.63 | 9.00 |
| Maximum | | 95.67 | 150.61 | 231.50 |
| Percentiles | 5 | 12.9649 | 17.7000 | 20.0589 |
| | 25 | 21.4730 | 37.8610 | 30.9922 |
| | 50 | 30.2970 | 55.2500 | 41.2000 |
| | 75 | 40.2290 | 75.2916 | 55.6875 |
| | 95 | 55.8748 | 102.0947 | 86.3931 |

Table 4.6.6 presents the pollutants' concentrations per cluster. Higher mean $NO_2$ concentrations are observed in clusters 3,6 and 8. Higher mean $O_3$ concentrations are observed in clusters 1,2 and 7. Higher mean $PM_{10}$ concentrations are observed in clusters 3,6 and 8.

*Table 4.6.6: Summary pollutant concentrations per cluster*

| | Cluster | | | | | | | |
|---|---|---|---|---|---|---|---|---|
| | 1 | 2 | 3 | 4 | 5 | 6 | 7 | 8 |
| | Mean (SD) | Mean (SD) | Mean (SD) | Mean (SD) | Mean (SD) | Mean (SD) | Mean (SD) | Mean (SD) |
| PM10 (µg/m3) | 40,56 (15,39) | 42,75 (17,51) | 52,13 (27,05) | 44,73 (16,86) | 45,64 (23,67) | 50,44 (23,67) | 42,68 (19,59) | 50,1 (24,22) |
| O3 (µg/m3) | 72,31 (22,82) | 68,09 (23,77) | 40,52 (18,84) | 61,47 (24,68) | 49,12 (23,14) | 42,77 (20,8) | 70,72 (22,4) | 41,2 (19,09) |
| NO2 (µg/m3) | 26,91 (11,49) | 29,56 (12,39) | 36,53 (14,09) | 31,54 (12,39) | 33,69 (13,78) | 35,5 (13,57) | 30,25 (11,96) | 35,34 (13,83) |

The differences in concentrations per cluster are shown in Figures 4.6.15-4.6.17.

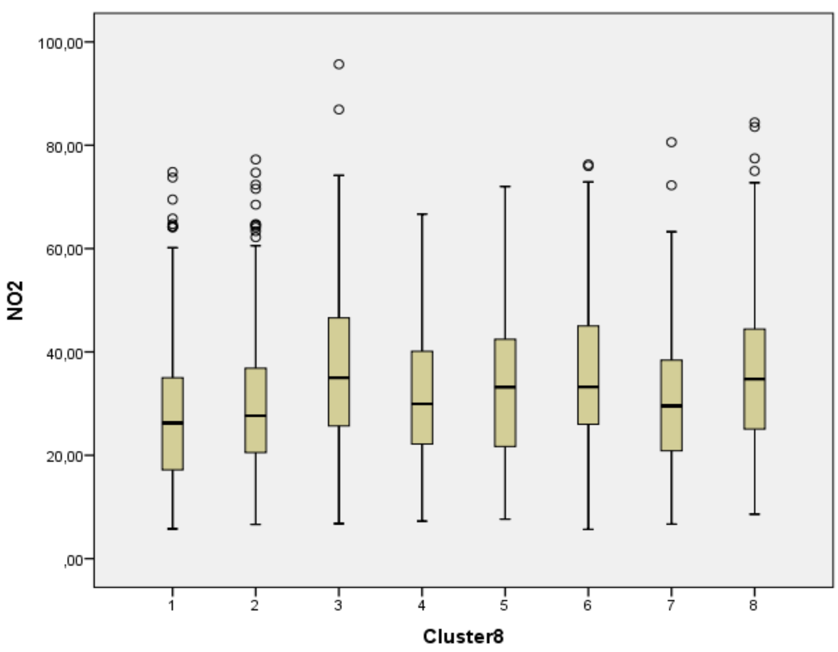


*Figure 4.6.15: $NO_2$ concentration statistics per cluster*

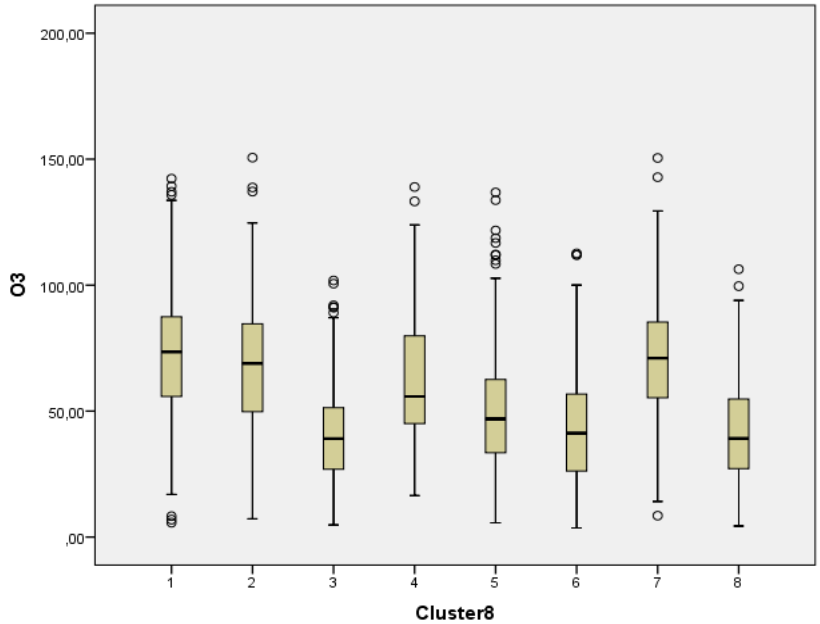


*Figure 4.6.16: $O_3$ concentration statistics per cluster*

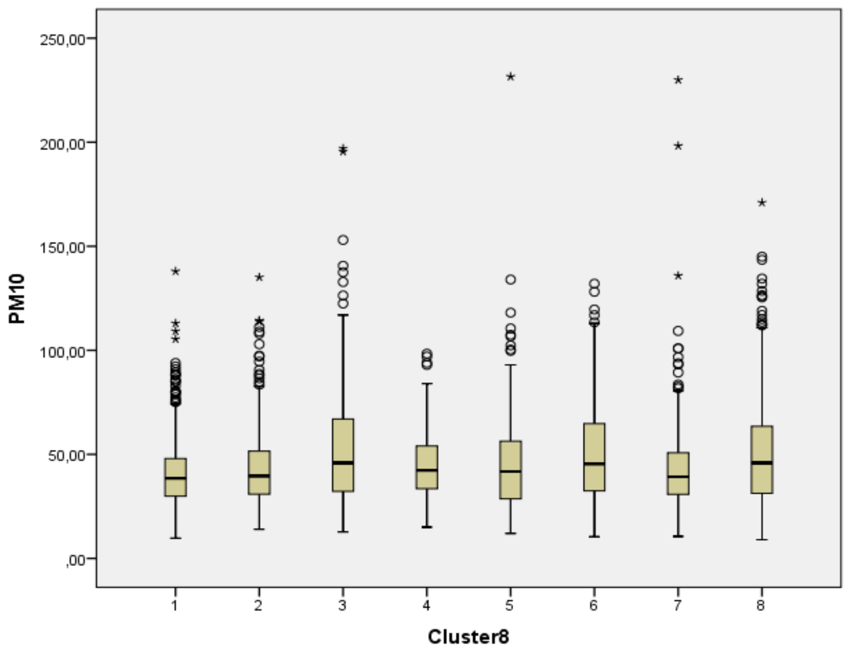


*Figure 4.6.17: $PM_{10}$ concentration statistics per cluster*

## Representative Days

In the following Table 4.6.7 are presented the selected RDs per 5-year period and per cluster.

*Table 4.6.7: Representative days per cluster and 5year period*

| Closest days to centroids per 5year per cluster | | | clusters | | | | | | | |
|---|---|---|---|---|---|---|---|---|---|---|
| | | | 1 | 2 | 3 | 4 | 5 | 6 | 7 | 8 |
| 5 year period | 2001-2005 | 1 | 2004-09-05 | 2005-06-02 | 2002-12-06 | 2001-11-03 | 2005-12-12 | 2003-03-25 | 2003-05-20 | 2002-03-21 |
| | 2006-2010 | 2 | 2006-07-25 | 2006-08-03 | 2006-10-21 | 2007-05-09 | 2009-10-05 | 2006-01-25 | 2007-04-25 | 2009-11-01 |
| | 2011-2015 | 3 | 2012-08-20 | 2013-08-10 | 2015-11-25 | 2015-06-28 | 2013-03-01 | 2011-09-30 | 2013-05-17 | 2014-11-25 |
| | 2016-2020 | 4 | 2019-07-02 | 2019-07-08 | 2018-01-12 | 2017-04-19 | 2017-01-21 | 2019-12-02 | 2018-05-18 | 2016-01-30 |
| | 2021-2025 | 5 | 2021-08-11 | 2022-06-01 | 2025-02-11 | 2024-06-10 | 2022-01-25 | 2022-01-28 | 2022-05-08 | 2023-02-09 |
| | 2026-2030 | 6 | 2029-09-01 | 2026-06-03 | 2030-12-13 | 2026-06-02 | 2029-10-27 | 2030-11-30 | 2028-06-05 | 2030-12-14 |
| | 2031-2035 | 7 | 2035-07-29 | 2034-04-22 | 2035-02-26 | 2034-04-28 | 2031-01-15 | 2032-01-15 | 2031-09-22 | 2031-01-19 |
| | 2036-2040 | 8 | 2037-06-04 | 2037-08-02 | 2038-12-08 | 2036-10-04 | 2039-01-08 | 2040-02-20 | 2040-05-05 | 2038-11-07 |
| | 2041-2045 | 9 | 2042-08-30 | 2042-06-01 | 2042-02-19 | 2042-04-19 | 2042-02-14 | 2041-01-15 | 2044-05-29 | 2045-11-03 |
| | 2046-2050 | 10 | 2048-05-22 | 2048-04-23 | 2048-10-22 | 2048-06-15 | 2050-10-14 | 2047-12-19 | 2049-05-31 | 2050-11-29 |

## Selected Clusters and RDs for modeling purposes

Selected RDs will be used to perform targeted weather and air quality simulations within each selected 5-year period estimating hourly/daily concentrations of the priority pollutants to assess the climatic effect on air quality evolution and the characteristics of air quality future episodes. The selection was based on 3-year periods (2016-2020, 2021-2025 and 2031-2035) and on the clusters with the most elevated concentrations of $PM_{10}$, $NO_2$ and $O_3$. In the case of Thessaloniki, cluster 1 for the case of $O_3$ and cluster 3 for the case of $NO_2$ and $PM_{10}$. In Table 4.5.8 are presented the selected days which was used for modeling purposes.

*Table 4.6.8: RDs for modeling purposes*

| **Period** | **Cluster 1 (O3)** | **Cluster 3 (NO2, PM)** |
|---|---|---|
| 2016-2020 | 2019-07-02 | 2018-01-12 |
| 2021-2025 | 2021-08-11 | 2025-02-11 |
| 2031-2035 | 2035-07-29 | 2035-02-26 |

### 4.6.3 Air Quality Modeling results

#### 4.6.3.1 Overall results

In Figure 4.6.18 the daily average concentrations of $NO_2$, $O_3$, $PM_{10}$ and $PM_{2.5}$ for selected RDs are presented.

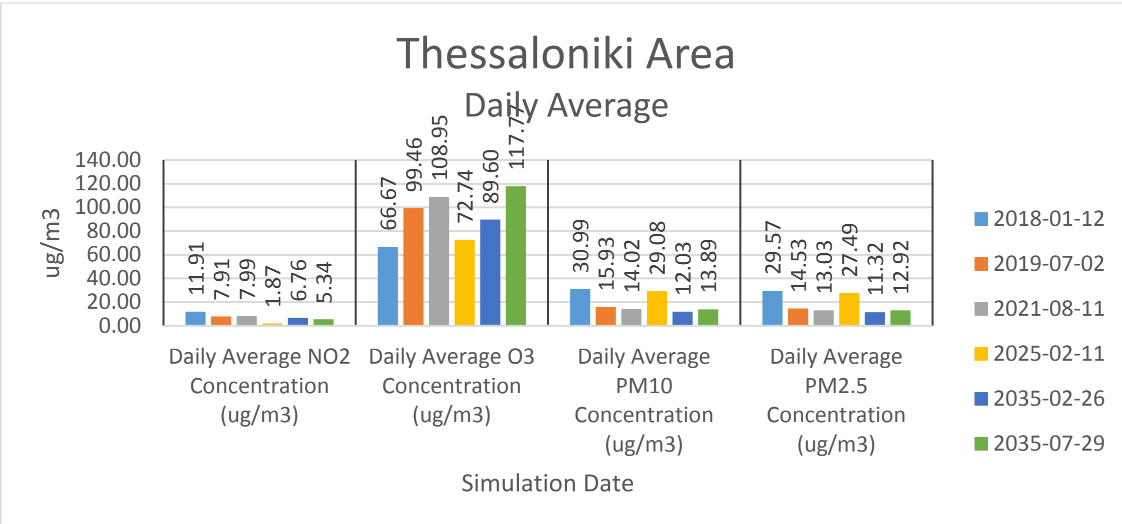


*Figure 4.6.18: Daily average concentrations*

In Figure 4.6.19 the obtained daily averaged concentrations are compared based on USTUTT and EGDAR HTAP emission inventories respectively. The results seem not to differ significantly.

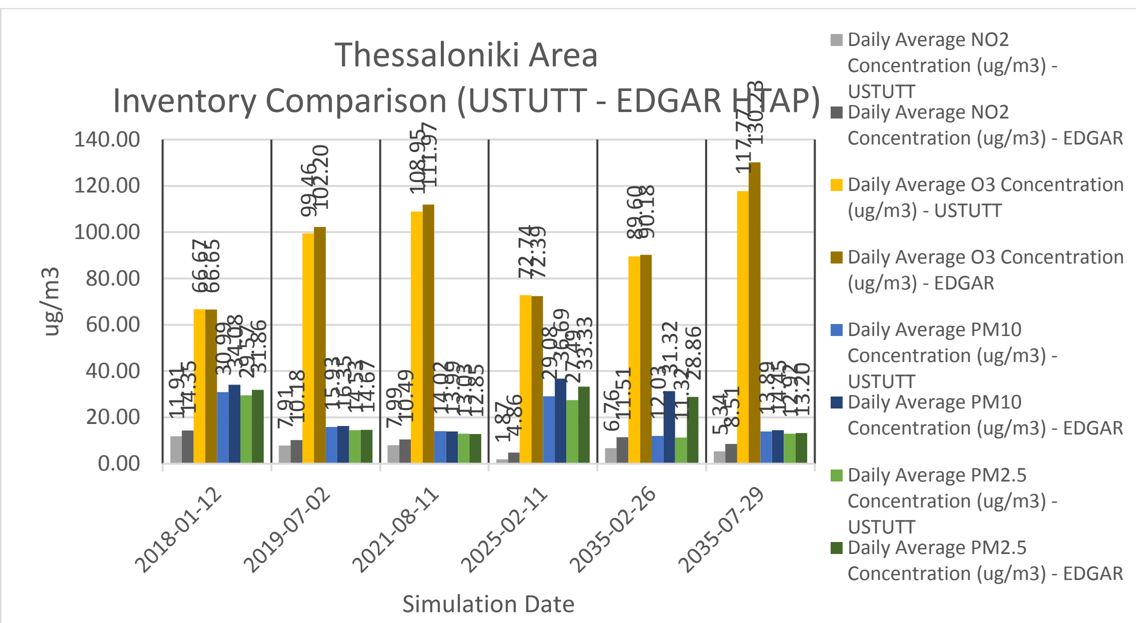


*Figure 4.6.19: Daily average concentrations – USTUTT vs EDGAR HTAP comparison*

### 4.6.3.2 Clusters results

$NO_2$ Concentrations (Cluster 3)

In Figure 4.6.20, the results are presented in terms of concentrations average, daily maximum and hourly maximum. The diurnal variations are shown in Figure 4.6.21.

Concentrations show a mixed picture. There is only one day in which the daily maximum concentration is below the EU and WHO yearly limit of 40μg/m$^3$. The maximum hourly concentrations are below the limit of 200μg/m$^3$.

$O_3$ Concentrations (Cluster 1)

In Figure 4.6.22, the results are presented in terms of concentrations average, daily maximum and hourly maximum. The diurnal variations are shown in Figure 4.6.23.

The daily average concentrations show an increasing trend with daily maximum values exceeding the WHO 8hr limit of 100μg/m$^3$. The maximum hourly concentrations exceed this limit as well as the EU 8hr limit of 120μg/m$^3$.

$PM_{10}$ Concentrations (Cluster 3)

In Figure 4.6.24, the results are presented in terms of concentrations average, daily maximum and hourly maximum. The diurnal variations are shown in Figure 4.6.25.

The daily maximum concentrations are above the WHO yearly limit of 20μg/m$^3$ showing a decreasing trend. In one day, the daily maximum concentration in also above the daily WHO limit of 50μg/m$^3$.

### $NO_2$-Cluster 3

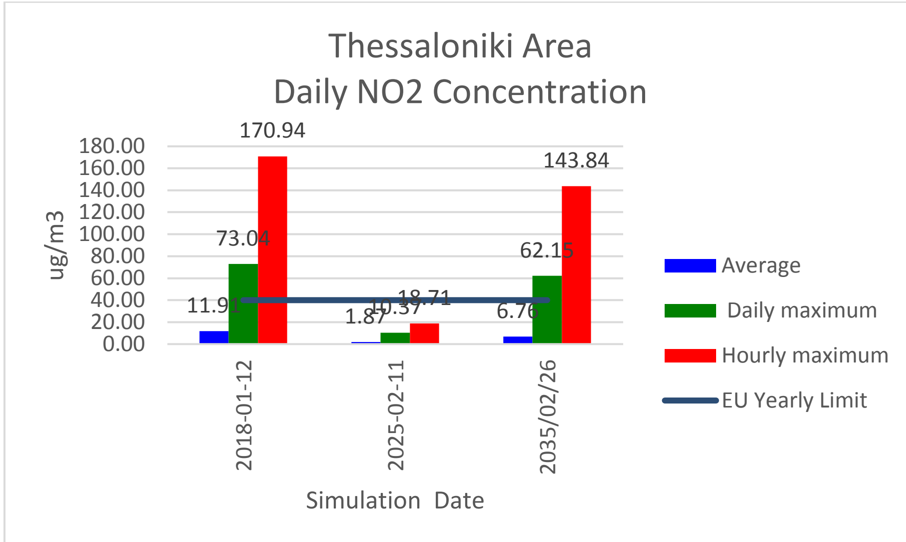


*Figure 4.6.20: $NO_2$ Day concentrations*

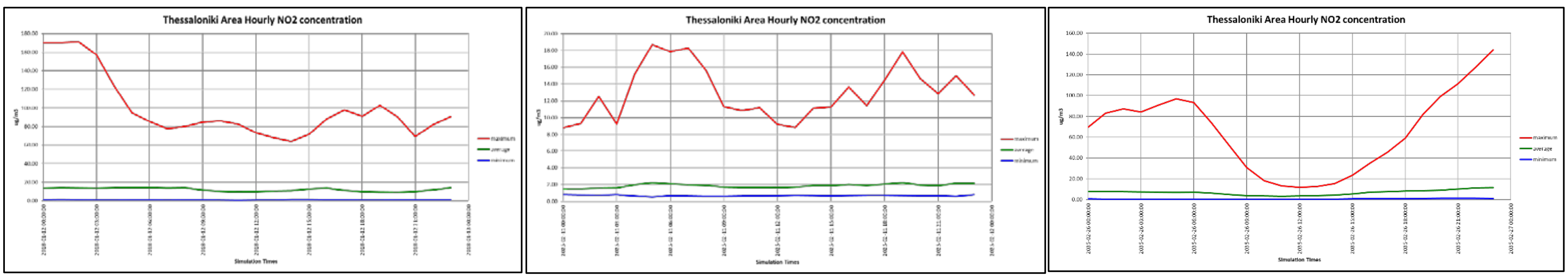


*Figure 4.6.21: Hourly $NO_2$ concentrations*

## $O_3$-Cluster 1

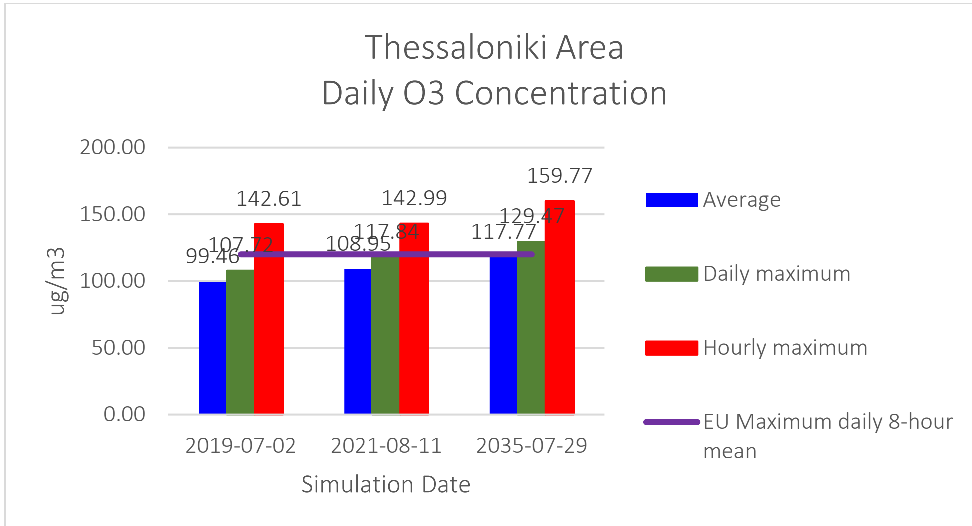


*Figure 4.6.22: $O_3$ Daily concentrations*

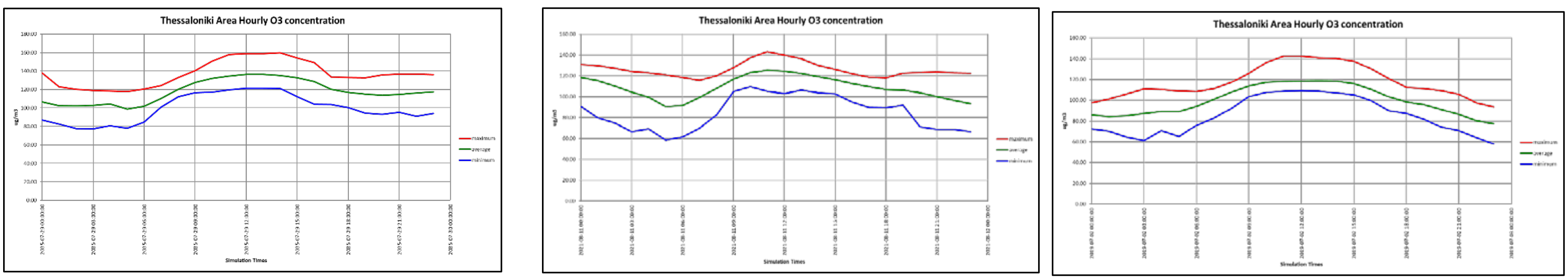


Figure 4.6.23: $O_3$ Hourly concentrations

## $PM_{10}$-Cluster 3

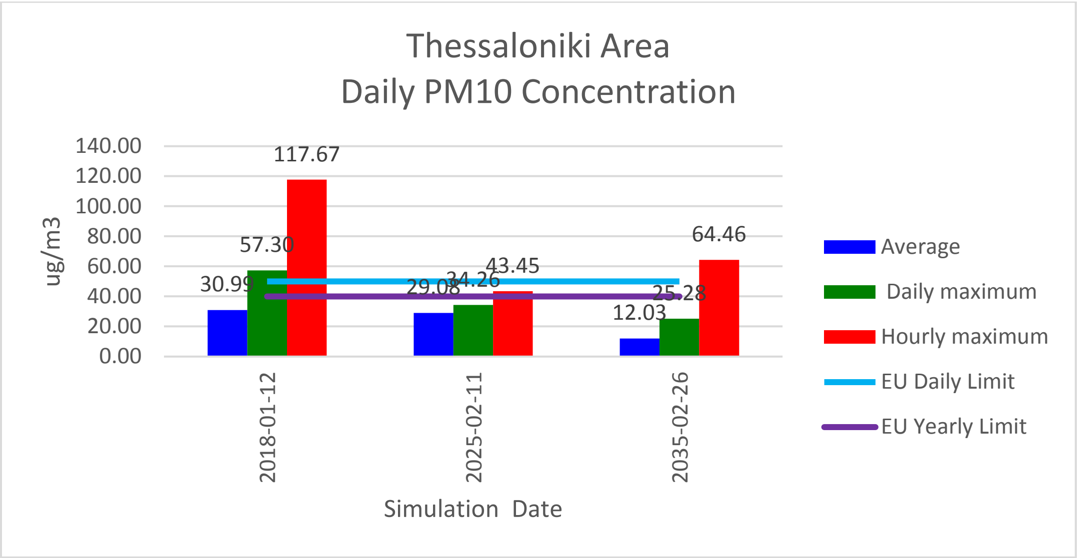


*Figure 4.6.24: $PM_{10}$ Daily concentrations*

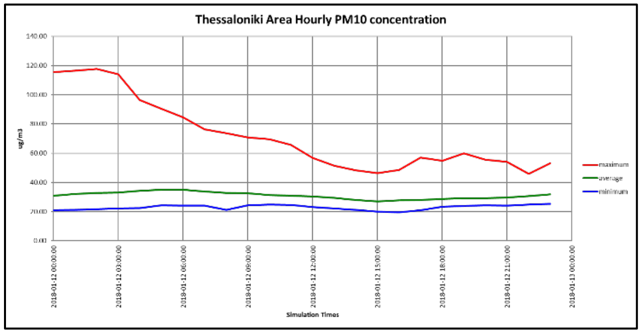


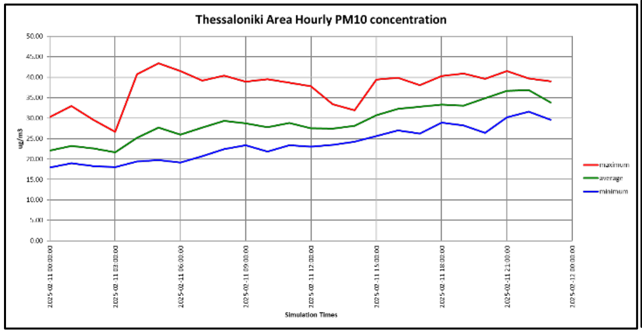


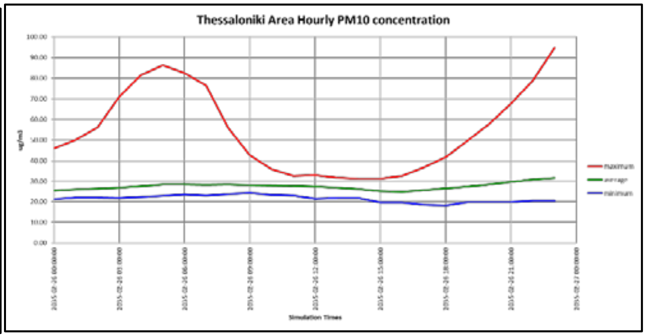


*Figure 4.6.25: $PM_{10}$ Hourly concentrations*

PM$_{2.5}$ Concentrations (Cluster 3)

In Figure 4.6.28, the results are presented in terms of concentrations average, daily maximum and hourly maximum.
The daily maximum concentrations are following a decreasing trend. The daily maximum concentrations are above the WHO yearly limit of 10μg/m$^3$.

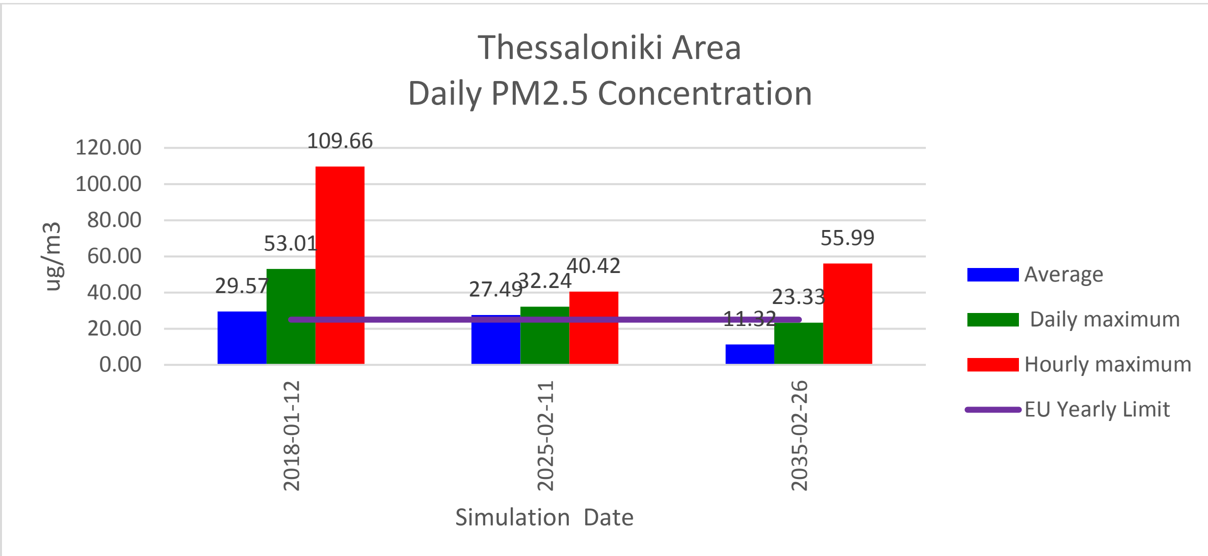


*Figure 4.6.26: PM$_{2.5}$ Day concentrations*

Figure 4.6.27 presents the estimated BaP daily concentrations contained in PM$_{2.5.}$ There is a decreasing trend. All days are above WHO annual limit of 0.12ng/m$^3$ however one day is below the EU annual limit of 1ng/m$^3$.

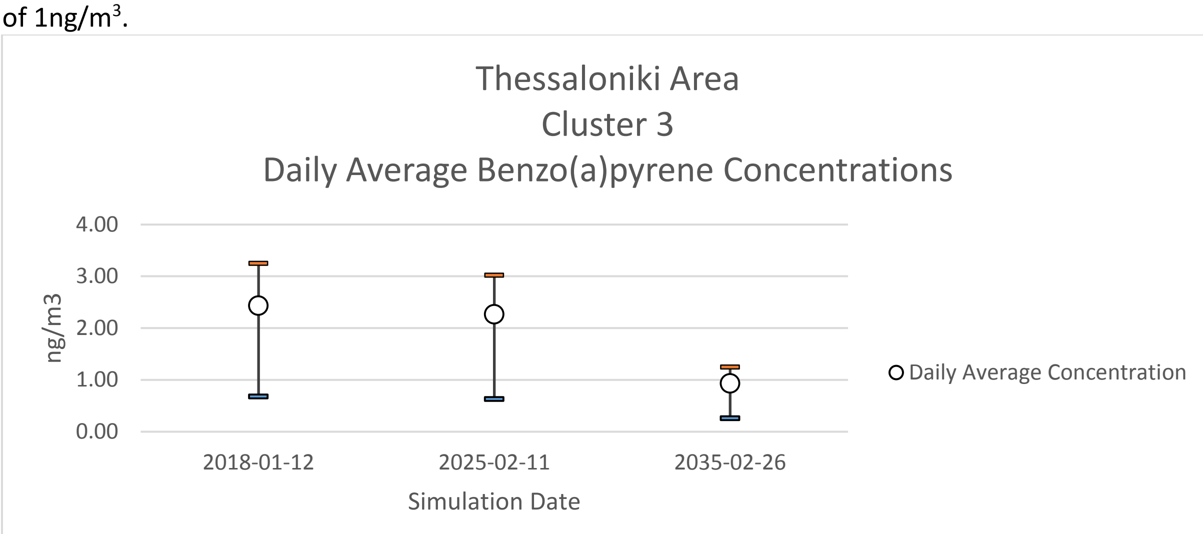


*Figure 4.6.27: BaP daily concentrations*

### 4.6.3.3 The Emission Inventory effect

Figures 4.6.28, 4.6.29, 4.6.30 and 4.6.31 illustrate the emission inventory temporal change effect on $NO_2$, $O_3$, $PM_{10}$ and $PM_{2.5}$ concentration levels respectively. There is a slight decreasing trend in all pollutants indicating the positive effect on emission reductions intervention.

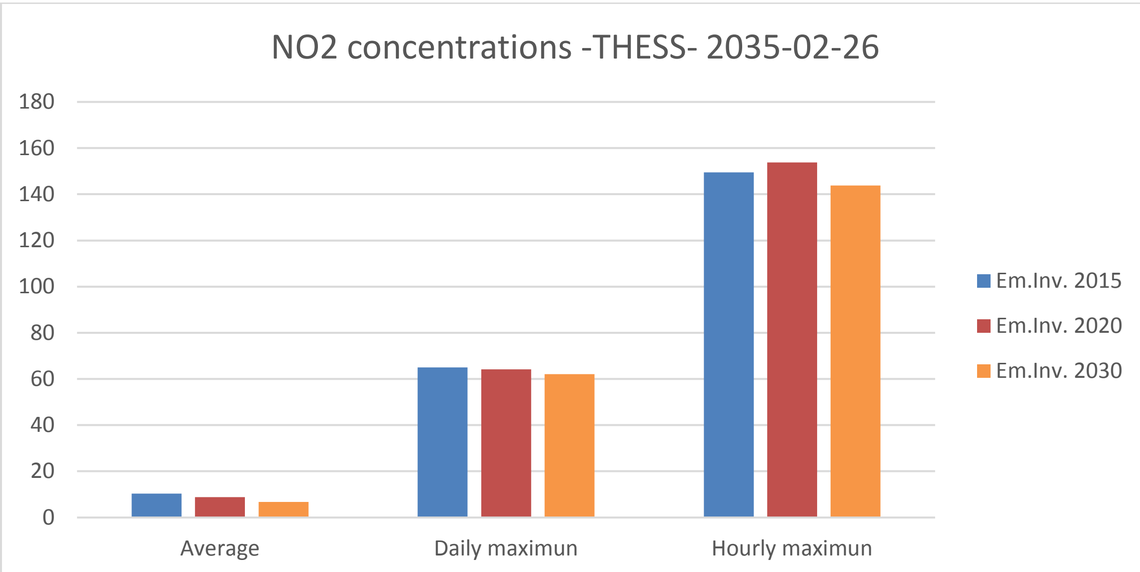


*Figure 4.6.28: $NO_2$ emission inventory comparison*

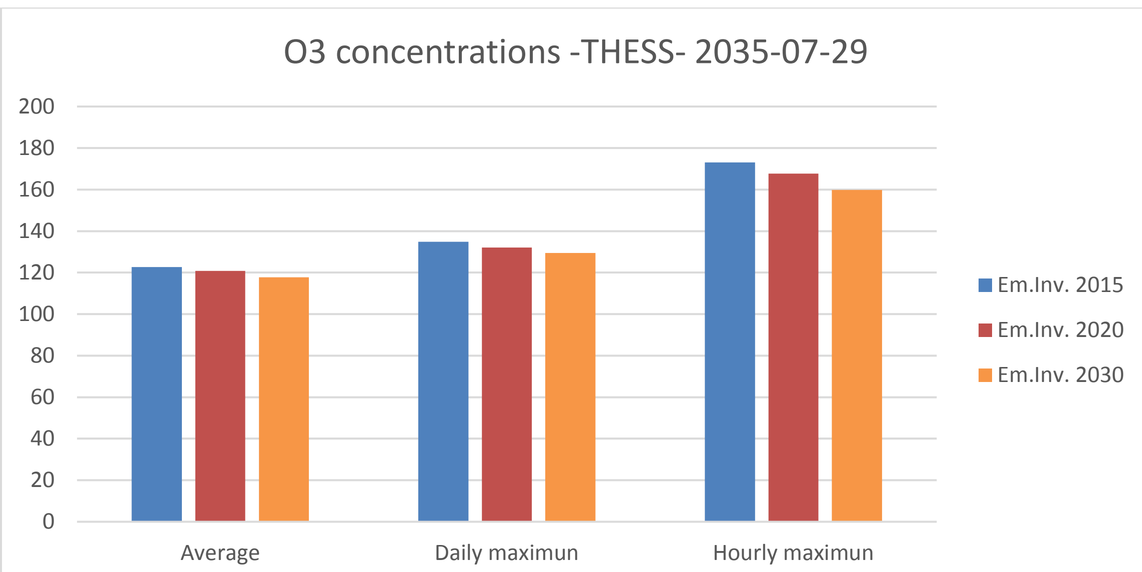


*Figure 4.6.29: $O_3$ emission inventory comparison*

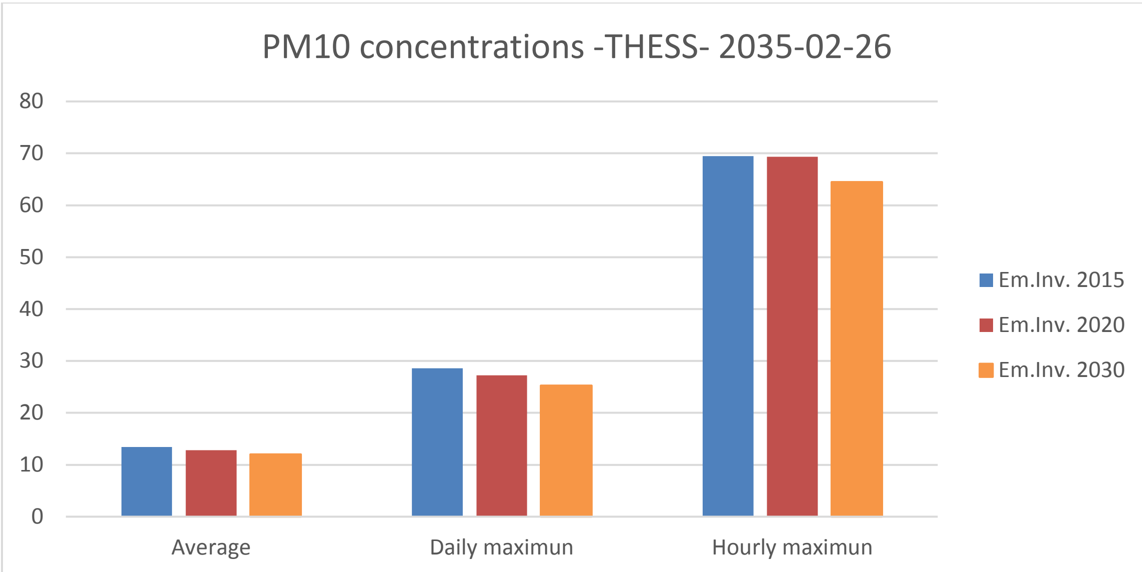


*Figure 4.6.30: $PM_{10}$ emission inventory comparison*

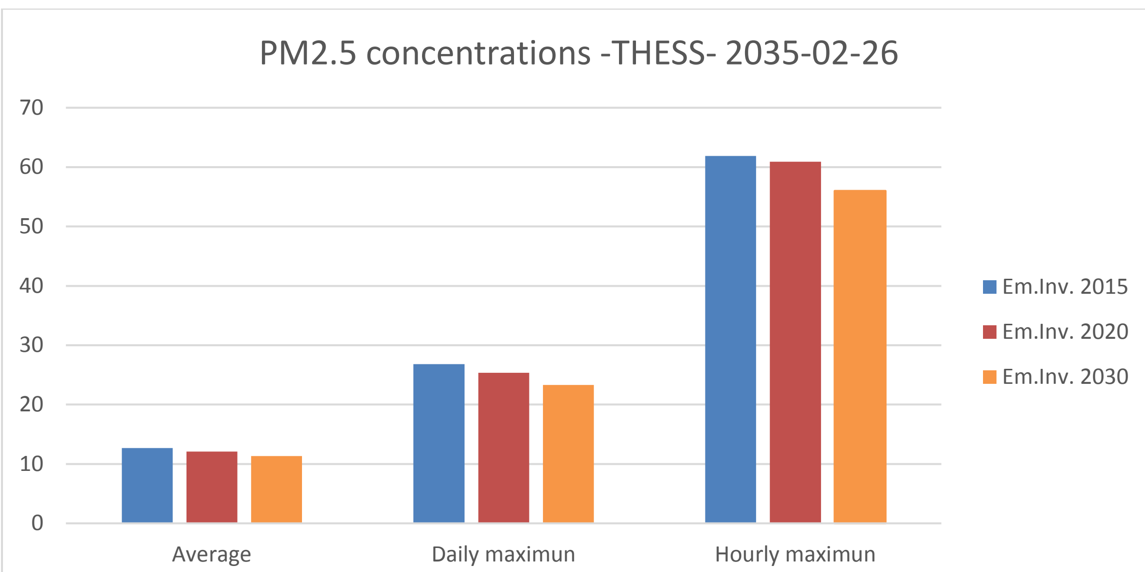


*Figure 4.6.31: $PM_{2.5}$ emission inventory comparison*

### 4.6.4 The GHGs Modeling results

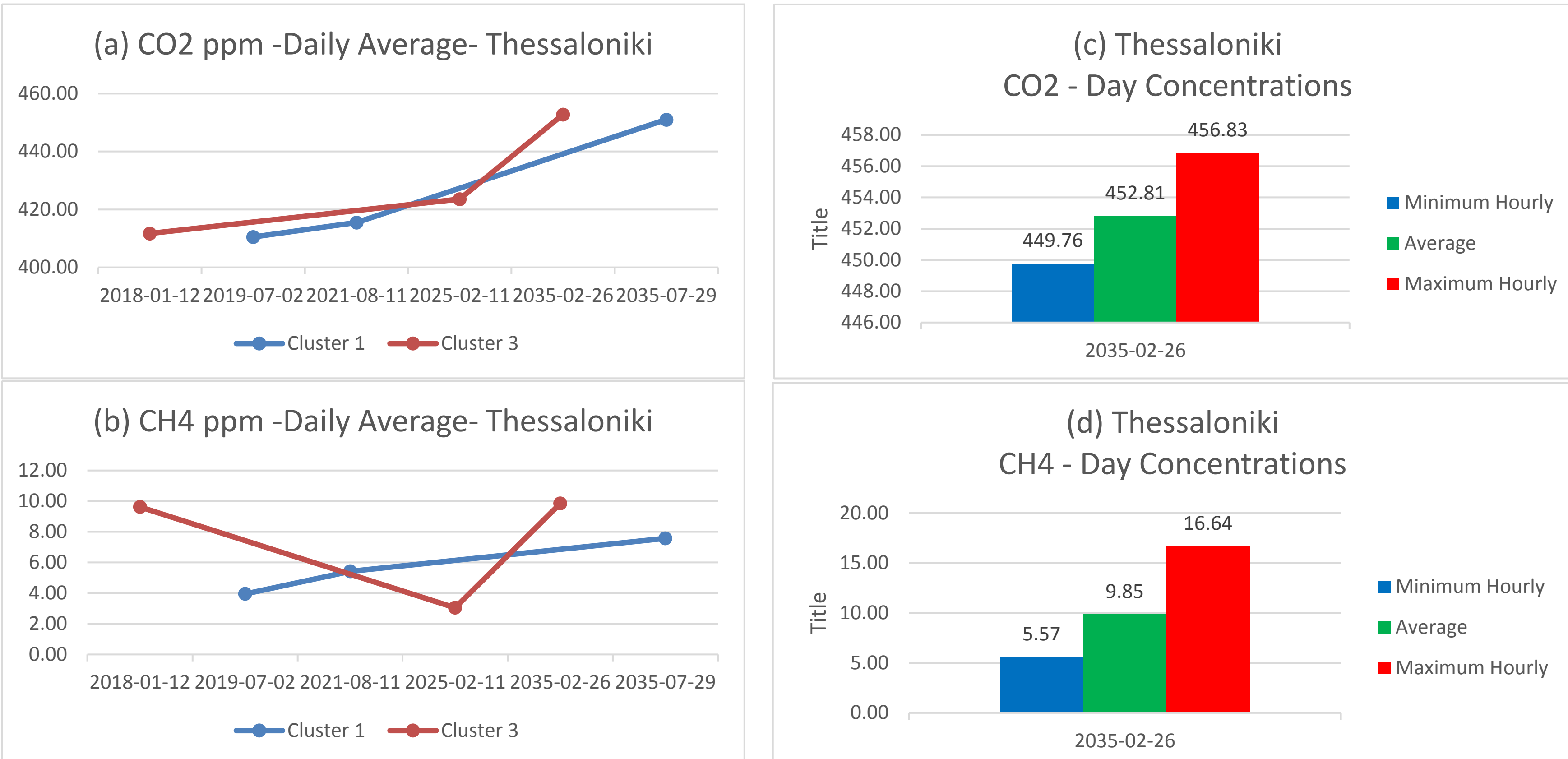


*Figure 4.6.32: (a),(b) $CO_2$ and $CH_4$ Daily average concentrations . (c),(d) $CO_2$ and $CH_4$ concentrations of the most polluted day*

### 4.6.5 Conclusions

For Thessaloniki greater area, clusters 3,5,6 and 8 could be categorized in cold period and on the other hand clusters 1,2 and 7 in warm period.

In clusters 1,7 and 8 there is a linear increase in frequency occurrence through the ten 5-year periods. On the other hand, clusters 3 and 4 show a linear decrease in frequency occurrence.

Heat wave occurrence show an increasing rate after 2031.The 5-year period 2046-2050 shows the highest number of heat waves. The most heat waves were associated with cluster 1 which correspond to cluster with days belong to warm period.

Cluster 3 is characterized with elevated $NO_2$ and PM concentrations and cluster 1 with elevated $O_3$ concentrations.

$NO_2$ concentrations show a mixed picture. There is only one day in which the daily maximum concentration is below the EU and WHO yearly limit of 40μg/m$^3$. The maximum hourly concentrations are below the limit of 200μg/m$^3$.

$O_3$ daily average concentrations show an increasing trend with daily maximum values exceeding the WHO 8hr limit of 100μg/m$^3$. The maximum hourly concentrations exceed this limit as well as the EU 8hr limit of 120μg/m$^3$.

$PM_{10}$ daily maximum concentrations are above the WHO yearly limit of 20μg/m$^3$ showing a decreasing trend. In one day, the daily maximum concentration in also above the daily WHO limit of 50μg/m$^3$.

$PM_{2.5}$ daily maximum concentrations are following a decreasing trend. The daily maximum concentrations are above the WHO yearly limit of 10μg/m$^3$.

For BaP concentrations, there is a decreasing trend. All days are above WHO annual limit of 0.12ng/m$^3$ however one day is below the EU annual limit of 1ng/m$^3$.

There is a slight decreasing trend in all pollutants indicating the positive effect on emission reductions intervention.

## 4.7 Milan

### 4.7.1 PCA results

The PCA analysis applied to the Milan data has led to the following results.

Three (3) principal components have been identified as factors for the cluster analysis (Table 4.7.1). Principal Components (PC) explaining 74.29% of the total variance in the initial data.

Factor 1 explains 35.59% of the total variance and contains negative sign of U wind component, V wind component, RH and precipitation.

Factor 2 explains 22.52% of the total variance and contains the 2 temperature variables, mean, daily temperature range, and the down ward short-wave radiation.

Factor 3 explains 16.17% of the total variance and contains precipitation and a negative sign of atmospheric boundary layer thickness and surface pressure.

*Table 4.7.1: The Principal Components results*

| | Component | | |
|---|---|---|---|
| | 1 | 2 | 3 |
| RH | .841 | | |
| U wind | -.744 | | |
| V wind | .737 | | |
| Precipitation | .669 | | |
| Downward short-wave surface radiation | | .918 | |
| Temperature | | .841 | |
| Temperature Range | | .780 | |
| Surface pressure | | | .743 |
| Atmospheric boundary layer thickness | | | -.598 |

### 4.7.2 Clustering results

#### Cluster description and trends

As explained in 3.4.4 the selected clusters of the city of Milan are 8. In Figure 4.7.1 are shown the number of days per cluster, where clusters 4 and 8 have the most days and cluster 5 and 6 have the less. The monthly distribution per cluster is presented in Table 4.7.2 and in Figure 4.7.2. By dividing the year in two periods, cold and warm, clusters 2,3,4 and 5 could be categorized in cold period and on the other hand clusters 1,6,7 and 8 in warm period.

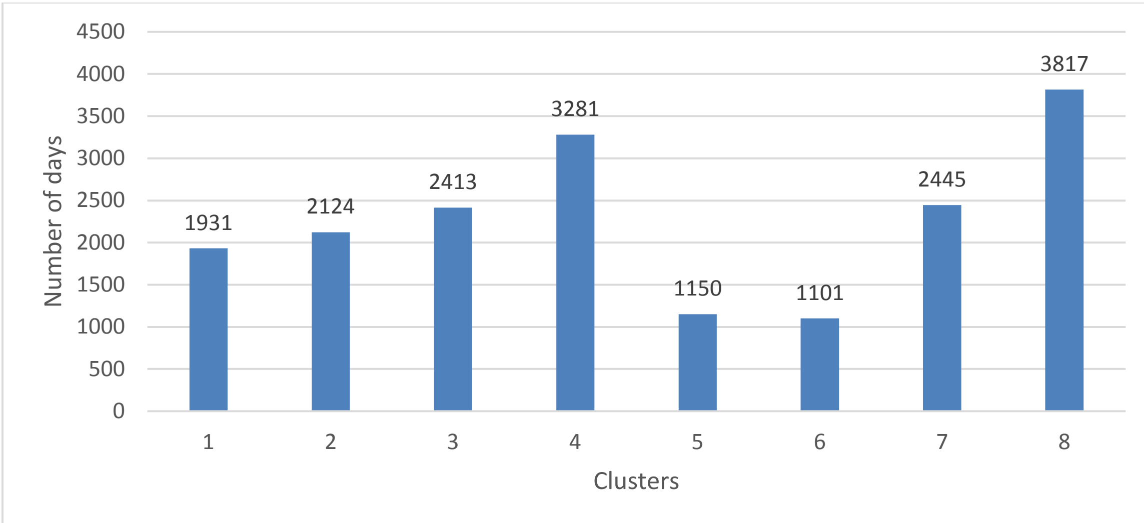


*Figure 4.7.1: Number of Days per cluster*

*Table 4.7.2: Monthly distribution per cluster*

| | | Month | | | | | | | | | | | | Total |
|---|---|---|---|---|---|---|---|---|---|---|---|---|---|---|
| | | Jan | Feb | Mar | Apr | May | Jun | Jul | Aug | Sep | Oct | Nov | Dec | |
| Cluster8 | 1 | 0 | 7 | 119 | 415 | 535 | 368 | 74 | 119 | 234 | 60 | 0 | 0 | 1931 |
| | 2 | 344 | 360 | 316 | 57 | 13 | 2 | 0 | 2 | 28 | 291 | 350 | 361 | 2124 |
| | 3 | 536 | 331 | 200 | 59 | 9 | 1 | 0 | 2 | 44 | 226 | 424 | 581 | 2413 |
| | 4 | 520 | 511 | 469 | 56 | 0 | 0 | 0 | 0 | 56 | 603 | 588 | 478 | 3281 |
| | 5 | 112 | 145 | 207 | 184 | 159 | 44 | 8 | 11 | 47 | 81 | 75 | 77 | 1150 |
| | 6 | 37 | 52 | 67 | 56 | 92 | 114 | 175 | 147 | 162 | 89 | 57 | 53 | 1101 |
| | 7 | 1 | 3 | 41 | 126 | 230 | 437 | 704 | 513 | 316 | 68 | 6 | 0 | 2445 |
| | 8 | 0 | 3 | 131 | 547 | 512 | 534 | 589 | 756 | 613 | 132 | 0 | 0 | 3817 |
| Total | | 1550 | 1412 | 1550 | 1500 | 1550 | 1500 | 1550 | 1550 | 1500 | 1550 | 1500 | 1550 | 18262 |

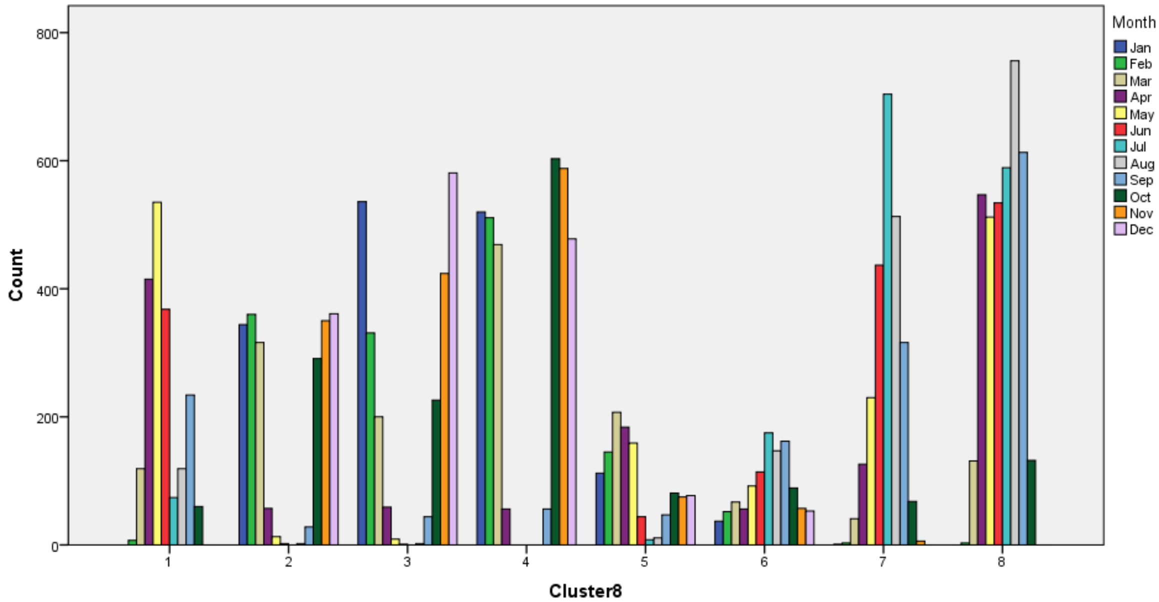


*Figure 4.7.2: Visualized bar chart of monthly distribution per cluster*

A trend analysis of the 5-year frequency of each cluster (Figure 4.7.3). There is an evidence that in clusters 4 and 8 there is a slight increase in frequency occurrence through the ten 5-year periods. On the other hand, clusters 1,3,5 and 6 show a linear decrease in frequency occurrence. In the rest clusters no clear trends could be pointed out.

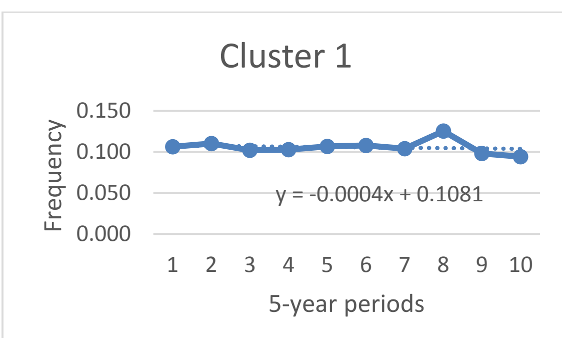


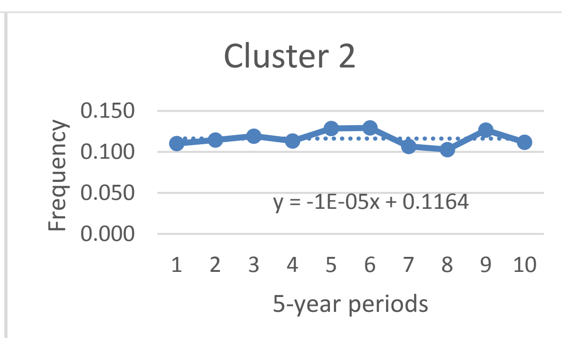

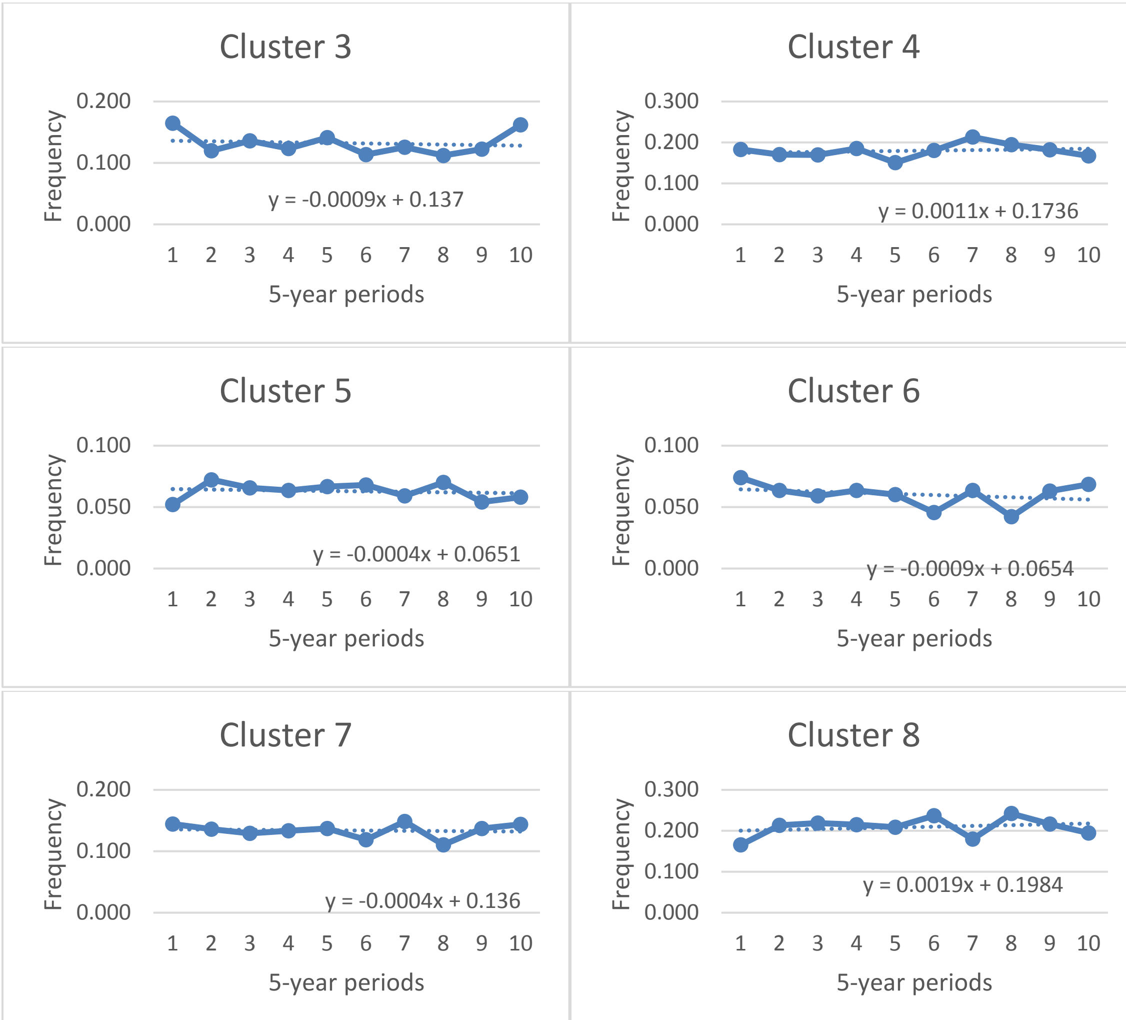


*Figure 4.7.3: Cluster 1-8 frequency trends*

## Cluster characterization

The clusters' implementation is based on the mean values of weather parameters which are displayed in Table 4.7.3.

*Table 4.7.3: Summary of the 8 clusters*

| | Cluster | | | | | | | |
|---|---|---|---|---|---|---|---|---|
| | 1 | 2 | 3 | 4 | 5 | 6 | 7 | 8 |
| | Mean (SD) | Mean (SD) | Mean (SD) | Mean (SD) | Mean (SD) | Mean (SD) | Mean (SD) | Mean (SD) |
| Temperature ( °C) | 15,37 (4,29) | 7,02 (4,09) | 6 (4,66) | 7,55 (4,59) | 9,27 (4,93) | 15,79 (6,48) | 20,53 (4,53) | 19,58 (5,08) |
| Daily Temperature Range ( °C) | 10,48 (1,74) | 8,13 (1,75) | 4,96 (1,88) | 8,95 (2,19) | 6,87 (1,69) | 5,31 (1,67) | 8,71 (1,43) | 11,63 (1,61) |
| Relative Humidity (%) | 42,12 (8,9) | 48,36 (12,19) | 80,89 (11,72) | 63,6 (14,82) | 34,79 (8,59) | 83,7 (6,82) | 72,54 (7,85) | 58,37 (10,64) |
| Surface Pressure (Pa) | 99119,15 (691,46) | 99350,19 (904,56) | 99518,11 (963,2) | 100798,59 (817,34) | 98934,68 (915,06) | 98858,67 (774,1) | 99245,81 (616,19) | 99900,3 (593,63) |
| Precipitation (kg/m2/s) | 0,000004 (0,000014 ) | 0,000004 (0,000014 ) | 0,000047 (0,000059 ) | 0,000001 (0,000006 ) | 0,000005 (0,000029 ) | 0,000288 (0,000136 ) | 0,000076 (0,000062 ) | 0,000005 (0,000012 ) |
| Downward Short Wave Radiation | 300,95 (60,02) | 127,36 (46,49) | 66,23 (40,33) | 126,07 (47,41) | 204,18 (89,52) | 134,1 (84,23) | 264,93 (58,75) | 293,51 (54,91) |
| u wind component (m/s) | 0,72 (1,06) | 0,78 (1,34) | -1,4 (1,49) | 0,04 (1,31) | 1,61 (1,72) | -2,97 (1,96) | -1,38 (1,2) | -0,3 (1,14) |
| v wind component (m/s) | -2,85 (1,62) | -2 (1,61) | 0 (1,04) | -0,34 (0,67) | -6,02 (2,05) | 0,39 (1,69) | 0,05 (0,94) | -0,12 (0,75) |
| V wind (m/s) | 3,22 (1,42) | 2,64 (1,41) | 1,9 (1,28) | 1,26 (0,84) | 6,55 (1,76) | 3,47 (1,91) | 1,76 (1,06) | 1,21 (0,71) |
| Atmospheric Boundary Layer Thickness (m) | 875,18 (188,62) | 464,82 (184) | 240,22 (137,76) | 234,19 (127,26) | 1065,68 (276,57) | 474,25 (166,68) | 562,96 (139,15) | 573,29 (152,48) |

In addition to the previous Table 4.7.3, Figure 4.7.4 presents the mean normalized (z-score) variables of each cluster, respectively showing the differences of the parameters per cluster.

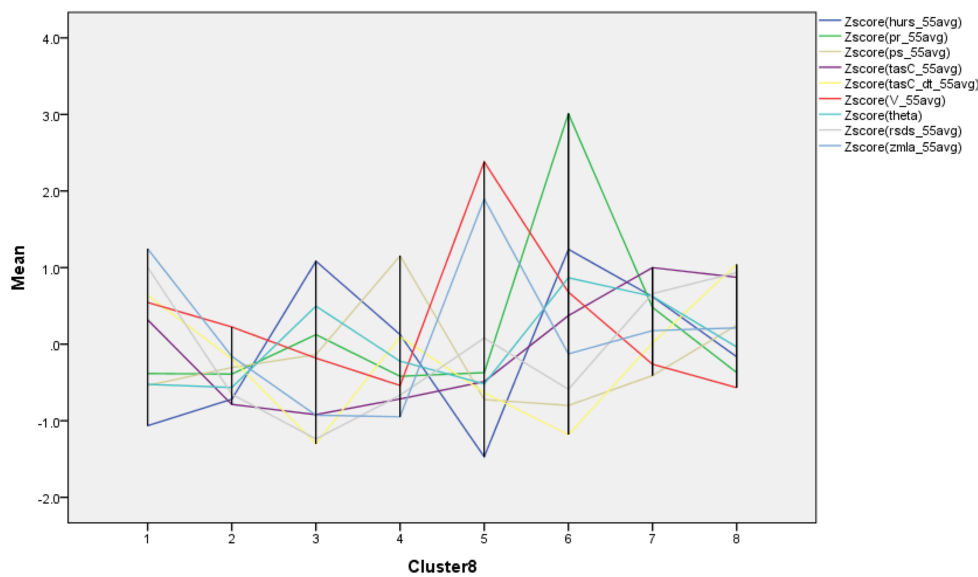


*Figure 4.7.4: Normalized variables (z-score) averaged for each cluster*

Daily, 10-meter from ground level, wind data were used to create the wind roses per each cluster as they are shown in Figures 4.7.5-4.7.12. Each wind direction distribution per cluster is presented in more details in Table 4.7.4.

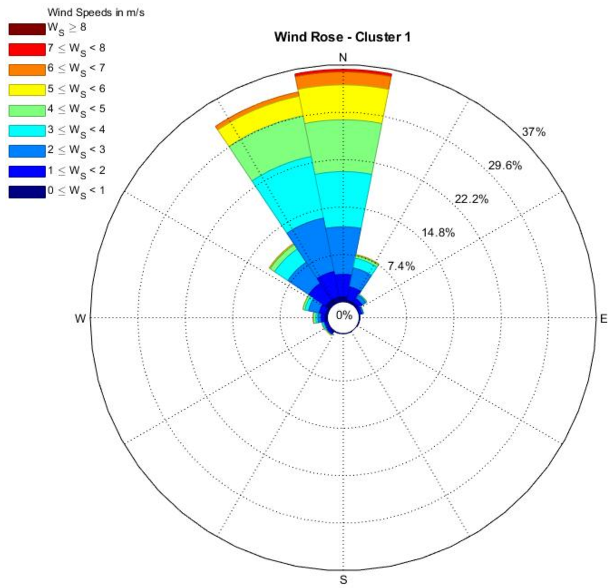


*Figure 4.7.5: Wind Rose - Cluster 1*

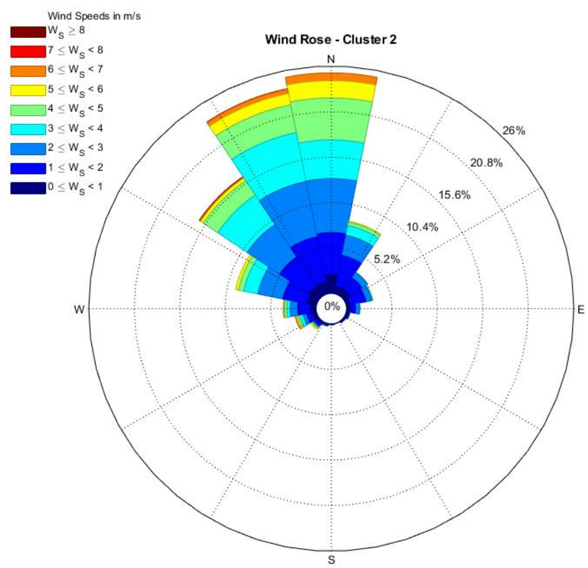


*Figure 4.7.6: Wind Rose - Cluster 2*

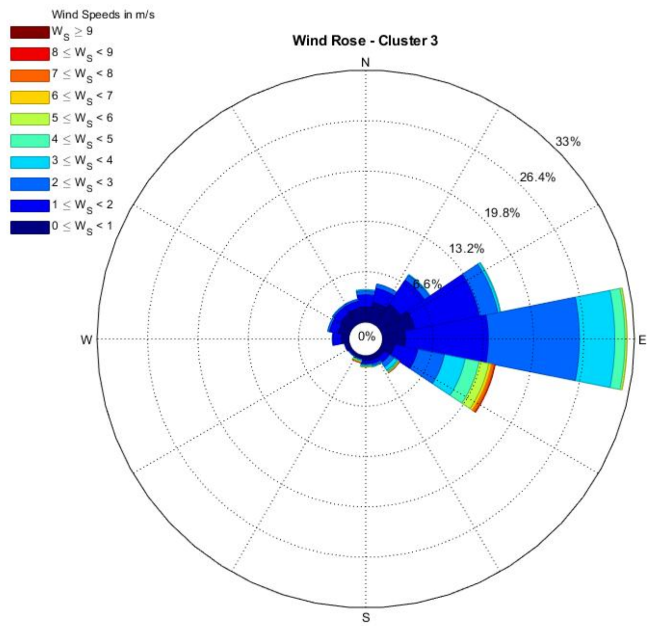


*Figure 4.7.7: Wind Rose - Cluster 3*

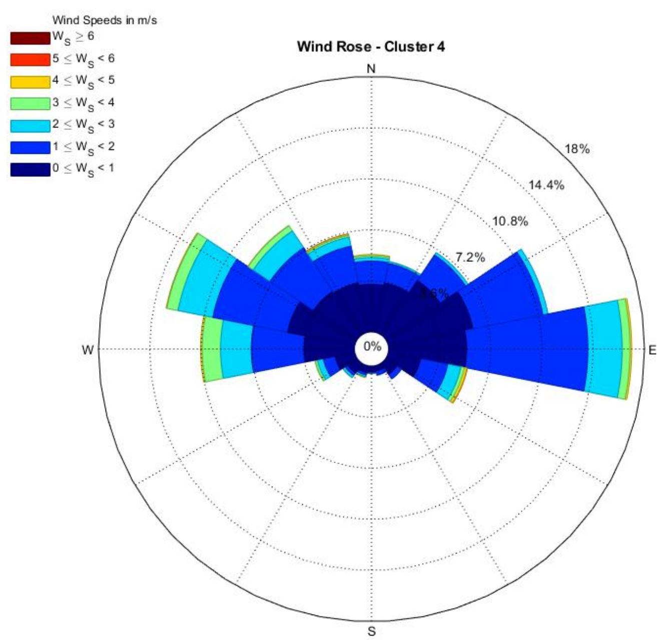


*Figure 4.7.8: Wind Rose - Cluster 4*

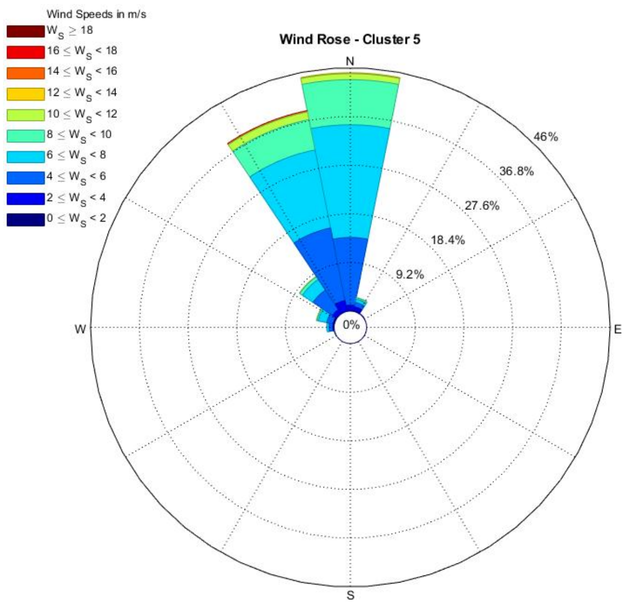


*Figure 4.7.9: Wind Rose - Cluster 5*

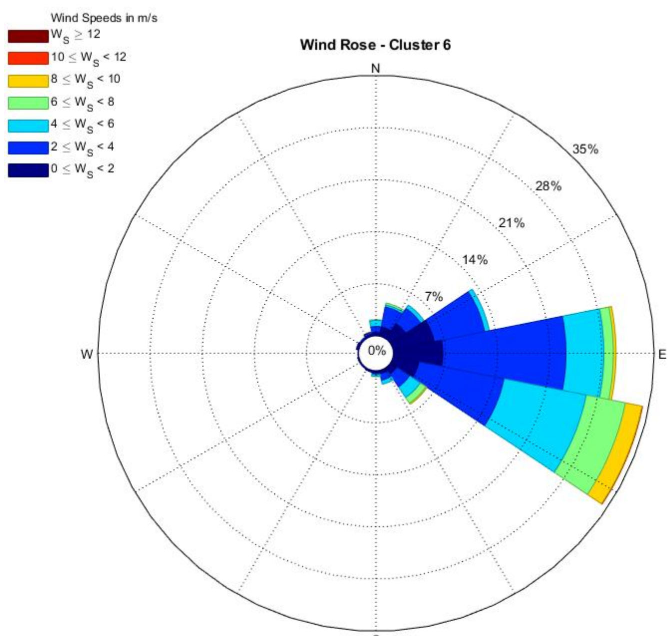


*Figure 4.7.10: Wind Rose - Cluster 6*

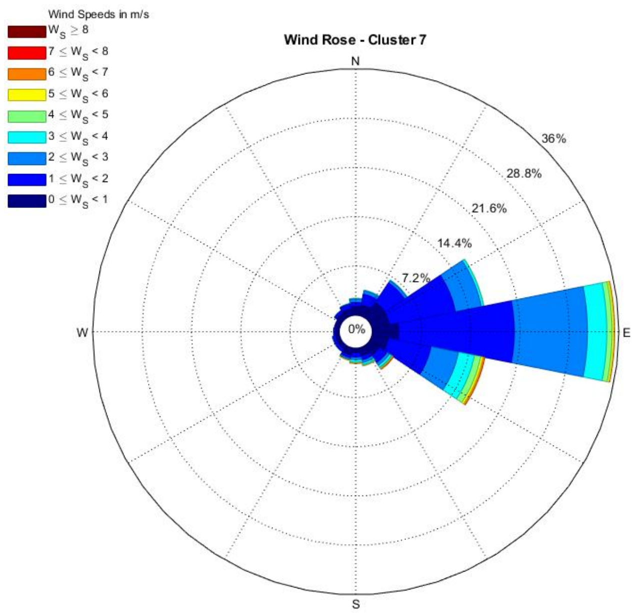


*Figure 4.7.11: Wind Rose - Cluster 7*

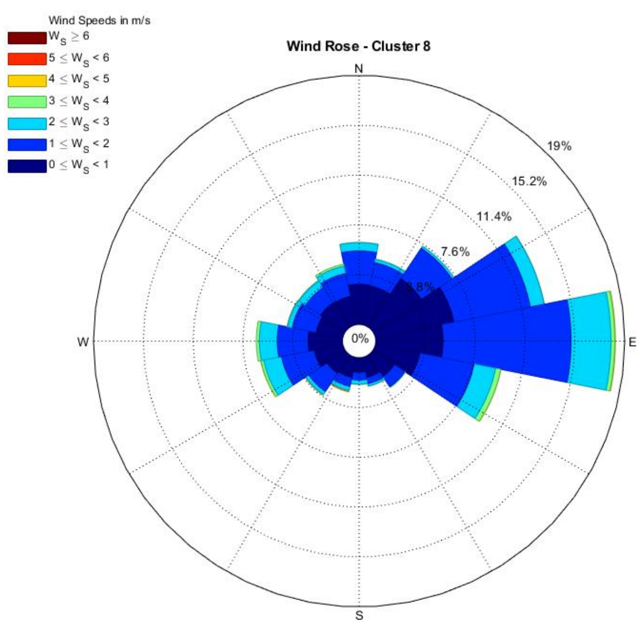


*Figure 4.7.12: Wind Rose - Cluster 8*

*Table 4.7.4: 16 Wind Direction distribution per cluster*

| | | | Wind16 | | | | | | | | | | | | | | | | Total |
|---|---|---|---|---|---|---|---|---|---|---|---|---|---|---|---|---|---|---|---|
| | | | S | SSW | SW | WSW | W | WNW | NW | NNW | N | NNE | NE | ENE | E | ESE | SE | SSE | |
| Cluster8 | 1 | Count | 1 | 2 | 17 | 19 | 43 | 77 | 221 | 645 | 701 | 146 | 38 | 15 | 3 | 2 | 0 | 1 | 1931 |
| | | % within Cluster8 | 0.1% | 0.1% | 0.9% | 1.0% | 2.2% | 4.0% | 11.4% | 33.4% | 36.3% | 7.6% | 2.0% | 0.8% | 0.2% | 0.1% | 0.0% | 0.1% | 100.0% |
| | 2 | Count | 3 | 7 | 24 | 53 | 80 | 200 | 349 | 508 | 535 | 180 | 70 | 66 | 33 | 10 | 5 | 1 | 2124 |
| | | % within Cluster8 | 0.1% | 0.3% | 1.1% | 2.5% | 3.8% | 9.4% | 16.4% | 23.9% | 25.2% | 8.5% | 3.3% | 3.1% | 1.6% | 0.5% | 0.2% | 0.0% | 100.0% |
| | 3 | Count | 36 | 24 | 13 | 16 | 53 | 70 | 74 | 75 | 103 | 124 | 192 | 382 | 773 | 364 | 76 | 38 | 2413 |
| | | % within Cluster8 | 1.5% | 1.0% | 0.5% | 0.7% | 2.2% | 2.9% | 3.1% | 3.1% | 4.3% | 5.1% | 8.0% | 15.8% | 32.0% | 15.1% | 3.1% | 1.6% | 100.0% |
| | 4 | Count | 18 | 28 | 41 | 94 | 355 | 444 | 304 | 232 | 179 | 167 | 229 | 376 | 561 | 186 | 44 | 23 | 3281 |
| | | % within Cluster8 | 0.5% | 0.9% | 1.2% | 2.9% | 10.8% | 13.5% | 9.3% | 7.1% | 5.5% | 5.1% | 7.0% | 11.5% | 17.1% | 5.7% | 1.3% | 0.7% | 100.0% |
| | 5 | Count | 0 | 0 | 0 | 1 | 16 | 40 | 98 | 445 | 518 | 31 | 1 | 0 | 0 | 0 | 0 | 0 | 1150 |
| | | % within Cluster8 | 0.0% | 0.0% | 0.0% | 0.1% | 1.4% | 3.5% | 8.5% | 38.7% | 45.0% | 2.7% | 0.1% | 0.0% | 0.0% | 0.0% | 0.0% | 0.0% | 100.0% |
| | 6 | Count | 9 | 3 | 2 | 2 | 1 | 4 | 3 | 7 | 24 | 50 | 60 | 145 | 329 | 376 | 65 | 21 | 1101 |
| | | % within Cluster8 | 0.8% | 0.3% | 0.2% | 0.2% | 0.1% | 0.4% | 0.3% | 0.6% | 2.2% | 4.5% | 5.4% | 13.2% | 29.9% | 34.2% | 5.9% | 1.9% | 100.0% |
| | 7 | Count | 55 | 46 | 28 | 27 | 21 | 19 | 34 | 45 | 61 | 93 | 163 | 408 | 865 | 411 | 103 | 66 | 2445 |
| | | % within Cluster8 | 2.2% | 1.9% | 1.1% | 1.1% | 0.9% | 0.8% | 1.4% | 1.8% | 2.5% | 3.8% | 6.7% | 16.7% | 35.4% | 16.8% | 4.2% | 2.7% | 100.0% |
| | 8 | Count | 78 | 102 | 141 | 244 | 251 | 166 | 164 | 180 | 239 | 195 | 284 | 502 | 698 | 373 | 114 | 86 | 3817 |
| | | % within Cluster8 | 2.0% | 2.7% | 3.7% | 6.4% | 6.6% | 4.3% | 4.3% | 4.7% | 6.3% | 5.1% | 7.4% | 13.2% | 18.3% | 9.8% | 3.0% | 2.3% | 100.0% |
| Total | | Count | 200 | 212 | 266 | 456 | 820 | 1020 | 1247 | 2137 | 2360 | 986 | 1037 | 1894 | 3262 | 1722 | 407 | 236 | 18262 |
| | | % within Cluster8 | 1.1% | 1.2% | 1.5% | 2.5% | 4.5% | 5.6% | 6.8% | 11.7% | 12.9% | 5.4% | 5.7% | 10.4% | 17.9% | 9.4% | 2.2% | 1.3% | 100.0% |

## Clusters and local Heat Waves

In Figures 4.7.13 and 4.7.12 are presented the heat waves occurrence per 5-year period and per cluster. The most heat waves seem to occur after 2036.The 5-year period 2041-2045 shows the highest number of heat waves, while the next 5-year period shows a decrease. The most heat waves were associated with clusters 7 and 8 which correspond to clusters with days belong to warm period (see Table 4.7.2).

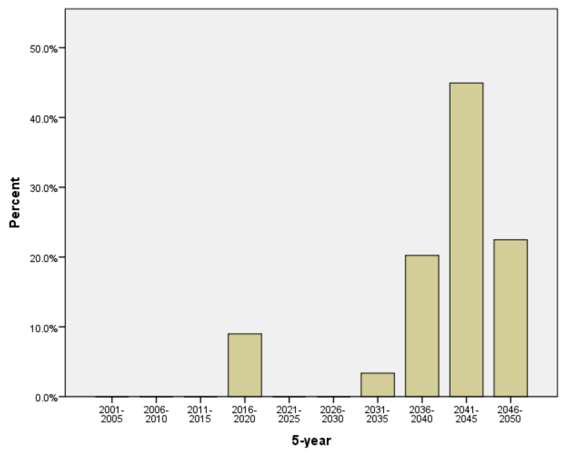


*Figure 4.7.13: Heat Waves per 5-year period*

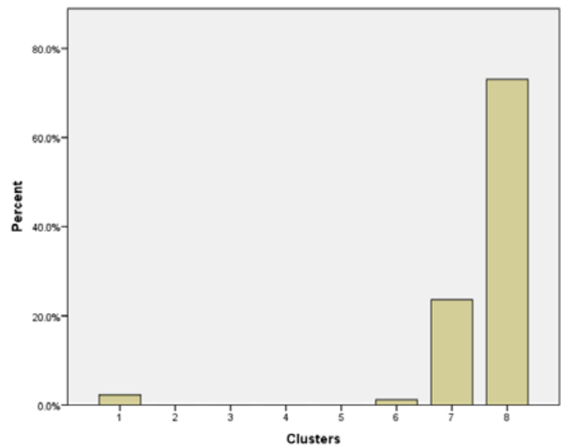


*Figure 4.7.14: Heat Waves per cluster*

## Clusters versus Air Quality level

As it can be seen in Table 4.1 two observation stations have been used for the present analysis. The descriptive statistics for $NO_2$, $O_3$ and $PM_{10}$ is given in Table 4.7.5.

*Table 4.7.5: Air pollutants descriptive statistics*

| | | NO2 | O3 | PM10 |
|---|---|---|---|---|
| Mean | | 58.04808 | 42.82351 | 48.94622 |
| Std. Deviation | | 23.774786 | 31.911888 | 30.993144 |
| Minimum | | 6.333 | 1.625 | 3.000 |
| Maximum | | 203.500 | 144.917 | 309.000 |
| Percentiles | 5 | 24.83300 | 6.08300 | 15.00000 |
| | 25 | 41.12500 | 12.91700 | 27.00000 |
| | 50 | 55.58300 | 36.10400 | 40.00000 |
| | 75 | 71.22900 | 69.11425 | 63.00000 |
| | 95 | 99.42930 | 98.99975 | 113.00000 |

Table 4.7.6 presents the pollutants' concentrations per cluster. Higher mean $NO_2$ concentrations are observed in clusters 2,3 and 4. Higher mean $O_3$ concentrations are observed in clusters 7 and 8. Higher mean $PM_{10}$ concentrations are observed in clusters 2,3 and 4.

*Table 4.7.6: Summary pollutant concentrations per cluster*

| | Cluster | | | | | | | |
|---|---|---|---|---|---|---|---|---|
| | 1 | 2 | 3 | 4 | 5 | 6 | 7 | 8 |
| | Mean (SD) | Mean (SD) | Mean (SD) | Mean (SD) | Mean (SD) | Mean (SD) | Mean (SD) | Mean (SD) |
| PM10 (µg/m3) | 34,37 (15,1) | 64,11 (34,07) | 68,92 (37,82) | 62,62 (31,41) | 53,68 (31,96) | 43,31 (25,87) | 32,15 (15,15) | 31,66 (14,56) |
| O3 (µg/m3) | 63,59 (25,23) | 18,17 (14,81) | 14,69 (11,08) | 19,75 (14,53) | 32,97 (25,29) | 52,39 (32,28) | 72,05 (24,63) | 65,83 (25,19) |
| NO2 (µg/m3) | 48,52 (16,65) | 69,26 (22,02) | 73,7 (23,38) | 70,27 (21,45) | 62,47 (20,76) | 53,74 (22,39) | 44,22 (18,83) | 43,56 (17,37) |

The differences in concentrations per cluster are shown in Figures 4.7.15-4.7.17.

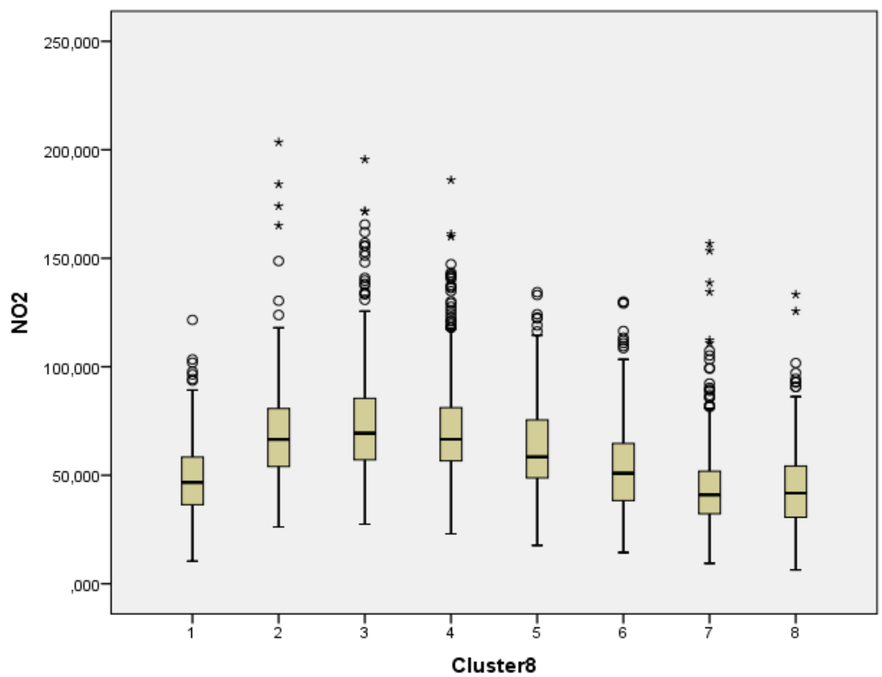


*Figure 4.7.15: $NO_2$ concentration statistics per cluster*

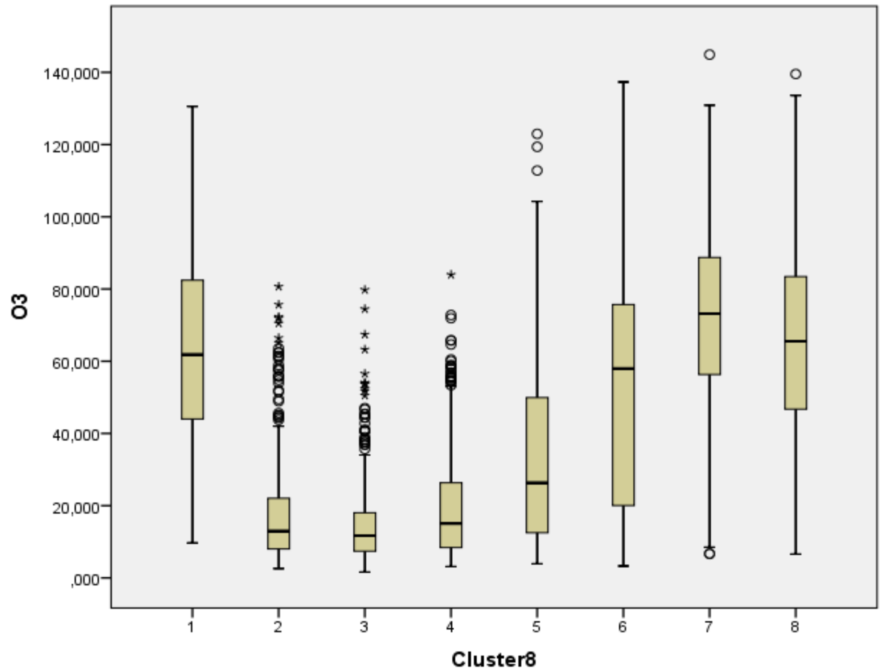


*Figure 4.7.16: $O_3$ concentration statistics per cluster*

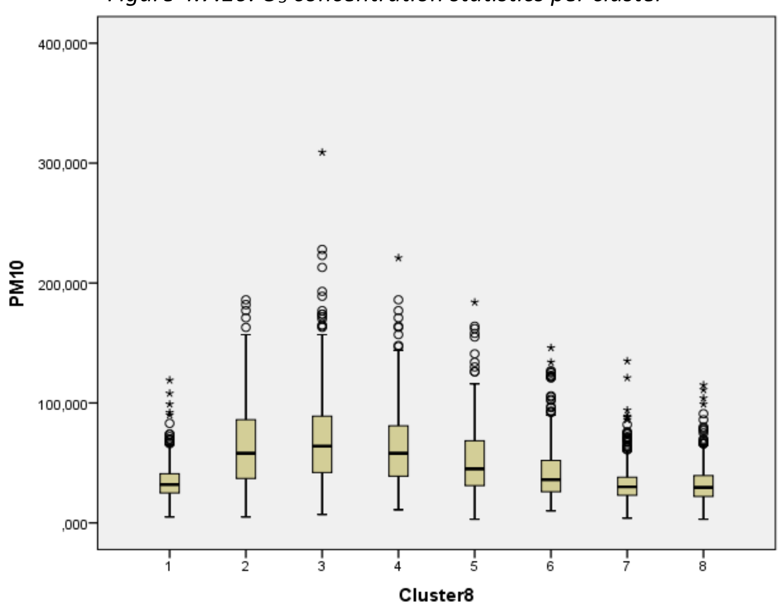


*Figure 4.7.17: $PM_{10}$ concentration statistics per cluster*

## Representative Days

In the following Table 4.7.7 are presented the selected RDs per 5-year period and per cluster.

*Table 4.7.7: Representative days per cluster and 5year period*

| Closest days to centroids per 5year per cluster | | | clusters | | | | | | | |
|---|---|---|---|---|---|---|---|---|---|---|
| | | | 1 | 2 | 3 | 4 | 5 | 6 | 7 | 8 |
| 5 year period | 2001-2005 | 1 | 2005/05/09 | 2002/02/03 | 2004/11/21 | 2002/02/11 | 2005/10/09 | 2004/09/10 | 2001/05/08 | 2005/05/05 |
| | 2006-2010 | 2 | 2009/05/04 | 2008/10/31 | 2008/10/27 | 2008/03/04 | 2010/10/02 | 2009/06/28 | 2006/07/11 | 2007/05/07 |
| | 2011-2015 | 3 | 2013/04/29 | 2014/11/26 | 2013/03/11 | 2014/01/26 | 2012/10/08 | 2012/05/13 | 2013/06/25 | 2011/08/31 |
| | 2016-2020 | 4 | 2016/05/15 | 2018/11/16 | 2019/10/29 | 2018/02/15 | 2016/10/10 | 2020/09/09 | 2017/07/30 | 2019/05/11 |
| | 2021-2025 | 5 | 2024/08/28 | 2021/01/25 | 2022/10/26 | 2024/11/05 | 2021/03/14 | 2025/08/29 | 2025/07/30 | 2021/05/15 |
| | 2026-2030 | 6 | 2028/04/28 | 2026/02/03 | 2030/11/28 | 2028/12/22 | 2029/02/20 | 2030/06/25 | 2030/06/11 | 2030/08/12 |
| | 2031-2035 | 7 | 2031/09/02 | 2033/02/28 | 2035/12/17 | 2034/11/22 | 2032/04/10 | 2033/07/31 | 2035/08/16 | 2034/05/04 |
| | 2036-2040 | 8 | 2038/05/08 | 2040/12/14 | 2037/12/31 | 2040/03/29 | 2037/03/23 | 2038/09/18 | 2038/08/25 | 2040/08/31 |
| | 2041-2045 | 9 | 2045/04/23 | 2041/11/29 | 2043/01/22 | 2041/11/17 | 2041/03/23 | 2043/07/04 | 2045/06/09 | 2041/05/17 |
| | 2046-2050 | 10 | 2049/04/25 | 2046/02/26 | 2049/02/20 | 2047/02/25 | 2047/09/29 | 2048/09/15 | 2046/06/25 | 2047/04/21 |

## Selected Clusters and RDs for modeling purposes

Selected RDs will be used to perform targeted weather and air quality simulations within each selected 5-year period estimating hourly/daily concentrations of the priority pollutants to assess the climatic effect on air quality evolution and the characteristics of air quality future episodes. The selection was based on 3-year periods (2016-2020, 2021-2025 and 2031-2035) and on the clusters with the most elevated concentrations of $PM_{10}$, $NO_2$ and $O_3$. In the case of Milan, cluster 3 recorded the most elevated values of $NO_2$ and $PM_{10}$ and cluster 7 for the case of $O_3$. In Table 4.7.8 are presented the selected days which was used for modeling purposes.

*Table 4.7.8: RDs for modeling purposes*

| **Period** | **Cluster 3 (NO2, PM)** | **Cluster 7 (O3)** |
|---|---|---|
| 2016-2020 | 2019-10-29 | 2017-07-30 |
| 2021-2025 | 2022-10-26 | 2025-07-30 |
| 2031-2035 | 2035-12-17 | 2035-08-16 |

### 4.7.3 Air Quality Modeling results

#### 4.7.3.1 Overall results

In Figure 4.7.18 the daily average concentrations of $NO_2$, $O_3$, $PM_{10}$ and $PM_{2.5}$ for selected RDs are presented.

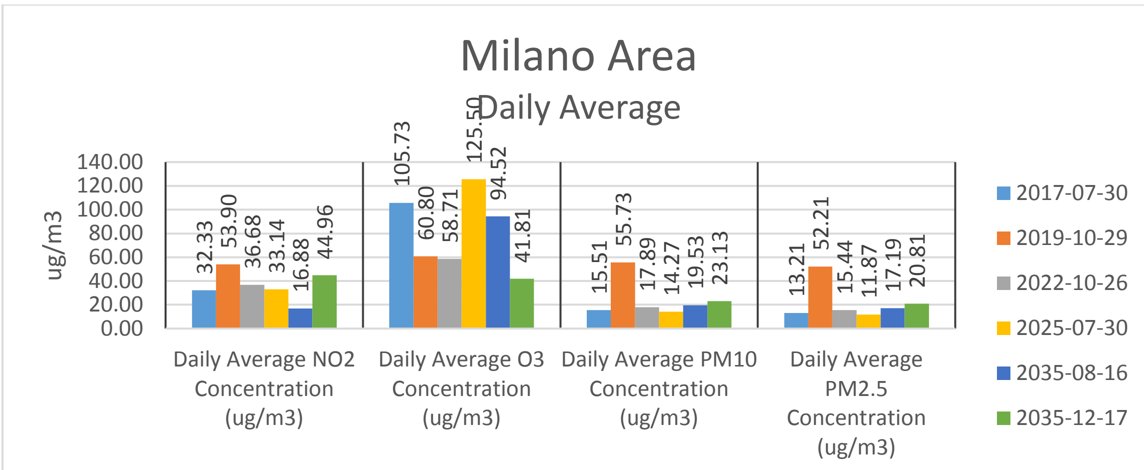


*Figure 4.7.18: Daily average concentrations*

In Figure 4.7.19 the obtained daily averaged concentrations are compared based on USTUTT and EGDAR HTAP emission inventories respectively. The results seem not to differ significantly.

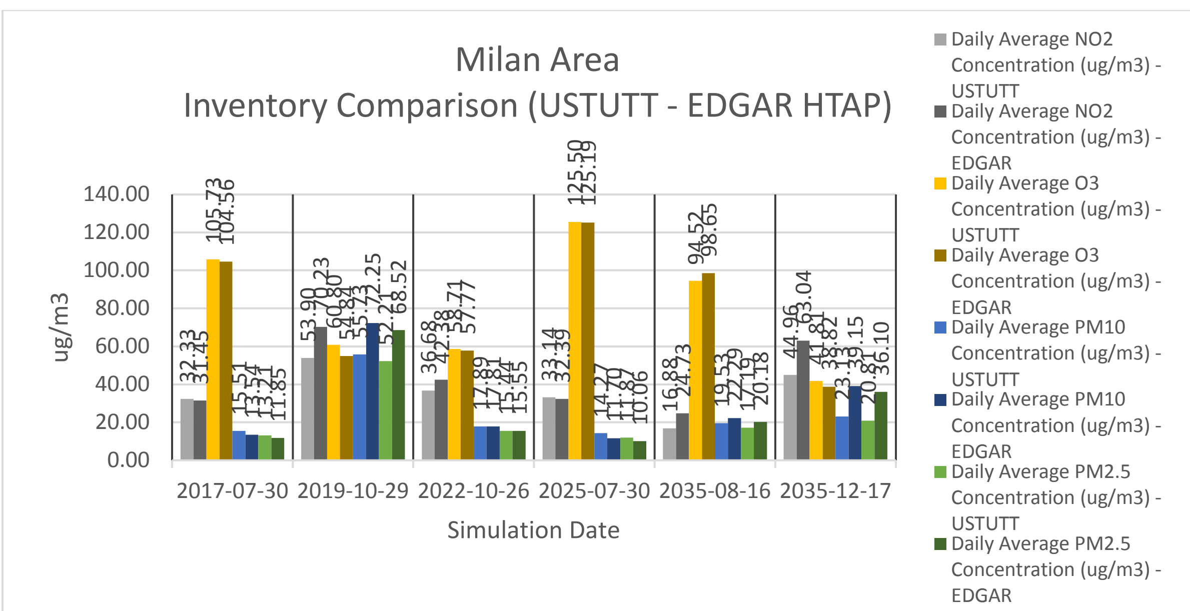


*Figure 4.7.19: Daily average concentrations – USTUTT vs EDGAR HTAP comparison*

#### 4.7.3.2 Clusters results

$NO_2$ Concentrations (Cluster 3)

In Figure 4.7.20, the results are presented in terms of concentrations average, daily maximum and hourly maximum. The diurnal variations are shown in Figure 4.7.21.

The daily maximum concentrations exceed the EU and WHO yearly limit of 40μg/m$^3$. The maximum hourly concentrations, being above the limit of 200μg/m$^3$, show a decreasing trend.

$O_3$ Concentrations (Cluster 7)

In Figure 4.7.22, the results are presented in terms of concentrations average, daily maximum and hourly maximum. The diurnal variations are shown in Figure 4.7.23.

The daily maximum values are above the WHO 8hr limit of 100μg/m$^3$. The maximum hourly concentrations exceed this limit as well as the EU 8hr limit of 120μg/m$^3$.

$PM_{10}$ Concentrations (Cluster 3)

In Figure 4.7.24, the results are presented in terms of concentrations average, daily maximum and hourly maximum. The diurnal variations are shown in Figure 4.7.25.

The daily maximum concentrations show maximum values above the WHO yearly limit of 20μg/m$^3$ with a decreasing rate. The hourly maximum concentrations have a decrease rate while showing values that exceed the WHO daily limit of 50μg/m$^3$.

### $NO_2$-Cluster 3

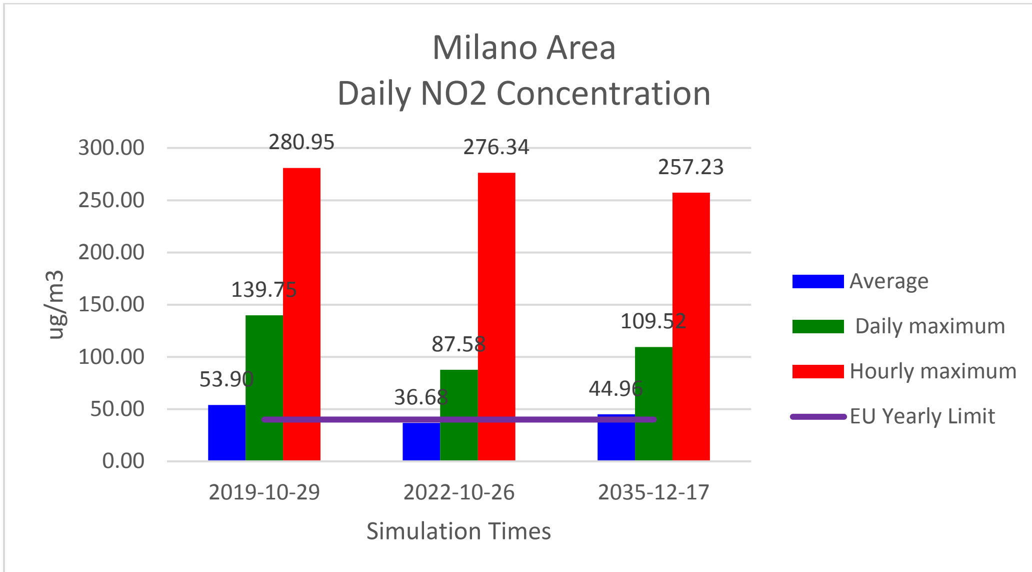


*Figure 4.7.20: $NO_2$ Day concentrations*

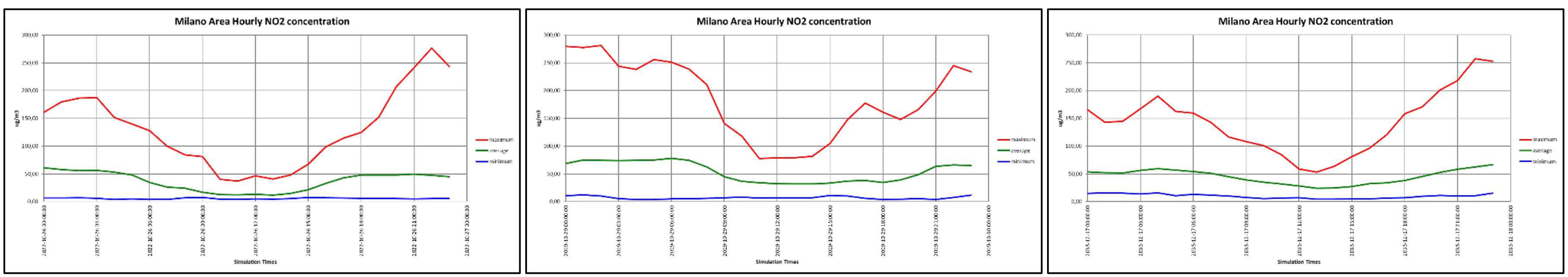


*Figure 4.7.21: Hourly $NO_2$ concentrations*

### $O_3$-Cluster 7

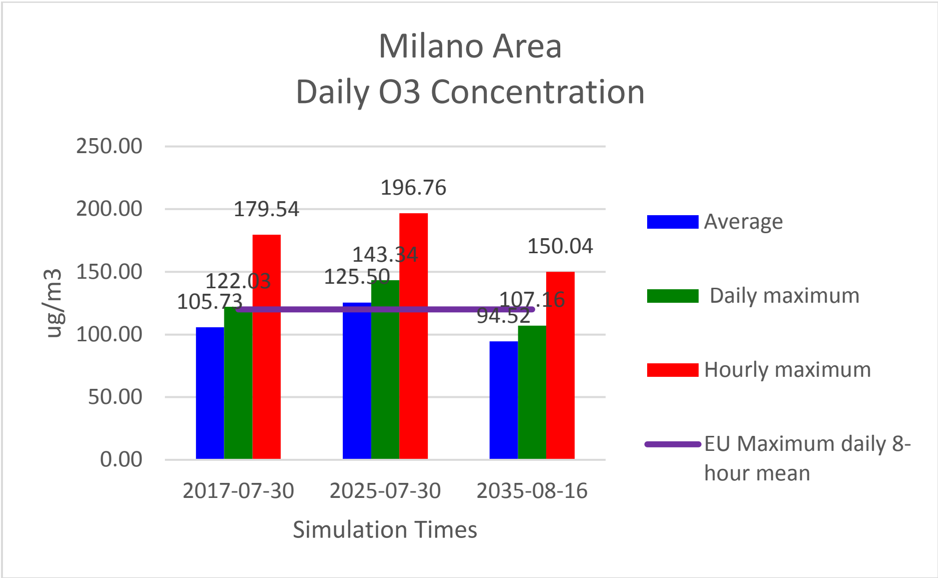


*Figure 4.7.22: $O_3$ Daily concentrations*

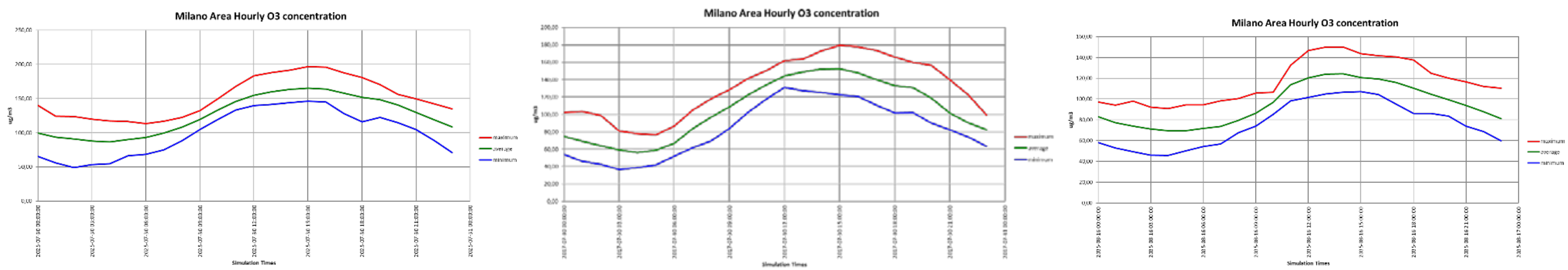


*Figure 4.7.23: $O_3$ Hourly concentrations*

### $PM_{10}$-Cluster 3

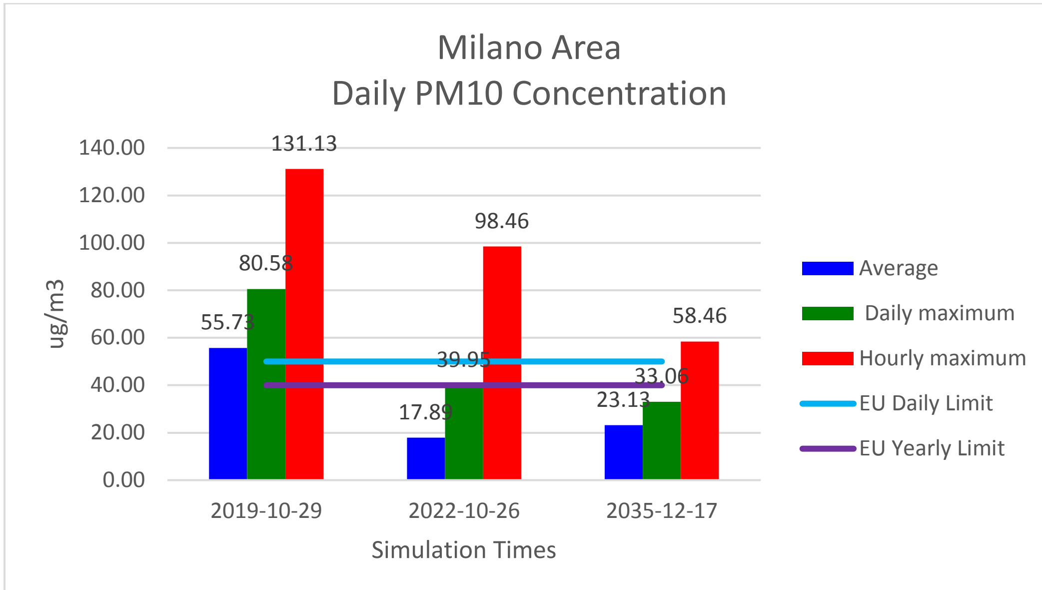


*Figure 4.7.24: $PM_{10}$ Daily concentrations*

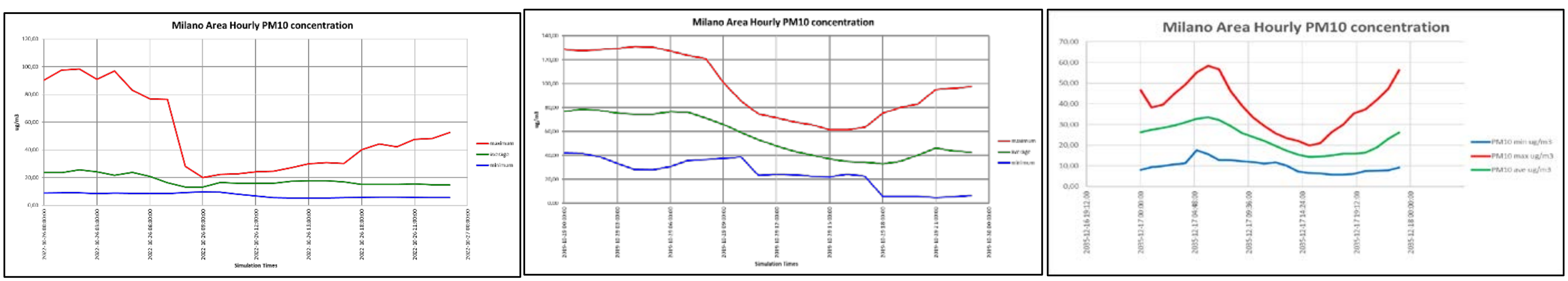


*Figure 4.7.25: $PM_{10}$ Hourly concentrations*

PM$_{2.5}$ Concentrations (Cluster 3)

In Figure 4.7.26, the results are presented in terms of concentrations average, daily maximum and hourly maximum.
The daily and hourly maximum concentrations are following a decreasing trend. The daily maximum concentrations are above the WHO yearly limit of 10μg/m$^3$.

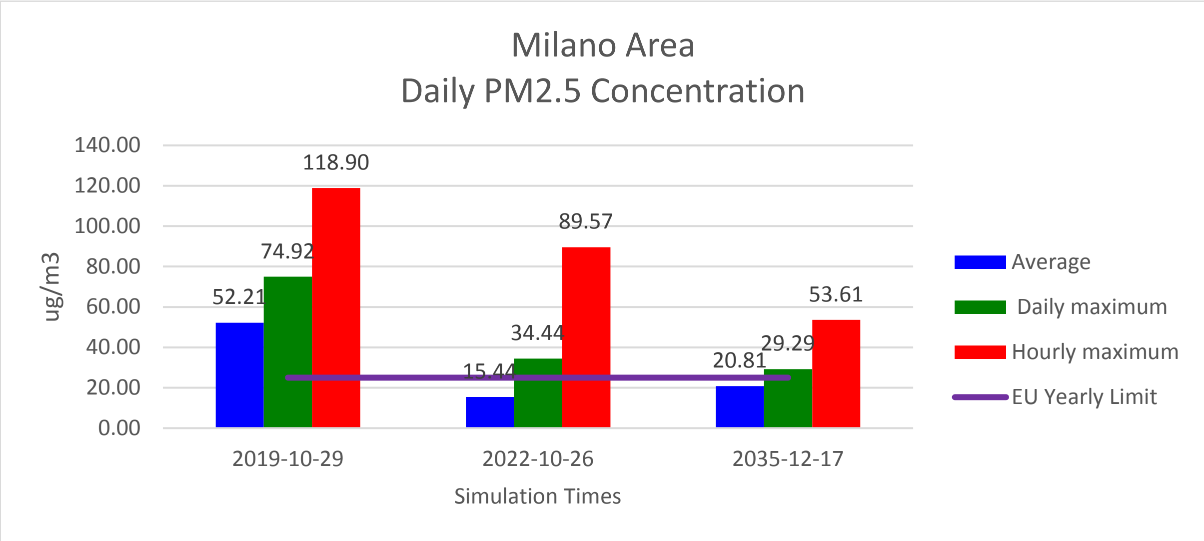


*Figure 4.7.26: PM$_{2.5}$ Day concentrations*

Figure 4.7.27 presents the estimated BaP daily concentrations contained in PM$_{2.5}$. All days are above WHO annual limit of 0.12ng/m$^3$ however one day is close to the EU annual limit of 1ng/m$^3$.

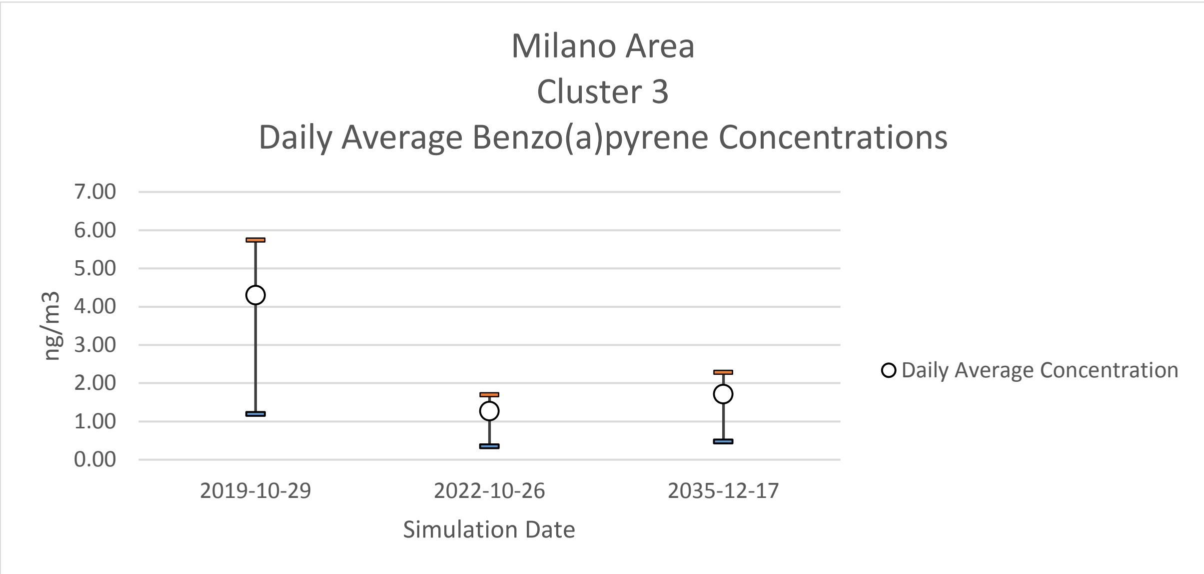


*Figure 4.7.27: BaP daily concentrations*

#### 4.7.3.3 The Emission Inventory effect

Figures 4.7.28, 4.7.29, 4.7.30 and 4.7.31 illustrate the emission inventory temporal change effect on $NO_2$, $O_3$, $PM_{10}$ and $PM_{2.5}$ concentration levels respectively. There is a decreasing trend in PM pollutants indicating the positive effect on emission reductions intervention. The picture in $NO_2$ and $O_3$ concentration levels is mixed.

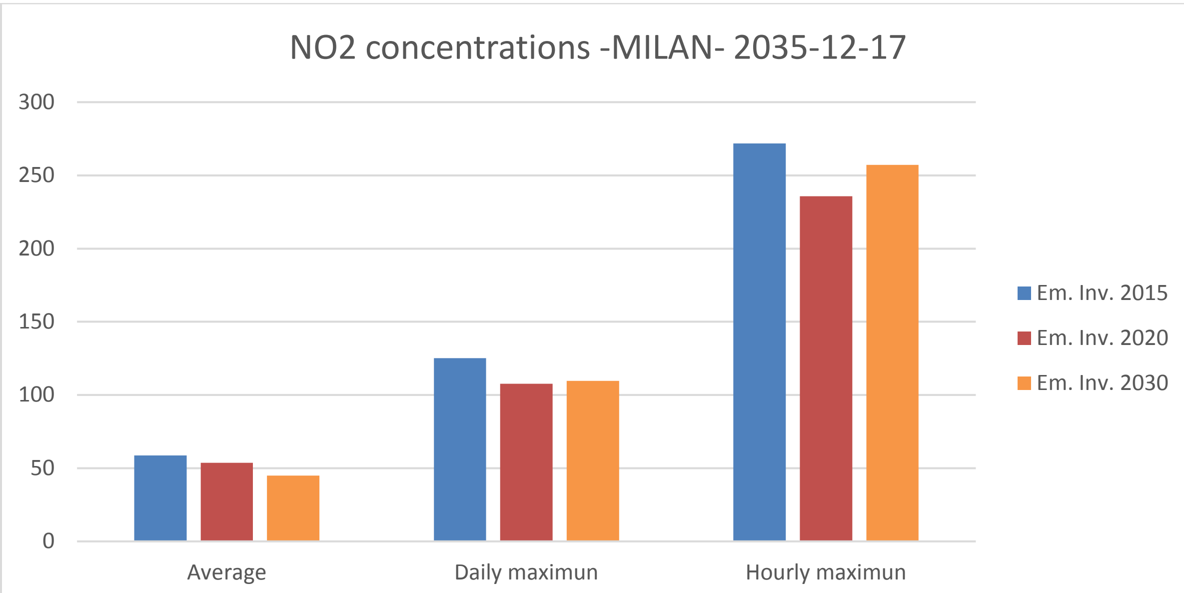


*Figure 4.7.28: $NO_2$ emission inventory comparison*

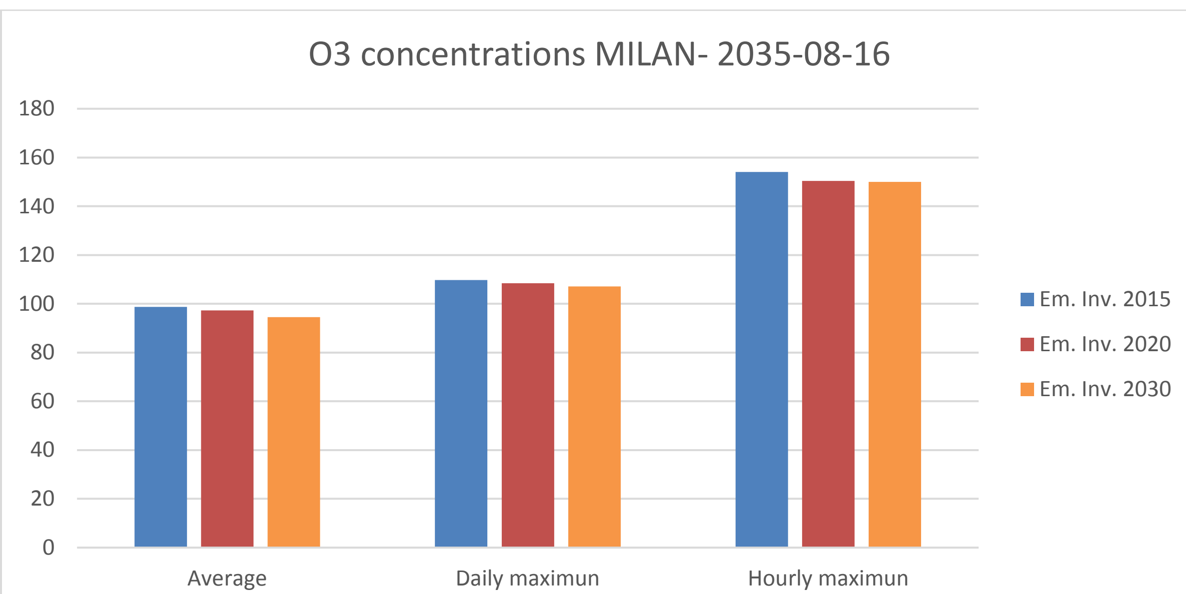


*Figure 4.7.29: $O_3$ emission inventory comparison*

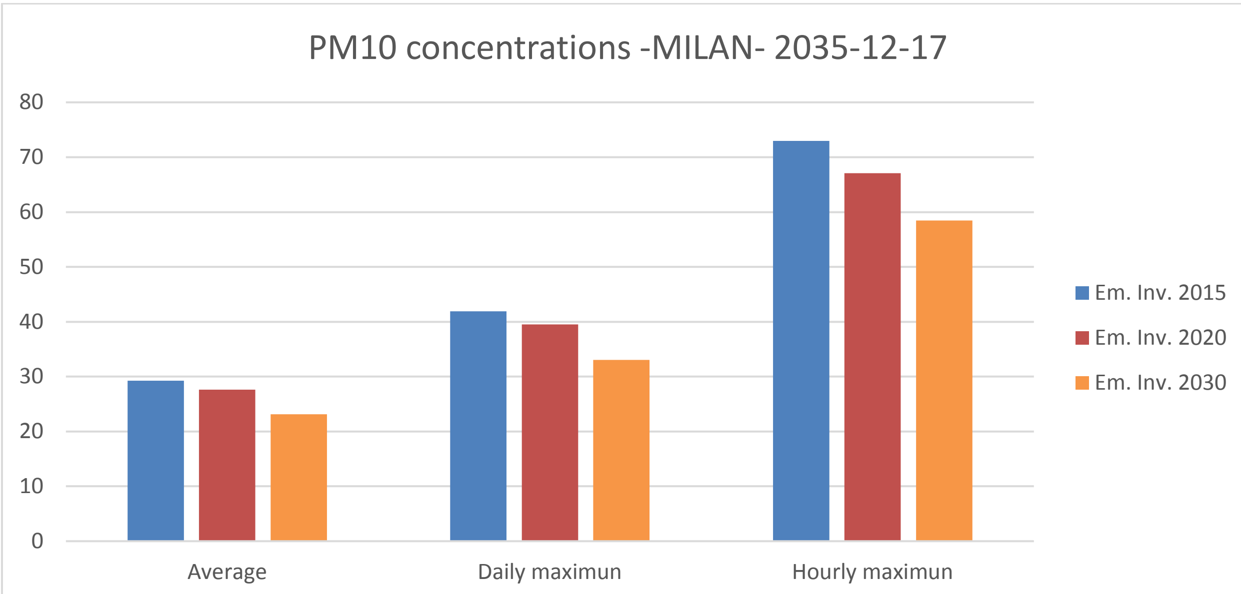


*Figure 4.7.30: $PM_{10}$ emission inventory comparison*

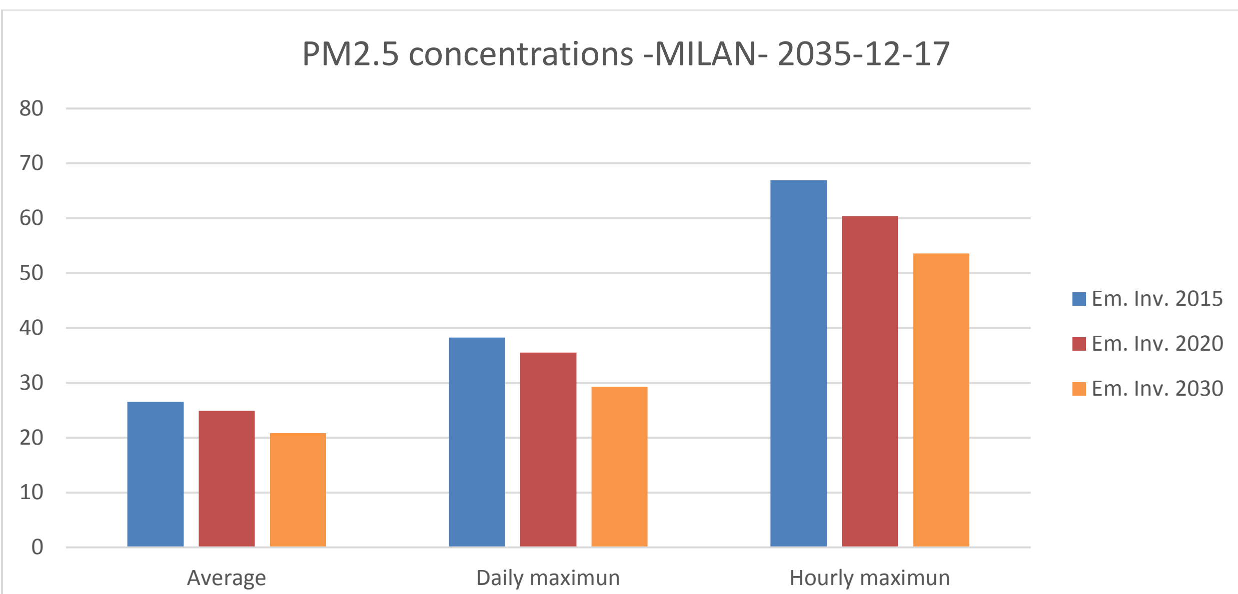


*Figure 4.7.31: $PM_{2.5}$ emission inventory comparison*

### 4.7.4 The GHGs Modeling results

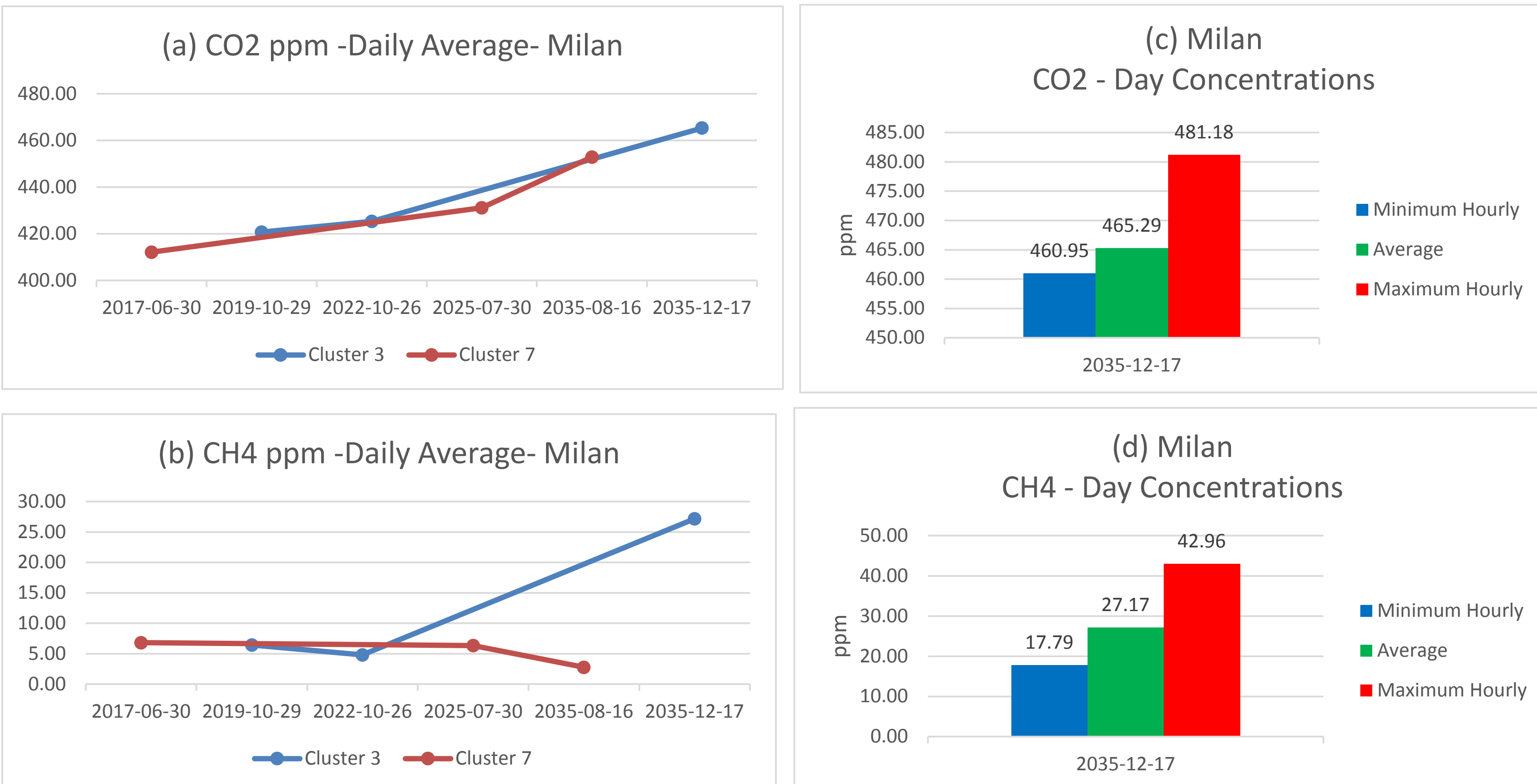


*Figure 4.7.32: (a),(b) $CO_2$ and $CH_4$ Daily average concentrations . (c),(d) $CO_2$ and $CH_4$ concentrations of the most polluted day*

### 4.7.5 Conclusions

For Milan greater area, clusters 2,3,4 and 5 could be categorized in cold period and on the other hand clusters 1,6,7 and 8 in warm period.

In clusters 4 and 8 there is a slight increase in frequency occurrence through the ten 5-year periods. On the other hand, clusters 1,3,5 and 6 show a linear decrease in frequency occurrence.

The most heat waves seem to occur after 2036.The 5-year period 2041-2045 shows the highest number of heat waves, while the next 5-year period shows a decrease. The most heat waves were associated with clusters 7 and 8 which correspond to clusters with days belong to warm period.

Cluster 3 is characterized with elevated $NO_2$ and PM concentrations and cluster 7 with elevated $O_3$ concentrations.

$NO_2$ daily maximum concentrations exceed the EU and WHO yearly limit of 40μg/m$^3$. The maximum hourly concentrations, being above the limit of 200μg/m$^3$, show a decreasing trend.

$O_3$ daily maximum values are above the WHO 8hr limit of 100μg/m$^3$. The maximum hourly concentrations exceed this limit as well as the EU 8hr limit of 120μg/m$^3$.

$PM_{10}$ daily maximum concentrations show maximum values above the WHO yearly limit of 20μg/m$^3$ with a decreasing rate. The hourly maximum concentrations have a decrease rate while showing values that exceed the WHO daily limit of 50μg/m$^3$.

$PM_{2.5}$ daily and hourly maximum concentrations are following a decreasing trend. The daily maximum concentrations are above the WHO yearly limit of 10μg/m$^3$.

For BaP concentrations, all days are above WHO annual limit of 0.12ng/m$^3$ however one day is close to the EU annual limit of 1ng/m$^3$.

There is a decreasing trend in PM pollutants indicating the positive effect on emission reductions intervention. The picture in $NO_2$ and $O_3$ concentration levels is mixed.

## 4.8 Madrid

### 4.8.1 PCA results

The PCA analysis applied to the Madrid data has led to the following results.

Three (3) principal components have been identified as factors for the cluster analysis (Table 4.8.1). Principal Components (PC) explaining 780.8% of the total variance in the initial data.

Factor 1 explains 43.34% of the total variance and contains the 2 temperature variables, mean, daily temperature range, the down ward short-wave radiation and a negative sign of RH and U wind component.

Factor 2 explains 23.07% of the total variance and contains the atmospheric boundary layer thickness and a negative sign of surface pressure.

Factor 3 explains 11.67% of the total variance and contains precipitation and V wind component.

*Table 4.8.1: The Principal Components results*

| | Component | | |
| --- | --- | --- | --- |
| | 1 | 2 | 3 |
| Temperature Range | .802 | | |
| Temperature | .772 | | |
| RH | -.768 | | |
| U wind | -.749 | | |
| Downward short-wave surface radiation | .744 | | |
| Surface pressure | | -.867 | |
| Atmospheric boundary layer thickness | | .863 | |
| V wind | | | .790 |
| Precipitation | | | .772 |

### 4.8.2 Clustering results

#### Cluster description and trends

As explained in 3.4.4 the selected clusters of the city of Madrid are 8. In Figure 4.8.1 are shown the number of days per cluster, where clusters 2,4 and 7 have the most days and cluster 3 and 5 have the less. The monthly distribution per cluster is presented in Table 4.8.2 and in Figure 4.8.2. By dividing the year in two periods, cold and warm, clusters 1,2,8 and 5 could be categorized in cold period and on the other hand clusters 4,7 and 9 in warm period.


*Figure 4.8.1: Number of Days per cluster*

*Table 4.8.2: Monthly distribution per cluster*

| | | Month | | | | | | | | | | | | Total |
|---|---|---|---|---|---|---|---|---|---|---|---|---|---|---|
| | | Jan | Feb | Mar | Apr | May | Jun | Jul | Aug | Sep | Oct | Nov | Dec | |
| Cluster10 | 1 | 245 | 252 | 271 | 130 | 22 | 5 | 0 | 0 | 19 | 249 | 208 | 203 | 1604 |
| | 2 | 541 | 487 | 255 | 5 | 0 | 0 | 0 | 0 | 0 | 120 | 530 | 498 | 2436 |
| | 3 | 102 | 125 | 153 | 160 | 163 | 60 | 16 | 13 | 66 | 110 | 95 | 87 | 1150 |
| | 4 | 0 | 0 | 26 | 249 | 618 | 551 | 446 | 336 | 401 | 62 | 0 | 0 | 2689 |
| | 5 | 56 | 59 | 54 | 19 | 12 | 9 | 27 | 35 | 17 | 40 | 54 | 94 | 476 |
| | 6 | 6 | 32 | 405 | 645 | 251 | 12 | 0 | 5 | 410 | 688 | 63 | 4 | 2521 |
| | 7 | 0 | 0 | 1 | 46 | 367 | 721 | 816 | 822 | 385 | 5 | 0 | 0 | 3163 |
| | 8 | 395 | 214 | 181 | 57 | 5 | 1 | 0 | 0 | 9 | 112 | 308 | 423 | 1705 |
| | 9 | 7 | 20 | 31 | 61 | 55 | 120 | 232 | 330 | 137 | 43 | 14 | 13 | 1063 |
| | 10 | 198 | 223 | 173 | 128 | 57 | 21 | 13 | 9 | 56 | 121 | 228 | 228 | 1455 |
| Total | | 1550 | 1412 | 1550 | 1500 | 1550 | 1500 | 1550 | 1550 | 1500 | 1550 | 1500 | 1550 | 18262 |

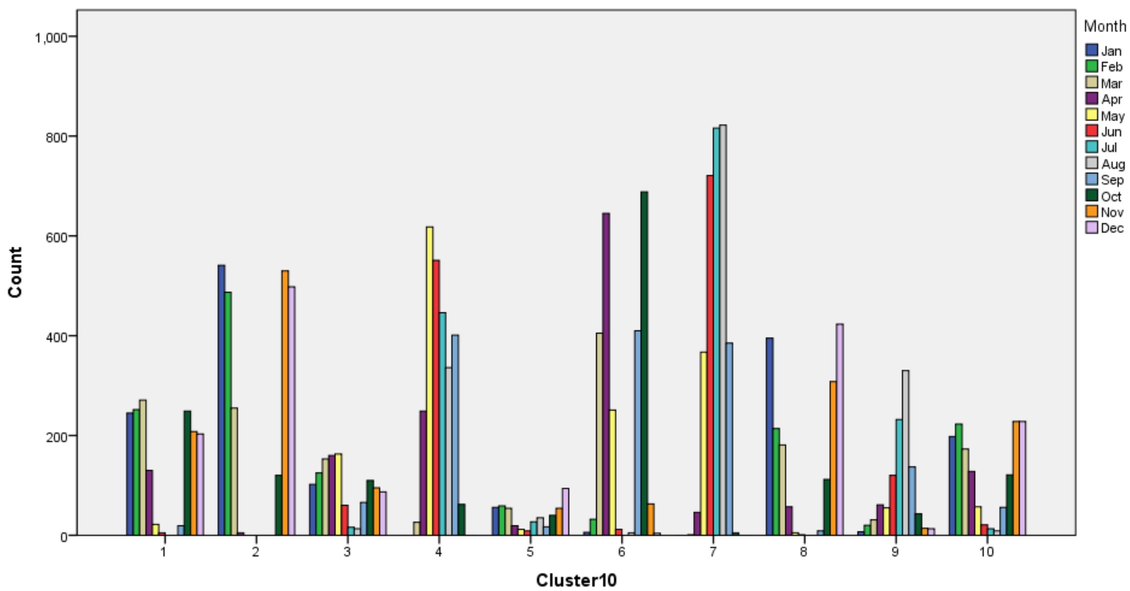


*Figure 4.8.2: Visualized bar chart of monthly distribution per cluster*

A trend analysis of the 5-year frequency of each cluster (Figure 4.8.3). There is an evidence that in clusters 1,8 and 9 there is a linear increase in frequency occurrence through the ten 5-year periods. On the other hand, clusters 3,4,5 and 10 show a linear decrease in frequency occurrence. In the rest clusters no clear trends could be pointed out.

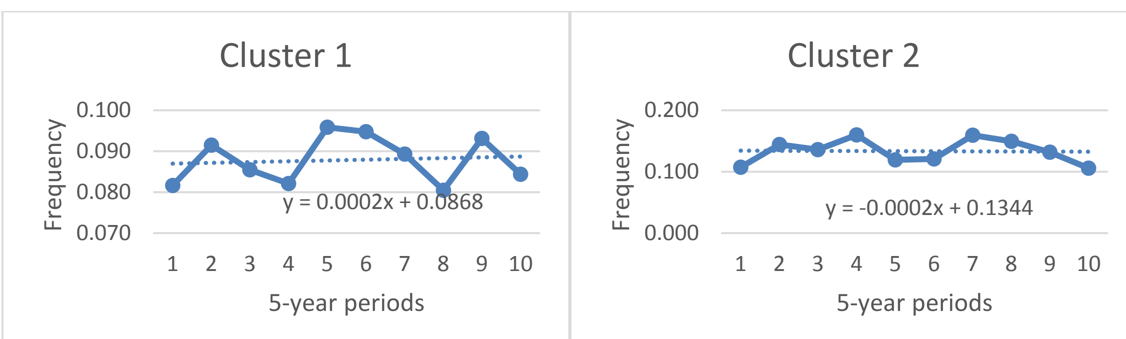

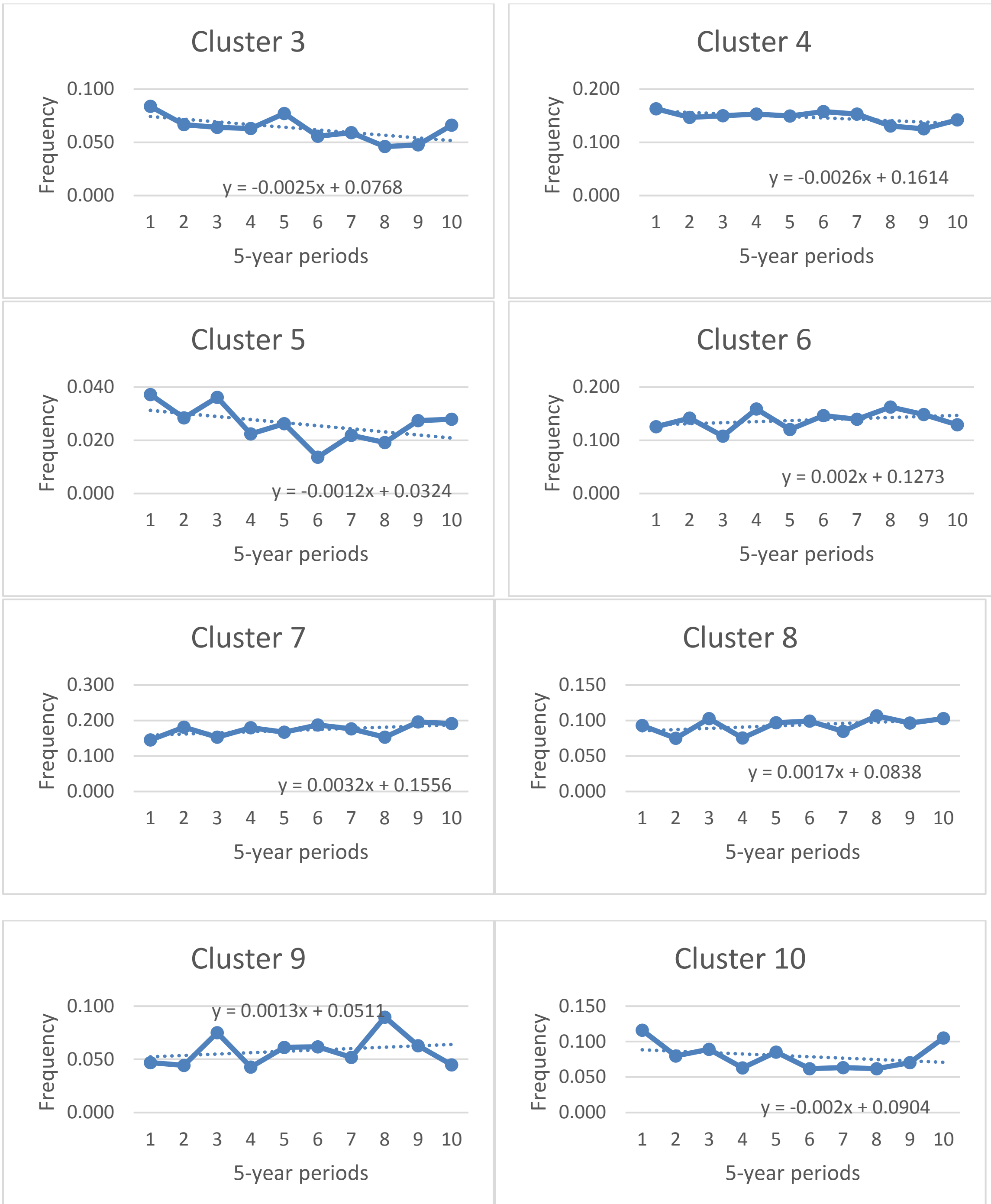


*Figure 4.8.3: Cluster 1-10 frequency trends*

## Cluster characterization

The clusters' implementation is based on the mean values of weather parameters which are displayed in Table 4.8.3.

*Table 4.8.3: Summary of the 10 clusters*

| | Cluster | | | | | | | | | |
|---|---|---|---|---|---|---|---|---|---|---|
| | 1 | 2 | 3 | 4 | 5 | 6 | 7 | 8 | 9 | 10 |
| | Mean (SD) | Mean (SD) | Mean (SD) | Mean (SD) | Mean (SD) | Mean (SD) | Mean (SD) | Mean (SD) | Mean (SD) | Mean (SD) |
| Temperature ( °C) | 7,21 (3,81) | 7,49 (3,16) | 8,25 (4,14) | 15,96 (4,24) | 11,23 (5,64) | 14,58 (3,93) | 21,99 (3,36) | 7,64 (3,12) | 21,08 (5,03) | 8,96 (3,69) |
| Daily Temperature Range ( °C) | 7,96 (2,04) | 10,55 (2,07) | 6,94 (1,99) | 10,35 (1,75) | 4,93 (1,93) | 12,77 (2,11) | 12,12 (1,74) | 6,22 (2,23) | 8,77 (2,04) | 5,01 (1,76) |
| Relative Humidity (%) | 63,82 (8,79) | 63,25 (13,22) | 57,77 (7,63) | 48,78 (6,72) | 80,86 (8,11) | 50,49 (9,84) | 43,67 (7,13) | 80,75 (9,17) | 58,4 (9,62) | 76,5 (8,28) |
| Surface Pressure (Pa) | 94326,78 (483,26) | 95160,57 (465,37) | 93512,72 (532,18) | 93859,25 (379,64) | 93117,44 (634,62) | 94510,76 (398,6) | 93980,06 (302,27) | 94323,17 (437,19) | 93778,13 (376,44) | 93271,47 (556,31) |
| Precipitation (kg/m2/s) | 0,000002 (0,000006) | 0 (0,000003) | 0,000006 (0,00001) | 0,000002 (0,000007) | 0,000198 (0,000083) | 0,000001 (0,000004) | 0,000003 (0,000008) | 0,000015 (0,000022) | 0,000053 (0,000041) | 0,000049 (0,000036) |
| Downward Short Wave Radiation | 165,16 (56,69) | 139,95 (39,6) | 223,18 (87,17) | 321,88 (52,27) | 84,15 (71,89) | 242,11 (60,37) | 330,11 (41,43) | 87,43 (48,73) | 254,04 (67,57) | 108,36 (70,7) |
| u wind component (m/s) | 2,35 (2,52) | -0,35 (1,55) | 4,38 (2,69) | 0,3 (2,38) | 3,13 (3,53) | -0,52 (1,95) | -1,45 (2,02) | 2,95 (2,03) | -0,56 (2,27) | 5,92 (2,1) |
| v wind component (m/s) | -2,11 (1,31) | -0,28 (0,87) | -3,55 (1,74) | -3,37 (1,36) | 2,47 (2,13) | -0,47 (1,24) | -1,57 (1,12) | 0,84 (0,98) | 0,44 (1,72) | 0,9 (1,54) |
| V wind (m/s) | 4,05 (1,28) | 1,51 (1,03) | 6,33 (1,45) | 4,2 (1,13) | 5,1 (2,63) | 2,07 (1,23) | 2,87 (1,29) | 3,44 (1,63) | 2,54 (1,46) | 6,25 (1,9) |
| Atmospheric Boundary Layer Thickness (m) | 676,79 (154,07) | 273,17 (127,62) | 1102,67 (186,17) | 1045,86 (153,98) | 741,89 (294,46) | 603,55 (168,91) | 1042,03 (145,67) | 437,91 (154,8) | 822 (189,44) | 844,7 (216,8) |

In addition to the previous Table 4.8.3, Figure 4.8.4 presents the mean normalized (z-score) variables of each cluster, respectively showing the differences of the parameters per cluster.

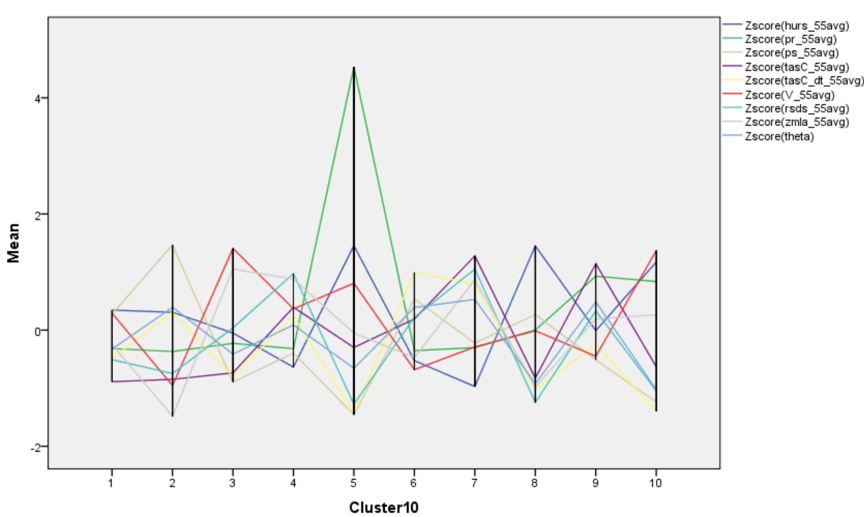


*Figure 4.8.4: Normalized variables (z-score) averaged for each cluster*

Daily, 10-meter from ground level, wind data were used to create the wind roses per each cluster as they are shown in Figures 4.8.5-4.8.14. Each wind direction distribution per cluster is presented in more details in Table 4.8.4.

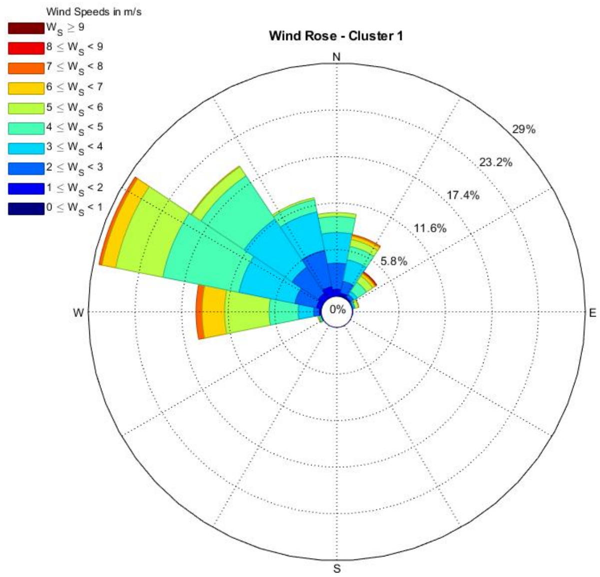


*Figure 4.8.5: Wind Rose - Cluster 1*

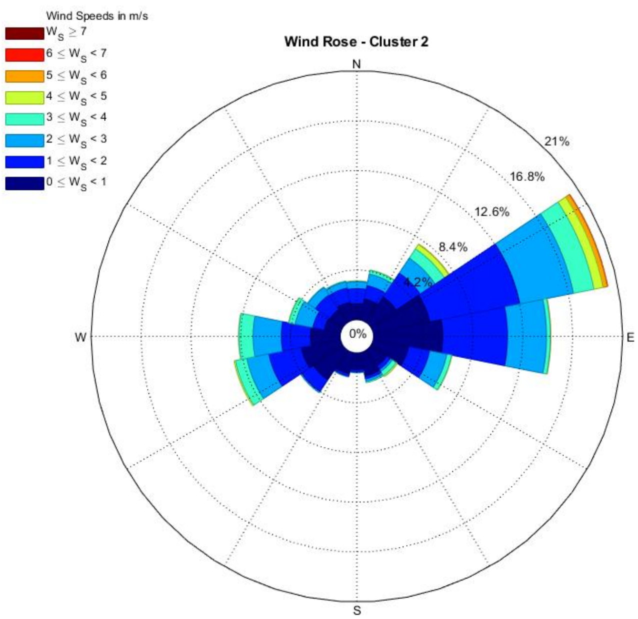


*Figure 4.8.6: Wind Rose - Cluster 2*

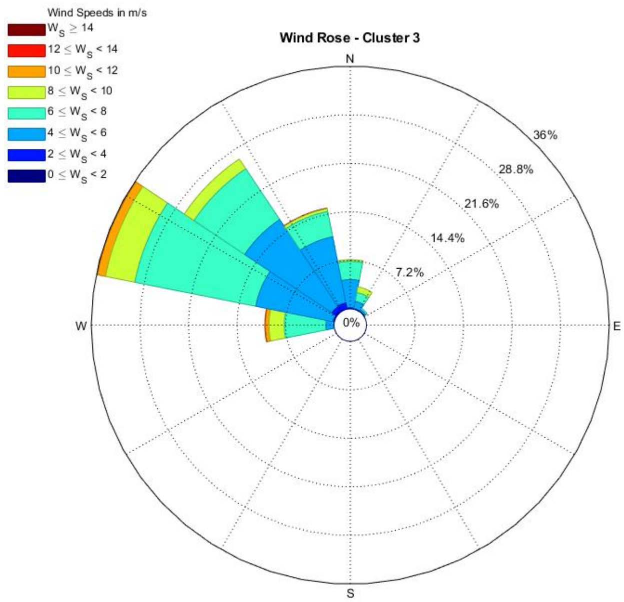


*Figure 4.8.7: Wind Rose - Cluster 3*

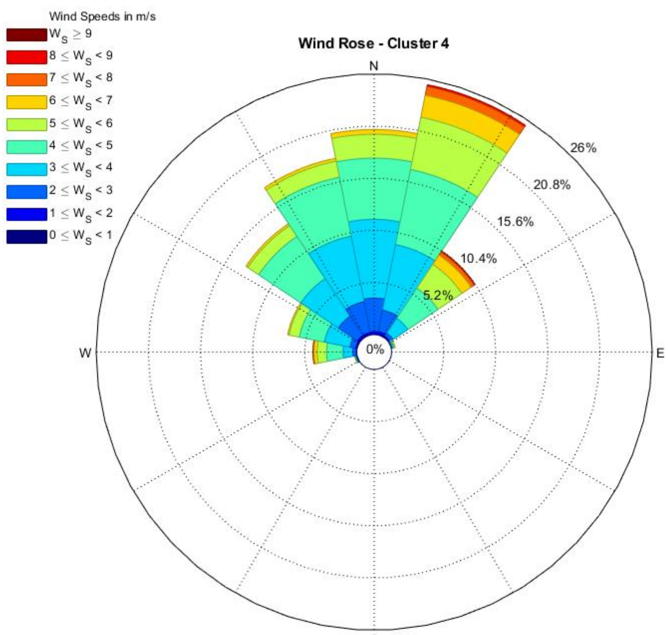


*Figure 4.8.8: Wind Rose - Cluster 4*

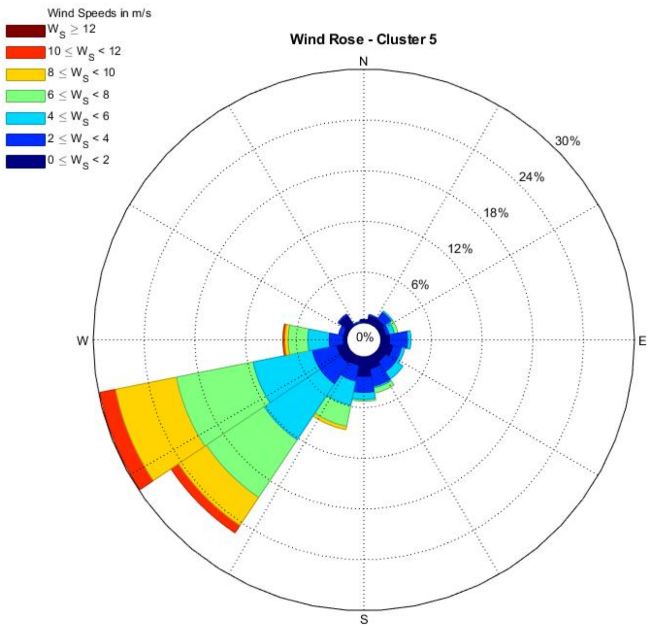


*Figure 4.8.9: Wind Rose - Cluster 5*

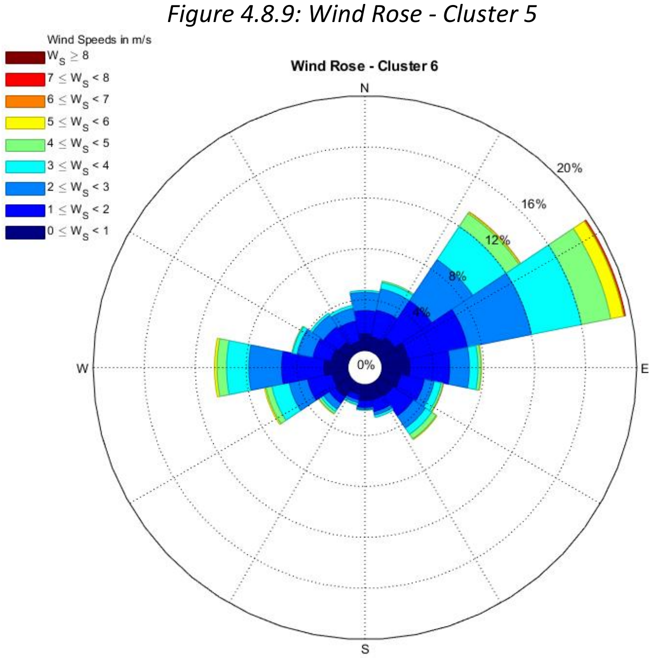


*Figure 4.8.10: Wind Rose - Cluster 6*

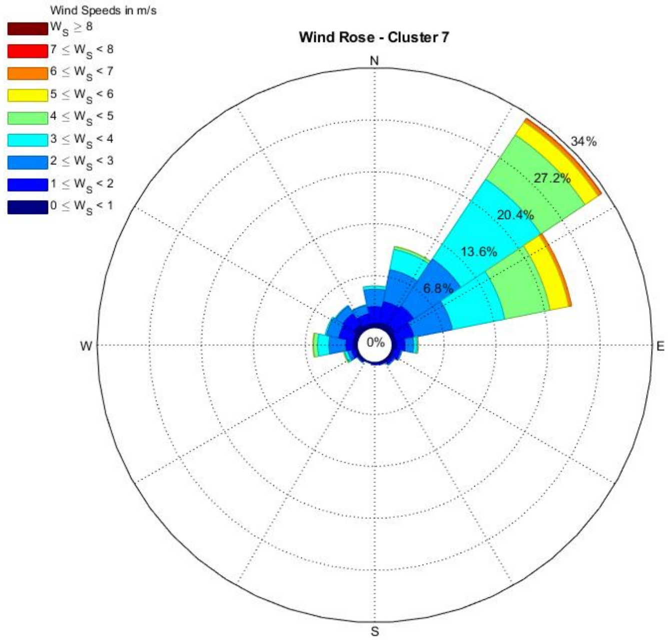


*Figure 4.8.11: Wind Rose - Cluster 7*

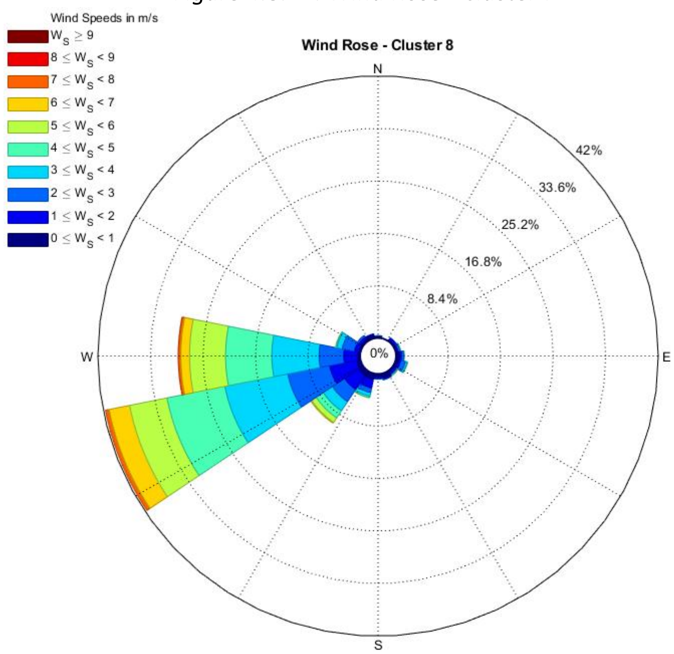


*Figure 4.8.12: Wind Rose - Cluster 8*

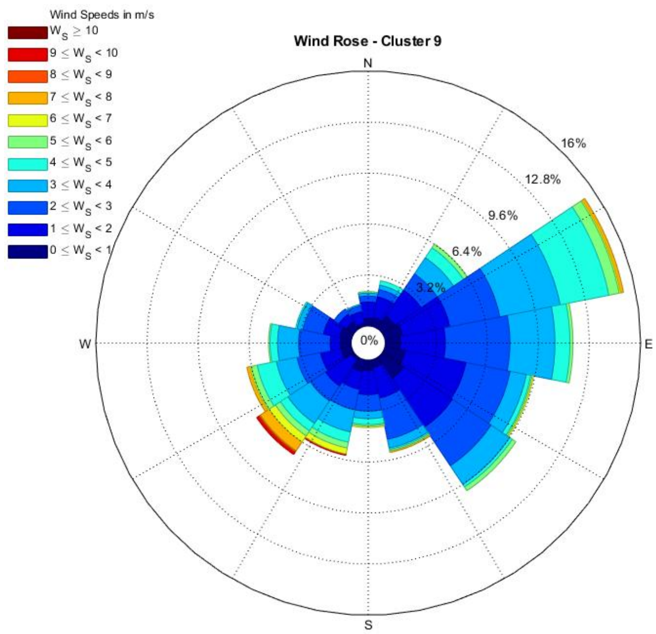


*Figure 4.8.13: Wind Rose - Cluster 9*

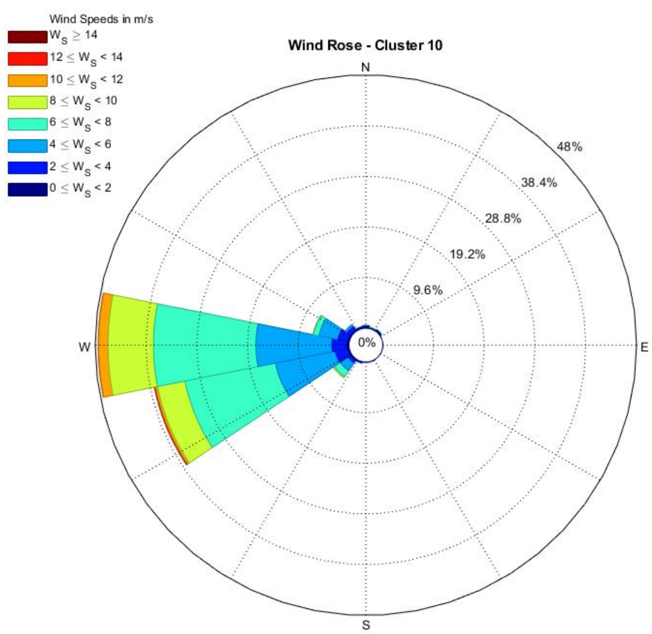


*Figure 4.8.14: Wind Rose - Cluster 10*

*Table 4.8.4: 16 Wind Direction distribution per cluster*

| | | | Wind16 | | | | | | | | | | | | | | | | Total |
|---|---|---|---|---|---|---|---|---|---|---|---|---|---|---|---|---|---|---|---|
| | | | S | SSW | SW | WSW | W | WNW | NW | NNW | N | NNE | NE | ENE | E | ESE | SE | SSE | |
| Cluster10 | 1 | Count | 0 | 0 | 0 | 8 | 250 | 453 | 319 | 201 | 167 | 126 | 65 | 14 | 1 | 0 | 0 | 0 | 1604 |
| | | % within Cluster10 | 0.0% | 0.0% | 0.0% | 0.5% | 15.6% | 28.2% | 19.9% | 12.5% | 10.4% | 7.9% | 4.1% | 0.9% | 0.1% | 0.0% | 0.0% | 0.0% | 100.0% |
| | 2 | Count | 41 | 51 | 105 | 223 | 209 | 109 | 88 | 82 | 80 | 105 | 194 | 491 | 364 | 165 | 66 | 63 | 2436 |
| | | % within Cluster10 | 1.7% | 2.1% | 4.3% | 9.2% | 8.6% | 4.5% | 3.6% | 3.4% | 3.3% | 4.3% | 8.0% | 20.2% | 14.9% | 6.8% | 2.7% | 2.6% | 100.0% |
| | 3 | Count | 0 | 0 | 0 | 0 | 118 | 413 | 313 | 176 | 84 | 39 | 7 | 0 | 0 | 0 | 0 | 0 | 1150 |
| | | % within Cluster10 | 0.0% | 0.0% | 0.0% | 0.0% | 10.3% | 35.9% | 27.2% | 15.3% | 7.3% | 3.4% | 0.6% | 0.0% | 0.0% | 0.0% | 0.0% | 0.0% | 100.0% |
| | 4 | Count | 0 | 0 | 0 | 7 | 118 | 190 | 367 | 483 | 550 | 684 | 279 | 11 | 0 | 0 | 0 | 0 | 2689 |
| | | % within Cluster10 | 0.0% | 0.0% | 0.0% | 0.3% | 4.4% | 7.1% | 13.6% | 18.0% | 20.5% | 25.4% | 10.4% | 0.4% | 0.0% | 0.0% | 0.0% | 0.0% | 100.0% |
| | 5 | Count | 25 | 42 | 121 | 142 | 36 | 5 | 8 | 1 | 2 | 5 | 10 | 10 | 17 | 14 | 17 | 21 | 476 |
| | | % within Cluster10 | 5.3% | 8.8% | 25.4% | 29.8% | 7.6% | 1.1% | 1.7% | 0.2% | 0.4% | 1.1% | 2.1% | 2.1% | 3.6% | 2.9% | 3.6% | 4.4% | 100.0% |
| | 6 | Count | 51 | 42 | 77 | 169 | 264 | 114 | 96 | 92 | 119 | 141 | 337 | 492 | 197 | 125 | 138 | 67 | 2521 |
| | | % within Cluster10 | 2.0% | 1.7% | 3.1% | 6.7% | 10.5% | 4.5% | 3.8% | 3.6% | 4.7% | 5.6% | 13.4% | 19.5% | 7.8% | 5.0% | 5.5% | 2.7% | 100.0% |
| | 7 | Count | 10 | 6 | 17 | 60 | 184 | 137 | 126 | 99 | 173 | 345 | 1056 | 758 | 108 | 43 | 28 | 13 | 3163 |
| | | % within Cluster10 | 0.3% | 0.2% | 0.5% | 1.9% | 5.8% | 4.3% | 4.0% | 3.1% | 5.5% | 10.9% | 33.4% | 24.0% | 3.4% | 1.4% | 0.9% | 0.4% | 100.0% |
| | 8 | Count | 16 | 69 | 173 | 710 | 497 | 71 | 20 | 14 | 8 | 3 | 12 | 16 | 24 | 35 | 18 | 19 | 1705 |
| | | % within Cluster10 | 0.9% | 4.0% | 10.1% | 41.6% | 29.1% | 4.2% | 1.2% | 0.8% | 0.5% | 0.2% | 0.7% | 0.9% | 1.4% | 2.1% | 1.1% | 1.1% | 100.0% |
| | 9 | Count | 45 | 65 | 78 | 71 | 55 | 38 | 16 | 15 | 23 | 31 | 68 | 162 | 125 | 101 | 107 | 63 | 1063 |
| | | % within Cluster10 | 4.2% | 6.1% | 7.3% | 6.7% | 5.2% | 3.6% | 1.5% | 1.4% | 2.2% | 2.9% | 6.4% | 15.2% | 11.8% | 9.5% | 10.1% | 5.9% | 100.0% |
| | 10 | Count | 1 | 5 | 62 | 547 | 690 | 102 | 22 | 6 | 8 | 4 | 6 | 0 | 1 | 0 | 0 | 1 | 1455 |
| | | % within Cluster10 | 0.1% | 0.3% | 4.3% | 37.6% | 47.4% | 7.0% | 1.5% | 0.4% | 0.5% | 0.3% | 0.4% | 0.0% | 0.1% | 0.0% | 0.0% | 0.1% | 100.0% |
| Total | | Count | 189 | 280 | 633 | 1937 | 2421 | 1632 | 1375 | 1169 | 1214 | 1483 | 2034 | 1954 | 837 | 483 | 374 | 247 | 18262 |
| | | % within Cluster10 | 1.0% | 1.5% | 3.5% | 10.6% | 13.3% | 8.9% | 7.5% | 6.4% | 6.6% | 8.1% | 11.1% | 10.7% | 4.6% | 2.6% | 2.0% | 1.4% | 100.0% |

## Clusters and local Heat Waves

In Figures 4.8.15 and 4.8.16 are presented the heat waves occurrence per 5-year period and per cluster. The 5-year period 2046-2050 shows the highest number of heat waves. The most heat waves were associated with clusters 7 and 9 which correspond to clusters with days belong to warm period (see Table 4.8.2).

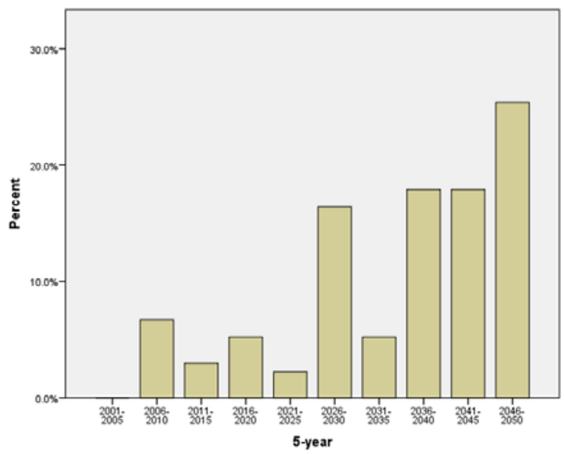


Figure 4.8.15: Heat Waves per 5-year period

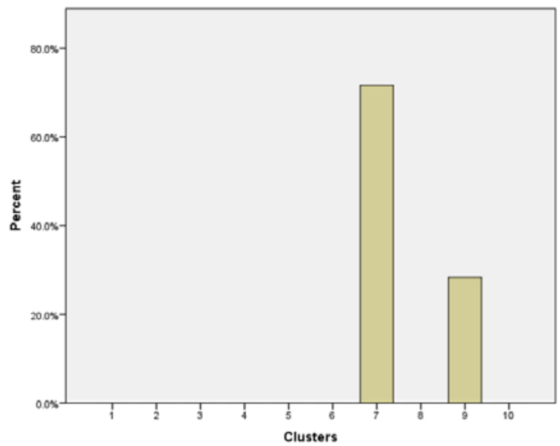


Figure 4.8.16: Heat Waves per cluster

## Clusters versus Air Quality level

As it can be seen in Table 4.1 two observation stations have been used for the present analysis. The descriptive statistics for $NO_2$, $O_3$ and $PM_{10}$ is given in Table 4.7.5.

Table 4.8.5: Air pollutants descriptive statistics

| | | NO2 | O3 | PM10 |
|---|---|---|---|---|
| Mean | | 48.1539 | 41.0876 | 28.0222 |
| Std. Deviation | | 18.85761 | 20.84879 | 14.96106 |
| Minimum | | 8.50 | 1.33 | 5.36 |
| Maximum | | 124.67 | 102.54 | 156.00 |
| Percentiles | 5 | 21.8861 | 8.2397 | 10.4342 |
| | 25 | 34.3349 | 23.4889 | 16.5684 |
| | 50 | 45.4264 | 42.0620 | 24.9680 |
| | 75 | 59.5620 | 56.7980 | 35.9044 |
| | 95 | 84.2917 | 74.7101 | 56.1959 |

Table 4.8.6 presents the pollutants' concentrations per cluster. Higher mean $NO_2$ concentrations are observed in clusters 1,2 and 8. Higher mean $O_3$ concentrations are observed in clusters 4 and 7. Higher mean $PM_{10}$ concentrations are observed in clusters 4,7 and 9.

*Table 4.8.6: Summary pollutant concentrations per cluster*

| | Cluster | | | | | | | | | |
|---|---|---|---|---|---|---|---|---|---|---|
| | 1 | 2 | 3 | 4 | 5 | 6 | 7 | 8 | 9 | 10 |
| | Mean (SD) | Mean (SD) | Mean (SD) | Mean (SD) | Mean (SD) | Mean (SD) | Mean (SD) | Mean (SD) | Mean (SD) | Mean (SD) |
| PM10 (μg/m3) | 26,31 (14,12) | 26,25 (17,44) | 27,34 (13,76) | 30,23 (14,2) | 27,9 (14,11) | 25,79 (14,09) | 31,35 (14,2) | 25,98 (14,83) | 30,23 (14,64) | 27,14 (15,56) |
| O3 (μg/m3) | 28,65 (17,39) | 25,46 (15,25) | 39,18 (18,38) | 56,46 (13,84) | 26,74 (16,95) | 43,48 (16,55) | 59,67 (12,42) | 23,42 (13,81) | 54,41 (17,77) | 29,5 (17,45) |
| NO2 (μg/m3) | 54,18 (19,83) | 55,24 (20,04) | 49,4 (17,27) | 42,52 (15,48) | 53,94 (19,47) | 46,25 (18,86) | 39,79 (14,55) | 54,99 (18,82) | 40,47 (14,76) | 53,74 (20,37) |

The differences in concentrations per cluster are shown in Figures 4.8.17-4.2.19.

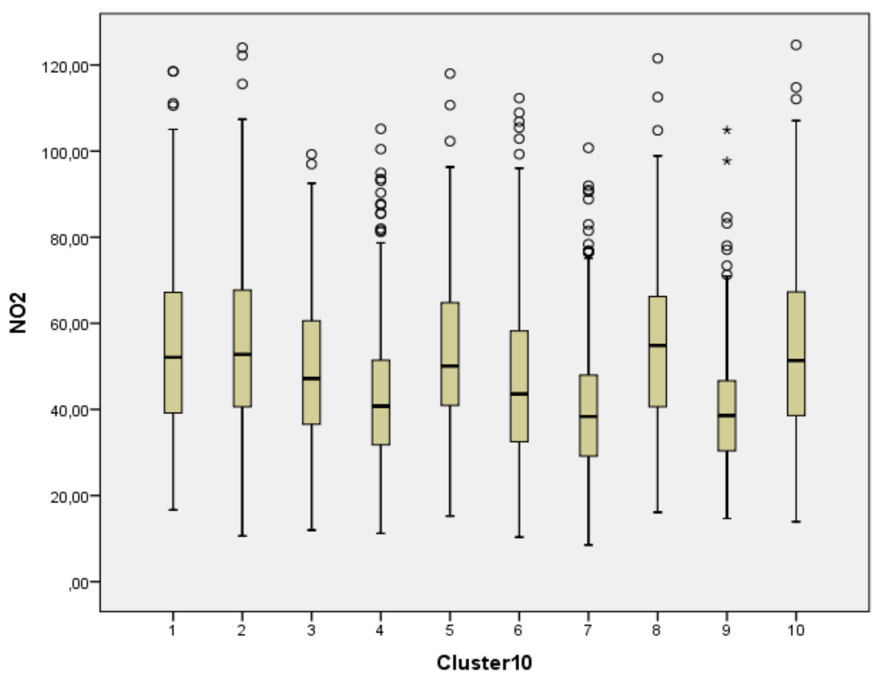


*Figure 4.8.17: $NO_2$ concentration statistics per cluster*

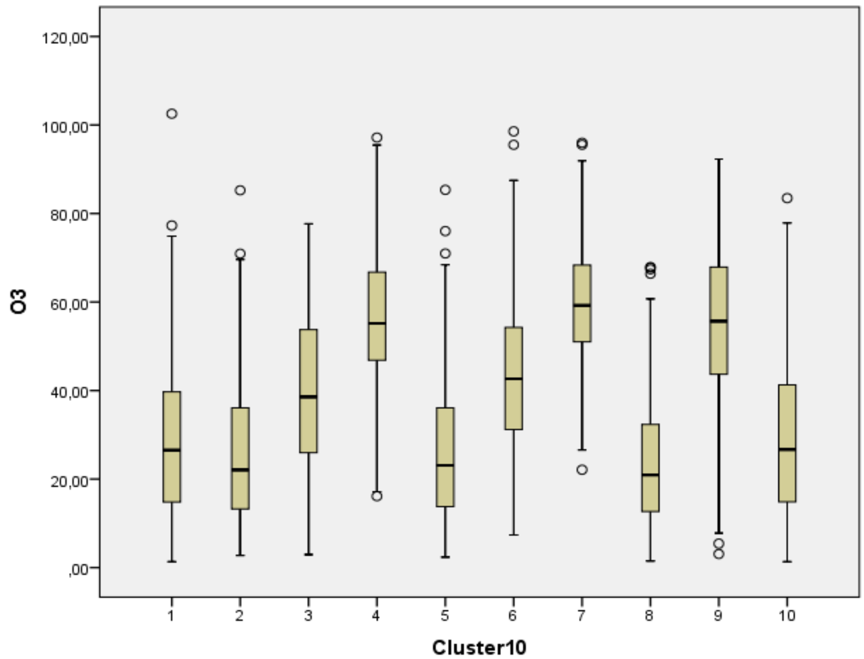


*Figure 4.8.18: $O_3$ concentration statistics per cluster*

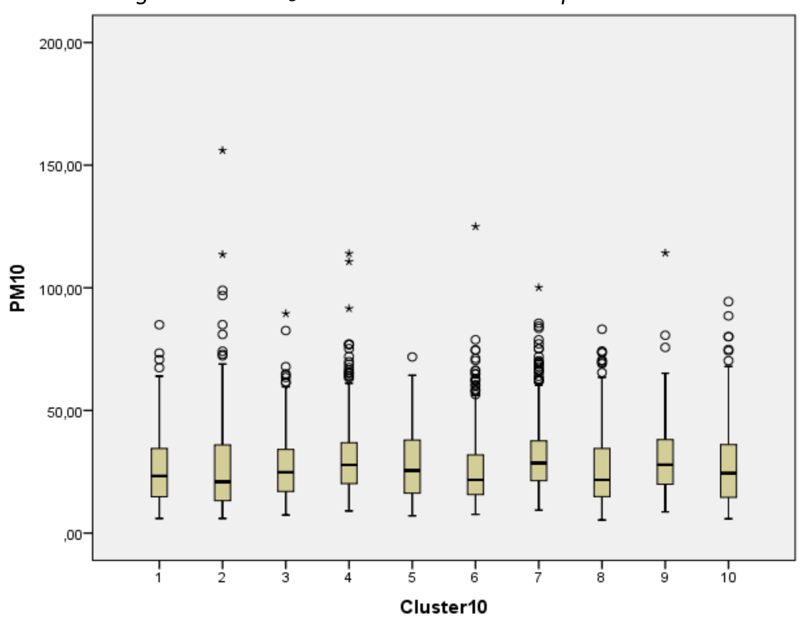


*Figure 4.8.19: $PM_{10}$ concentration statistics per cluster*

### Representative Days

In the following Table 4.8.7 are presented the selected RDs per 5-year period and per cluster.

*Table 4.8.7: Representative days per cluster and 5year period*

| Closest days to centroids per 5year per cluster | | | clusters | | | | | | | | | |
|---|---|---|---|---|---|---|---|---|---|---|---|---|
| | | | 1 | 2 | 3 | 4 | 5 | 6 | 7 | 8 | 9 | 10 |
| 5 year period | 2001-2005 | 1 | 2005/10/27 | 2005/12/07 | 2004/05/05 | 2003/05/28 | 2001/10/19 | 2001/09/25 | 2005/08/30 | 2003/11/22 | 2004/08/23 | 2002/11/30 |
| | 2006-2010 | 2 | 2009/02/25 | 2008/11/28 | 2009/03/10 | 2007/09/05 | 2007/11/23 | 2009/04/27 | 2008/07/09 | 2006/01/07 | 2006/06/15 | 2006/11/20 |
| | 2011-2015 | 3 | 2012/03/25 | 2011/01/28 | 2013/09/29 | 2011/06/09 | 2013/10/06 | 2011/04/14 | 2013/06/25 | 2014/11/08 | 2015/06/29 | 2015/03/23 |
| | 2016-2020 | 4 | 2016/11/07 | 2017/11/21 | 2017/03/02 | 2019/05/25 | 2018/06/19 | 2019/04/22 | 2018/06/21 | 2019/11/05 | 2018/07/28 | 2020/01/17 |
| | 2021-2025 | 5 | 2025/02/18 | 2021/11/12 | 2025/04/14 | 2025/05/24 | 2024/11/19 | 2023/03/28 | 2021/06/18 | 2022/02/26 | 2024/06/08 | 2021/01/26 |
| | 2026-2030 | 6 | 2028/11/06 | 2029/11/06 | 2029/03/17 | 2027/09/11 | 2030/12/17 | 2026/10/06 | 2026/08/08 | 2029/01/13 | 2030/06/18 | 2029/12/29 |
| | 2031-2035 | 7 | 2035/03/02 | 2031/02/16 | 2033/03/22 | 2034/08/31 | 2032/12/06 | 2033/10/09 | 2033/06/14 | 2035/12/15 | 2032/04/27 | 2035/03/17 |
| | 2036-2040 | 8 | 2037/11/06 | 2040/11/19 | 2036/02/28 | 2040/06/05 | 2038/12/02 | 2037/04/15 | 2039/06/04 | 2040/01/29 | 2040/09/03 | 2036/05/09 |
| | 2041-2045 | 9 | 2042/03/19 | 2041/01/29 | 2044/10/21 | 2044/05/23 | 2041/02/12 | 2041/10/03 | 2045/06/05 | 2041/11/19 | 2045/08/25 | 2045/03/27 |
| | 2046-2050 | 10 | 2048/10/26 | 2048/01/19 | 2046/03/24 | 2050/09/02 | 2046/03/18 | 2050/03/22 | 2046/08/11 | 2048/01/29 | 2046/06/30 | 2046/01/23 |

### Selected Clusters and RDs for modeling purposes

Selected RDs will be used to perform targeted weather and air quality simulations within each selected 5-year period estimating hourly/daily concentrations of the priority pollutants to assess the climatic effect on air quality evolution and the characteristics of air quality future episodes. The selection was based on 3-year periods (2016-2020, 2021-2025 and 2031-2035) and on the clusters with the most elevated concentrations of $PM_{10}$, $NO_2$ and $O_3$. In the case of Madrid, cluster 8 recorded the most elevated values of $NO_2$, cluster 7 for the case of $O_3$ and $PM_{10}$. In Table 4.8.8 are presented the selected days which was used for modeling purposes.

*Table 4.8.8: RDs for modeling purposes*

| **Period** | **Cluster 7 (O3, PM)** | **Cluster 8 (NO2)** |
|---|---|---|
| 2016-2020 | 2018-06-21 | 2019-11-05 |
| 2021-2025 | 2021-06-18 | 2022-02-26 |
| 2031-2035 | 2033-06-14 | 2035-12-15 |

### 4.8.3 Air Quality Modeling results

#### 4.8.3.1 Overall results

In Figure 4.8.20 the daily average concentrations of $NO_2$, $O_3$, $PM_{10}$ and $PM_{2.5}$ for selected RDs are presented.

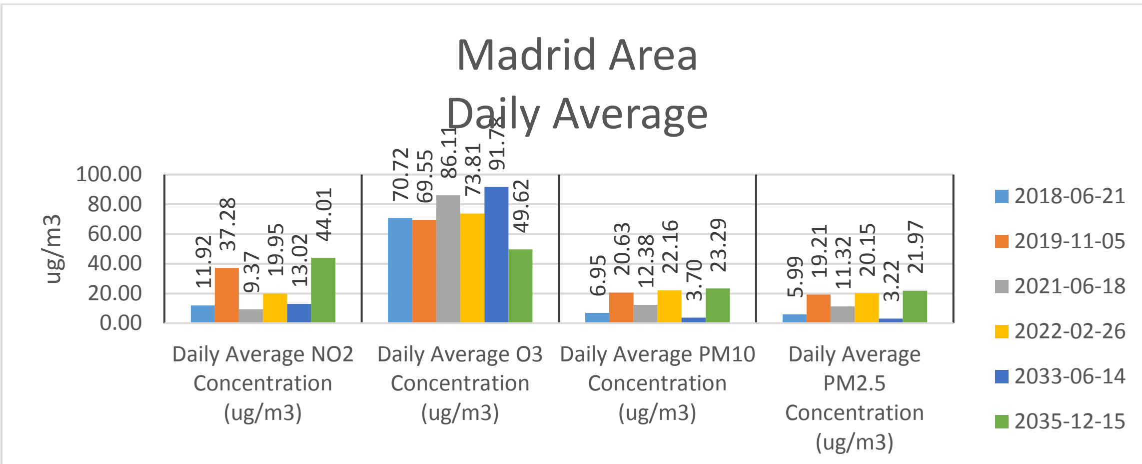


*Figure 4.8.20: Daily average concentrations*

In Figure 4.8.21 the obtained daily averaged concentrations are compared based on USTUTT and EGDAR HTAP emission inventories respectively. The results seem not to differ significantly expect in some days in PM concentrations.

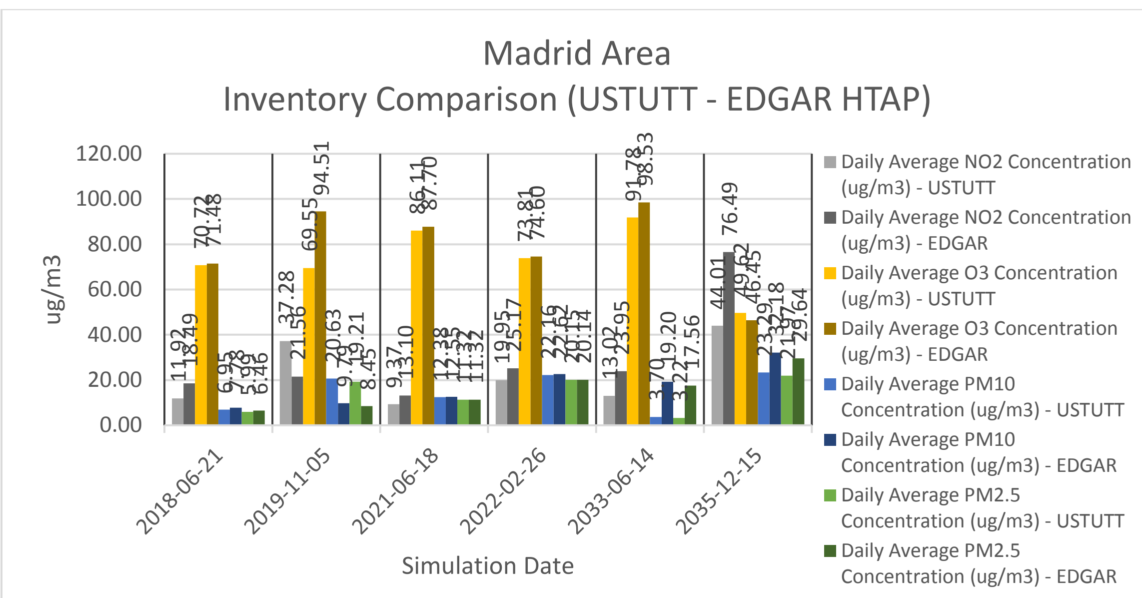


*Figure 4.8.21: Daily average concentrations – USTUTT vs EDGAR HTAP comparison*

#### 4.8.3.2 Clusters results

$NO_2$ Concentrations (Cluster 8)

In Figure 4.8.22, the results are presented in terms of concentrations average, daily maximum and hourly maximum. The diurnal variations are shown in Figure 4.8.23.

The daily maximum concentrations exceed the EU and WHO yearly limit of 40μg/m$^3$.

$O_3$ Concentrations (Cluster 7)

In Figure 4.8.24, the results are presented in terms of concentrations average, daily maximum and hourly maximum. The diurnal variations are shown in Figure 4.8.25.

The daily average concentrations show an increasing trend with maximum values very close to the WHO 8hr limit of 100μg/m$^3$. The maximum hourly concentrations exceed this limit.

$PM_{10}$ Concentrations (Cluster 7)

In Figure 4.8.26, the results are presented in terms of concentrations average, daily maximum and hourly maximum. The diurnal variations are shown in Figure 4.8.27.

The daily maximum concentrations show maximum values below the WHO yearly limit of 20μg/m$^3$.

## $NO_2$-Cluster 8

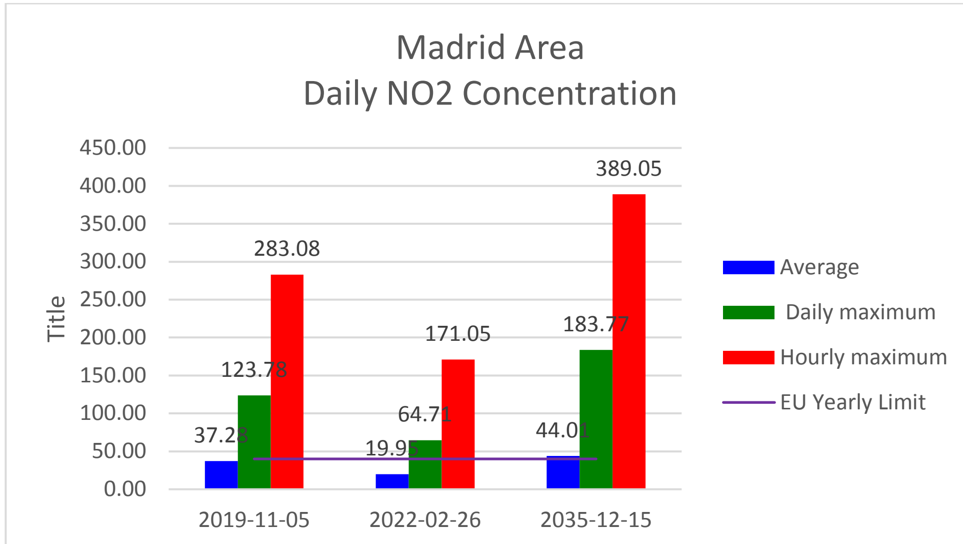


*Figure 4.8.22: $NO_2$ Day concentrations*

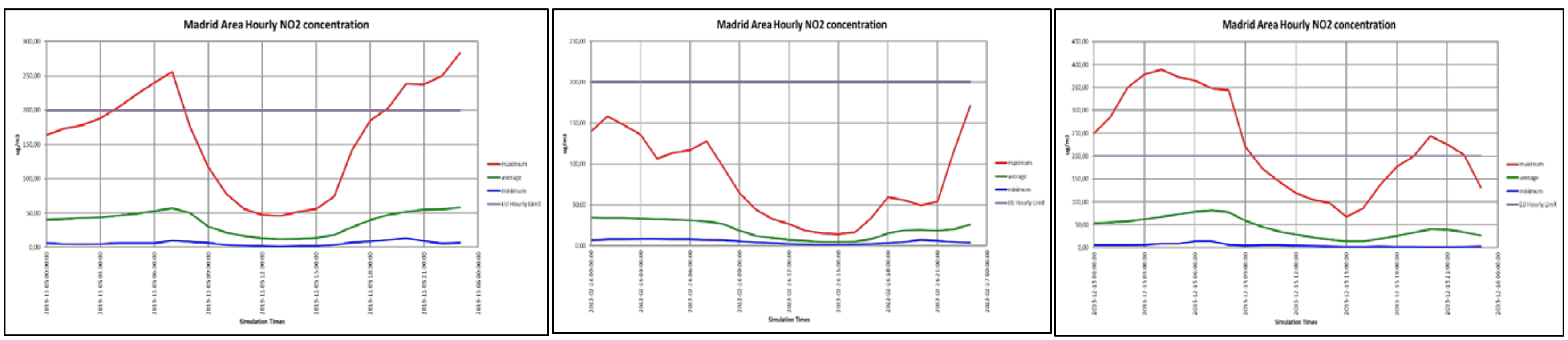


**Figu***re 4.8.23: NO2 Hourly concentrations*

### $O_3$-Cluster 7

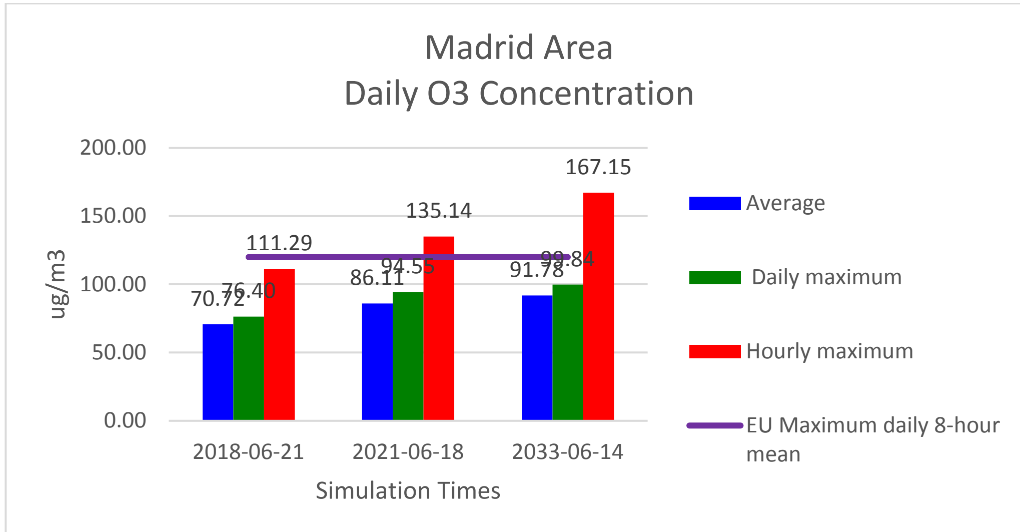


*Figure 4.8.24: $O_3$ Daily concentrations*

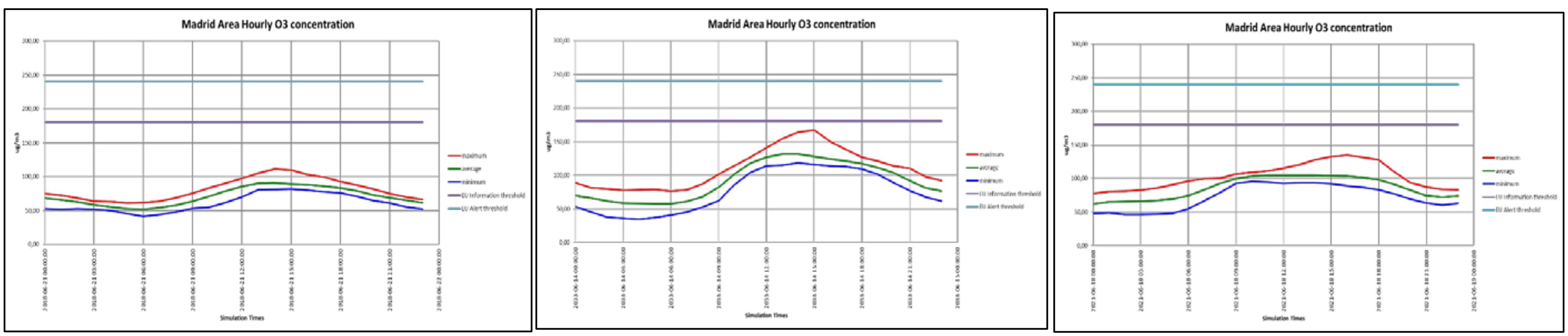


*Figure 4.8.25: $O_3$ Hourly concentrations*

### $PM_{10}$-Cluster 7

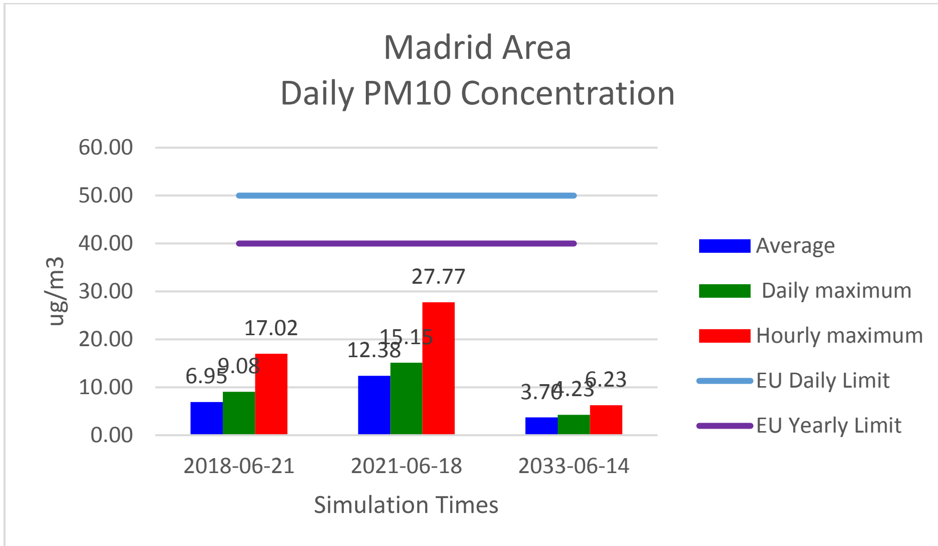


*Figure 4.8.26: $PM_{10}$ Daily concentrations*

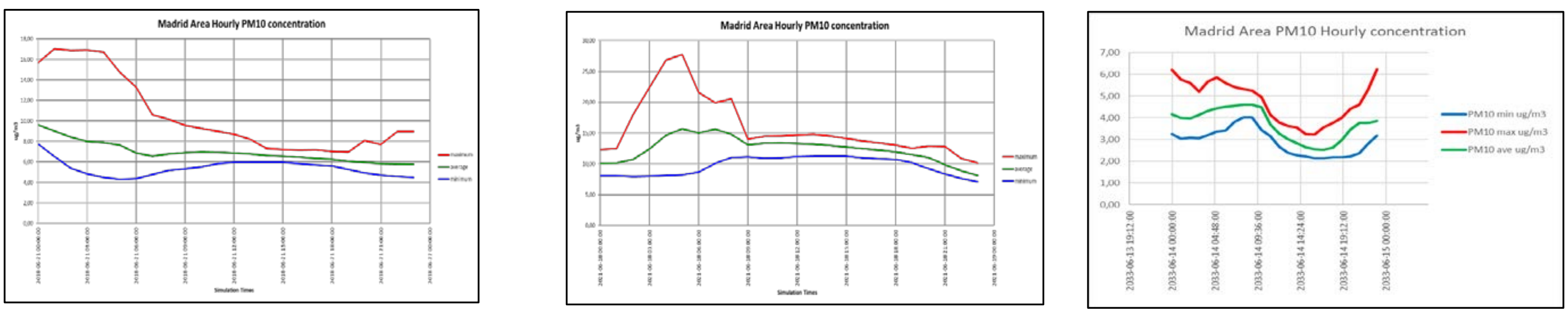


*Figure 4.8.27: $PM_{10}$ Hourly concentrations*

PM2.5 Concentrations (Cluster 7)

In Figure 4.8.28, the results are presented in terms of concentrations average, daily maximum and hourly maximum.
The daily maximum concentrations are below the WHO yearly limit of 10μg/m$^3$ in two days and below the WHO daily limit of 25μg/m$^3$ in all days.

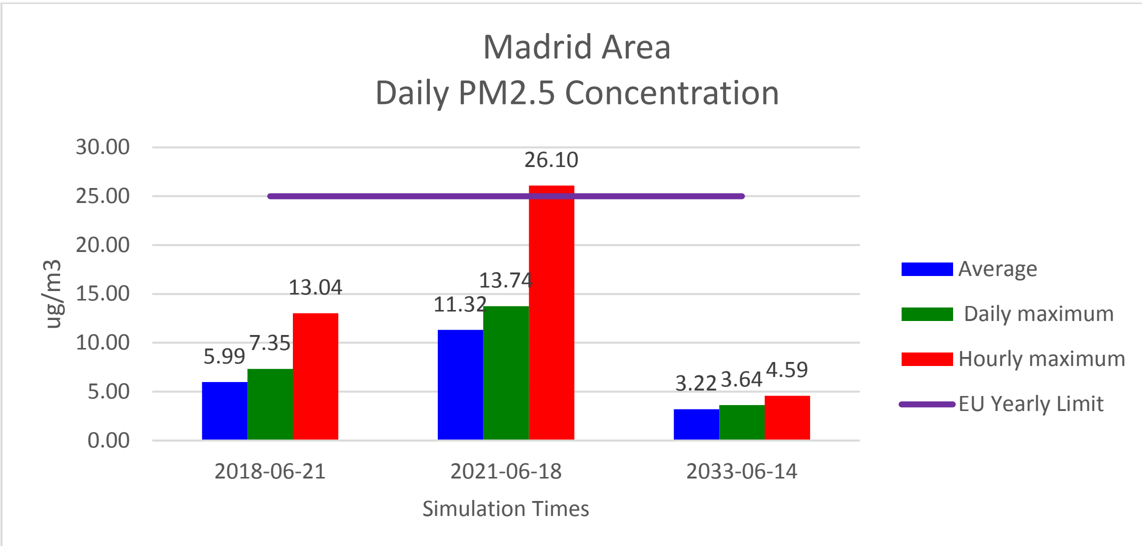


*Figure 4.8.28: PM2.5 Day concentrations*

Figure 4.8.29 presents the estimated BaP daily concentrations contained in PM2.5. All days are above WHO annual limit of 0.12ng/m$^3$ however the average values are below the EU annual limit of 1ng/m$^3$.

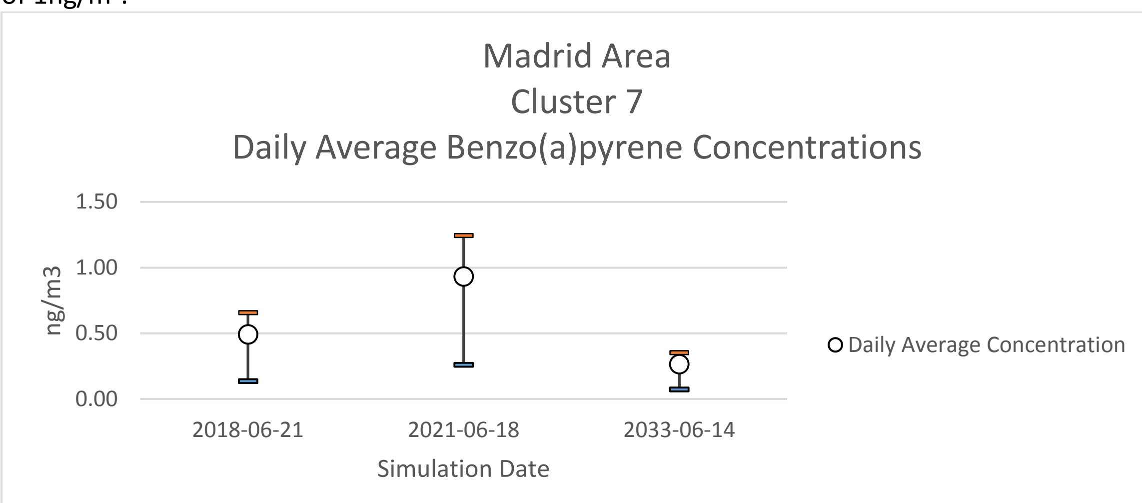


*Figure 4.8.29: BaP daily concentrations*

### 4.8.3.3 The Emission Inventory effect

Figures 4.8.30, 4.8.31, 4.8.32 and 4.8.33 illustrate the emission inventory temporal change effect on $NO_2$, $O_3$, $PM_{10}$ and $PM_{2.5}$ concentration levels respectively. There is a decreasing trend in $NO_2$ and $PM_{10}$ concentrations. $O_3$ and $PM_{2.5}$ concentrations seem to be stable; a quality check of the emission inventory could clarify more the outcome.

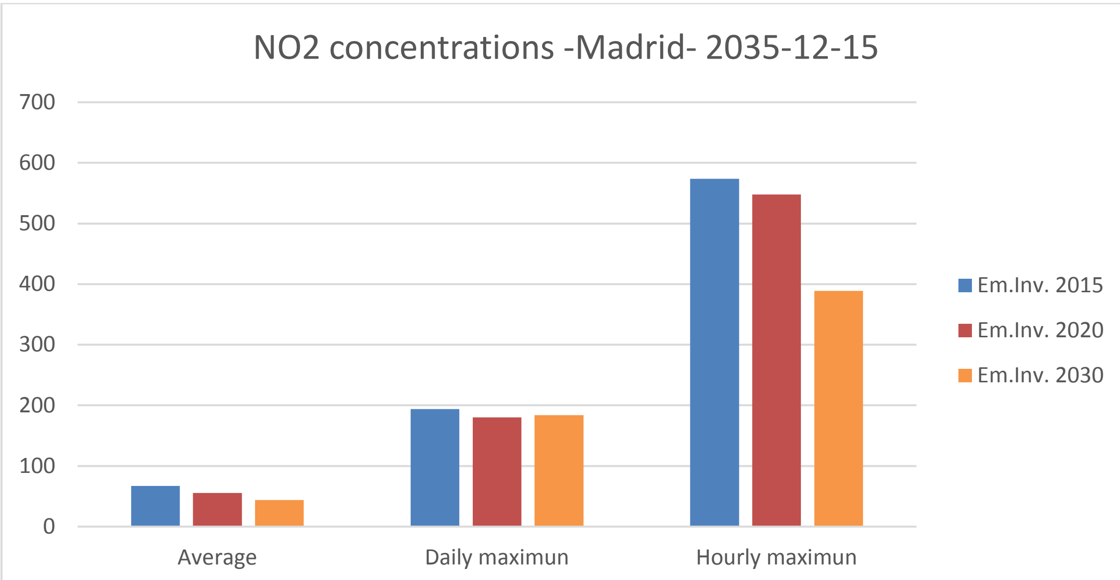


*Figure 4.8.30: $NO_2$ emission inventory comparison*

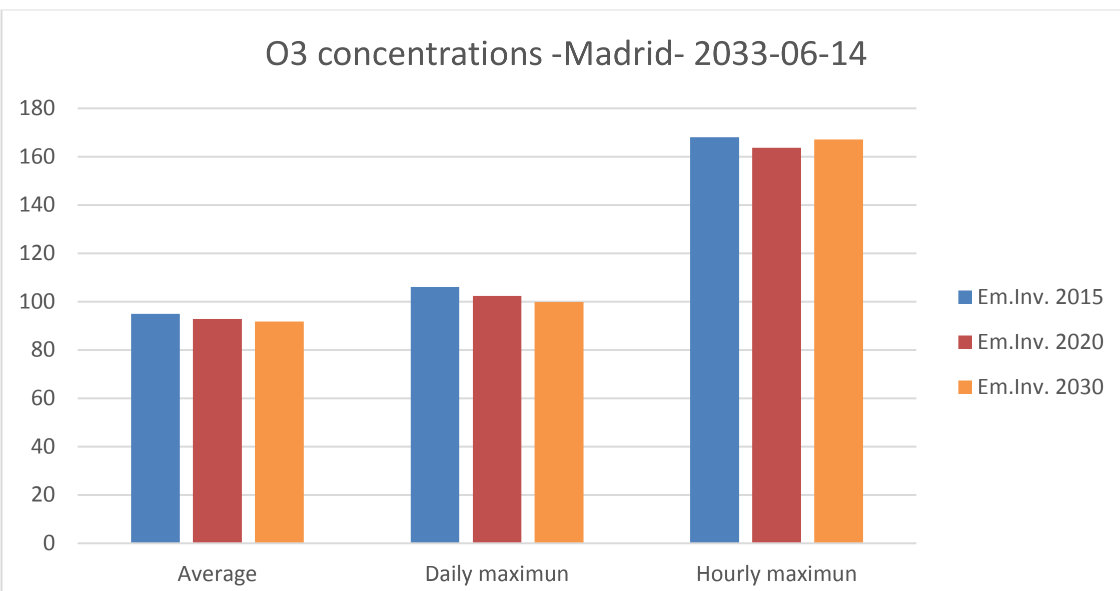


*Figure 4.8.31: $O_3$ emission inventory comparison*

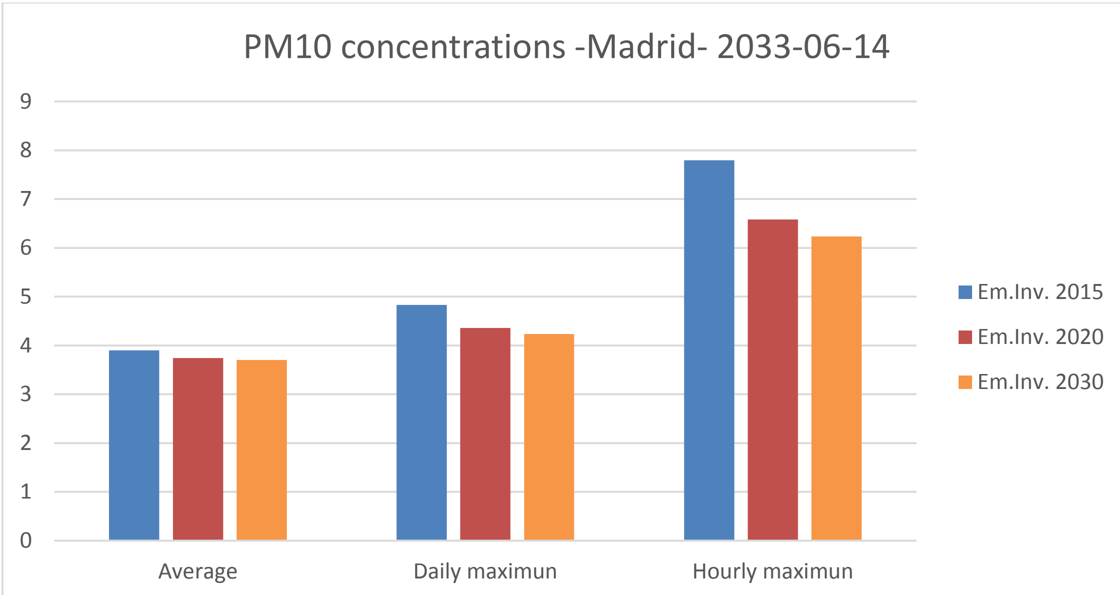


*Figure 4.8.32: $PM_{10}$ emission inventory comparison*

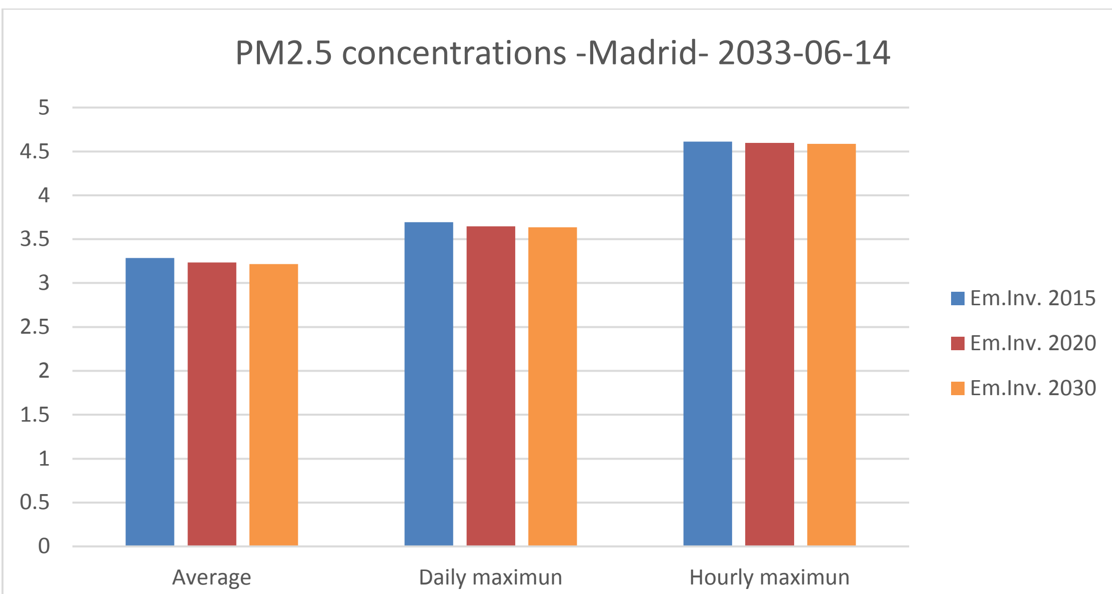


*Figure 4.8.33: $PM_{2.5}$ emission inventory comparison*

### 4.8.4 The GHGs Modeling result

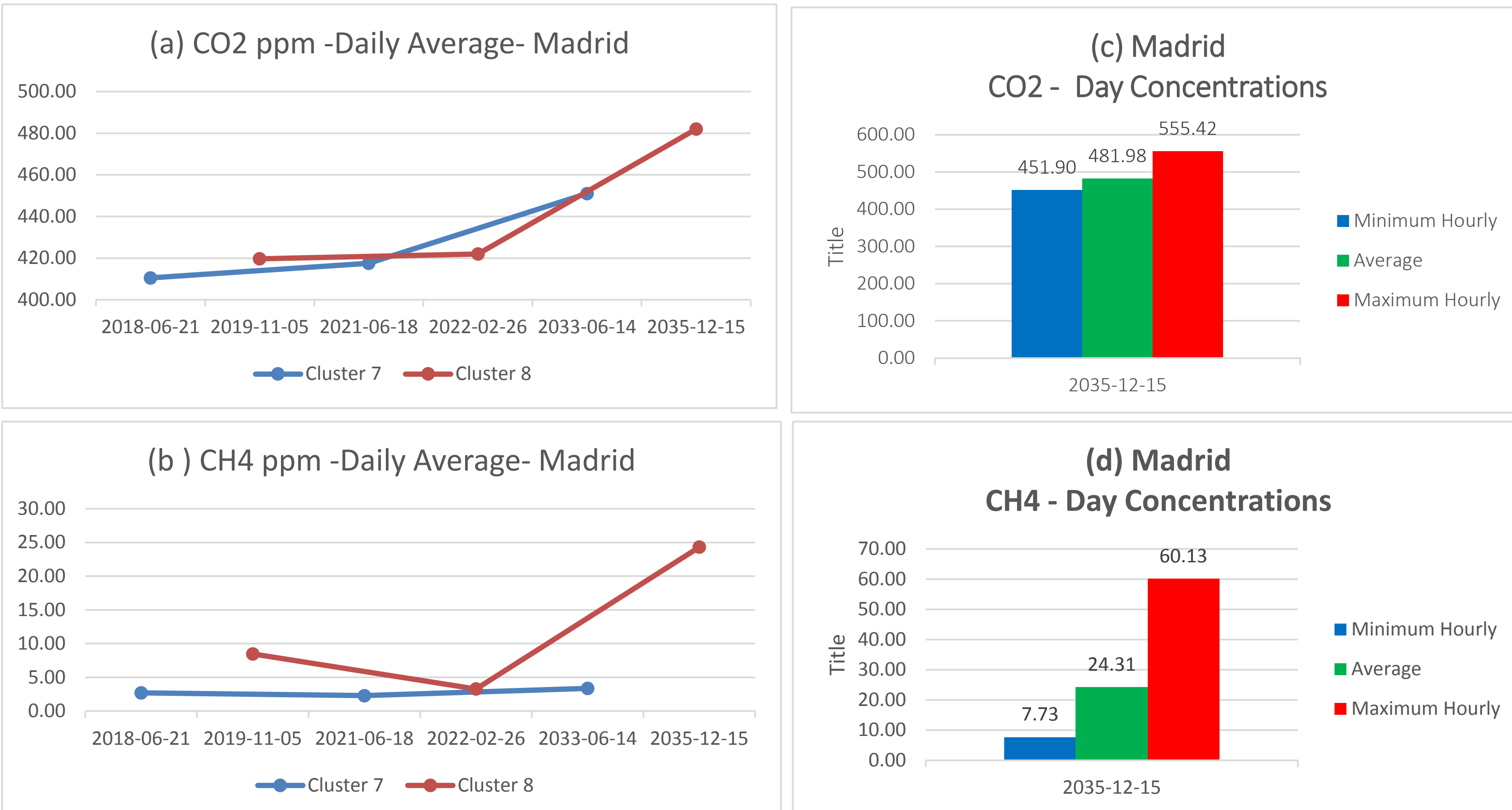


*Figure 4.8.34: (a),(b) $CO_2$ and $CH_4$ Daily average concentrations . (c),(d) $CO_2$ and $CH_4$ concentrations of the most polluted day*

### 4.8.5 Conclusions

For Madrid greater area, clusters 1,2,8 and 5 could be categorized in cold period and on the other hand clusters 4,7 and 9 in warm period.

In clusters 1,8 and 9 there is a linear increase in frequency occurrence through the ten 5-year periods. On the other hand, clusters 3,4,5 and 10 show a linear decrease in frequency occurrence.

The 5-year period 2046-2050 shows the highest number of heat waves. The most heat waves were associated with clusters 7 and 9 which correspond to clusters with days belong to warm period.

Cluster 8 is characterized with elevated $NO_2$ and cluster 7 with elevated $O_3$ and PM concentrations.

$NO_2$ daily maximum concentrations exceed the EU and WHO yearly limit of 40μg/$m^3$.

$O_3$ daily average concentrations show an increasing trend with maximum values very close to the WHO 8hr limit of 100μg/$m^3$. The maximum hourly concentrations exceed this limit.

$PM_{10}$ daily maximum concentrations show maximum values below the WHO yearly limit of 20μg/$m^3$.

$PM_{2.5}$ daily maximum concentrations are below the WHO yearly limit of 10μg/$m^3$ in two days and below the WHO daily limit of 25μg/$m^3$ in all days.

For BaP concentrations, all days are above WHO annual limit of 0.12ng/$m^3$ however the average values are below the EU annual limit of 1ng/$m^3$.

Regarding the emission reductions intervention effect, there is a decreasing trend in $NO_2$ and $PM_{10}$ concentrations. $O_3$ and $PM_{2.5}$ concentrations seem to be stable; a quality check of the emission inventory could clarify more the outcome.

## 4.9 Copenhagen – Roskilde

### 4.9.1 PCA results

The PCA analysis applied to the Copenhagen - Roskilde data has led to the following results.

Three (3) principal components have been identified as factors for the cluster analysis (Table 4.9.1). Principal Components (PC) explaining 66.66% of the total variance in the initial data.

Factor 1 explains 32.91% of the total variance and contains the 2 temperature variables, mean, daily temperature range, the down ward short-wave radiation and a negative sign of RH.

Factor 2 explains 19.34% of the total variance and contains the atmospheric boundary layer thickness and the U wind component.

Factor 3 explains 14.41% of the total variance and contains precipitation, V wind component and a negative sign of surface pressure.

*Table 4.9.1: The Principal Components results*

| | Component | | |
|---|---|---|---|
| | 1 | 2 | 3 |
| Downward short-wave surface radiation | .872 | | |
| Temperature | .841 | | |
| Temperature Range | .778 | | |
| RH | -.571 | | |
| Atmospheric boundary layer thickness | | .920 | |
| U wind | | .668 | |
| Precipitation | | | .776 |
| V wind | | | .665 |
| Surface pressure | | | -.574 |

### 4.9.2 Clustering results

<u>**Cluster description and trends**</u>

As explained in 3.4.4 the selected clusters of the Copenhagen -Roskilde are 8. In Figure 4.9.1 are shown the number of days per cluster, where clusters 4 and 7 have the most days and cluster 2 and 8 have the less. The monthly distribution per cluster is presented in Table 4.9.2 and in Figure 4.9.2. By dividing the year in two periods, cold and warm, clusters 1,3,5 and 7 could be categorized in cold period and on the other hand clusters 4 and 6 in warm period.


*Figure 4.9.1: Number of Days per cluster*

*Table 4.9.2: Monthly distribution per cluster*

| | | Month | | | | | | | | | | | | Total |
|---|---|---|---|---|---|---|---|---|---|---|---|---|---|---|
| | | Jan | Feb | Mar | Apr | May | Jun | Jul | Aug | Sep | Oct | Nov | Dec | |
| Cluster | 1 | 256 | 269 | 369 | 232 | 46 | 7 | 0 | 4 | 95 | 330 | 240 | 230 | 2078 |
| | 2 | 97 | 61 | 79 | 76 | 99 | 106 | 79 | 134 | 144 | 162 | 139 | 155 | 1331 |
| | 3 | 415 | 417 | 486 | 188 | 39 | 5 | 1 | 1 | 47 | 165 | 239 | 294 | 2297 |
| | 4 | 0 | 0 | 29 | 203 | 598 | 898 | 983 | 815 | 321 | 52 | 0 | 1 | 3900 |
| | 5 | 261 | 175 | 141 | 134 | 78 | 35 | 25 | 52 | 202 | 358 | 384 | 361 | 2206 |
| | 6 | 0 | 4 | 21 | 217 | 394 | 340 | 416 | 411 | 374 | 66 | 2 | 1 | 2246 |
| | 7 | 455 | 417 | 333 | 279 | 198 | 63 | 15 | 41 | 117 | 253 | 379 | 443 | 2993 |
| | 8 | 66 | 69 | 92 | 171 | 98 | 46 | 31 | 92 | 200 | 164 | 117 | 65 | 1211 |
| Total | | 1550 | 1412 | 1550 | 1500 | 1550 | 1500 | 1550 | 1550 | 1500 | 1550 | 1500 | 1550 | 18262 |

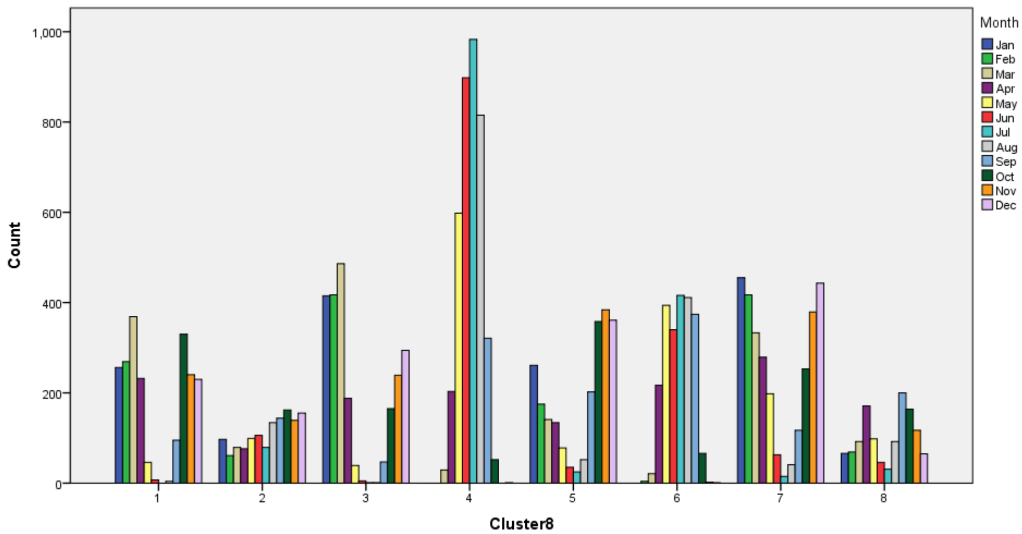


*Figure 4.9.2: Visualized bar chart of monthly distribution per cluster*

A trend analysis of the 5-year frequency of each cluster (Figure 4.9.3). There is an evidence that in clusters 2 and 5 there is a linear increase in frequency occurrence through the ten 5-year periods. On the other hand, clusters 3 and 8 show a linear decrease in frequency occurrence. In the rest clusters no clear trends could be pointed out.

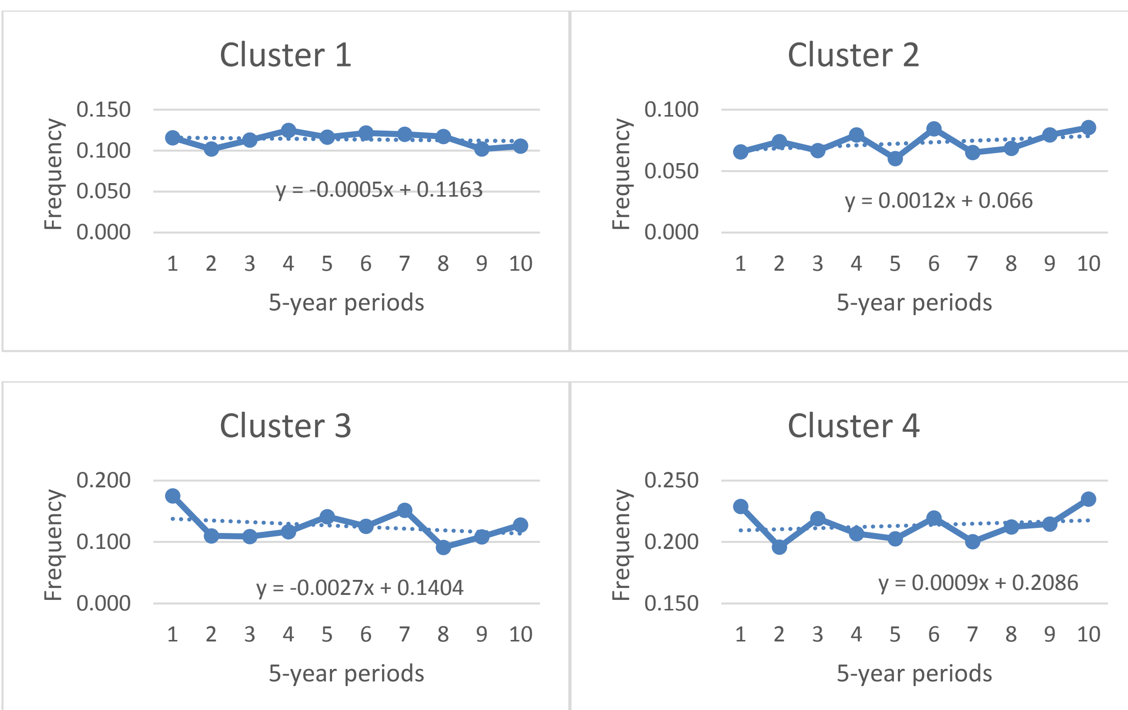


*Figure 4.9.3: Cluster 1-8 frequency trends*

## Cluster characterization

The clusters' implementation is based on the mean values of weather parameters which are displayed in Table 4.9.3.

*Table 4.9.3: Summary of the 8 clusters*

| | Cluster | | | | | | | |
|---|---|---|---|---|---|---|---|---|
| | 1 | 2 | 3 | 4 | 5 | 6 | 7 | 8 |
| | Mean (SD) | Mean (SD) | Mean (SD) | Mean (SD) | Mean (SD) | Mean (SD) | Mean (SD) | Mean (SD) |
| Temperature ( °C) | 2,76 (4,97) | 10 (5,94) | 1,39 (4,84) | 16,61 (4,77) | 7,62 (3,84) | 13,63 (5,07) | 5,08 (4,73) | 7,98 (5,13) |
| Daily Temperature Range ( °C) | 3,09 (1,32) | 3,77 (1,53) | 3,14 (1,46) | 6,06 (1,34) | 2,64 (1,16) | 5,14 (1,17) | 2,81 (1,3) | 3,33 (1,2) |
| Relative Humidity (%) | 79,8 (6,82) | 88,04 (4,71) | 89,27 (5,66) | 80,5 (6,24) | 82,71 (4,45) | 74,64 (5,75) | 90,31 (4,58) | 71,35 (6,14) |
| Surface Pressure (Pa) | 100950,01 (1127,47) | 99490,95 (1005,75) | 101676,79 (1178,65) | 101317,21 (798,04) | 99464,8 (996,22) | 101078,5 (812,9) | 100086,54 (1062,76) | 100271,08 (941,21) |
| Precipitation (kg/m2/s) | 0,000008 (0,000012) | 0,000137 (0,000082) | 0,000008 (0,000012) | 0,00001 (0,000021) | 0,000042 (0,000033) | 0,000008 (0,000015) | 0,000038 (0,000033) | 0,000012 (0,000016) |
| Downward Short Wave Radiation | 91,67 (64,54) | 87,12 (83,29) | 69,24 (53,26) | 274,2 (63,23) | 67,84 (64,85) | 255,17 (70,88) | 58,58 (54,69) | 158,39 (93,7) |
| u wind component (m/s) | 1,62 (4,94) | 0,18 (4,4) | -1,24 (4,09) | -1,94 (3,07) | 6,71 (3,2) | 1,49 (4,06) | -0,04 (4,39) | 7,01 (3,84) |
| v wind component (m/s) | -2,9 (3,62) | 4,33 (3,79) | -0,84 (3,12) | 0,73 (2,5) | 3,38 (3,38) | -1,43 (3,07) | 2,62 (3,35) | -3,41 (3,44) |

| | | | | | | | | |
|---|---|---|---|---|---|---|---|---|
| V wind (m/s) | 6,49 (2,53) | 6,67 (2,82) | 4,79 (2,4) | 3,9 (2,17) | 8,51 (2,4) | 5,12 (1,99) | 5,54 (2,6) | 8,98 (2,59) |
| Atmospheric Boundary Layer Thickness (m) | 553,22 (126,07) | 477,89 (154,14) | 329,51 (109,38) | 288,51 (97,05) | 707,62 (133,2) | 548,32 (142,54) | 392,39 (119,96) | 915,9 (162,24) |

In addition to the previous Table 4.9.3, Figure 4.9.4 presents the mean normalized (z-score) variables of each cluster, respectively showing the differences of the parameters per cluster.

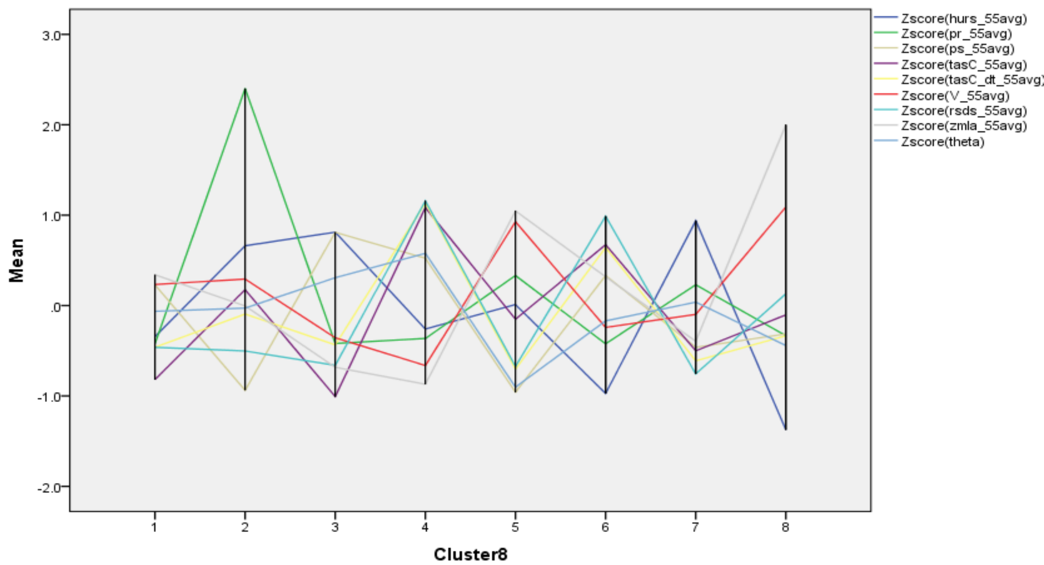


*Figure 4.9.4: Normalized variables (z-score) averaged for each cluster*

Daily, 10-meter from ground level, wind data were used to create the wind roses per each cluster as they are shown in Figures 4.9.5-4.9.12. Each wind direction distribution per cluster is presented in more details in Table 4.9.4.

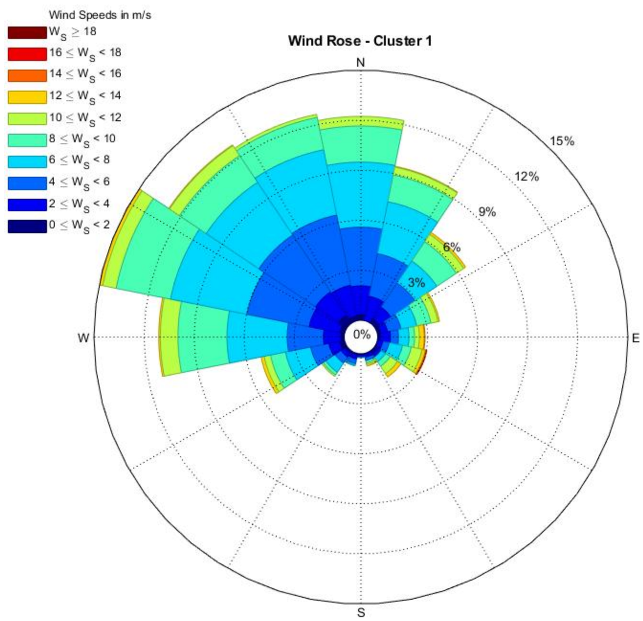


*Figure 4.9.5: Wind Rose - Cluster 1*

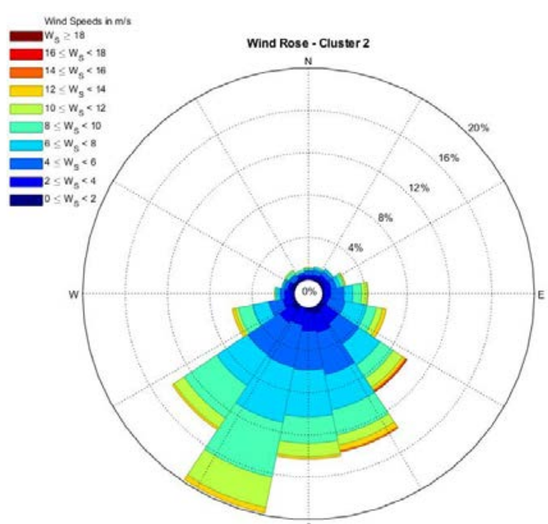


*Figure 4.9.6: Wind Rose - Cluster 2*

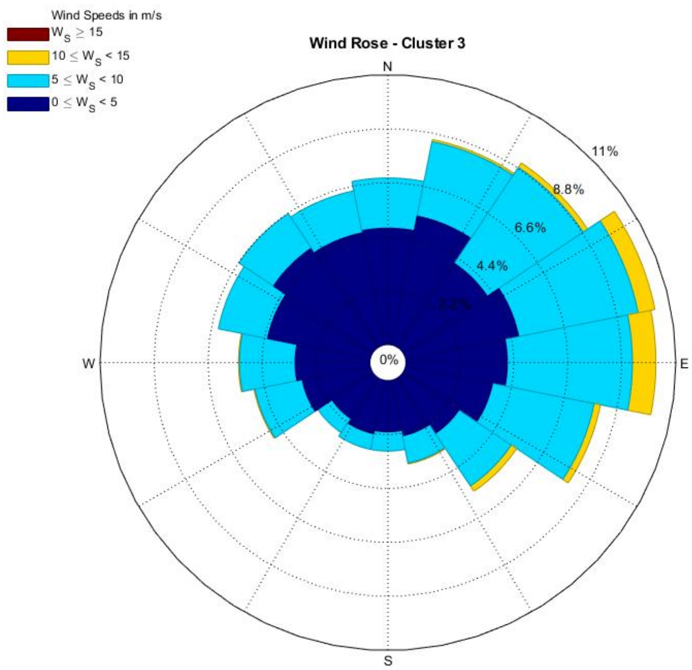


*Figure 4.9.7: Wind Rose - Cluster 3*

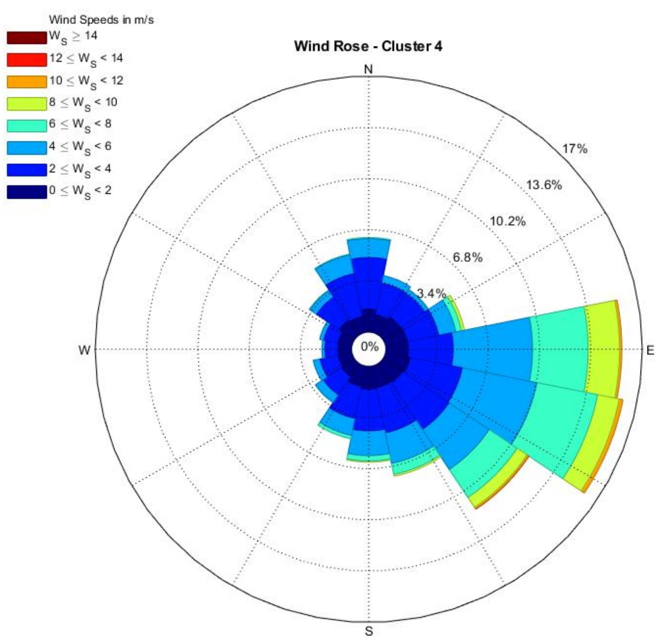


*Figure 4.9.8: Wind Rose - Cluster 4*

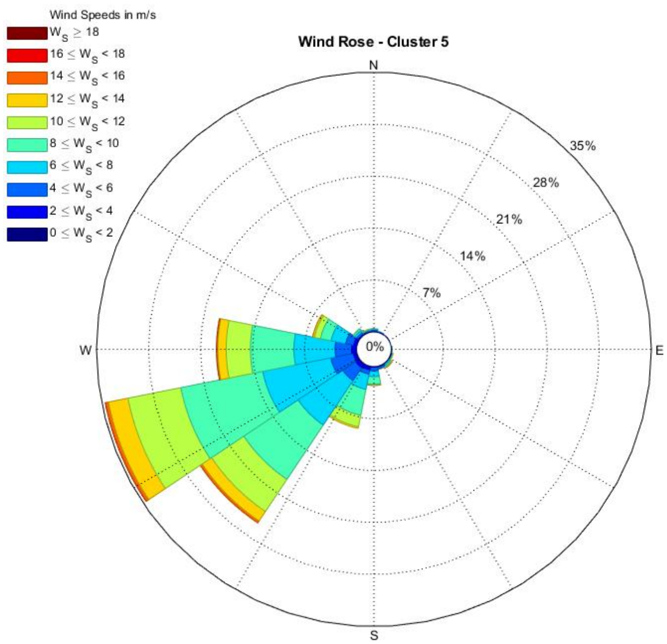


*Figure 4.9.9: Wind Rose - Cluster 5*

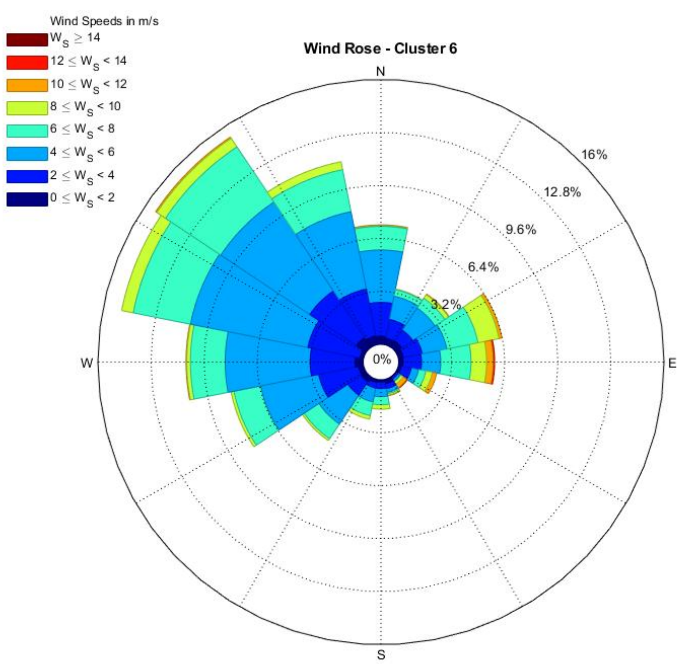


*Figure 4.9.10: Wind Rose - Cluster 6*

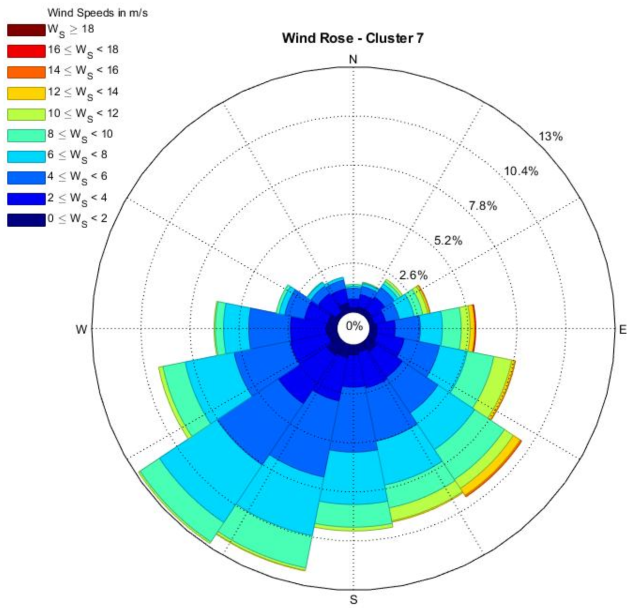


*Figure 4.9.11: Wind Rose - Cluster 7*

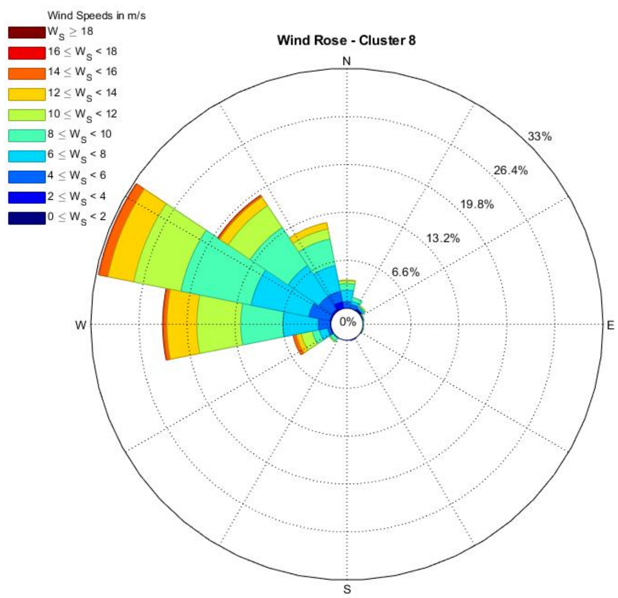


*Figure 4.9.12: Wind Rose - Cluster 8*

*Table 4.9.4: 16 Wind Direction distribution per cluster*

| | | | Wind16 | | | | | | | | | | | | | | | | Total |
|---|---|---|---|---|---|---|---|---|---|---|---|---|---|---|---|---|---|---|---|
| | | | S | SSW | SW | WSW | W | WNW | NW | NNW | N | NNE | NE | ENE | E | ESE | SE | SSE | |
| Cluster8 | 1 | Count | 5 | 16 | 38 | 106 | 231 | 311 | 267 | 262 | 254 | 196 | 136 | 79 | 59 | 63 | 39 | 16 | 2078 |
| | | % within Cluster8 | 0.2% | 0.8% | 1.8% | 5.1% | 11.1% | 15.0% | 12.8% | 12.6% | 12.2% | 9.4% | 6.5% | 3.8% | 2.8% | 3.0% | 1.9% | 0.8% | 100.0% |
| | 2 | Count | 190 | 263 | 188 | 80 | 25 | 17 | 18 | 13 | 15 | 17 | 20 | 30 | 57 | 82 | 131 | 185 | 1331 |
| | | % within Cluster8 | 14.3% | 19.8% | 14.1% | 6.0% | 1.9% | 1.3% | 1.4% | 1.0% | 1.1% | 1.3% | 1.5% | 2.3% | 4.3% | 6.2% | 9.8% | 13.9% | 100.0% |
| | 3 | Count | 66 | 66 | 62 | 111 | 123 | 145 | 151 | 147 | 156 | 196 | 208 | 238 | 234 | 186 | 128 | 80 | 2297 |
| | | % within Cluster8 | 2.9% | 2.9% | 2.7% | 4.8% | 5.4% | 6.3% | 6.6% | 6.4% | 6.8% | 8.5% | 9.1% | 10.4% | 10.2% | 8.1% | 5.6% | 3.5% | 100.0% |
| | 4 | Count | 248 | 192 | 122 | 102 | 77 | 85 | 141 | 207 | 245 | 150 | 142 | 208 | 610 | 626 | 454 | 291 | 3900 |
| | | % within Cluster8 | 6.4% | 4.9% | 3.1% | 2.6% | 2.0% | 2.2% | 3.6% | 5.3% | 6.3% | 3.8% | 3.6% | 5.3% | 15.6% | 16.1% | 11.6% | 7.5% | 100.0% |
| | 5 | Count | 56 | 188 | 569 | 762 | 416 | 134 | 23 | 10 | 10 | 3 | 1 | 0 | 3 | 7 | 14 | 10 | 2206 |
| | | % within Cluster8 | 2.5% | 8.5% | 25.8% | 34.5% | 18.9% | 6.1% | 1.0% | 0.5% | 0.5% | 0.1% | 0.0% | 0.0% | 0.1% | 0.3% | 0.6% | 0.5% | 100.0% |
| | 6 | Count | 40 | 55 | 104 | 183 | 240 | 334 | 343 | 253 | 162 | 77 | 87 | 143 | 130 | 53 | 19 | 23 | 2246 |
| | | % within Cluster8 | 1.8% | 2.4% | 4.6% | 8.1% | 10.7% | 14.9% | 15.3% | 11.3% | 7.2% | 3.4% | 3.9% | 6.4% | 5.8% | 2.4% | 0.8% | 1.0% | 100.0% |
| | 7 | Count | 295 | 366 | 384 | 289 | 195 | 99 | 63 | 57 | 44 | 49 | 68 | 98 | 168 | 236 | 295 | 287 | 2993 |
| | | % within Cluster8 | 9.9% | 12.2% | 12.8% | 9.7% | 6.5% | 3.3% | 2.1% | 1.9% | 1.5% | 1.6% | 2.3% | 3.3% | 5.6% | 7.9% | 9.9% | 9.6% | 100.0% |
| | 8 | Count | 0 | 0 | 9 | 65 | 280 | 395 | 232 | 146 | 47 | 19 | 11 | 3 | 1 | 2 | 0 | 1 | 1211 |
| | | % within Cluster8 | 0.0% | 0.0% | 0.7% | 5.4% | 23.1% | 32.6% | 19.2% | 12.1% | 3.9% | 1.6% | 0.9% | 0.2% | 0.1% | 0.2% | 0.0% | 0.1% | 100.0% |
| Total | | Count | 900 | 1146 | 1476 | 1698 | 1587 | 1520 | 1238 | 1095 | 933 | 707 | 673 | 799 | 1262 | 1255 | 1080 | 893 | 18262 |
| | | % within Cluster8 | 4.9% | 6.3% | 8.1% | 9.3% | 8.7% | 8.3% | 6.8% | 6.0% | 5.1% | 3.9% | 3.7% | 4.4% | 6.9% | 6.9% | 5.9% | 4.9% | 100.0% |

## Clusters and local Heat Waves

In Figures 4.9.13 and 4.9.14 are presented the heat waves occurrence per 5-year period and per cluster. The most heat waves seem to occur after 2021 and are spread through 2050. The 5-year period 2041-2045 shows the highest number of heat waves, while the next 5-year period shows a decrease. The most heat waves were associated with cluster 4 which correspond to clusters with days belong to warm period (see Table 4.9.2).

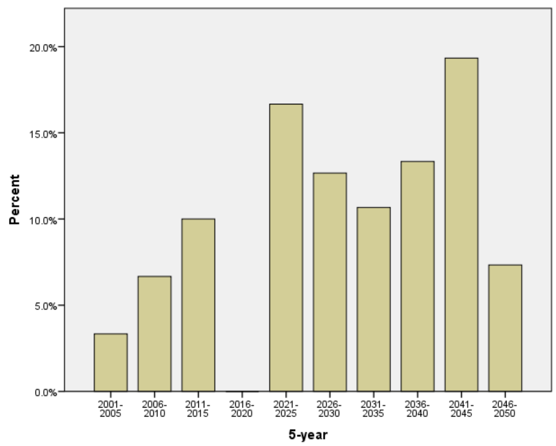


*Figure 4.9.13: Heat Waves per 5-year period*

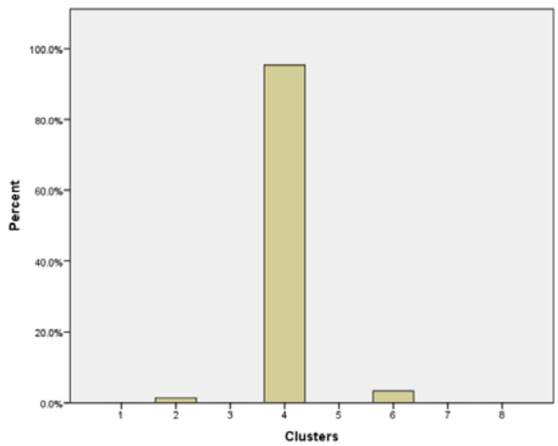


*Figure 4.9.14: Heat Waves per cluster*

## Clusters versus Air Quality level

As it can be seen in Table 4.1 three observation stations have been used for the present analysis. The descriptive statistics for $NO_2$, $O_3$ and $PM_{10}$ is given in Table 4.9.5.

*Table 4.9.5: Air pollutants descriptive statistics*

| | | NO2 | O3 | PM10 |
|---|---|---|---|---|
| Mean | | 38.9441 | 39.5671 | 29.6071 |
| Std. Deviation | | 13.41391 | 16.96380 | 13.15144 |
| Minimum | | 6.88 | 1.21 | 3.51 |
| Maximum | | 112.33 | 103.63 | 216.00 |
| Percentiles | 5 | 18.4611 | 11.6394 | 14.3003 |
| | 25 | 29.3075 | 26.9553 | 20.8500 |
| | 50 | 38.0780 | 39.6980 | 27.2590 |
| | 75 | 47.4075 | 51.6553 | 35.3120 |
| | 95 | 62.5037 | 67.1509 | 54.1510 |

Table 4.9.6 presents the pollutants' concentrations per cluster. Higher mean $NO_2$ concentrations are observed in clusters 1 and 7. Higher mean $O_3$ concentrations are observed in clusters 4 and 6. Higher mean $PM_{10}$ concentrations are observed in clusters 1,3 and 7.

*Table 4.9.6: Summary pollutant concentrations per cluster*

| | Cluster | | | | | | | |
|---|---|---|---|---|---|---|---|---|
| | 1 | 2 | 3 | 4 | 5 | 6 | 7 | 8 |
| | Mean (SD) | Mean (SD) | Mean (SD) | Mean (SD) | Mean (SD) | Mean (SD) | Mean (SD) | Mean (SD) |
| PM10 (µg/m3) | 31,91 (15,16) | 28,04 (12,36) | 31,94 (14,56) | 27,95 (9,61) | 28,38 (13,31) | 28,33 (11,79) | 31,73 (15,19) | 27,35 (12,27) |
| O3 (µg/m3) | 34,75 (16,47) | 37,86 (18,18) | 34,97 (16,86) | 48,78 (13,26) | 32,84 (15,85) | 46,52 (14,31) | 35 (17,59) | 39,19 (15,21) |
| NO2 (µg/m3) | 41,03 (14) | 38,31 (13,3) | 38,61 (12,9) | 37,84 (13,38) | 38,51 (12,82) | 38,12 (14,24) | 40,47 (13,18) | 38,85 (13,18) |

The differences in concentrations per cluster are shown in Figures 4.9.15-4.2.17.

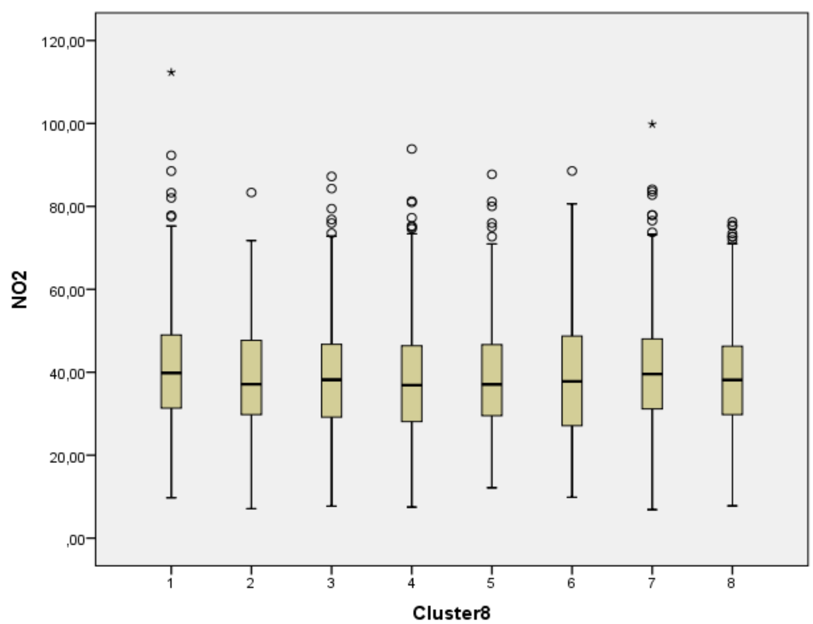


*Figure 4.9.15: $NO_2$ concentration statistics per cluster*

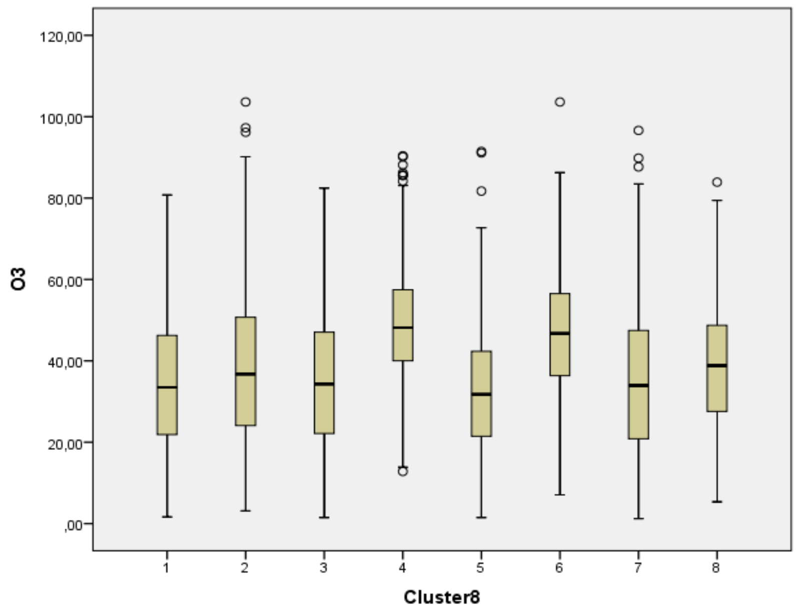


*Figure 4.9.16: $O_3$ concentration statistics per cluster*

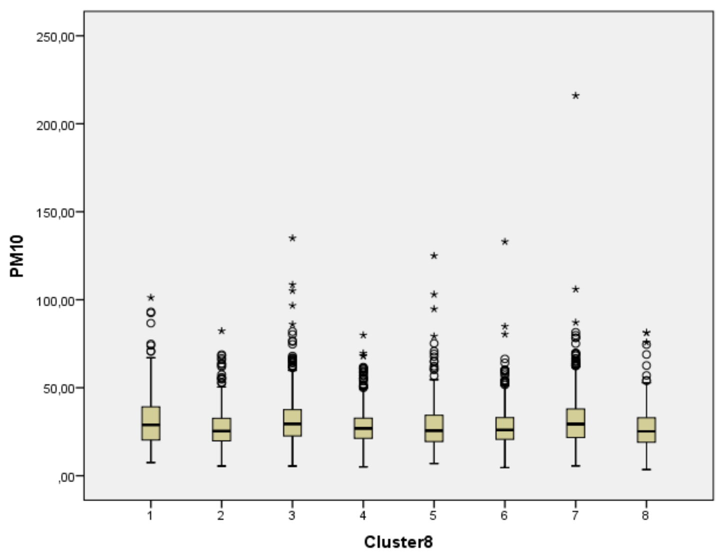


*Figure 4.9.17: $PM_{10}$ concentration statistics per cluster*

## Representative Days

In the following Table 4.9.7 are presented the selected RDs per 5-year period and per cluster.

*Table 4.9.7: Representative days per cluster and 5year period*

| Closest days to centroids per 5year per cluster | | | clusters | | | | | | | |
|---|---|---|---|---|---|---|---|---|---|---|
| | | | 1 | 2 | 3 | 4 | 5 | 6 | 7 | 8 |
| 5 year period | 2001-2005 | 1 | 2002/04/11 | 2003/10/19 | 2005/03/25 | 2004/06/03 | 2004/12/01 | 2004/06/13 | 2005/04/27 | 2001/04/21 |
| | 2006-2010 | 2 | 2006/11/08 | 2010/11/18 | 2009/03/12 | 2006/05/29 | 2010/04/10 | 2010/06/11 | 2006/04/21 | 2007/09/25 |
| | 2011-2015 | 3 | 2015/03/15 | 2011/05/06 | 2014/10/31 | 2015/07/07 | 2011/10/04 | 2013/06/17 | 2013/01/15 | 2014/04/18 |
| | 2016-2020 | 4 | 2018/02/21 | 2016/01/09 | 2017/03/01 | 2017/08/07 | 2018/11/20 | 2018/08/24 | 2020/02/17 | 2018/09/30 |
| | 2021-2025 | 5 | 2022/03/28 | 2023/09/30 | 2025/02/09 | 2024/07/17 | 2023/02/25 | 2023/08/30 | 2022/11/20 | 2023/05/11 |
| | 2026-2030 | 6 | 2028/02/22 | 2030/10/22 | 2028/12/05 | 2030/06/02 | 2029/12/04 | 2027/07/30 | 2026/11/21 | 2027/04/22 |
| | 2031-2035 | 7 | 2031/12/08 | 2032/11/06 | 2031/01/03 | 2035/06/10 | 2032/11/02 | 2032/06/07 | 2035/03/02 | 2031/04/15 |
| | 2036-2040 | 8 | 2040/03/12 | 2040/11/11 | 2036/03/22 | 2039/06/13 | 2037/01/17 | 2036/06/11 | 2039/05/18 | 2038/04/01 |
| | 2041-2045 | 9 | 2041/03/05 | 2045/10/02 | 2041/02/18 | 2044/08/12 | 2041/11/02 | 2043/05/09 | 2045/03/02 | 2043/04/09 |
| | 2046-2050 | 10 | 2048/03/29 | 2047/05/17 | 2048/11/11 | 2050/05/22 | 2050/12/08 | 2046/08/02 | 2047/10/20 | 2048/08/01 |

## Selected Clusters and RDs for modeling purposes

Selected RDs will be used to perform targeted weather and air quality simulations within each selected 5-year period estimating hourly/daily concentrations of the priority pollutants to assess the climatic effect on air quality evolution and the characteristics of air quality future episodes. The selection was based on 3-year periods (2016-2020, 2021-2025 and 2031-2035) and on the clusters with the most elevated concentrations of $PM_{10}$, $NO_2$ and $O_3$. In the case of Copenhagen/Roskilde, cluster 1 recorded the most elevated values of $NO_2$, cluster 4 for the case of $O_3$ and cluster 3 for the case of $PM_{10}$. In Table 4.9.8 are presented the selected days which was used for modeling purposes.

*Table 4.9.8: RDs for modeling purposes*

| **Period** | **Cluster 1 (NO2)** | **Cluster 3 (PM)** | **Cluster 4 (O3)** |
|---|---|---|---|
| 2016-2020 | 2018-02-21 | 2017-03-01 | 2017-08-07 |
| 2021-2025 | 2022-03-28 | 2025-02-09 | 2024-07-17 |
| 2031-2035 | 2031-12-08 | 2031-01-03 | 2035-06-10 |

### 4.9.3 Air Quality Modeling results – Roskilde wider area

#### 4.9.3.1 Overall results

In Figure 4.9.18 the daily average concentrations of $NO_2$, $O_3$, $PM_{10}$ and $PM_{2.5}$ for selected RDs are presented.

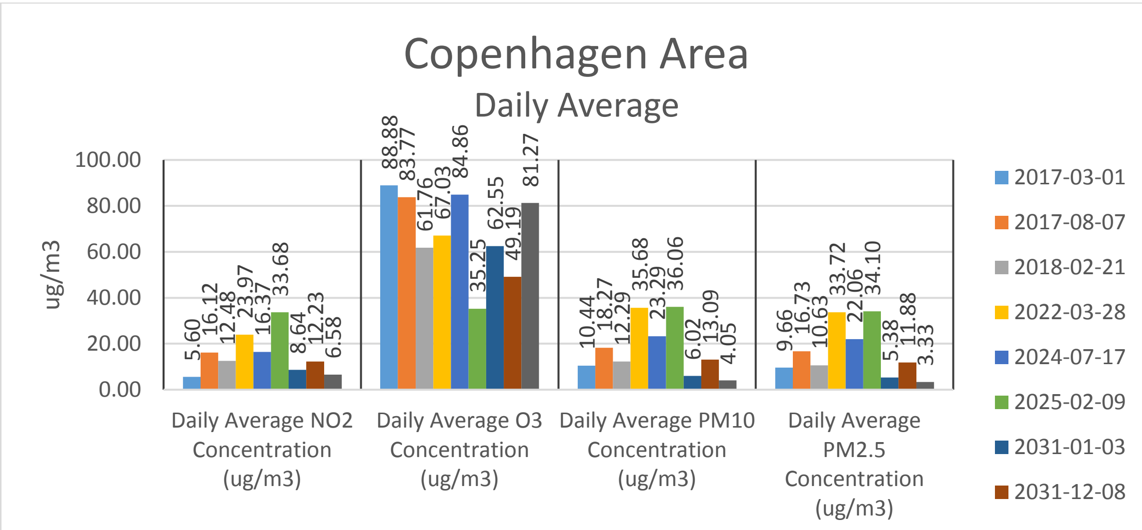


*Figure 4.9.18: Daily average concentrations*

In Figure 4.9.19 the obtained daily averaged concentrations are compared based on USTUTT and EGDAR HTAP emission inventories respectively. The results seem not to differ significantly.

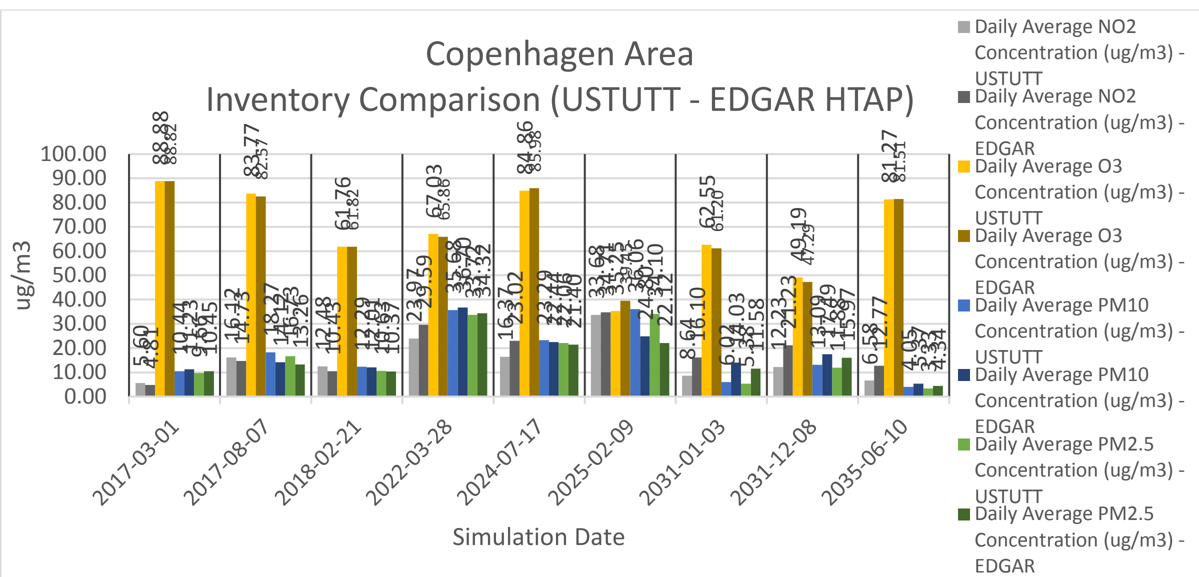


*Figure 4.9.19: Daily average concentrations – USTUTT vs EDGAR HTAP comparison*

#### 4.9.3.2 Clusters results

$NO_2$ Concentrations (Cluster 1)

In Figure 4.9.20, the results are presented in terms of concentrations average, daily maximum and hourly maximum. The diurnal variations are shown in Figure 4.9.21.

The daily maximum concentrations seem to be very close or exceed the EU and WHO yearly limit of 40μg/$m^3$.

$O_3$ Concentrations (Cluster 4)

In Figure 4.9.22, the results are presented in terms of concentrations average, daily maximum and hourly maximum. The diurnal variations are shown in Figure 4.9.23.

Both daily average and maximum concentrations are below the WHO 8hr limit of 100μg/$m^3$.

$PM_{10}$ Concentrations (Cluster 3)

In Figure 4.9.24, the results are presented in terms of concentrations average, daily maximum and hourly maximum. The diurnal variations are shown in Figure 4.9.25.

The picture is mixed. The daily maximum concentrations are below the WHO yearly limit of 20μg/$m^3$ in two days. In one day, the daily maximum value exceeds the WHO daily limit of 50μg/$m^3$.

## $NO_2$-Cluster 1

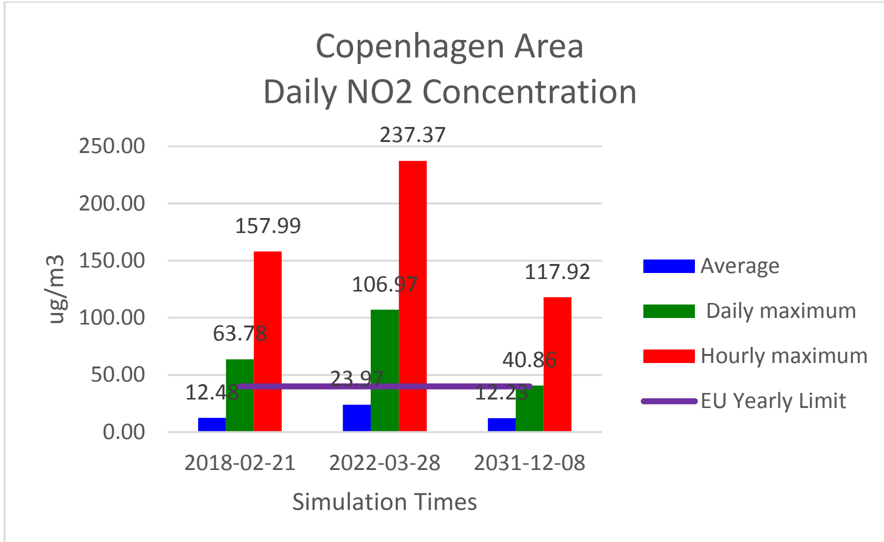


*Figure 4.9.20: $NO_2$ Day concentrations*

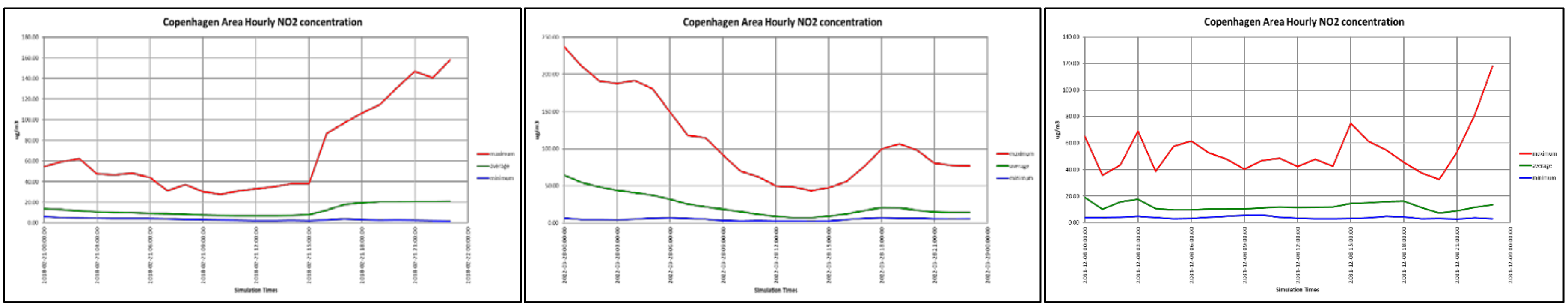


*Figure 4.9.21: Hourly $NO_2$ concentrations*

### $O_3$-Cluster 4

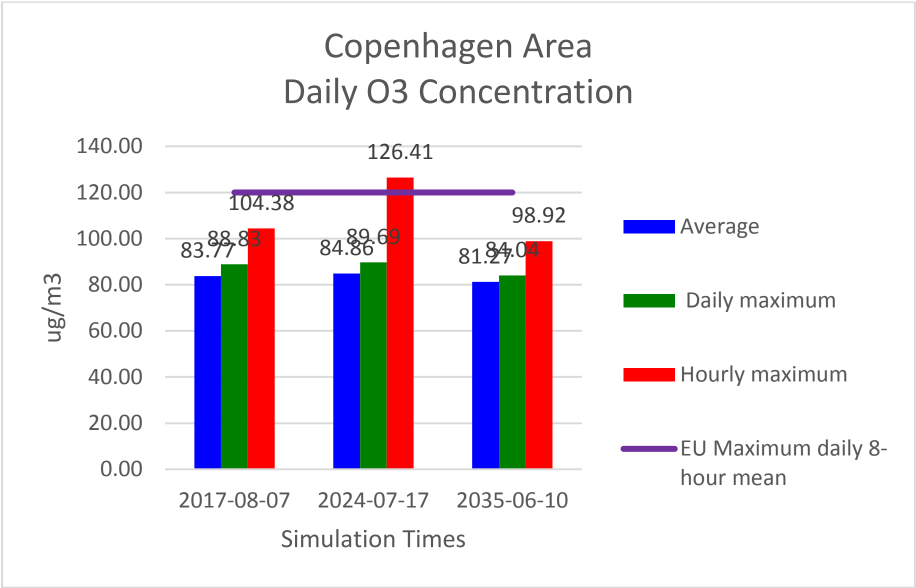


*Figure 4.9.22: $O_3$ Daily concentrations*

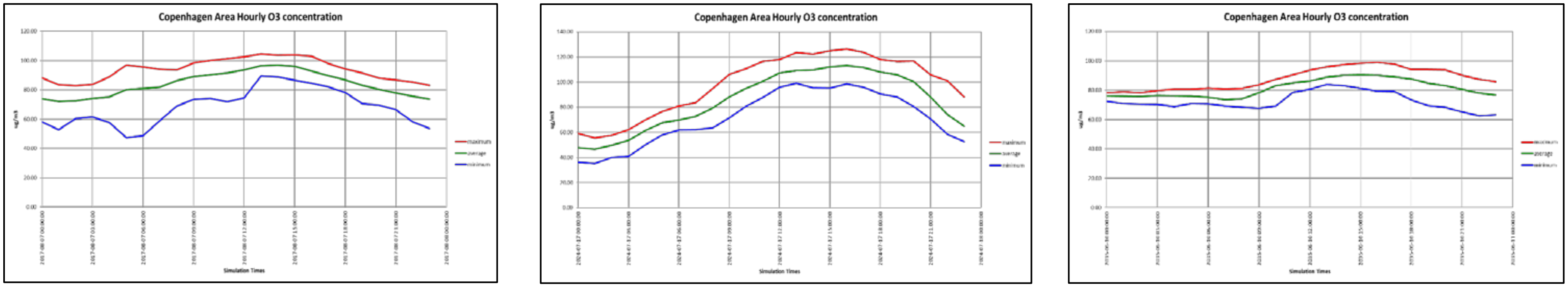


*Figure 4.9.23: $O_3$ Hourly concentrations*

## $PM_{10}$-Cluster 3

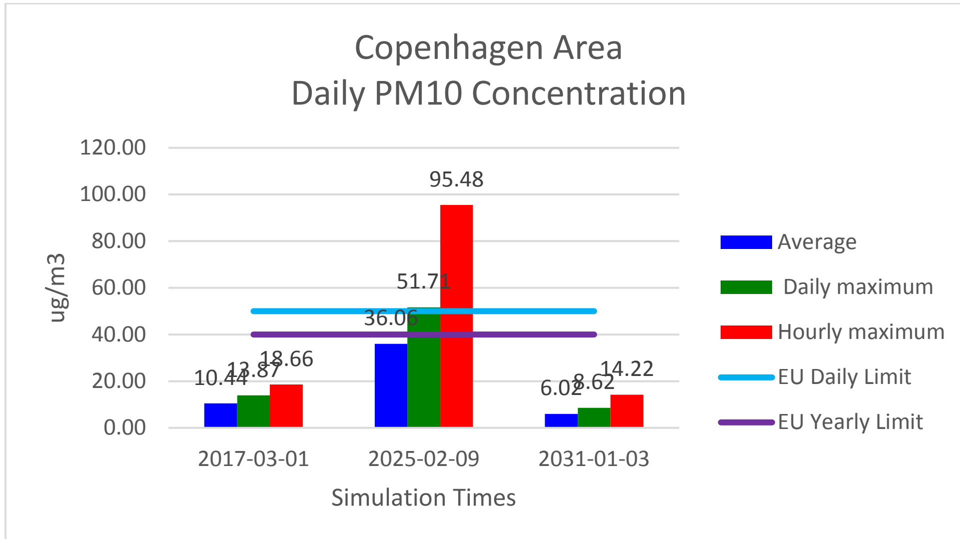


*Figure 4.9.24: $PM_{10}$ Daily concentrations*

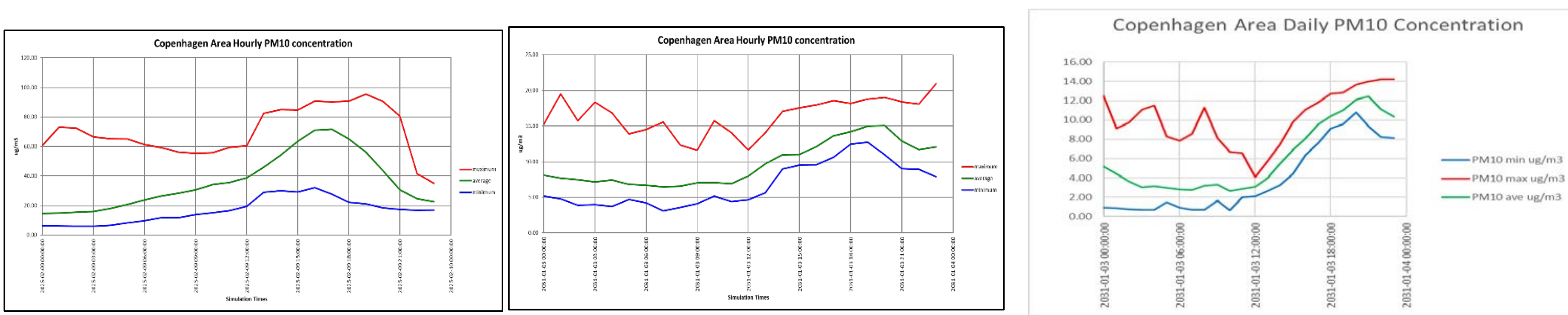


*Figure 4.9.25: $PM_{10}$ Hourly concentrations*

PM$_{2.5}$ Concentrations (Cluster 3)

In Figure 4.9.29, the results are presented in terms of concentrations average, daily maximum and hourly maximum.
The picture about the PM$_{2.5}$ concentration is mixed. The daily maximum concentration is well above the WHO yearly limit of 10μg/m$^3$ in one day and on and below it the rest days.

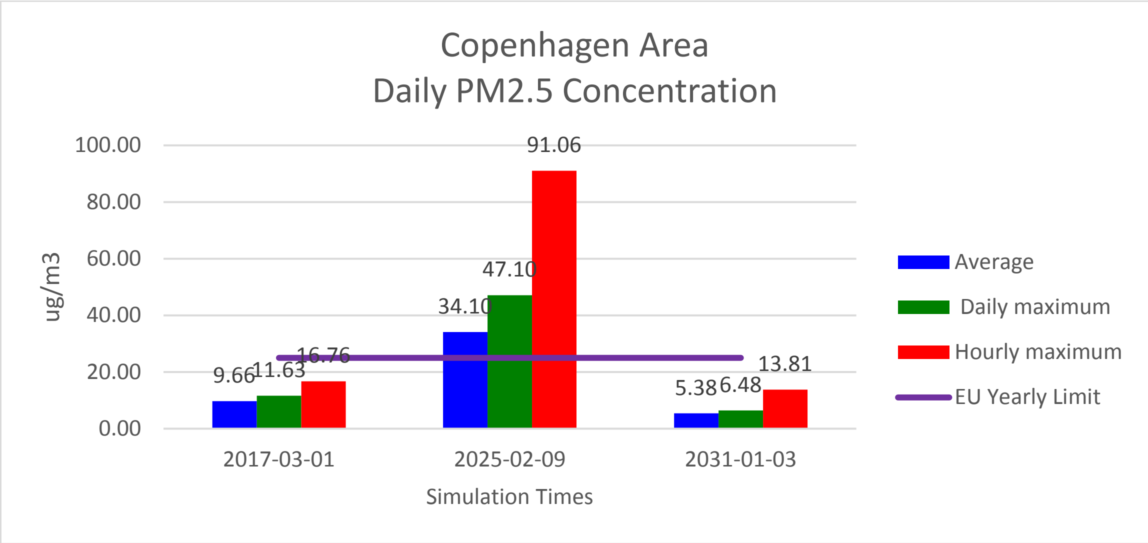


*Figure 4.9.26: PM$_{2.5}$ Day concentrations*

Figure 4.9.27 presents the estimated BaP daily concentrations contained in PM$_{2.5}$. All days are above WHO annual limit of 0.12ng/m$^3$ however two days are below the EU annual limit of 1ng/m$^3$.

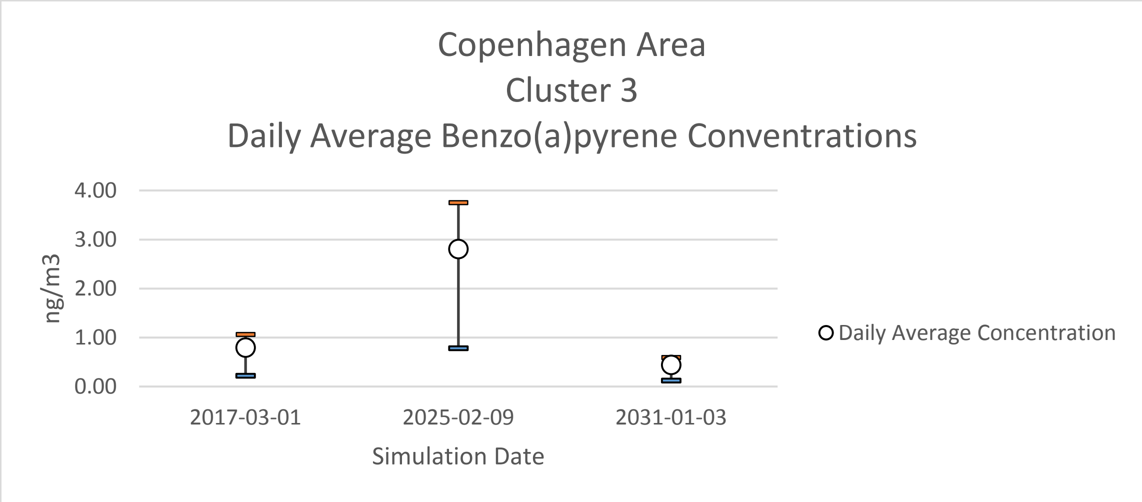


*Figure 4.9.27: BaP daily concentrations*

### 4.9.3.3 The Emission Inventory effect

Figures 4.9.28, 4.9.29, 4.9.30 and 4.9.31 illustrate the emission inventory temporal change effect on $NO_2$, $O_3$, $PM_{10}$ and $PM_{2.5}$ concentration levels respectively. There is a decreasing trend in $NO_2$, $PM_{10}$ and $PM_{2.5}$ pollutants indicating the positive effect on emission reductions intervention. In the case of $O_3$, concentrations seem to be stable.

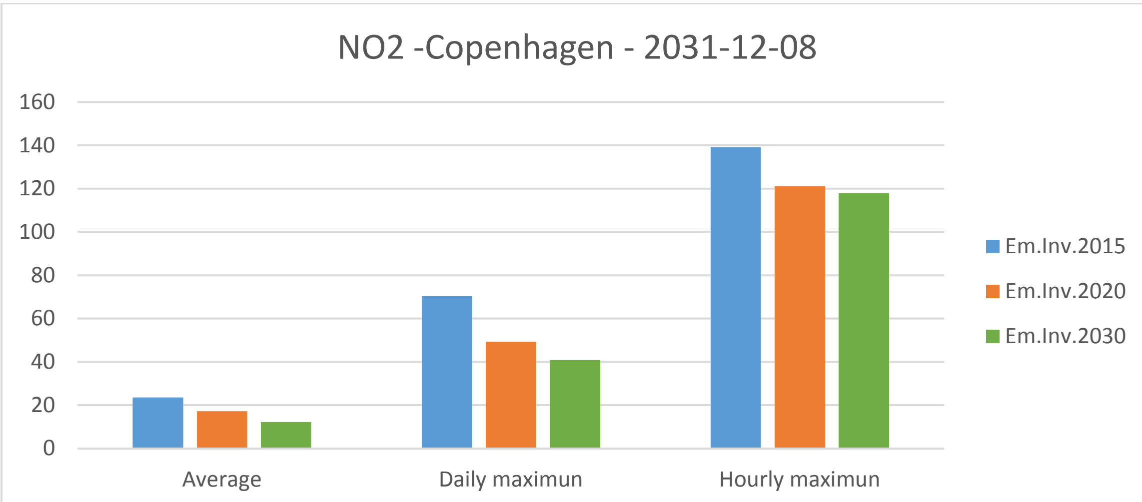


*Figure 4.9.28: $NO_2$ emission inventory comparison*

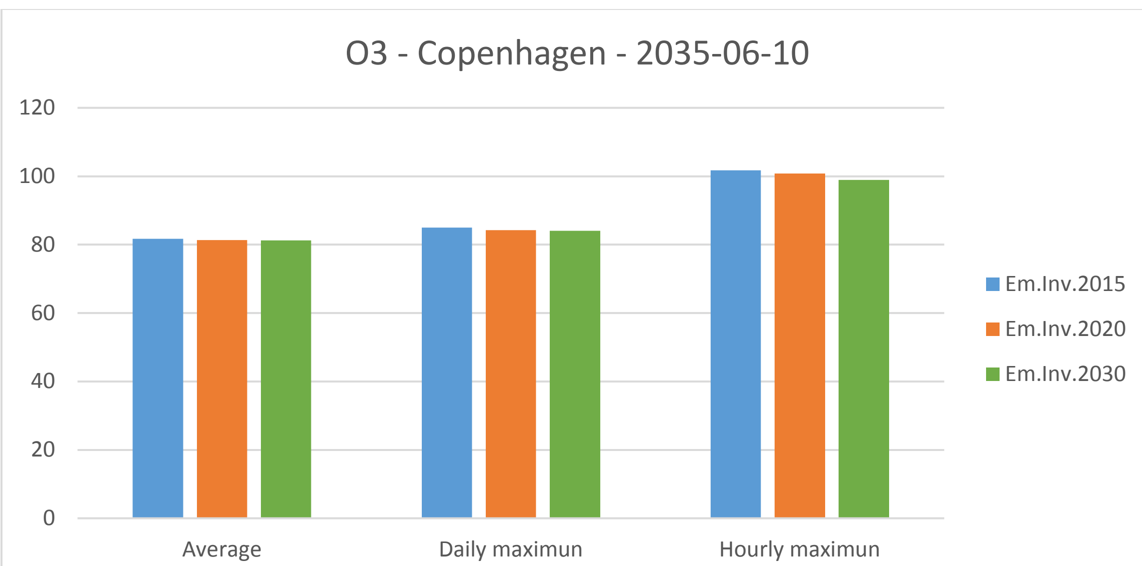


*Figure 4.9.29: $O_3$ emission inventory comparison*

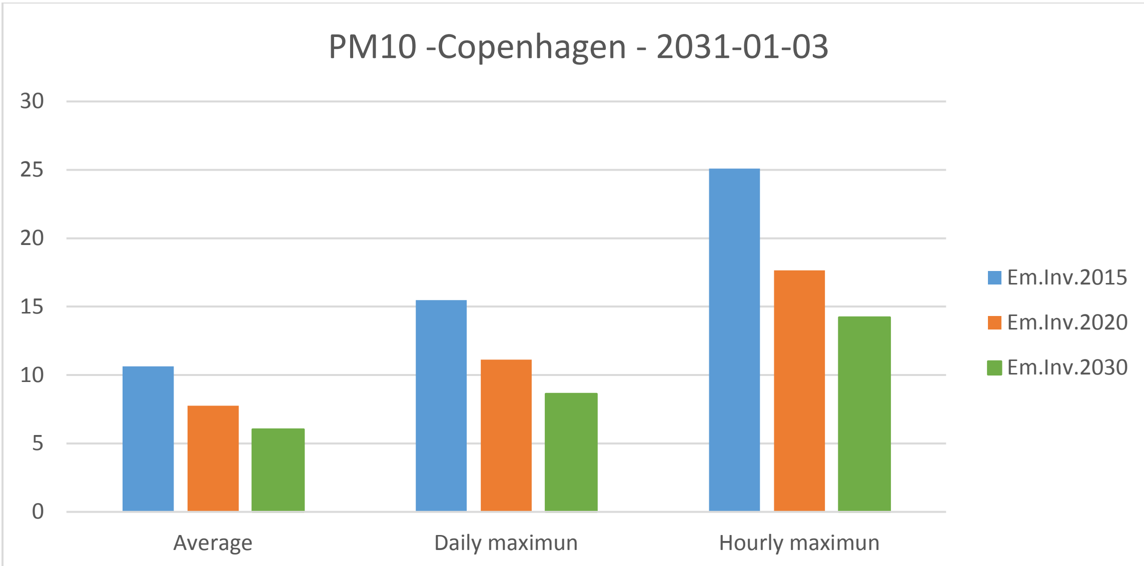


*Figure 4.9.30: $PM_{10}$ emission inventory comparison*

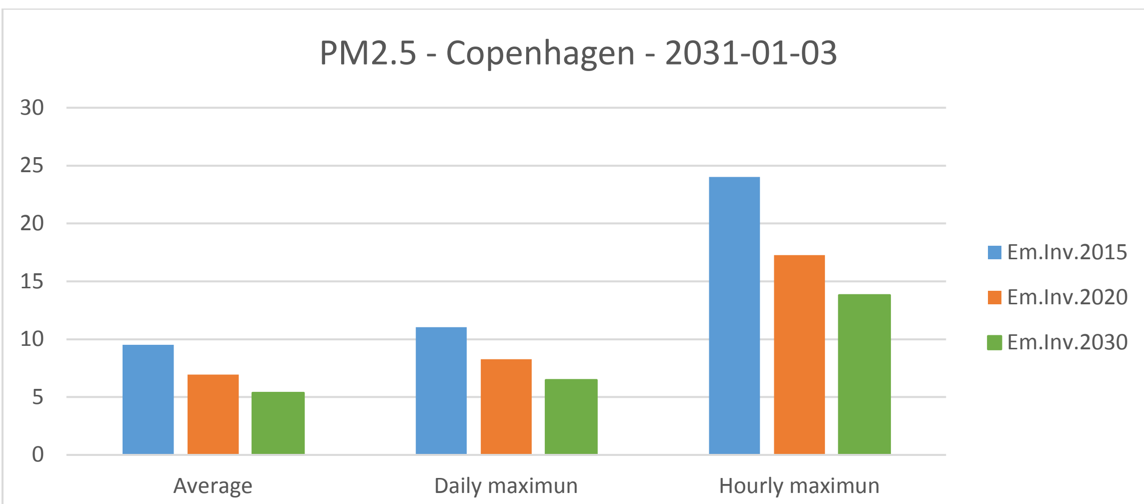


*Figure 4.9.31: $PM_{2.5}$ emission inventory comparison*

### 4.9.4 Air Quality Modeling results – Copenhagen wider area

#### 4.9.4.1 Overall results

In Figure 4.9.32 the daily average concentrations of $NO_2$, $O_3$, $PM_{10}$ and $PM_{2.5}$ for selected RDs are presented.

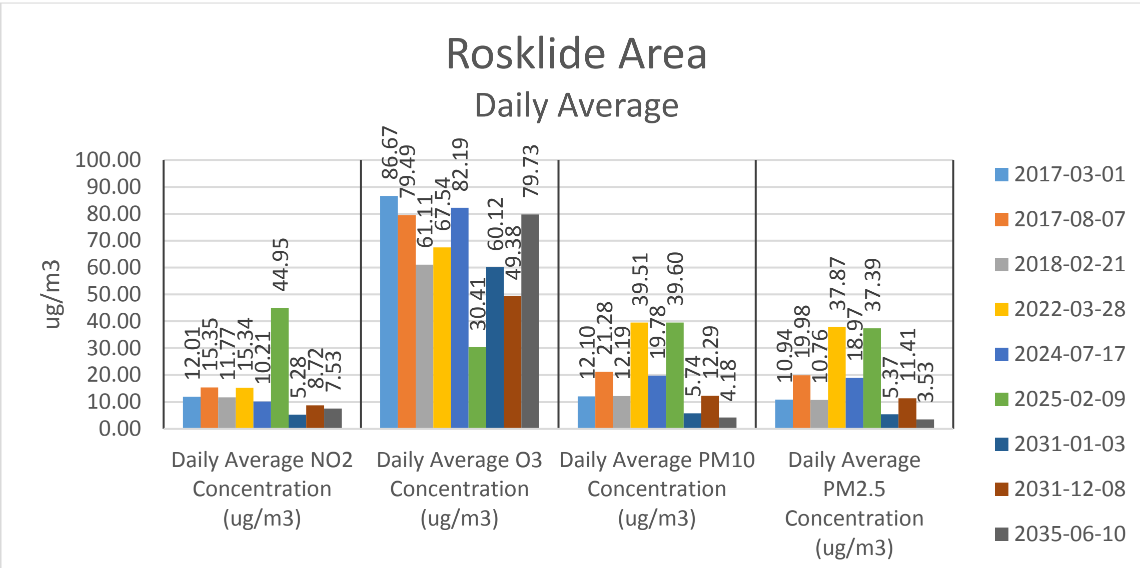


*Figure 4.9.32: Daily average concentrations*

#### 4.9.4.2 Clusters results

$NO_2$ Concentrations (Cluster 1)

In Figure 4.9.33, the results are presented in terms of concentrations average, daily maximum and hourly maximum. The diurnal variations are shown in Figure 4.9.34.

The daily maximum concentrations are below EU and WHO yearly limit of 40μg/$m^3$. The hourly maximum concentrations are below the WHO hourly limit of 20 μg/$m^3$.

$O_3$ Concentrations (Cluster 4)

In Figure 4.9.35, the results are presented in terms of concentrations average, daily maximum and hourly maximum. The diurnal variations are shown in Figure 4.9.36.

Both daily average and maximum concentrations are below the WHO 8hr limit of 100μg/$m^3$. The maximum hourly concentrations are below the EU limit of 120μg/$m^3$.

$PM_{10}$ Concentrations (Cluster 3)

In Figure 4.9.37, the results are presented in terms of concentrations average, daily maximum and hourly maximum. The diurnal variations are shown in Figure 4.9.38.

The picture is mixed. The daily maximum concentrations are below the WHO yearly limit of 20μg/$m^3$ in two days. All daily maximum values are below the WHO daily limit of 50μg/$m^3$.

### $NO_2$-Cluster 1

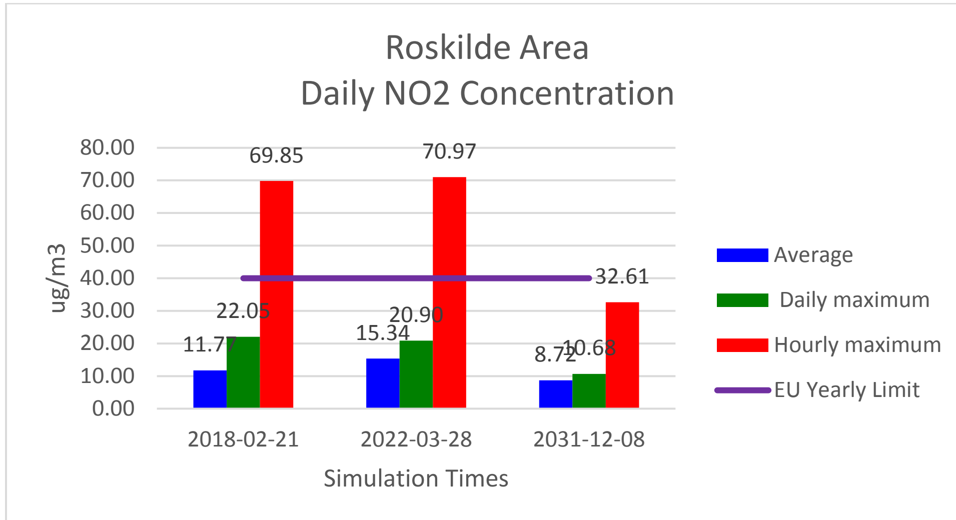


*Figure 4.9.33: $NO_2$ Day concentrations*

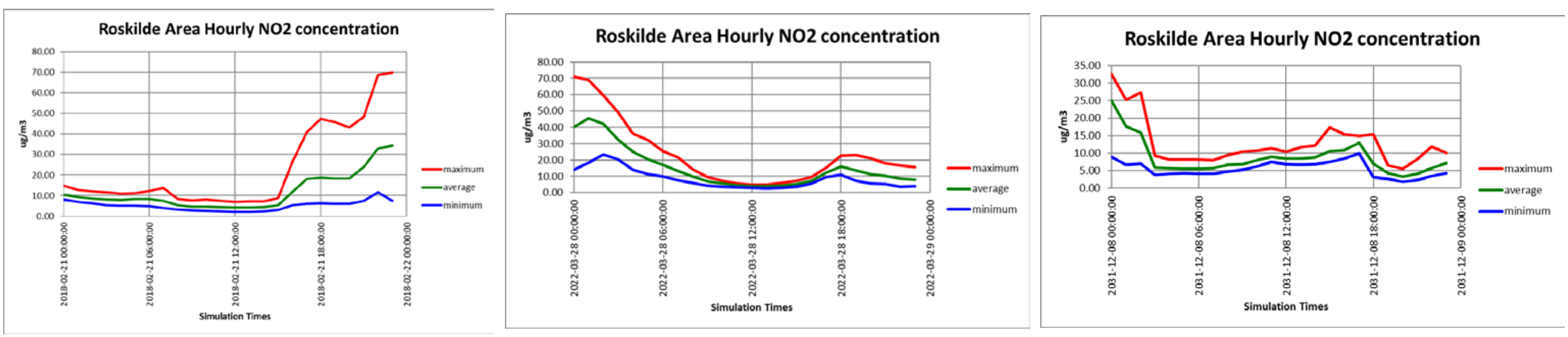


*Figure 4.9.34: Hourly $NO_2$ concentrations*

### $O_3$-Cluster 4

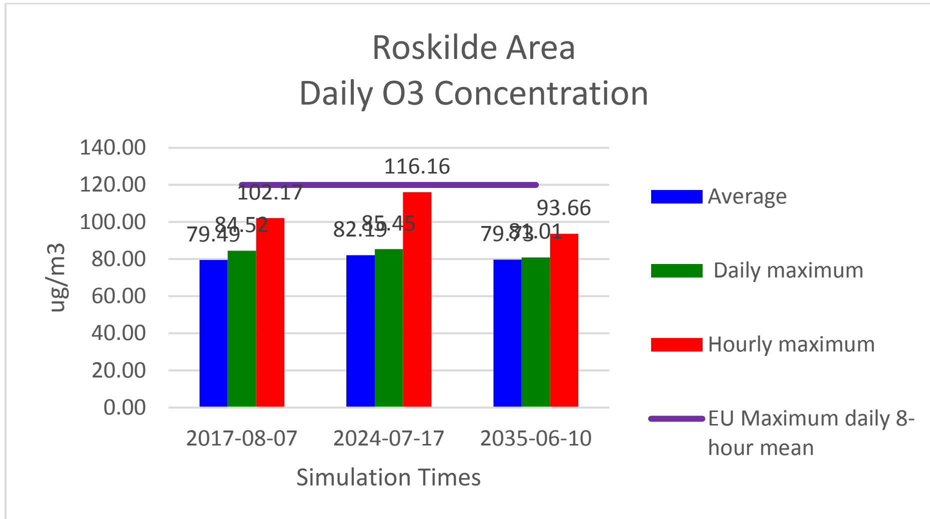


*Figure 4.9.35: $O_3$ Daily concentrations*

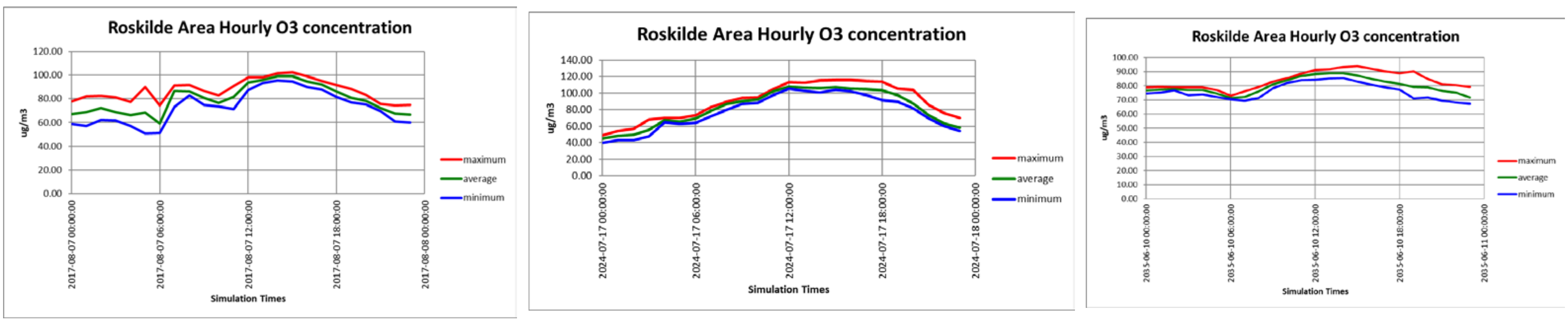


*Figure 4.9.36: $O_3$ Hourly concentrations*

### $PM_{10}$-Cluster 3

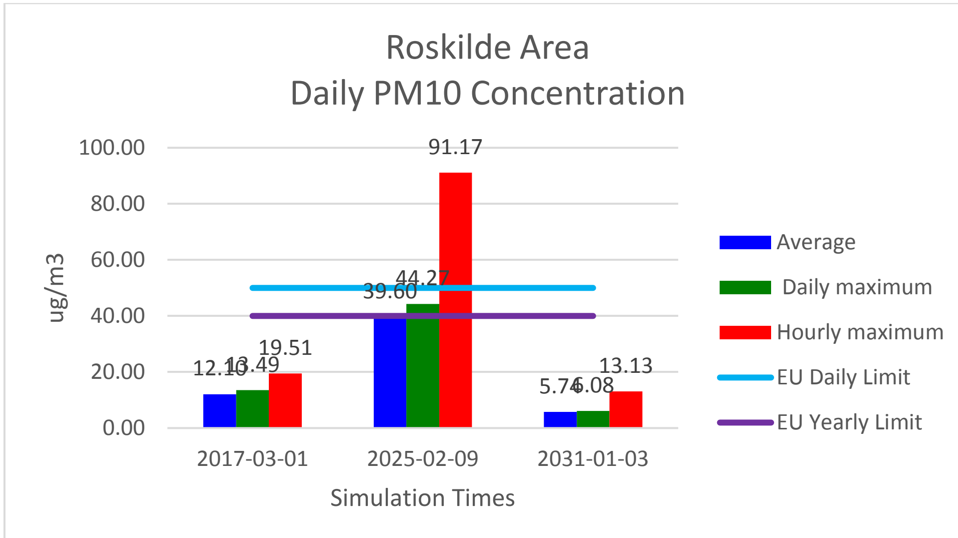


*Figure 4.9.37: $PM_{10}$ Daily concentrations*

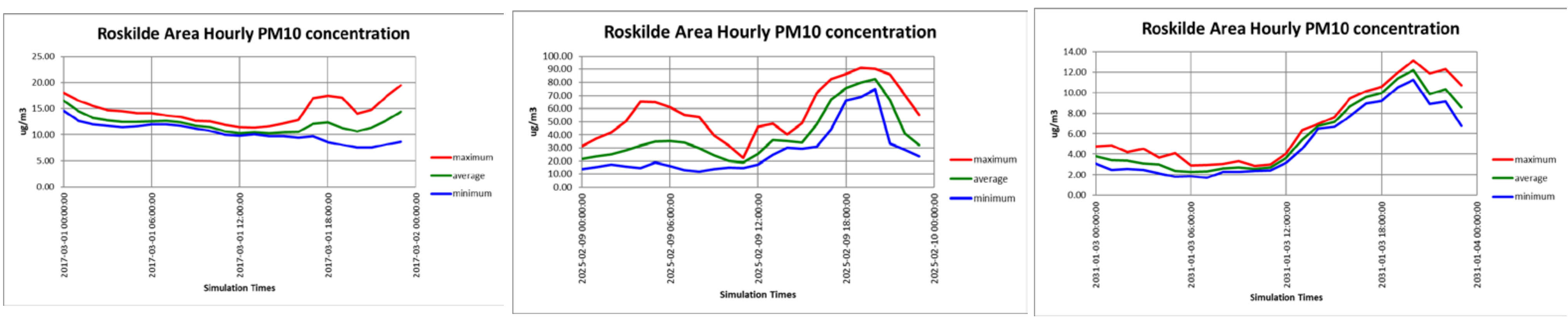


*Figure 4.9.38: $PM_{10}$ Hourly concentrations*

PM$_{2.5}$ Concentrations (Cluster 3)

In Figure 4.9.39, the results are presented in terms of concentrations average, daily maximum and hourly maximum.

The picture about the PM$_{2.5}$ concentration is mixed. The daily maximum concentration is well above the WHO yearly limit of 10μg/m$^3$ in one day. On the other hand its well below in another day.

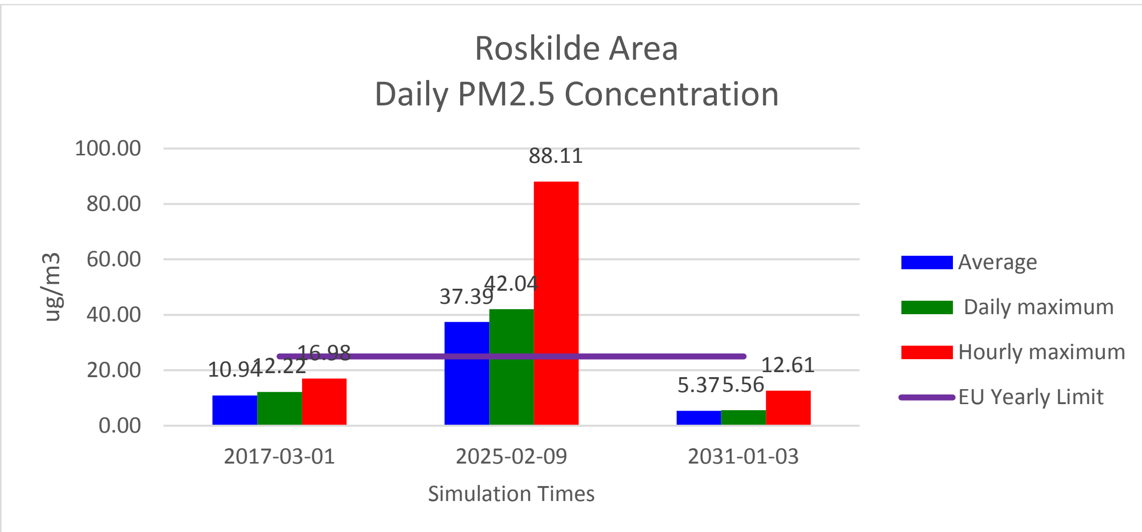


*Figure 4.9.39: PM$_{2.5}$ Day concentrations*

Figure 4.9.40 presents the estimated BaP daily concentrations contained in PM$_{2.5}$. All days are above WHO annual limit of 0.12ng/m$^3$ however two days are below the EU annual limit of 1ng/m$^3$.

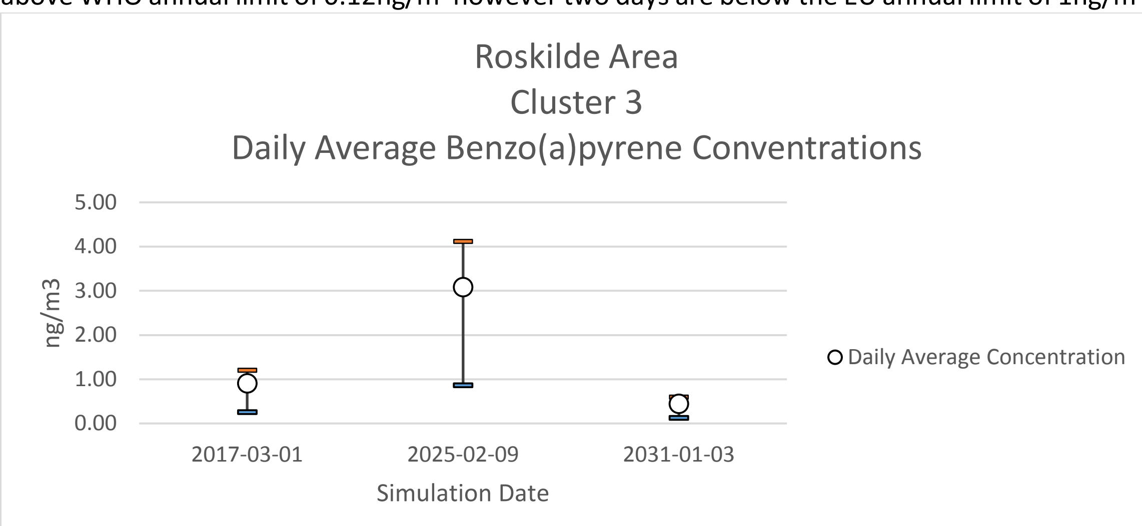


*Figure 4.9.40: BaP daily concentrations*

### 4.9.4.3 The Emission Inventory effect

Figures 4.9.41, 4.9.42, 4.9.43 and 4.9.44 illustrate the emission inventory temporal change effect on $NO_2$, $O_3$, $PM_{10}$ and $PM_{2.5}$ concentration levels respectively. There is a clearly decreasing trend in $NO_2$, $PM_{10}$ and $PM_{2.5}$ pollutants indicating the positive effect on emission reductions intervention. In the case of $O_3$, concentrations seem to be stable.

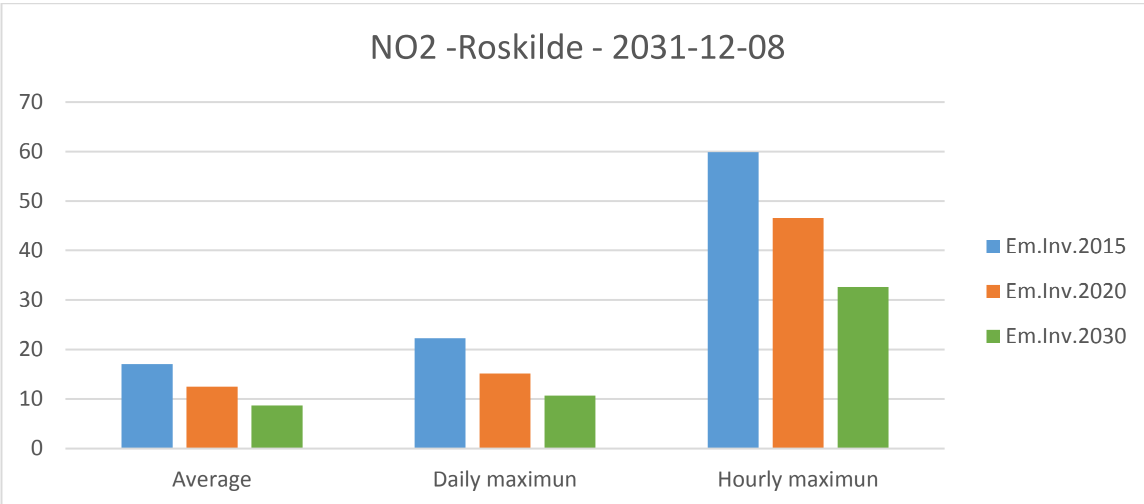


*Figure 4.9.41: $NO_2$ emission inventory comparison*

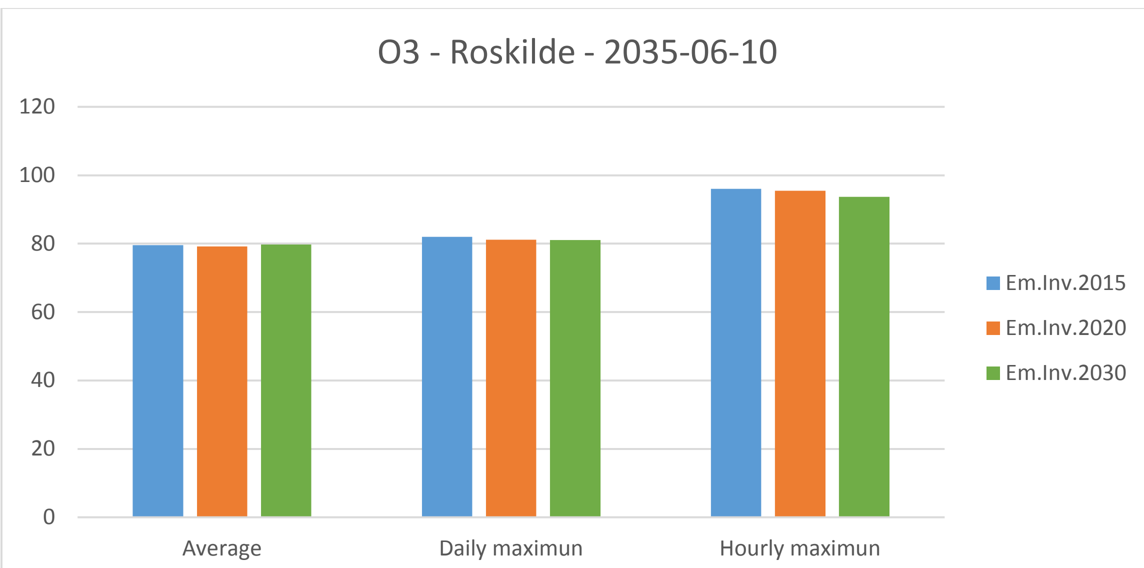


*Figure 4.9.42: $O_3$ emission inventory comparison*

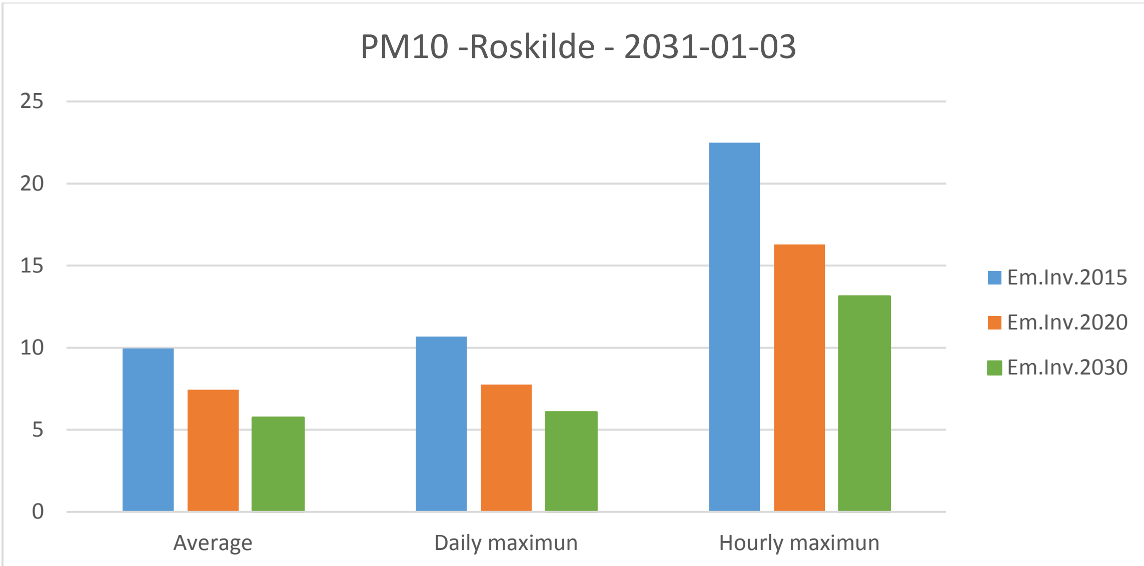


*Figure 4.9.43: $PM_{10}$ emission inventory comparison*

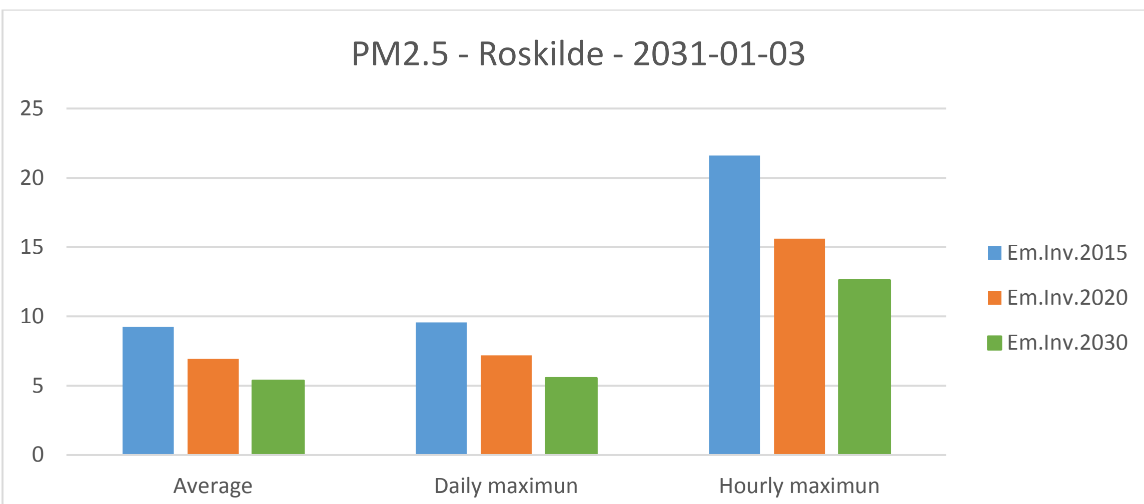


*Figure 4.9.44: $PM_{2.5}$ emission inventory comparison*

### 4.9.5 The GHGs Modeling results

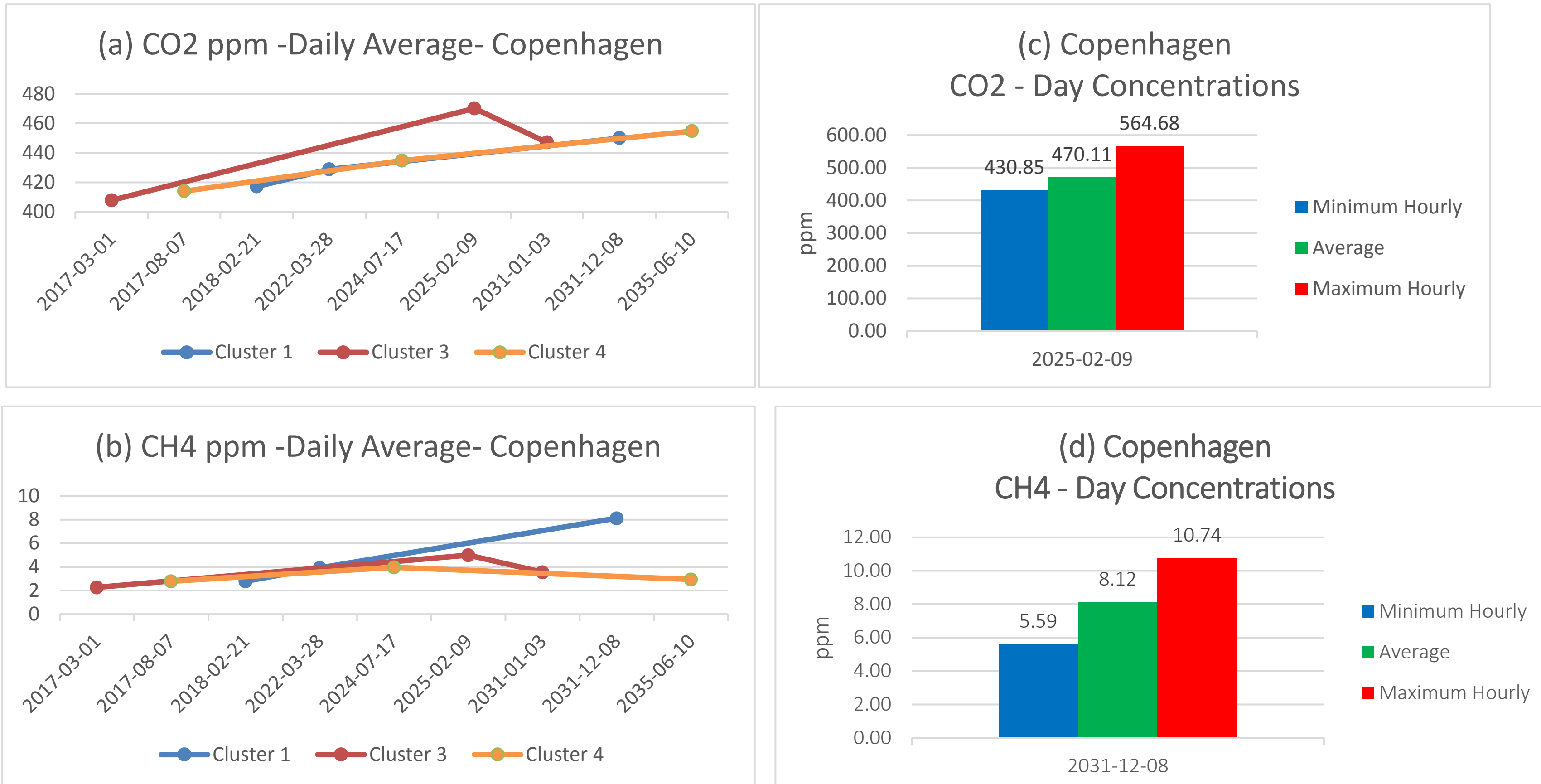


*Figure 4.9.45: (a),(b) $CO_2$ and $CH_4$ Daily average concentrations . (c),(d) $CO_2$ and $CH_4$ concentrations of the most polluted day*

### 4.9.6 Conclusions

**Copenhagen – Roskilde**

For Copenhagen – Roskilde greater area, clusters 1,3,5 and 7 could be categorized in cold period and on the other hand clusters 4 and 6 in warm period.

In in clusters 2 and 5 there is a linear increase in frequency occurrence through the ten 5-year periods. On the other hand, clusters 3 and 8 show a linear decrease in frequency occurrence.

The most heat waves seem to occur after 2021 and are spread through 2050. The 5-year period 2041-2045 shows the highest number of heat waves, while the next 5-year period shows a decrease. The most heat waves were associated with cluster 4 which correspond to clusters with days belong to warm period

Cluster 1 is characterized with elevated $NO_2$ concentrations, cluster 4 with elevated $O_3$ concentrations and cluster 3 with elevated PM concentrations.

**Copenhagen wider area**

$NO_2$ daily maximum concentrations seem to be very close or exceed the EU and WHO yearly limit of 40μg/m$^3$.

Both $O_3$ daily average and maximum concentrations are below the WHO 8hr limit of 100μg/m$^3$.

For $PM_{10}$ the picture is mixed. The daily maximum concentrations are below the WHO yearly limit of 20μg/m$^3$ in two days. In one day, the daily maximum value exceeds the WHO daily limit of 50μg/m$^3$.

The picture about the $PM_{2.5}$ concentration is mixed. The daily maximum concentration is well above the WHO yearly limit of 10μg/m$^3$ in one day and on and below it the rest days.

For BaP concentrations, all days are above WHO annual limit of 0.12ng/m$^3$ however two days are below the EU annual limit of 1ng/m$^3$.

There is a decreasing trend in $NO_2$, $PM_{10}$ and $PM_{2.5}$ pollutants indicating the positive effect on emission reductions intervention. In the case of $O_3$, concentrations seem to be stable.

**Roskilde wider area**

$NO_2$ daily maximum concentrations are below EU and WHO yearly limit of 40μg/m$^3$. The hourly maximum concentrations are below the WHO hourly limit of 20 μg/m$^3$.

Both $O_3$ daily average and maximum concentrations are below the WHO 8hr limit of 100μg/m$^3$. The maximum hourly concentrations are below the EU limit of 120μg/m$^3$.

For $PM_{10}$ the picture is mixed. The daily maximum concentrations are below the WHO yearly limit of 20μg/m$^3$ in two days. All daily maximum values are below the WHO daily limit of 50μg/m$^3$.

The picture about the $PM_{2.5}$ concentration is mixed. The daily maximum concentration is well above the WHO yearly limit of 10μg/m$^3$ in one day. On the other hand, its well below in another day.

For BaP concentrations, all days are above WHO annual limit of 0.12ng/m$^3$ however two days are below the EU annual limit of 1ng/m$^3$

There is a clearly decreasing trend in $NO_2$, $PM_{10}$ and $PM_{2.5}$ pollutants indicating the positive effect on emission reductions intervention. In the case of $O_3$, concentrations seem to be stable.

## 4.10 Ljubljana

### 4.10.1 PCA results

The PCA analysis applied to Ljubljana data has led to the following results.

Four (4) principal components have been identified as factors for the cluster analysis (Table 4.10.1). Principal Components (PC) explaining 80.85% of the total variance in the initial data.

Factor 1 explains 31.58% of the total variance and contains the 2 temperature variables, mean, daily temperature range and the down ward short-wave radiation.

Factor 2 explains 18.70% of the total variance and contains precipitation and RH.

Factor 3 explains 15.70% of the total variance and contains U and V wind components.

Factor 4 explains 11.53% of the total variance and contains atmospheric boundary layer thickness and surface pressure.

*Table 4.10.1: The Principal Components results*

| | Component | | | |
|---|---|---|---|---|
| | 1 | 2 | 3 | 4 |
| Downward short-wave surface radiation | .860 | | | |
| Temperature | .859 | | | |
| Temperature Range | .754 | | | |
| Precipitation | | .826 | | |
| RH | | .826 | | |
| U wind | | | .903 | |
| V wind | | | .892 | |
| Atmospheric boundary layer thickness | | | | .838 |
| Surface pressure | | | | -.667 |

### 4.10.2 Clustering results

#### Cluster description and trends

As explained in 3.4.4 the selected clusters of the city of Ljubljana are 6. In Figure 4.10.1 are shown the number of days per cluster, where cluster 3 have the most days and cluster 5 have the less. The monthly distribution per cluster is presented in Table 4.10.2 and in Figure 4.10.2. By dividing the year in two periods, cold and warm, clusters 2,5 and 6 could be categorized in cold period and on the other hand clusters 3 and 4 in warm period.


*Figure 4.10.1: Number of Days per cluster*

*Table 4.10.2: Monthly distribution per cluster*

| | | Month | | | | | | | | | | | | Total |
|---|---|---|---|---|---|---|---|---|---|---|---|---|---|---|
| | | Jan | Feb | Mar | Apr | May | Jun | Jul | Aug | Sep | Oct | Nov | Dec | |
| Cluster 6 | 1 | 161 | 218 | 470 | 506 | 350 | 119 | 72 | 24 | 129 | 180 | 162 | 123 | 2514 |
| | 2 | 560 | 470 | 360 | 163 | 17 | 0 | 0 | 0 | 79 | 379 | 485 | 597 | 3110 |
| | 3 | 0 | 0 | 49 | 403 | 718 | 929 | 1083 | 1230 | 780 | 86 | 0 | 0 | 5278 |
| | 4 | 118 | 127 | 165 | 165 | 302 | 396 | 371 | 280 | 352 | 250 | 177 | 112 | 2815 |
| | 5 | 181 | 212 | 207 | 232 | 161 | 55 | 24 | 15 | 59 | 152 | 178 | 226 | 1702 |
| | 6 | 530 | 385 | 299 | 31 | 2 | 1 | 0 | 1 | 101 | 503 | 498 | 492 | 2843 |
| Total | | 1550 | 1412 | 1550 | 1500 | 1550 | 1500 | 1550 | 1550 | 1500 | 1550 | 1500 | 1550 | 18262 |

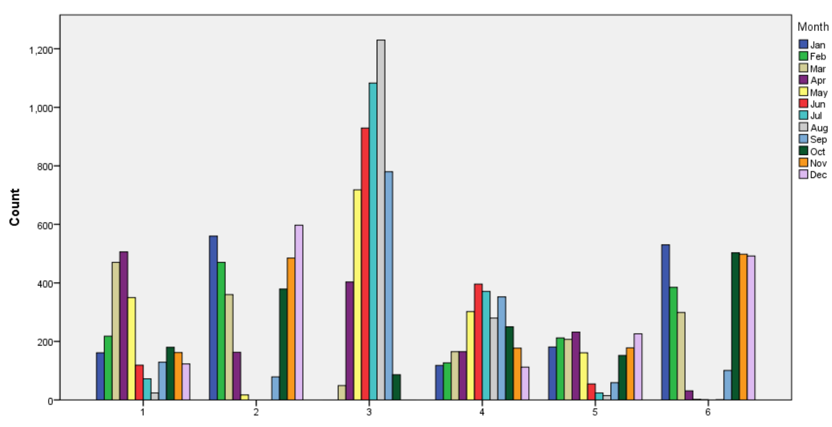


*Figure 4.10.2: Visualized bar chart of monthly distribution per cluster*

A trend analysis of the 5-year frequency of each cluster (Figure 4.9.3). There is an evidence that in clusters 2 and 5 there is a linear increase in frequency occurrence through the ten 5-year periods. On the other hand, clusters 3 and 8 show a linear decrease in frequency occurrence. In the rest clusters no clear trends could be pointed out.


*Figure 4.10.3: Cluster 1-6 frequency trends*

## Cluster characterization

The clusters' implementation is based on the mean values of weather parameters which are displayed in Table 4.10.3.

*Table 4.10.3: Summary of the 6 clusters*

| | Cluster | | | | | |
|---|---|---|---|---|---|---|
| | 1 | 2 | 3 | 4 | 5 | 6 |
| | Mean (SD) | Mean (SD) | Mean (SD) | Mean (SD) | Mean (SD) | Mean (SD) |
| Temperature ( ºC) | 4,86 (6,35) | 4,99 (4,53) | 17,05 (4,9) | 11,45 (7,11) | 8,55 (4,25) | 3,29 (5,65) |
| Daily Temperature Range ( ºC) | 7,26 (2,05) | 6,28 (2,14) | 10,02 (1,66) | 5,6 (1,85) | 5,88 (2,07) | 7,19 (2,29) |
| Relative Humidity (%) | 55,07 (9,87) | 74,15 (13,5) | 69,63 (9,59) | 86,25 (5,63) | 77,79 (10,54) | 73 (13,61) |
| Surface Pressure (Pa) | 94530,57 (871,18) | 94809,35 (801,68) | 94941,36 (592,4) | 94120,34 (715,03) | 93716,59 (755,61) | 95778,31 (795,39) |
| Precipitation (kg/m2/s) | 0,000011 (0,000025) | 0,000015 (0,000029) | 0,000026 (0,000038) | 0,000165 (0,000103) | 0,000106 (0,000109) | 0,000007 (0,000017) |
| Downward Short Wave Radiation | 208,73 (87,54) | 104,72 (56,78) | 288,44 (49,61) | 137,4 (79,73) | 132,69 (87,43) | 112,56 (50,2) |
| u wind component (m/s) | -0,95 (2,75) | 3,18 (1,39) | -0,57 (2,06) | -1,72 (1,79) | 3,7 (1,82) | -0,14 (2,08) |
| v wind component (m/s) | -2,68 (1,69) | 1,55 (1,12) | -0,12 (1,1) | -0,54 (1,61) | 3,33 (1,83) | 0,01 (0,82) |
| V wind (m/s) | 3,9 (1,8) | 3,69 (1,44) | 2,1 (1,18) | 2,6 (1,51) | 5,28 (1,87) | 1,91 (1,18) |
| Atmospheric Boundary Layer Thickness (m) | 887,84 (228,96) | 487,29 (133,6) | 615,53 (136,63) | 455,07 (147,24) | 812,2 (202,89) | 309,34 (132,03) |

In addition to the previous Table 4.10.3, Figure 4.10.4 presents the mean normalized (z-score) variables of each cluster, respectively showing the differences of the parameters per cluster.

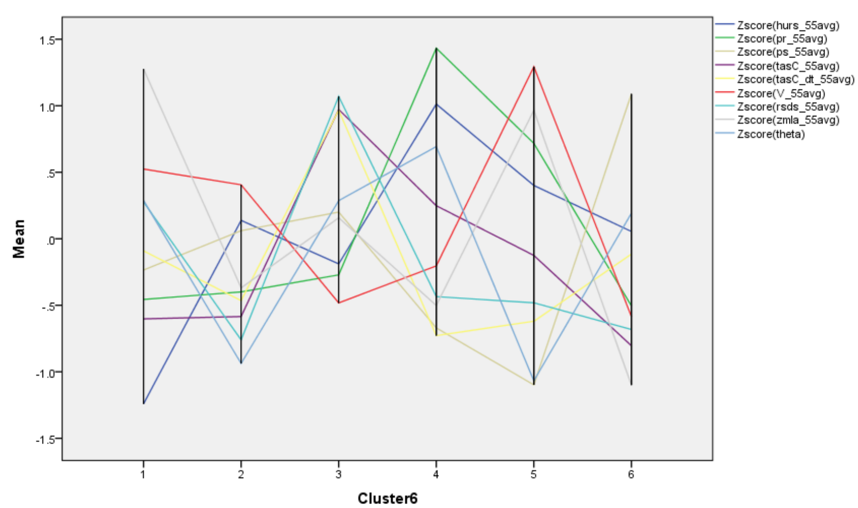


*Figure 4.10.4: Normalized variables (z-score) averaged for each cluster*

Daily, 10-meter from ground level, wind data were used to create the wind roses per each cluster as they are shown in Figures 4.10.5-4.10.14. Each wind direction distribution per cluster is presented in more details in Table 4.10.4.

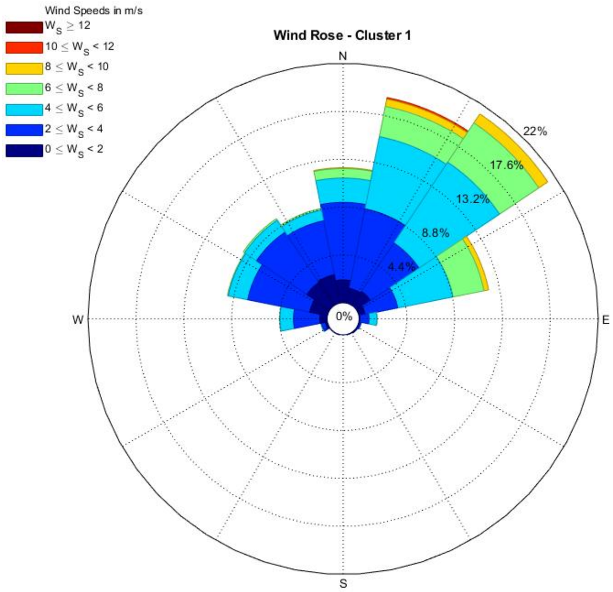


*Figure 4.10.5: Wind Rose - Cluster 1*

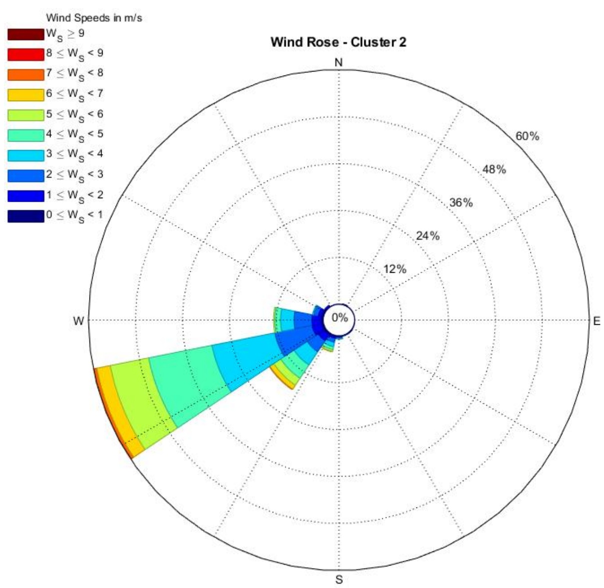


*Figure 4.10.6: Wind Rose - Cluster 2*

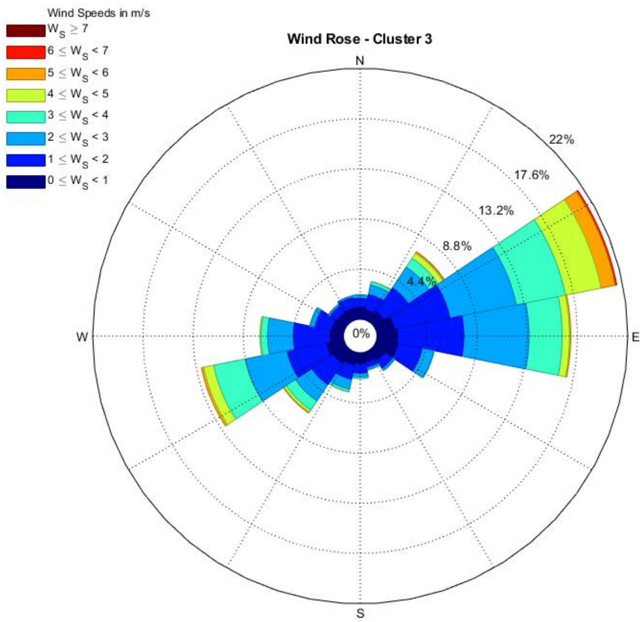


*Figure 4.10.7: Wind Rose - Cluster 3*

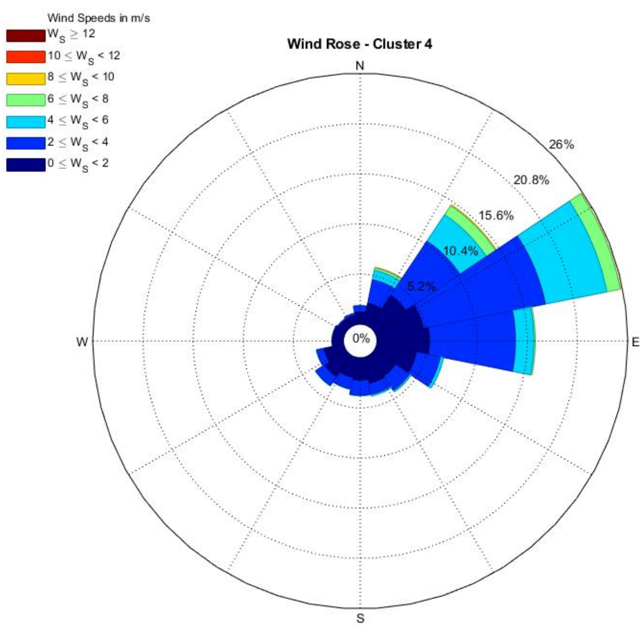


*Figure 4.10.8: Wind Rose - Cluster 4*

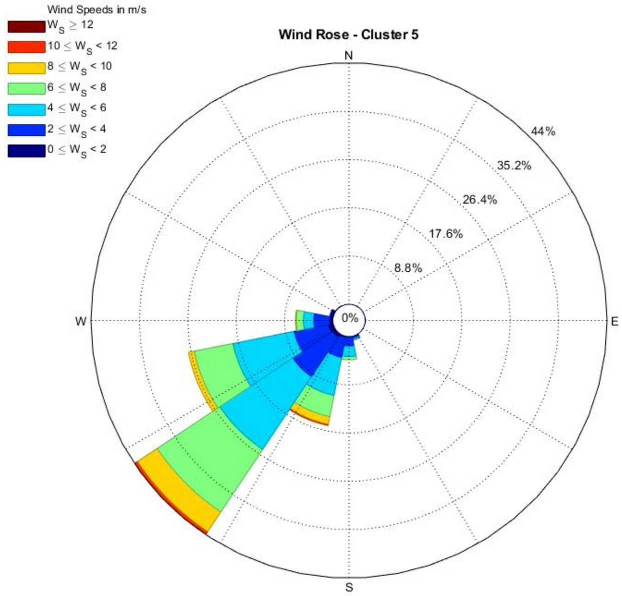


*Figure 4.10.9: Wind Rose - Cluster 5*

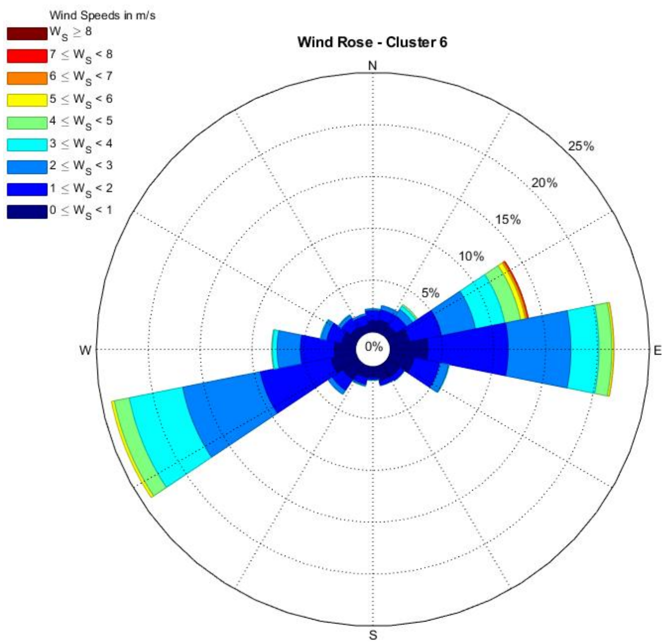


*Figure 4.10.10: Wind Rose - Cluster 6*

*Table 4.10.4: 16 Wind Direction distribution per cluster*

| | | | Wind16 | | | | | | | | | | | | | | | | Total |
|---|---|---|---|---|---|---|---|---|---|---|---|---|---|---|---|---|---|---|---|
| | | | S | SSW | SW | WSW | W | WNW | NW | NNW | N | NNE | NE | ENE | E | ESE | SE | SSE | |
| Cluster6 | 1 | Count | 0 | 1 | 1 | 16 | 110 | 236 | 241 | 223 | 312 | 484 | 532 | 306 | 42 | 6 | 3 | 1 | 2514 |
| | | % within Cluster6 | 0.0% | 0.0% | 0.0% | 0.6% | 4.4% | 9.4% | 9.6% | 8.9% | 12.4% | 19.3% | 21.2% | 12.2% | 1.7% | 0.2% | 0.1% | 0.0% | 100.0% |
| | 2 | Count | 28 | 134 | 541 | 1863 | 395 | 91 | 18 | 3 | 3 | 7 | 3 | 2 | 2 | 4 | 8 | 8 | 3110 |
| | | % within Cluster6 | 0.9% | 4.3% | 17.4% | 59.9% | 12.7% | 2.9% | 0.6% | 0.1% | 0.1% | 0.2% | 0.1% | 0.1% | 0.1% | 0.1% | 0.3% | 0.3% | 100.0% |
| | 3 | Count | 120 | 187 | 351 | 672 | 387 | 161 | 100 | 112 | 114 | 180 | 391 | 1134 | 897 | 272 | 116 | 84 | 5278 |
| | | % within Cluster6 | 2.3% | 3.5% | 6.7% | 12.7% | 7.3% | 3.1% | 1.9% | 2.1% | 2.2% | 3.4% | 7.4% | 21.5% | 17.0% | 5.2% | 2.2% | 1.6% | 100.0% |
| | 4 | Count | 111 | 95 | 109 | 82 | 34 | 34 | 30 | 34 | 55 | 170 | 429 | 726 | 462 | 199 | 130 | 115 | 2815 |
| | | % within Cluster6 | 3.9% | 3.4% | 3.9% | 2.9% | 1.2% | 1.2% | 1.1% | 1.2% | 2.0% | 6.0% | 15.2% | 25.8% | 16.4% | 7.1% | 4.6% | 4.1% | 100.0% |
| | 5 | Count | 72 | 282 | 748 | 457 | 116 | 12 | 1 | 0 | 0 | 0 | 0 | 0 | 1 | 0 | 0 | 13 | 1702 |
| | | % within Cluster6 | 4.2% | 16.6% | 43.9% | 26.9% | 6.8% | 0.7% | 0.1% | 0.0% | 0.0% | 0.0% | 0.0% | 0.0% | 0.1% | 0.0% | 0.0% | 0.8% | 100.0% |
| | 6 | Count | 38 | 56 | 101 | 683 | 230 | 100 | 67 | 52 | 64 | 75 | 100 | 387 | 613 | 166 | 57 | 54 | 2843 |
| | | % within Cluster6 | 1.3% | 2.0% | 3.6% | 24.0% | 8.1% | 3.5% | 2.4% | 1.8% | 2.3% | 2.6% | 3.5% | 13.6% | 21.6% | 5.8% | 2.0% | 1.9% | 100.0% |
| Total | | Count | 369 | 755 | 1851 | 3773 | 1272 | 634 | 457 | 424 | 548 | 916 | 1455 | 2555 | 2017 | 647 | 314 | 275 | 18262 |
| | | % within Cluster6 | 2.0% | 4.1% | 10.1% | 20.7% | 7.0% | 3.5% | 2.5% | 2.3% | 3.0% | 5.0% | 8.0% | 14.0% | 11.0% | 3.5% | 1.7% | 1.5% | 100.0% |

## Clusters and local Heat Waves

In Figures 4.10.11 and 4.10.12 are presented the heat waves occurrence per 5-year period and per cluster. The most heat waves seem to occur after 2036.The 5-year period 2041-2045 shows the highest number of heat waves, while the next 5-year period shows a decrease. The most heat waves were associated with cluster 3 which correspond to clusters with days belong to warm period (see Table 4.10.2).

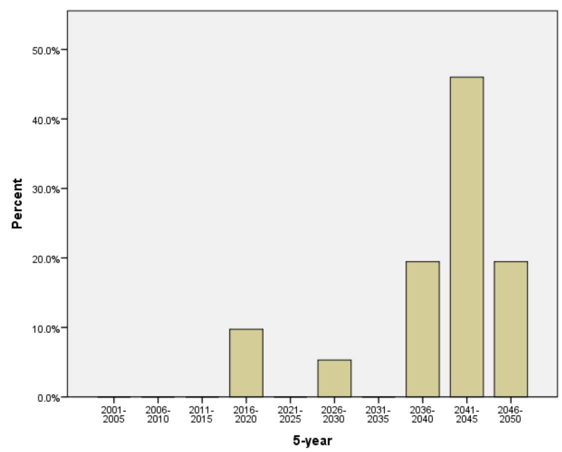


*Figure 4.10.11: Heat Waves per 5-year period*

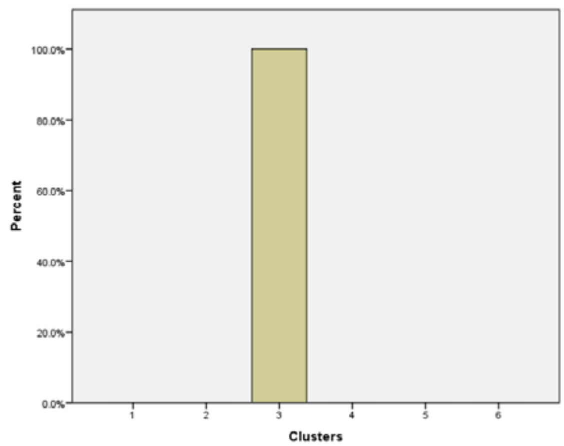


*Figure 4.10.12: Heat Waves per cluster*

## Clusters versus Air Quality level

As it can be seen in Table 4.1 one observation station have been used for the present analysis. The descriptive statistics for $NO_2$, $O_3$ and $PM_{10}$ is given in Table 4.10.5.

*Table 4.10.5: Air pollutants descriptive statistics*

| | | NO2 | O3 | PM10 |
|---|---|---|---|---|
| Mean | | 30.18989 | 43.14679 | 33.83737 |
| Std. Deviation | | 15.187291 | 26.674553 | 20.264830 |
| Minimum | | 2.174 | 0.355 | 1.446 |
| Maximum | | 139.252 | 142.665 | 170.900 |
| Percentiles | 5 | 11.74160 | 5.23900 | 10.92680 |
| | 25 | 20.09150 | 20.10000 | 20.36700 |
| | 50 | 26.98700 | 41.95500 | 29.23000 |
| | 75 | 37.23050 | 62.81300 | 41.58300 |
| | 95 | 58.51660 | 89.23900 | 71.86580 |

Table 4.10.6 presents the pollutants' concentrations per cluster. Higher mean $NO_2$ concentrations are observed in clusters 2 and 6. Higher mean $O_3$ concentrations are observed in cluster 6. Higher mean $PM_{10}$ concentrations are observed in clusters 2 and 6.

*Table 4.10.6: Summary pollutant concentrations per cluster*

| | Cluster | | | | | |
|---|---|---|---|---|---|---|
| | 1 | 2 | 3 | 4 | 5 | 6 |
| | Mean (SD) | Mean (SD) | Mean (SD) | Mean (SD) | Mean (SD) | Mean (SD) |
| PM10 (μg/m3) | 33,46 (19,72) | 40,48 (22,25) | 25,3 (11,6) | 32,72 (20,59) | 37,53 (21,78) | 41,35 (23,23) |
| O3 (μg/m3) | 46,8 (27,2) | 24,55 (19,09) | 60,38 (21,14) | 48,23 (25,61) | 37,13 (26,18) | 25,8 (18,61) |
| NO2 (μg/m3) | 30,9 (15,89) | 37,86 (16,72) | 22,06 (7,62) | 28,38 (15,24) | 33,35 (15,9) | 36,38 (15,33) |

The differences in concentrations per cluster are shown in Figures 4.10.13-4.10.15.

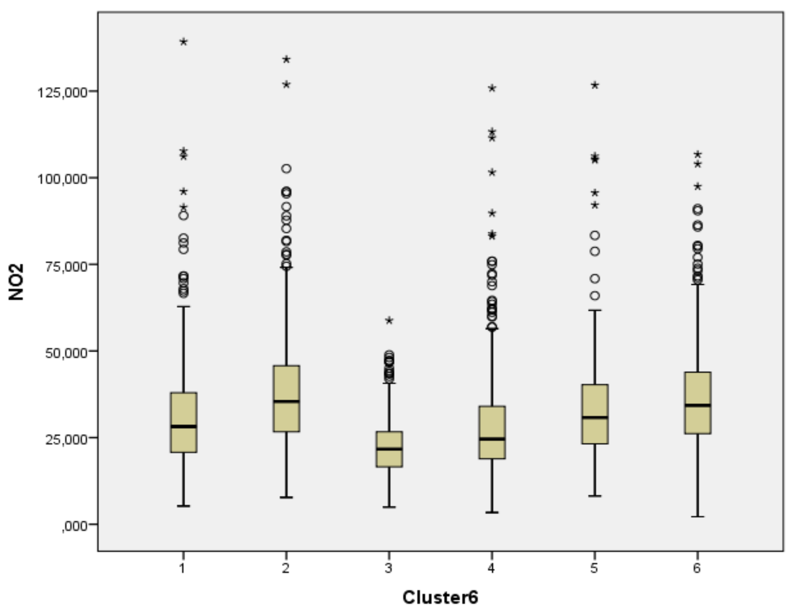


*Figure 4.10.13: $NO_2$ concentration statistics per cluster*

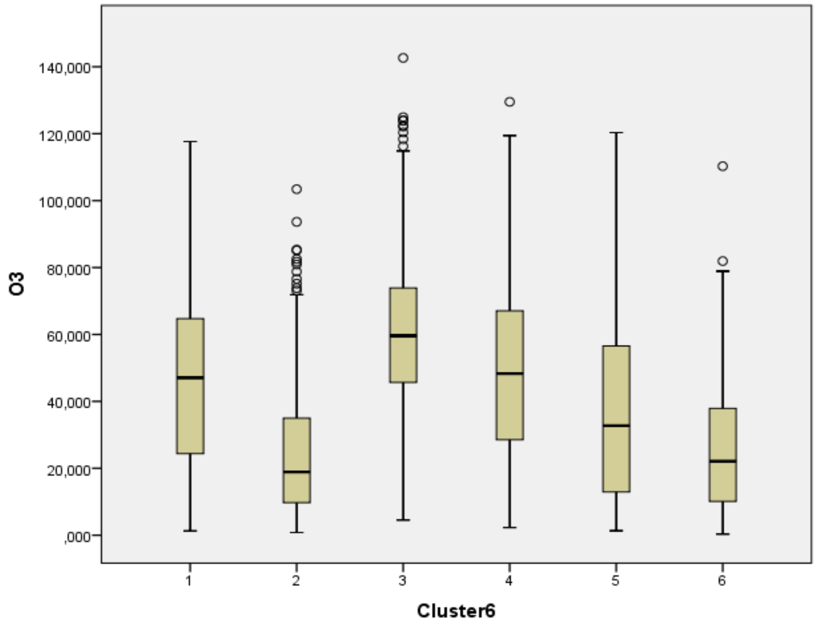


*Figure 4.10.14: $O_3$ concentration statistics per cluster*

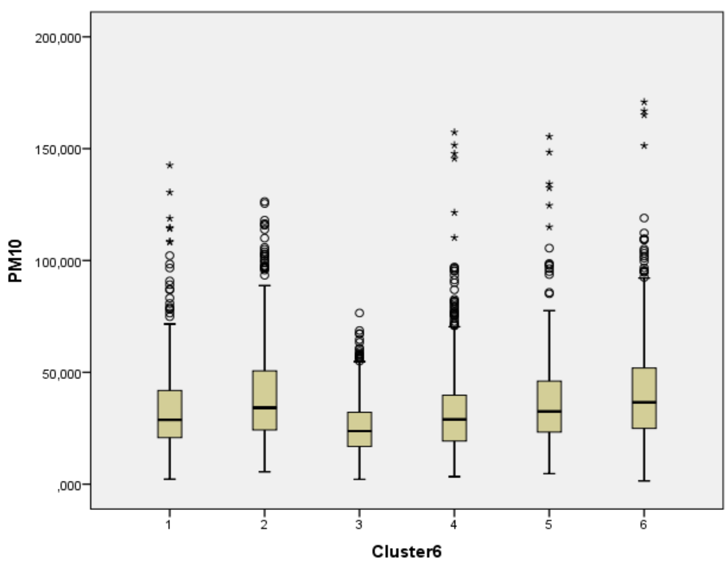


*Figure 4.10.15: $PM_{10}$ concentration statistics per cluster*

## Representative Days

In the following Table 4.10.7 are presented the selected RDs per 5-year period and per cluster.

*Table 4.10.7: Representative days per cluster and 5year period*

| Closest days to centroids per 5year per cluster | | | clusters | | | | | |
|---|---|---|---|---|---|---|---|---|
| | | | 1 | 2 | 3 | 4 | 5 | 6 |
| 5 year period | 2001-2005 | 1 | 2005/10/10 | 2004/11/26 | 2005/06/15 | 05-09-2004 | 2003/05/04 | 2002/11/01 |
| | 2006-2010 | 2 | 2006/03/29 | 2007/02/07 | 2009/05/19 | 2008/06/17 | 2006/05/13 | 2007/12/06 |
| | 2011-2015 | 3 | 2015/10/03 | 2012/11/13 | 2011/09/03 | 2012/06/20 | 2014/10/13 | 2015/02/04 |
| | 2016-2020 | 4 | 2020/03/25 | 2017/11/29 | 2018/06/01 | 2016/05/31 | 2020/10/15 | 2017/11/05 |
| | 2021-2025 | 5 | 2025/03/29 | 2025/12/12 | 2025/07/31 | 2023/06/23 | 2025/03/08 | 2023/01/24 |
| | 2026-2030 | 6 | 2030/04/03 | 2029/10/25 | 2029/05/25 | 2030/06/07 | 2026/03/09 | 2027/02/26 |
| | 2031-2035 | 7 | 2033/03/23 | 2033/11/26 | 2031/05/27 | 2035/05/16 | 2034/04/09 | 2033/11/15 |
| | 2036-2040 | 8 | 2038/04/21 | 2040/11/19 | 2036/06/08 | 2037/04/21 | 2038/12/09 | 2040/11/10 |
| | 2041-2045 | 9 | 2041/03/19 | 2045/02/02 | 2041/06/02 | 2045/05/11 | 2041/03/18 | 2042/12/14 |
| | 2046-2050 | 10 | 2047/03/15 | 2047/11/22 | 2050/05/10 | 2049/05/29 | 2049/03/10 | 2046/03/11 |

## Selected Clusters and RDs for modeling purposes

Selected RDs will be used to perform targeted weather and air quality simulations within each selected 5-year period estimating hourly/daily concentrations of the priority pollutants to assess the climatic effect on air quality evolution and the characteristics of air quality future episodes. The selection was based on 3-year periods (2016-2020, 2021-2025 and 2031-2035) and on the clusters with the most elevated concentrations of $PM_{10}$, $NO_2$ and $O_3$. In the case of Ljubljana, cluster 2 recorded the most elevated values of $NO_2$, cluster 3 for the case of $O_3$ and cluster 6 for the case of $PM_{10}$. In Table 4.10.8 are presented the selected days which was used for modeling purposes.

*Table 4.10.8: RDs for modeling purposes*

| **Period** | **Cluster 2 (NO2)** | **Cluster 3 (O3)** | **Cluster 6 (PM)** |
|---|---|---|---|
| 2016-2020 | 2017-11-29 | 2018-06-01 | 2017-11-05 |
| 2021-2025 | 2025-12-12 | 2025-07-31 | 2023-01-24 |
| 2031-2035 | 2033-11-26 | 2031-05-27 | 2033-11-15 |

### 4.10.3 Air Quality Modeling results

#### 4.10.3.1 Overall results

In Figure 4.10.16 the daily average concentrations of $NO_2$, $O_3$, $PM_{10}$ and $PM_{2.5}$ for selected RDs are presented.

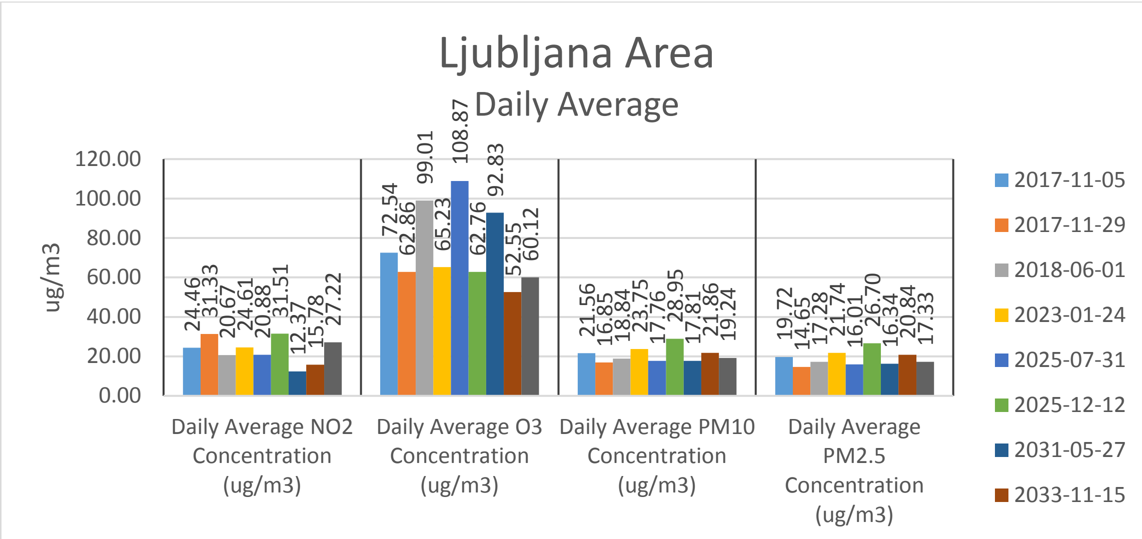


*Figure 4.10.16: Daily average concentrations*

In Figure 4.9.19 the obtained daily averaged concentrations are compared based on USTUTT and EGDAR HTAP emission inventories respectively. The results seem not to differ significantly.

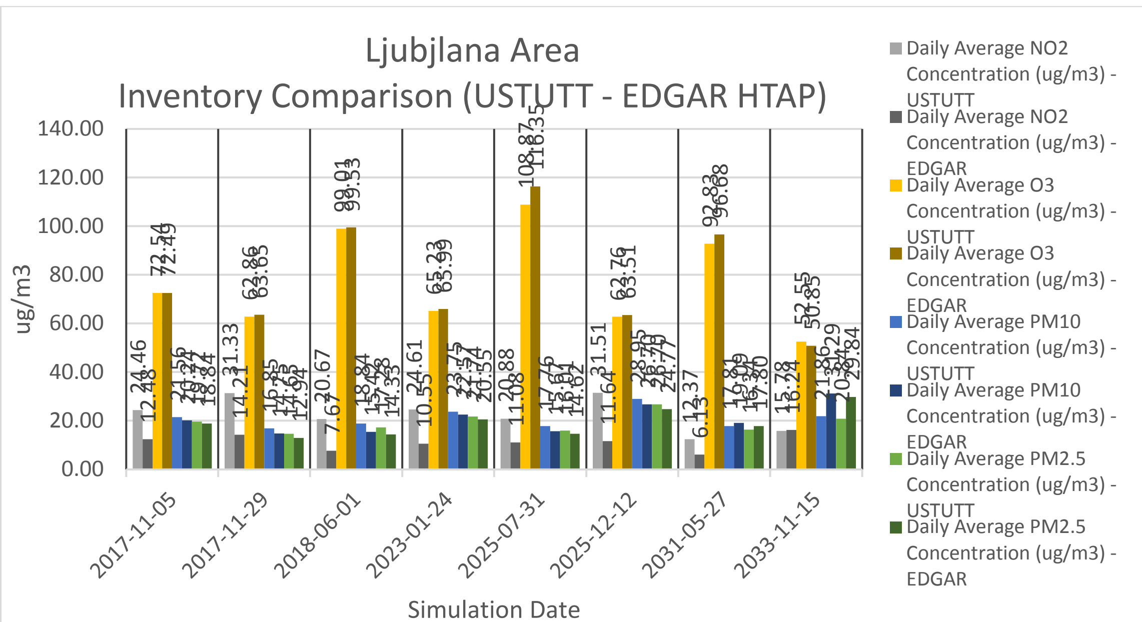


*Figure 4.10.17: Daily average concentrations – USTUTT vs EDGAR HTAP comparison*

#### 4.10.3.2 Clusters results

$NO_2$ Concentrations (Cluster 2)

In Figure 4.10.18, the results are presented in terms of concentrations average, daily maximum and hourly maximum. The diurnal variations are shown in Figure 4.10.19.

The daily maximum concentrations seem to well exceed the EU and WHO yearly limit of 40μg/m$^3$. The maximum hourly concentrations are above the limit of 200μg/m$^3$.

$O_3$ Concentrations (Cluster 5)

In Figure 4.10.20, the results are presented in terms of concentrations average, daily maximum and hourly maximum. The diurnal variations are shown in Figure 4.10.21.

The daily maximum concentrations are very close and above the WHO 8hr limit of 100μg/m$^3$. The maximum hourly concentrations exceed this limit as well as the EU 8hr limit of 120μg/m$^3$.

$PM_{10}$ Concentrations (Cluster 7)

In Figure 4.10.22, the results are presented in terms of concentrations average, daily maximum and hourly maximum. The diurnal variations are shown in Figure 4.10.23.

The daily maximum concentrations are above the WHO yearly limit of 20μg/m$^3$. Both daily maximum and hourly maximum values show a decreasing rate.

### $NO_2$-Cluster 2

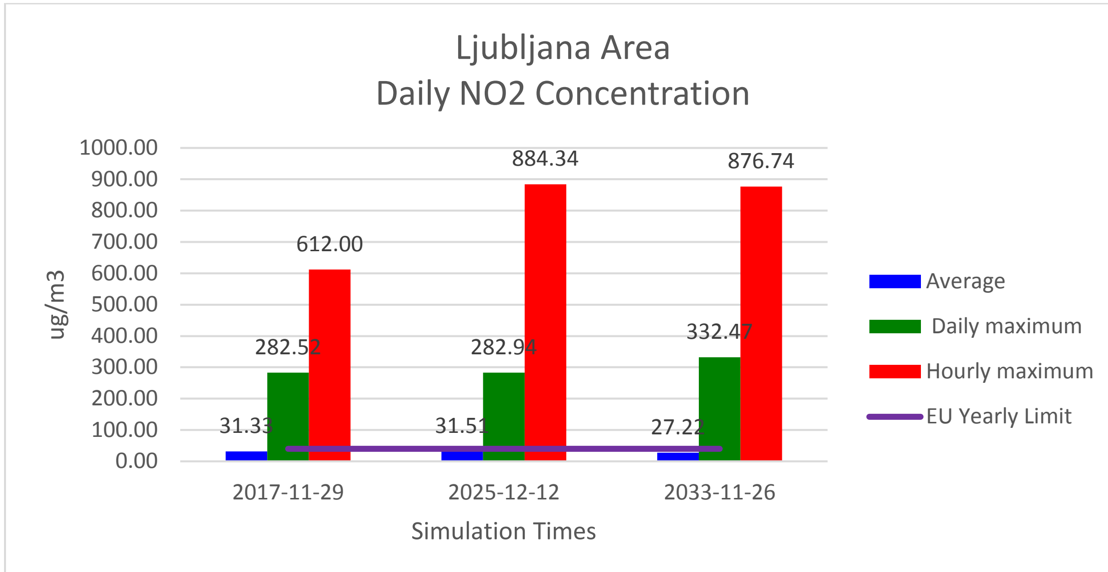


*Figure 4.10.18: $NO_2$ Day concentrations*

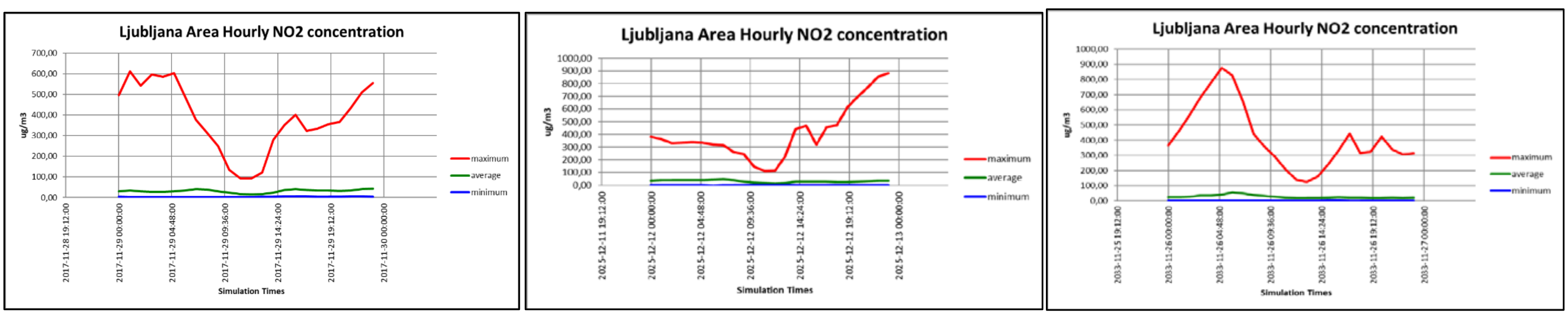


*Figure 4.10.19: Hourly $NO_2$ concentrations*

## $O_3$-Cluster 3

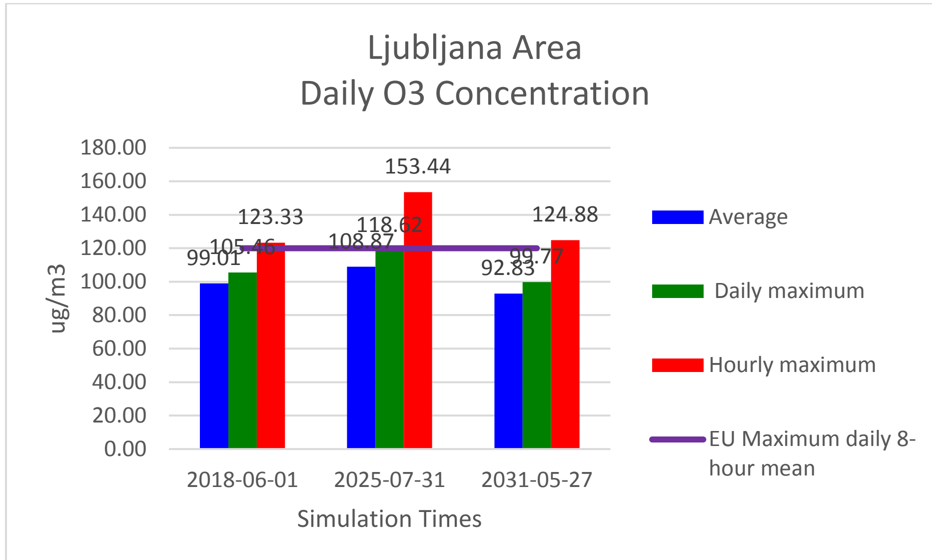


*Figure 4.10.20: $O_3$ Daily concentrations*

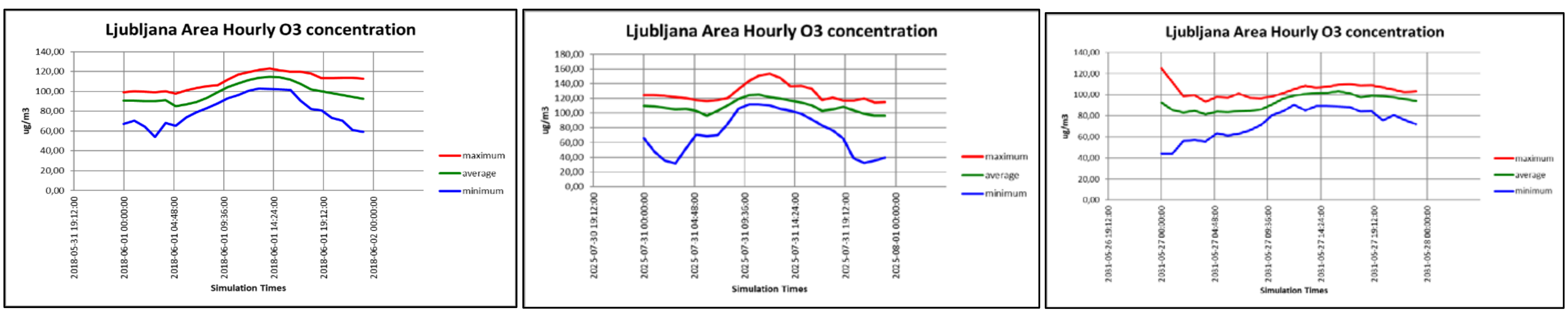


*Figure 4.10.21: $O_3$ Hourly concentrations*

## $PM_{10}$-Cluster 6

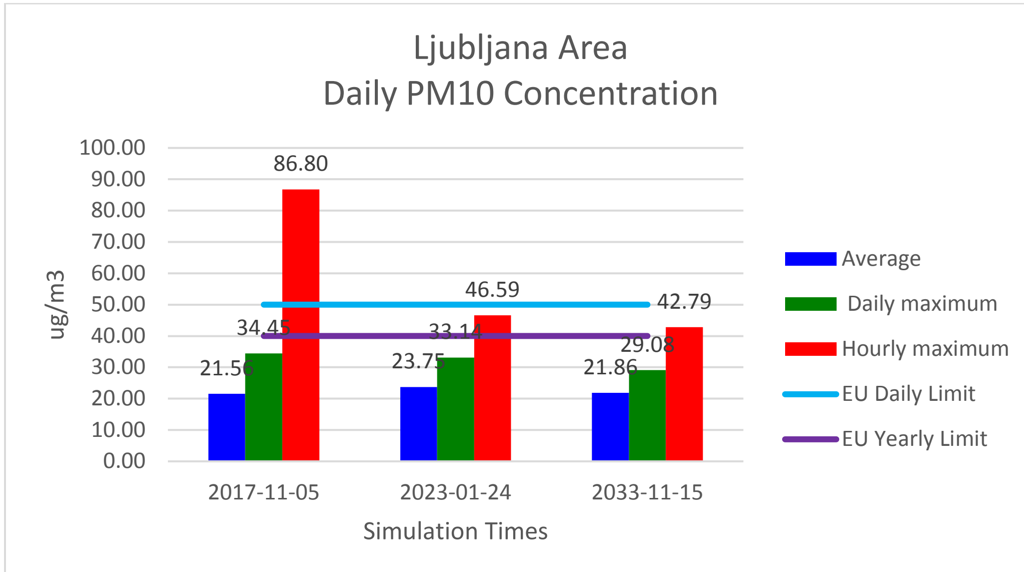


*Figure 4.10.22: $PM_{10}$ Daily concentrations*

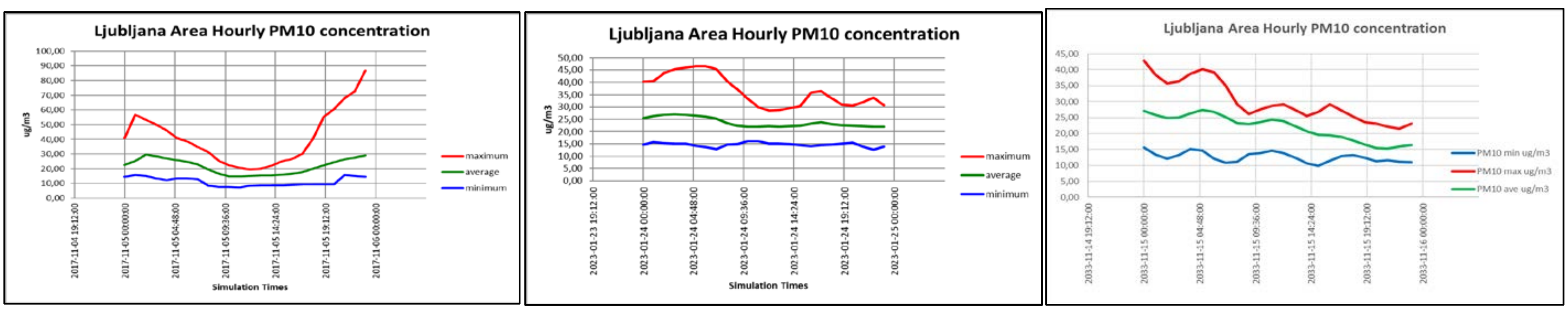


*Figure 4.10.23: $PM_{10}$ Hourly concentrations*

PM$_{2.5}$ Concentrations (Cluster 6)

In Figure 4.10.24, the results are presented in terms of concentrations average, daily maximum and hourly maximum.
The daily maximum concentrations are well above the WHO yearly limit of 10μg/m$^3$ in all days.

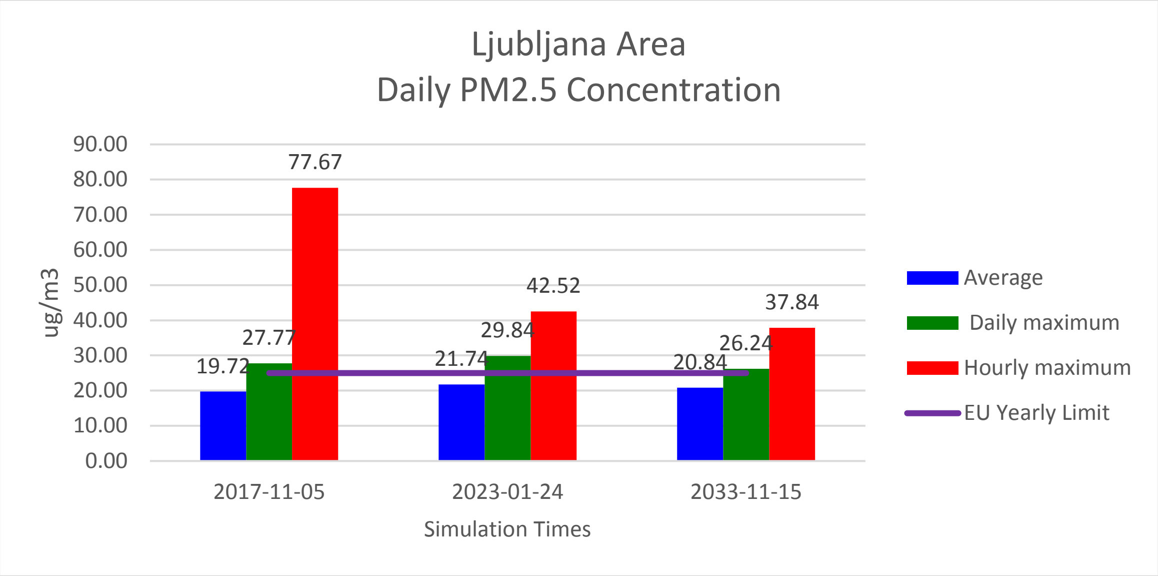


*Figure 4.10.24: PM$_{2.5}$ Day concentrations*

Figure 4.5.29 presents the estimated BaP daily concentrations contained in PM$_{2.5}$. All days are above WHO annual limit of 0.12ng/m$^3$ . Concentrations are closer (but above) to the EU annual limit of 1ng/m$^3$.

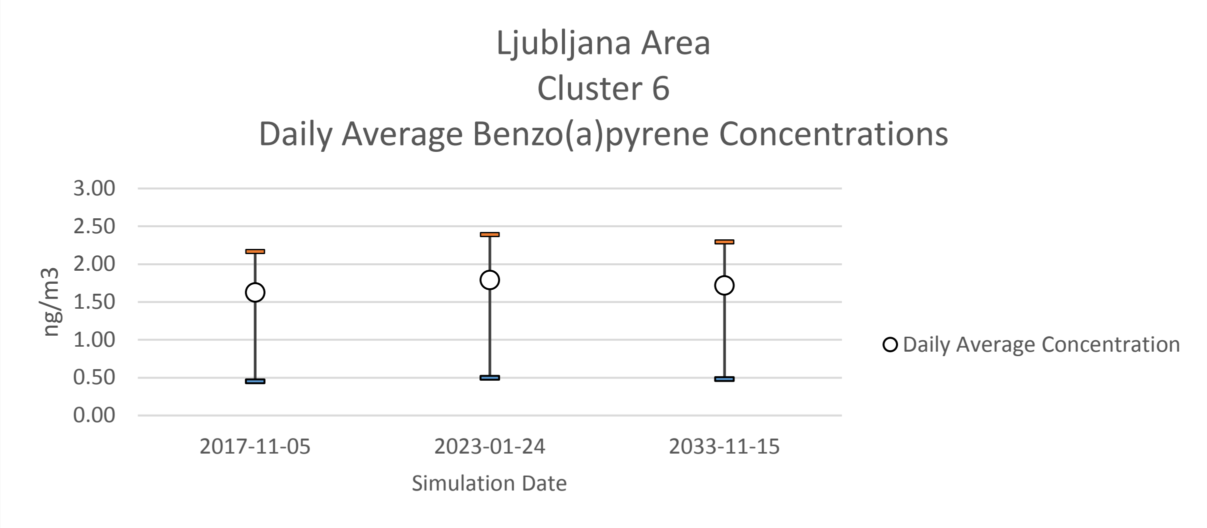


*Figure 4.10.25: BaP daily concentrations*

#### 4.10.3.3 The Emission Inventory effect

Figures 4.10.26, 4.10.27, 4.10.28 and 4.10.29 illustrate the emission inventory temporal change effect on $NO_2$, $O_3$, $PM_{10}$ and $PM_{2.5}$ concentration levels respectively. There is a slight decreasing trend in PM pollutants and an even slighter decrease in $NO_2$ and $O_3$ concentrations.

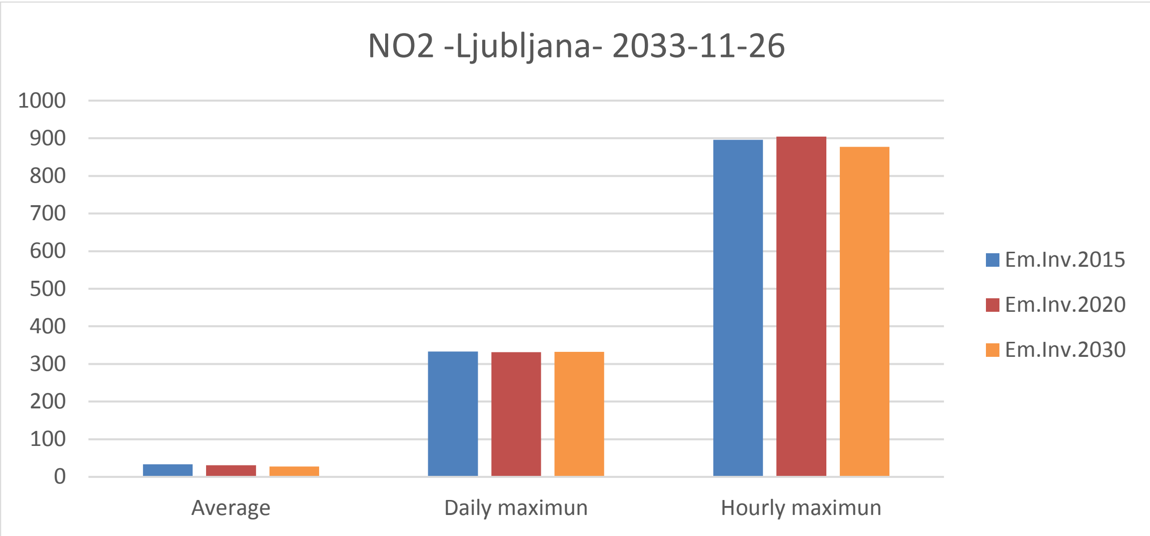


*Figure 4.10.26: $NO_2$ emission inventory comparison*

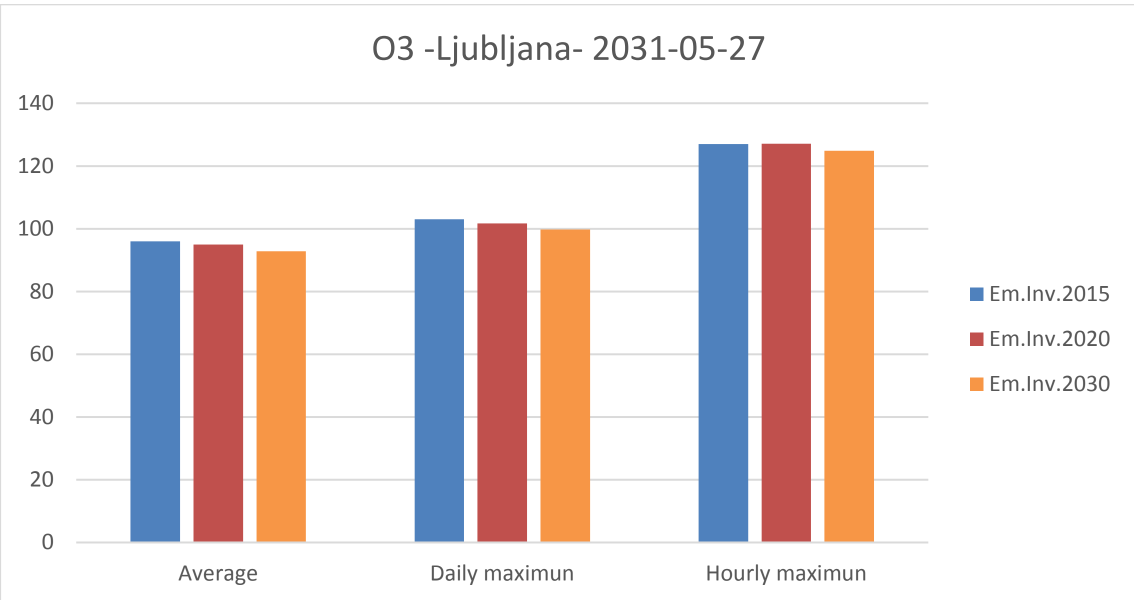


*Figure 4.10.27: $O_3$ emission inventory comparison*

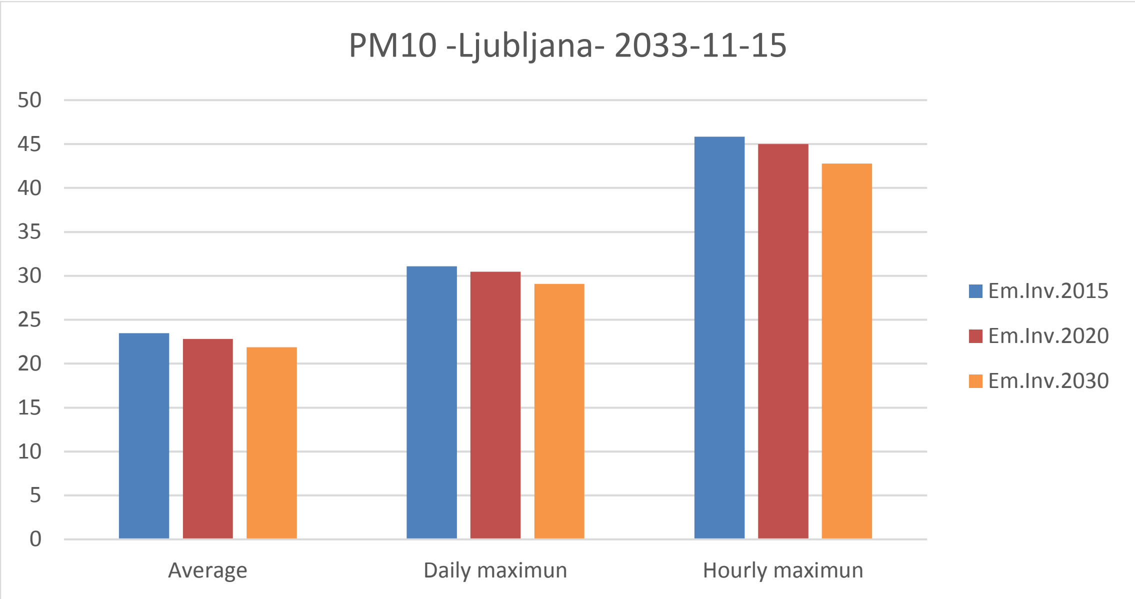


*Figure 4.10.28: $PM_{10}$ emission inventory comparison*

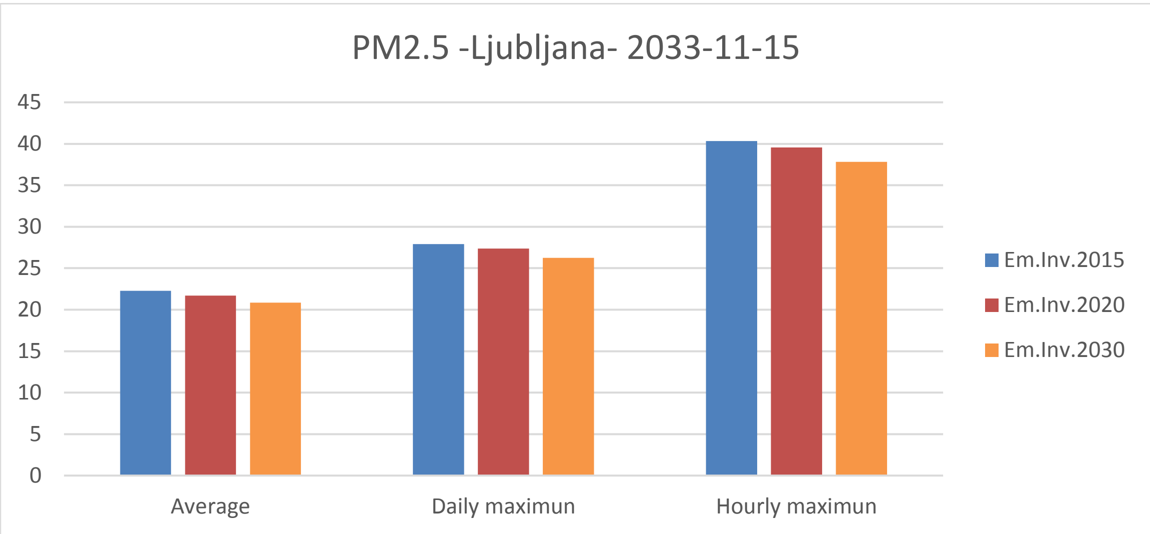


*Figure 4.10.29: $PM_{2.5}$ emission inventory comparison*

### 4.10.4 The GHGs Modeling results

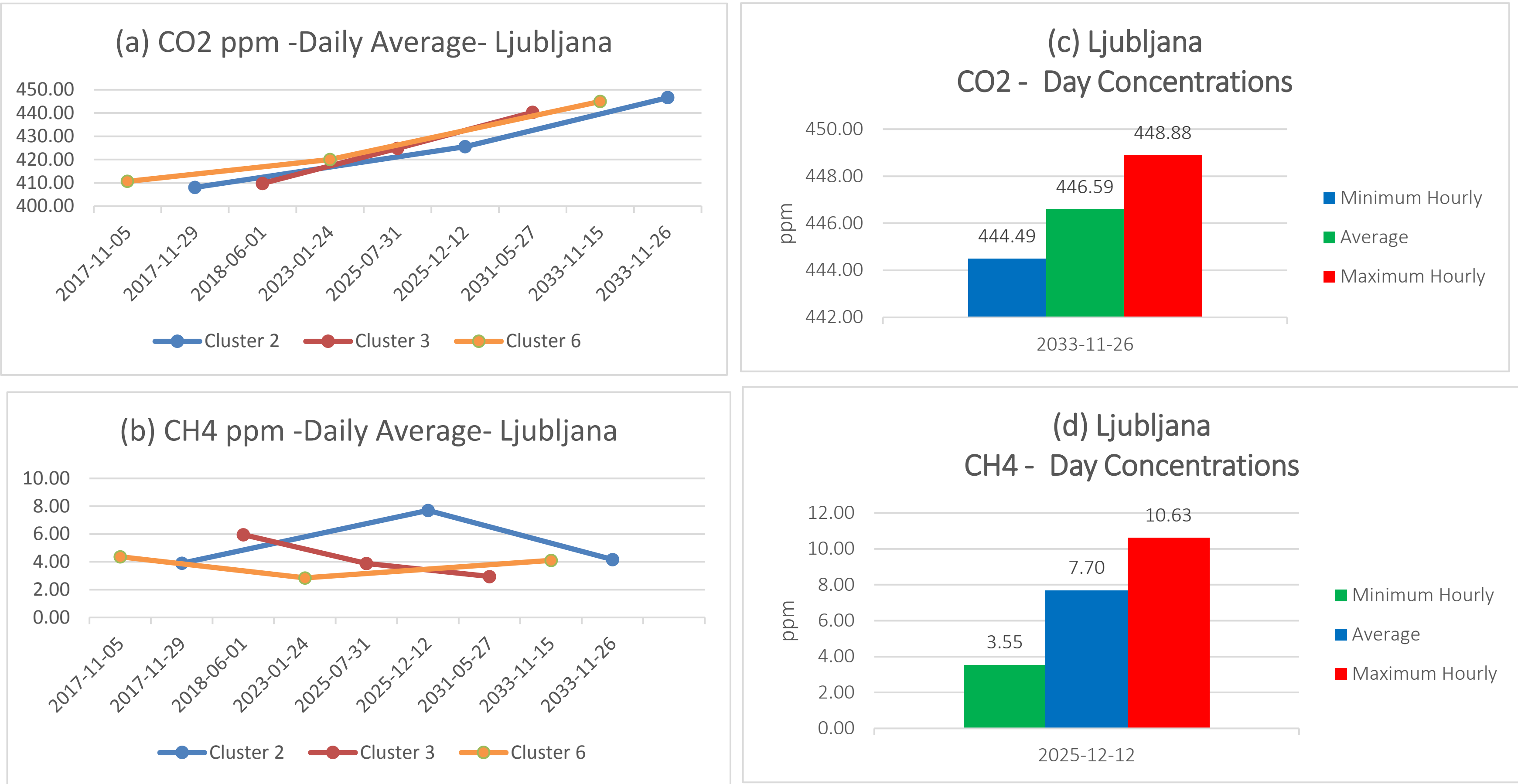


*Figure 4.10.30: (a),(b) $CO_2$ and $CH_4$ Daily average concentrations . (c),(d) $CO_2$ and $CH_4$ concentrations of the most polluted day*

### 4.10.5 Conclusions

For Ljubljana greater area, clusters 2,5 and 6 could be categorized in cold period and on the other hand clusters 3 and 4 in warm period.

In clusters 2 and 5 there is a linear increase in frequency occurrence through the ten 5-year periods. On the other hand, clusters 3 and 8 show a linear decrease in frequency occurrence.

The most heat waves seem to occur after 2036.The 5-year period 2041-2045 shows the highest number of heat waves, while the next 5-year period shows a decrease. The most heat waves were associated with cluster 3 which correspond to clusters with days belong to warm period.

Cluster 2 is characterized with elevated $NO_2$ concentrations, cluster 3 with elevated $O_3$ concentrations and cluster 6 with elevated PM concentrations.

$NO_2$ daily maximum concentrations seem to well exceed the EU and WHO yearly limit of 40μg/m$^3$. The maximum hourly concentrations are above the limit of 200μg/m$^3$.

$O_3$ daily maximum concentrations are very close and above the WHO 8hr limit of 100μg/m$^3$. The maximum hourly concentrations exceed this limit as well as the EU 8hr limit of 120μg/m$^3$.

$PM_{10}$ daily maximum concentrations are above the WHO yearly limit of 20μg/m$^3$. Both daily maximum and hourly maximum values show a decreasing rate.

$PM_{2.5}$ daily maximum concentrations are well above the WHO yearly limit of 10μg/m$^3$ in all days.

For BaP concentrations, all days are above WHO annual limit of 0.12ng/m$^3$. Concentrations are closer (but above) to the EU annual limit of 1ng/m$^3$.

Regarding the emission reductions intervention effect, there is a slight decreasing trend in PM pollutants and an even slighter decrease in $NO_2$ and $O_3$ concentrations.

## 4.11 Local heat waves versus $O_3$ concentrations

In Table 4.11.1 are presented the clusters' number associated with heat waves and elevated $O_3$ concentrations.

Table 4.11.1: Local heat waves versus O3 concentrations

| City | $O_3$-Cluster | Heat wave -Cluster |
|---|---|---|
| Stuttgart | 5 | 4,5 |
| Athens | 4 | 4,5 |
| Thessaloniki | 1 | 1,7 |
| Milan | 7 | 8,7 |
| Madrid | 7 | 7,9 |
| Ljubljana | 3 | 3 |
| Copenenhagen/Roskilde | 4 | 4 |
| Basel | 2 | 2 |
| Brno | 4 | 5,4 |

# 5. Concluding Remarks

To study future climatic change effects on certain subjects such as atmospheric processes and air quality one should consider the inherent uncertainties in trying to mathematically describe the associated phenomena and quantify the relevant input due mainly to lack of knowledge and missing accurate enough input data. In addition, for answers that require high temporal and spatial refinements one may add also the issue computational capacity. Therefore, when quantifying such processes is more reliable to talk about trends rather than absolute values.

In studying climatic trends in the atmosphere, one should consider also the additional difficulty due to high temporal variability of the defining parameters not only on the level of hour and day but also on the level of the year and even beyond.

The objective of the present study is to provide high space and time resolution ground concentrations reflecting climatic trends for the period 2001-2050, of major air pollutants ($PM_{10}$, $PM_{2.5}$, $NO_2$, $O_3$, BaP) and major Greenhouse Gases ($CO_2$, $CH_4$) in Europe, focusing on the nine ICARUS cities i.e. Thessaloniki, Athens, Madrid, Stuttgart, Ljubljana, Brno, Milan, Basel and Copenhagen/Roskilde and to assess the effect of climate and emissions changes over time on the air concentration levels of the abovementioned pollutants.

To achieve such an objective and given the today computational capacity limitations, the common approach in the past has been to perform weather and air quality simulations for a complete year but only for a limited number of years. Such an approach has the inherent weakness that the results represent the selected year only and not the neighboring ones due to the inherent high yearly variability.

Taking into consideration all the above-mentioned complexities, the effort in the present study was to come up with a new and smart approach that fulfills the project objective by introducing proper trend indicators and targeted weather and air quality simulations. The adopted methodology is based on weather clustering that has been widely used in the past for weather classification which successfully met the project objectives.

Thus, a novel approach based on weather clustering is inaugurated to study climate change effect on air quality levels. The adopted clustering technique has been applied in daily weather data of 50-year period (from 2001 to 2050) to estimate the appropriate number of clusters. For the years 2006-2050 the weather predictions are based on the future emission scenarios developed by the last IPCC assessment report. In fact, the moderate Representative Concentration Pathway - RCP4.5 was selected which follows a rising radiative forcing pathway leading to 4.5W/$m_2$ in 2100. The detailed weather data were derived from the Coordinated Regional Climate Downscaling Experiment (CORDEX) provided from the Earth System Grid Federation (ESGF) index nodes. The Regional Climate Model (RCM) INERIS-WRF331F was selected, using the EUR 11 (about 10 km resolution) horizontal domain projection.

To cope with the abovementioned high temporal weather variability, the clustering exercise results are examined over 5-year periods, i.e. 2001-2005, 2006-2010, 2011-2015, 2016-2020, 2021-2025, 2026-2030, 2031-2035, 2036-2040, 2041-2045 and 2046-2050, instead of one year.

Under these circumstances, the detailed atmospheric modeling has been restricted to cluster representative days in each of the above mentioned 5-years period. It should be reminded that a representative day per cluster per 5-year period is identified as the one with the closest distance from the cluster's centroid.

The results obtained have shown the following key conclusions:

1. The ICARUS studies on climatic change reinforces the view that the greenhouse effect is likely to be 'felt' even under a moderate climatic scenario such as RCP4.5. For the cities of Stuttgart, Ljubljana, Brno, Milan, Basel and Copenhagen/Roskilde the present results indicate that adverse effects at least in terms of heat wave event frequency for this specific scenario, seem to reach maxima in the early 40s. For the cities of the south (Athens, Thessaloniki, Madrid) the maxima shift late 40s and probably beyond.
2. The elevated numbers of heat waves are associated with specific weather clusters;
3. There is a correlation between weather patterns with higher heat wave events and weather patterns with elevated $O_3$ concentrations. This is an indication that the greenhouse effect seems to lead to elevated $O_3$ concentrations likely due to the intensified atmospheric photochemical activity.
4. With respect to cluster frequency trend over the 50year period slight changes are observed. More specifically:
    - For all cities, the clusters associated with elevated heat wave events and $O_3$ concentrations show an increase.
    - The clusters associated with elevated PM show an increase only in Stuttgart and Madrid.
    - The clusters with elevated $NO_2$ concentrations show an increase in the five cities: Stuttgart, Brno, Basel, Madrid and Ljubljana.
5. Concerning the influence of the foreseen emission inventory changes on air pollutant concentrations levels, the detailed atmospheric simulations have shown that the policies incorporated into the adopted emission patterns seem to lead to $NO_2$ decreases and $O_3$ slight decreases. In the case of PM, the picture is mixed. For example, in Stuttgart, Milan, Basel and Athens the indication is of clear decrease whereas in Brno there are slight increases. In Madrid and Ljubljana slight decreases in PM concentrations were estimated.
6. The detailed atmospheric modelling simulations suggest also that the problem of meeting health standards for $NO_2$, $O_3$, PM and BaP will still continue to be an issue in the future.

The present results indicate that climatic change seems to increase atmospheric photochemical activity. Such phenomena could lead to $O_3$ and SOA concentration increases. On the other hand a significant part of coarse PM is water/minerals. The temperature and humidity is expected to play a significant role due to condensation processes. Hot and dry atmosphere is expected to decrease such a mass fraction.

The results obtained introduce the following hypotheses which need to be verified on experimental and theoretical basis:

1. The greenhouse effect intensifies the atmospheric photochemical activity leading to increase of $O_3$ and SOA concentrations in fine PM fraction.
2. The greenhouse effect affects condensation equilibrium due to temperature rising and leading to the reduction of water/minerals PM mass fraction.

## 6. References

Austin E., Zanobetti A., Coull B., Schwartz J., Gold D.R. and Koutrakis P. (2014) Ozone trends and their relationship to characteristic weather patterns. Journal of Exposure Science and Environmental Epidemiology, 1–11

Beck C., Philipp A. (2010) Evaluation and comparison of circulation type classifications for the European domain. Physics and Chemistry of the Earth 35, 374–387

Bejaran R.A., Camilloni I.A. (2003) Objective method for classifying air masses: an application to the analysis of Buenos Aires's urban heat island intensity. Theor Appl Climatol 74: 93–103

Cahynova M., Huth R. (2010) Circulation vs. climatic changes over the Czech Republic: A comprehensive study based on the COST733 database of atmospheric circulation classifications. Physics and Chemistry of the Earth 35, 422–428

Chang W., ZhanJ. (2017) The association of weather patterns with haze episodes: Recognition by PM2.5 oriented circulation classification applied in Xiamen, Southeastern China. Atmospheric Research 197, 425–436"

Clarke L.E., Edmonds J.A., Jacoby H.D., Pitcher H., Reilly J.M., Richels R. (2007) Scenarios of greenhouse gas emissions and atmospheric concentrations. Sub-report 2.1a of Synthesis and Assessment Product 2.1. Climate Change Science Program and the Subcommittee on Global Change Research, Washington DC

Demuzere M., and N. P. M. van Lipzig, (2010) A new method to estimate air-quality levels using a synoptic-regression approach. Part I: Present-day O3 and PM10 analysis. Atmos. Environ., 44, 1341–1355

Di Filippo P., Riccardi C., Pomata D., Gariazzo C., Buiarelli F. (2010) Seasonal Abundance of Particle-Phase Organic Pollutants in an Urban/Industrial Atmosphere Water Air Soil Pollut, 211, 231-250

EEA (2016) Air Quality in Europe – 2016 Report, No 28/2016, ISBN 978-92-9213-847-9, ISSN 1977-8449, doi:10.2800/80982

ETC/ACM (2011) Evaluation of current limit and target values as set in the EU Air Quality Directive, de Leeuw, F. and Ruyssenaars, P., Technical Paper 2011/3, European Topic Centre on Air Pollution and Climate Change Mitigation

EU, 2004. Directive 2004/107/EC of the European Parliament and of the Council of 15 December 2004 Relating to Arsenic, Cadmium, Mercury, Nickel and Polycyclic Aromatic Hydrocarbons in Ambient Air. OJ L 23, 26.1.2005, pp. 3-16"

Fujino J., Nair R., Kainuma M., Masui T., Matsuoka Y. (2006) Multigas mitigation analysis on stabilization scenarios using aim global model. The Energy Journal Special issue #3:343–354

Guerreiro C.B.B., Horalek J., de Leeuw F., Couvidat F. (2016) Benzo(a)pyrene in Europe: Ambient air concentrations, population exposure and health effects. Environmental Pollution, 214, 657-667

Guerreiro S. B., Dawson R. J, Kilsby C., Lewis E. and Ford A. (2018) Future heat-waves, droughts and floods in 571 European cities. Environ. Res. Lett. 13:034009

Hellén H., Kangas L., Kousa A., Vestenius M., Teinilä K., Karppinen A., Kukkonen J., Niemi J.V. (2017) Evaluation of the impact of wood combustion on benzo[a]pyrene (BaP) concentrations; ambient measurements and dispersion modeling in Helsinki, Finland, Atmos. Chem. Phys., 17, 3475–3487

Hijioka Y., Matsuoka Y., Nishimoto H., Masui T., Kainuma M. (2008) Global GHG emission scenarios under GHG concentration stabilization targets. J Glob Environ Eng 13:97–108

Hoffmann P. and Schlunzen K.H. (2013) Weather Pattern Classification to Represent the Urban Heat Island in Present and Future Climate. American Meteorological Society DOI: 10.1175/JAMC-D-12-065.1

Huth R., Beck C., Philipp A., Demuzere M., Ustrnul Z., Cahynová M., Kyselý J., Tveito O. (2008) Classifications of Atmospheric Circulation Patterns. Trends and Directions in Climate Research: Ann. N.Y. Acad. Sci. 1146: 105–152

IARC (2012) Chemical Agents and Related Occupations - Volume 100 F - A Review of Human Carcinogens. In: International Agency for Research on Cancer (IARC) Monographs on the Evaluation of Carcinogenic Risks to Humans, 100F

Kinney P. (2008) Climate Change, Air Quality, and Human Health , Am J Prev Med, 35(5):459–467

Kliucininkas L., Martuzevicius D., Krugly E., Prasauskas T., Kauneliene V., Molnar P., Strandberg B. (2011) Indoor and outdoor concentrations of fine particles, particle-bound PAHs and volatile organic compounds in Kaunas, Lithuania, J. Environ. Monit., 13, 182–191

Kozlowska W.R., Kozielska B., Klejnowski K., Szopa S. (2013),Hazardous compounds in urban PM in the central part of Upper Silesia (Poland) in winter, Archives of Environmental Protection, 39, 53-65

Lloyd  Stuart P. (1982) Least Squares Quantization in PCM. IEEE Transactions on Information Theory. Vol. 28, pp. 129–137

Makkonen U., Hellén H., Anttila P., Ferm M., (2010) Size distribution and chemical composition of airborne particles in south-eastern Finland during different seasons and wildfire episodes in 2006, Science of the Total Environment 408, 644–651

Makra L., Mika J., Bartzokas A., Béczi R., Borsos E., Sümeghy Z. (2006) An objective classification system of air mass types for Szeged, Hungary, with special interest in air pollution levels. Meteorol. Atmos. Phys. 92: 115

Moertini V.S. (2002) Introduction to five data clustering algorithms. Integral, Vol. 7, No. 2

Preisendorfer R.W., Mobley C.D. (1988) Principal components analysis in meteorology and oceanography. Developments in Atmospheric Sciences 17, Elsevier,Amsterdam

Riahi K., Grübler A., Nakicenovic N. (2007) Scenarios of long-term socio-economic and environmental development under climate stabilization. Technol Forecast Soc Chang 74:887–935

Rimetz-Planchon J., Perdrix E., Sobanska S., Bremard C. (2008) PM10 air quality variations in an urbanized and industrialized harbor. Atmospheric Environment 42, 7274–7283

Saarnio K., Sillanpaa M., Hillamo R., Sandell E., Pennanen A.S., Salonen R.O. (2008) Polycyclic aromatic hydrocarbons in size-segregated particulate matter from six urban sites in Europe , Atmospheric Environment 42, 9087-9097

Serra C., Fernadez-Mills G., Periago M.C., and Lana X. (1999) Winter synoptic types in Catalonia and their linkage with minimum temperature anomalies. Int J Climatol 19:1675–1695

Serra C., Fernadez-Mills G., Periago M.C., and Lana X. (1999) Winter synoptic types in Catalonia and their linkage with minimum temperature anomalies. Int J Climatol 19:1675–1695

Sfetsos A., Bartzis J. (2007) Real time, high resolution regional weather and air quality forecasting system in west Macedonia, Greece, Proceedings of the 11th International Conference on Harmonisation within Atmospheric Dispersion Modelling for Regulatory Purposes

Sfetsos A., Vlachogiannis D., Gounaris N., Stubos A.K. (2005) On the identification of representative samples from large data sets, with application to synoptic climatology. Theor. Appl. Climatol. 82, 177–182

Smith S.J., Wigley T.M.L. (2006) MultiGas forcing stabilization with minicam. The Energy Journal Special issue #3:373–392

Taylor K.E., Stouffer R.J., and Meehl G.A. (2012) An Overview of CMIP5 and the Experiment Design. Bull. Amer. Meteorol. Soc., 93:485–498doi:10.1175/BAMS-D-11-00094.1

Thomson A.M., Calvin K.V., Smith S.J., Kyle G.P., Volke A., Patel P., Delgado-Arias S., Bond- Lamberty B., Wise M.A., Clarke L.E., and Edmonds J.A. (2011) RCP4.5: a pathway! For stabilization of radiative forcing by 2100. Climatic&Change,109,77Q94

van Vuuren D.P., Edmonds J., Kainuma M. et al. (2011) The representative concentration pathways: an overview. Climatic Change, 109:5–31

Van Vuuren DP, Den Elzen MGJ, Lucas PL, Eickhout B, Strengers BJ, Van Ruijven B, Wonink S, Van Houdt R (2007a) Stabilizing greenhouse gas concentrations at low levels: an assessment of reduction strategies and costs. Clim Chang 81:119–159

VanVuuren D.P., Eickhout B., Lucas P..L, den Elzen M.G.J. (2006) Long-termmulti-gas scenarios to stabilise radiative forcing—exploring costs and benefits within an integrated assessment framework. Energ J 27:201–233

Vercauteren J., Matheeussen C., Wauters E., Roekens E., van Grieken R., Krata A., Makarovska Y., Maenhaut W., Chi X., Geypens B., (2011) Chemkar PM10: An extensive look at the local differences in chemical composition of PM10 in Flanders, Belgium, Atmospheric Environment 45, 108-116

WHO (2010), WHO guidelines for indoor air quality: selected pollutants, World Health Organization, European Centre for Environment and Health, Bonn

Wise M., Calvin K., Thomson A., Clarke L., Bond-Lamberty B., Sands R., Smith S.J., Janetos A., Edmonds J. (2009) Implications of limiting CO2 concentrations for land use and energy. Science 324:1183– 1186